Department of Civil and Environmental Engineering
University of Alberta
Edmonton

Structural Engineering Report No. 214

TRANSMISSION OF HIGH STRENGTH CONCRETE COLUMN LOADS THROUGH CONCRETE SLABS

BY
CARLOS E. OSPINA
SCOTT D. B. ALEXANDER

JANUARY 1997

"Transmission of High Strength Concrete Column Loads through Concrete Slabs"
by Carlos E. Ospina and Scott D.B. Alexander

Page	REVISION
6	Sixth line of fifth paragraph: revise "from 0.67 to 0.74" to read "from 0.45 to 0.54".
9	Third line of first paragraph: revise "from 1.11 to 1.23" to read "from 0.76 to 0.83".
9	Fourth line of first paragraph: revise "from 0.57 to 1.38" to read "from 0.79 to 0.97".
9	Eq. 2.5: replace "$0.47 f'_{cs}$" by "$0.47 f'_{cc}$".
11	Fifth line of third paragraph: revise "from 0.43 to 1.23" to read "from 0.45 to 0.87".
18	Table 2.1: Some of the values for ρ_{col} and ρ_{slab} are incorrect. An updated Table is attached.
36	Table 3.1: The majority of ρ_{slab} values are incorrect. An updated Table is attached.
37	Table 3.2: Revise "kN.m" to read "kN.m/m"
43	Moment units in Figs. 3.5 and 3.6 must be kN.m/m.
47	In the sketch of the top mat reinforcement, please revise "1 @ 600 (A2)" to read "2 @ 300 (A2)". Also change "2 @ 300 (A1,A3,A4)" to read "3 @ 200 (A1,A3,A4)".
59	Eq. 4.1: Please correct the equation as follows:

$$f_c = \frac{P_{col} - f_s A_{st}}{A_g - A_{st}} \quad , \quad f_s \leq f_y$$

Page	REVISION
75	Fig. 4.13: The drawing must show the slab segment deflecting downwards.
101	Table 6.1: The corresponding $f'_{ce,calc}$ value for specimen B-1 should be 70.10 instead of 72.10. Statistical values are correct though.
164	Fig. B.61: The curve for the strain through slab got interrupted due to a problem with the LVDT.

Second Revision: Sept. 9, 1998.

		Dimensions (mm)					Approx. Reinforcement Ratios (%)	
Reference	Type	a	b	c	e	h	ρ_{col}	ρ_{slab}
Bianchini et al.	ISP	788	788	279	635	178	1.46	0.47
	ESP	533	788	279	635	178	1.46	0.45 0.54
	CSP	533	533	279	635	178	1.46	0.52
	SC	-	-	279	635	178	1.46	-
Gamble & Klinar	ISP	1067	1067	254	610	127 178	1.76	0.76~0.83
	ESP	762	1067	254	610	127	1.76	0.79~0.84 0.92~0.97
Shu and Hawkins	SC	-	-	152	305	25~458	1.22	-
Kayani	ESP	762	1067	254	610	178	3.52	0.45 0.87
	SC	-	-	254	610	178	1.76~3.52	-

Nomenclature: ISP   : Interior Sandwich Plate
ESP   : Edge Sandwich Plate
CSP   : Corner Sandwich Plate
SC   : Sandwich Column

Notes: 1. Slab flexural reinforcement ratios were calculated based on the average effective depth.
2. For the edge sandwich plates, the first value or range for ρ_{slab} corresponds to the amount of reinforcement perpendicular to the free edge. The second value or range corresponds to the amount of reinforcement parallel to the free edge.

Table 2.1   Description of Test Specimens Found in the Literature

Specimen	Dimensions (mm)					Concrete Strength (MPa)		Approx. Reinf. Ratios (%)	
Mark	a	b	c	e	h	f'_{cc}	f'_{cs}	ρ_{col}	ρ_{slab}
A1-A,B,C	1380	1380	200	500	100	105 (27)	40 (28)	4.00	0.59
A2-A,B,C	1380	1380	200	500	100	112 (29)	46 (28)	4.00	0.44
A3-A,B,C	1380	1380	200	500	150	89 (27)	25 (28)	4.00	0.35
A4-A,B,C	1380	1380	200	500	150	106 (29)	23 (28)	4.00	0.35
B-1	1350	1350	250	625	250	104 (51)	42 (49)	1.28	0.27
B-2	1350	1350	250	675	150	104 (56)	42 (54)	1.28	0.63
B-3	1350	1350	250	625	250	113 (44)	44 (42)	1.28	0.27
B-4	1350	1350	250	675	150	113 (45)	44 (43)	1.28	0.63
B-5	1350	1350	250	625	250	95 (17)	15 (20)	1.28	0.27
B-6	1350	1350	250	675	150	95 (18)	15 (21)	1.28	0.63
B-7	1350	1350	175x350	625	250	120 (21)	19 (23)	1.28	0.27
B-8	1350	1350	175x350	675	150	120 (22)	19 (24)	1.28	0.63
C1-A	680	1220	230	465	170	107 (34)	32 (33)	3.02	0.32,0.31
C1-B	680	1220	230	465	170	107 (34)	35 (33)	3.02	0.32,0.31
C1-C	680	1220	230	465	170	107 (34)	34 (33)	3.02	0.32,0.31
C2-A	680	1220	230	435	230	108 (29)	31 (28)	3.02	0.23,0.21
C2-B	680	1220	230	435	230	108 (29)	34 (28)	3.02	0.23,0.21
C2-C	680	1220	230	435	230	108 (29)	33 (28)	3.02	0.23,0.21
D-SC1	-	-	250	712.5	75	105 (24)	17 (27)	1.28	-
D-SC2	-	-	250	687.5	125	105 (24)	17 (27)	1.28	-
D-SC3	-	-	250	675	150	107 (22)	17 (25)	1.28	-
D-SC4	-	-	250	625	250	105 (23)	17 (26)	1.28	-

Notes: 1. Concrete strengths correspond to those at time of testing. Numbers in parentheses indicate column and slab concrete age in days at time of testing.
2. Column strengths are those from upper or lower column end, whichever was lower.
3. Slab flexural reinforcement ratios were calculated based on the average effective depth and a 20 mm concrete cover.
4. For the edge specimens (C Series), the first value for ρ_{slab} corresponds to the ratio of slab reinforcement perpendicular to the free edge. The second value corresponds to the ratio of slab reinforcement parallel to the free edge.

Table 3.1   Description of Test Specimens

TRANSMISSION OF HIGH STRENGTH CONCRETE COLUMN LOADS THROUGH CONCRETE SLABS

by

Carlos E. Ospina

and

Scott D. B. Alexander

Department of Civil Engineering

University of Alberta

Edmonton, Alberta

Canada

January, 1997

Abstract

For economic reasons, columns in multistorey reinforced concrete buildings are built with high-strength concrete whereas slabs are built with concrete of weaker strength. In the preferred method of construction, the columns are first cast up to the soffit of the slab they will support. Then, the slab concrete is cast continuous through the columns. This process is repeated until the last floor is cast. As a result, the axial load that is transmitted from a column above the floor must pass through a layer of weaker concrete before reaching the column below the floor. A design question arises as to what concrete compressive strength should be used in the design of the column.

The behaviour of a slab-column joint is affected not only by the column load but by the slab load. Load on the slab causes flexural tension within the slab-column joint. Provisions in ACI 318-95 to evaluate the effective compressive strength of reinforced concrete columns intersected by concrete slabs are based on tests of slab-column connection specimens with unloaded slabs. Neither the design provisions in ACI 318-95 nor those in CSA A23.3-94 account for the effects of slab and column geometry on the joint compressive strength.

This report presents test data from a total of thirty connection specimens. Of these, nineteen were either interior or edge slab-column connections with loaded slabs. The test program examined the effects of slab loading and of connection geometry. Design provisions for interior, edge and corner connections are presented.

Acknowledgments

Table of Contents

List of Tables

List of Figures

Notation

A_g	Column gross area
A_{st}	Total area of column longitudinal reinforcement
c	Column width
CSP	Corner sandwich plate
ESP	Edge sandwich plate
f_c	Average compressive stress applied on column
f'_c	Specified compressive strength of concrete
f'_{cc}	Cylinder strength of column concrete
f'_{cs}	Cylinder strength of slab concrete
f'_{ce}	Effective compressive strength of column
f_y	Yield strength of steel reinforcement
h	Slab or joint concrete thickness
ISP	Interior sandwich plate
m	Distance between the column threaded rods closer to the slab and the slab top and bottom levels
P_{col}	Applied load on column
$P_{col,max}$	Maximum load applied on column
P_o	Nominal axial load resistance at zero eccentricity of a reinforced concrete short tied column
P_{s1}	Slab load intensity (applied to both interior and edge sandwich plates)
P_{s2}	Slab load intensity (applied only to the edge sandwich plates)
SC	Sandwich column specimen
α_1	Ratio of average stress in rectangular compression block to the specified concrete compressive strength
ε_{col}	Column longitudinal strain outside the joint region
ε_{mid}	Column longitudinal strain at specimen mid-height (includes strain contribution from both column stubs and slab)
$\varepsilon_{bot\,col}$	Column longitudinal strain measured along bottom column stub

$\varepsilon_{top\ col}$ Column longitudinal strain measured along top column stub

ε_{tt} Column longitudinal strain through slab thickness

ρ_{col} Column flexural reinforcement ratio

ρ_{slab} Slab flexural reinforcement ratio

1. INTRODUCTION

1.1 Description of the Problem

In multistorey reinforced concrete building construction, significant economy may be achieved by building the columns with high-strength concrete and the floors with a concrete of lower strength. With an increase in concrete strength, a column of smaller dimensions would carry the load that a larger normal-strength concrete column would sustain. A reduction in the column cross-sectional dimensions increases the amount of rentable space and is beneficial when architectural considerations restrict the size of the columns.

Use of concrete higher than 80 MPa in multistorey building columns is becoming more common in modern construction. For example, column concrete reaching 80 MPa has been reported for the Kuala Lumpur City Centre twin towers which at the time of completion will rank as the tallest buildings in the world (CEB Bulletin d'Information No. 222, 1994). Column concrete strengths ranging from 96.5 to 124 MPa have been reported by Howard and Leatham (1992), and by Randall and Foot (1992), for office buildings in Seattle. Concrete columns made of 82.7 MPa high-strength concrete were reported for the 311 South Wacker Drive tower in Chicago. Column concrete of 117 MPa was reported by Moreno (1992) for the 31 storey 225 West Wacker Drive tower, also in Chicago.

In the construction of multistorey reinforced concrete buildings it is accepted practice to cast the columns up to the bottom level of the slab they will support and then to cast the slab concrete continuous through the columns. Then, columns are cast up to the next floor level. This results in the slab concrete intersecting the high-strength concrete columns at each floor level. In other words, the axial load that is transmitted from the column above the floor must traverse a layer of weaker concrete before reaching the column immediately below the floor. A design question arises as to what compressive strength should be used in the design of the column.

Design provisions in CSA A23.3-M84 (Section 10.13) and in ACI 318-95 (Section 10.15) are based on the experimental work carried out by Bianchini, Woods and Kesler in 1960. These test results correspond to slab-column connection specimens subjected to column load only. Design guidelines in CSA A23.3-94 (Section 10.12) were developed by adding to the supporting data base a limited set of test results of interior connection specimens with loaded slabs.

There is a need to extend the work of Bianchini et al. for slab-column connection specimens subjected to both column and slab loading. It is also necessary to study the effect that column and slab dimensions may have on the column compressive strength. The range of column strengths should also be extended bearing in mind that column concrete strengths used in current practice greatly exceed those used three decades ago.

1.2 Objectives and Scope

Three design options are available to determine what compressive strength should be used to design a concrete column intersected by concrete floors.

The first solution consists of placing column concrete within the joint region and designing the connection based on the cylinder strength of the column concrete. The second design method is based on the floor concrete cylinder strength with the addition of dowels and spirals, as required. The third provision is to estimate an effective compressive strength of the slab portion of the column as a weighted average of the column and slab concrete cylinder strengths. Of these three design guidelines, the first is the most frequently adopted. Selection of either the first or the second method has implications on ease of construction and quality assurance.

This investigation will deal mainly with the third design option. The primary objective of this study is the development of design provisions to determine the effective strength of interior, edge and corner concrete columns intersected by concrete slabs.

The main variables accounted for in this research program are the amount of slab loading applied to the specimens and the ratio of slab thickness to column width, h/c.

Two types of test specimens were adopted throughout the experimental program. The first type consisted of two high-strength reinforced concrete column stubs framing into a normal-strength concrete slab segment. These specimens modeled interior and edge slab-column connections. Specimen dimensions representative of both flat plate and flat slab systems were tested. Column loads were applied to all of the specimens. Different levels of gravity load were also applied to the slab segments.

The second type of specimen consisted of two high-strength reinforced concrete column stubs sandwiching a layer of normal-strength concrete with same cross-sectional dimensions of those of the column stubs. No segment of normal-strength concrete was cast around the joint. These specimens were subjected to column load only and were intended to study the behaviour of unconfined joints.

In this experimental program, column concrete compressive strengths ranged from 89 to 120 MPa. Slab concrete compressive strengths varied from 15 to 46 MPa.

1.3 Organization of the Report

Chapter 2 presents a literature survey. It outlines the work reported by previous researchers and reviews the recommendations and design procedures that have been proposed. Chapter 3 presents a detailed description of the specimens tested throughout this experimental program. It also contains a description of the fabrication, instrumentation and testing procedures that were followed. Test results, observations and a comprehensive

description of the specimen behaviour are presented in Chapter 4. In Chapter 5, the analysis of test results is presented by describing the effect that slab loading and the slab thickness-to-column width ratio, h/c, have on the strength of high-strength concrete columns intersected by normal-strength concrete slabs. Chapter 6 presents the development of design provisions for interior, edge and corner columns and finally, a summary and relevant conclusions of this research work are reported in Chapter 7.

2. BACKGROUND

2.1 Introduction

In the design of interior columns intersected by concrete slabs of weaker strength, the joint concrete is assumed to be confined, and therefore capable of carrying compressive stresses in excess of the cylinder strength of the slab concrete. This increased strength, defined as an *effective* compressive strength, results from the lateral restraint provided to the joint by stresses acting in the plane of the slab. The restraint conditions vary according to the type of connection, either interior, edge, or corner.

Past researchers (Bianchini et al. (1960), Gamble and Klinar (1991), Shu and Hawkins (1992), and Kayani (1992)) have attributed the joint restraint effect to the slab concrete around the joint periphery and to the high-strength concrete column ends framing into the joint. Their test observations lead to the following description of the joint behaviour.

Under column compressive load the joint concrete shortens longitudinally and, due to Poisson's ratio, expands laterally. Across its height, the joint lateral expansion is resisted by the top and bottom slab reinforcing bars passing through the joint and by the surrounding floor concrete.

The joint is also restrained at the top and bottom levels by the column ends framing into the connection. The high-strength column ends restrain the joint concrete in the same way that testing machine platens restrain a concrete cylinder. In a compression test, the strength of the specimen depends on its aspect ratio, defined as the ratio of the specimen height to its diameter (cylinder) or width (prism). As this aspect ratio increases, the strength decreases.

A slab-column joint may be viewed as a concrete prism being pressed between two stronger column ends. It is likely that the aspect ratio of the joint, defined as the slab thickness divided by the column side dimension, h/c, affects the compressive strength of the connection.

2.2 Literature Survey

2.2.1 General

Sketches of test specimens simulating slab-column connections tested in the past are presented in Figs. 2.1 through 2.4.

A typical slab-column connection specimen consists of two high-strength concrete column stubs framing into a segment of slab concrete. Figures 2.1, 2.2 and 2.3 illustrate typical interior, edge and corner specimens.

In this report, a slab-column connection specimen will be referred to as a *sandwich plate* since this type of connection may be viewed as a concrete plate sandwiched by the column ends framing into the joint.

Figure 2.4 illustrates a typical *sandwich column* specimen. It consists of a high-strength column intersected by a layer of floor concrete at the column mid-height. No slab segment is cast around the joint faces. In effect, the slab concrete is cut off at the joint periphery.

2.2.2 Chronological Report of Published Test Results and Code Provisions

2.2.2.1 Bianchini, Woods and Kesler (1960)

Bianchini et al. tested 29 sandwich plate specimens. Of these, there were 11 interior, nine edge and nine corner connection specimens. They also tested four sandwich column specimens. The first objective of testing was to define how large a ratio of column concrete to slab concrete cylinder strength, f'_{cc}/f'_{cs}, could be tolerated without reducing the axial load capacity of the column. The second objective was to determine the effective axial load capacity of the column when this limiting value was exceeded.

The major variables accounted for in this study were the ratio of column concrete strength to slab concrete strength, f'_{cc}/f'_{cs}, and the joint type, either interior, edge or corner. The slab thickness, column size and amount of column reinforcement were kept constant. Type and dimensions of the test specimens are reported in Table 2.1.

Column cylinder strengths, f'_{cc}, ranged between 15.8 to 56 MPa whereas slab cylinder strengths, f'_{cs}, varied from 8.8 to 24.8 MPa. For the sandwich plate specimens, columns were longitudinally reinforced with four No. 6 deformed bars and with No. 2 stirrups spaced 200 mm apart. Slabs were reinforced at top and bottom with No. 4 deformed bars. Spacing of these bars varied according to the type of connection being examined. Slab reinforcement ratios in the sandwich plate specimens varied approximately from 0.67 to 0.74 %. The yield strength of the steel reinforcement ranged from 295 MPa to 323 MPa. Sandwich columns were reinforced with four No. 6 deformed bars with No. 2 ties spaced at 200 mm. This amount of reinforcement was also kept constant. Testing age of specimens was set at 28 days. Load was applied only to the columns. Duration of the tests ranged between 1.5 to 2 hours.

For the interior specimens, cracking started on the vertical face of the slab at mid-edge and progressed inwards to the column, directly over the slab reinforcement. Then, cracks formed around the slab-column contact surface. Later, cracks formed in the columns above and below the slab. Interior specimens failed either on the top or the bottom column stubs.

For the edge and corner specimens, vertical cracks formed first in the visible face (or faces) of the joint. Then, cracks formed in the slab top and bottom levels around the column. Cracks then extended towards the slab edges, in line with the slab reinforcement.

6

Failure occurred either in the visible face (or faces) of the joint or in the top or bottom column stubs.

For the sandwich columns, the first cracks were vertical splitting cracks in the sandwiched concrete joint. Failure occurred later at the joint region.

Bianchini et al. reported their test results by plotting ratios of the column effective compressive strength to the floor concrete strength, f'_{ce}/f'_{cs}, against ratios of the column concrete cylinder strength to the floor concrete cylinder strength, f'_{cc}/f'_{cs}. The term f'_{cc} represents the top or bottom column stub cylinder strength, whichever is lower.

Bianchini et al. calculated the column effective compressive strength from the ACI code design equation for short tied columns, given as

$$P_o = 0.85 f'_c \left(A_g - A_{st} \right) + f_y A_{st} \qquad [2.1]$$

Re-arranging terms, and replacing the f'_c term by f'_{ce} yields

$$f'_{ce} = \frac{P_o - f_y A_{st}}{0.85 \left(A_g - A_{st} \right)} \qquad [2.2]$$

where $P_o = P_{col,max}$, the maximum column load applied in a test.

Failure of the different test specimens was found to be dependent of the ratio of column to slab compressive strength, f'_{cc}/f'_{cs}. They concluded that under certain f'_{cc}/f'_{cs} values, the presence of the weaker slab concrete may reduce the axial compressive strength of the column. For interior columns, this critical value was found to be equal to 1.5. For edge and corner specimens, the value was 1.4.

When exceeding these ratios, Bianchini et al. concluded that, for interior columns, only 75 percent of the column concrete strength may be effective in sustaining the column load. For edge and corner columns, Bianchini et al. found that no significant benefits may be obtained by increasing the column concrete strength beyond 1.4 times the floor concrete strength.

2.2.2.2 CSA A23.3-M84 and ACI 318-95

Both CSA A23.3-M84 and ACI 318-95 standards use the test results reported by Bianchini et al. as the background for their design provisions on the subject of transmission of column loads through concrete floors. The design guidelines given in ACI 318-95 are, in essence, the same as those originally given in the ACI 318-63 code. Since these provisions have remained intact for more than 30 years, any reported observation or comment on the subject concerning the ACI 318 code provisions within this period of time will be referred to ACI 318-95.

Design provisions in ACI 318-95 and CSA A23.3-M84 establish that when the column concrete strength does not exceed by more than 40 % the slab concrete strength, the design of the connection is based on the column concrete cylinder strength. When this limit is exceeded, three solutions are presented.

The first solution refers to the construction procedure of *puddling* in which column concrete is placed within the slab-column connection region. Since both column and slab concrete should be cast simultaneously, special care must be taken to avoid placement of the weaker concrete within the joint region. The top surface of the puddled column concrete must extend at least 600 mm (2 ft) from the face of the column. Proper vibration of the column and slab concretes should be accomplished to guarantee an optimum integration between both materials.

The second provision states that the axial load capacity of the column may be calculated based on the lower intervening concrete cylinder strength (usually that cast in the floor) plus the addition of vertical dowels and spirals to the connection. This results in the following design equation.

$$\frac{f'_{cc}}{f'_{cs}} > 1.4 \quad ; \quad f'_{ce} = f'_{cs} \qquad [2.3]$$

The third design recommendation is an equation to calculate the column effective compressive strength as a weighted average of column and slab concrete cylinder strengths. The use of this equation is limited to interior slab or slab/beam column connections and is given as follows.

$$\frac{f'_{cc}}{f'_{cs}} > 1.4 \quad ; \quad f'_{ce} = 0.35 f'_{cs} + 0.75 f'_{cc} \qquad [2.4]$$

2.2.2.3 Gamble and Klinar (1991)

Gamble and Klinar tested 6 edge and 6 interior sandwich plate specimens. Dimensions of the test specimens are presented in Table 2.1. Their test program extended the range of values of column to slab concrete compressive strength, f'_{cc}/f'_{cs}, and yield strength of the reinforcement, f_y. Major parameters involved were the type of specimen and the ratio of the column compressive strength to the slab compressive strength, f'_{cc}/f'_{cs}.

Column concrete strengths ranged between 72.4 and 104.8 MPa. Slab concrete varied from 15.9 to 45.5 MPa. The size of the aggregate used in the slab concrete was 19 mm (3/4 in). Specimens were tested at ages between 61 to 157 days. The amount of column reinforcement was held constant. Four No. 6 deformed bars were placed for this purpose. Transverse reinforcement for the columns was also kept constant with 1/4" diameter stirrups spaced at 250 mm. The slab top reinforcement consisted of No. 4 deformed bars. One specimen (edge-type) had 3/8 in-diameter negative reinforcement bars running in the

8

direction perpendicular to the slab free edge. Spacing of the top slab rebar varied. Bottom reinforcement, if any, limited to two No. 4 bars passing through the joint in each direction. Slab flexural reinforcement ratio varied approximately from 1.11 to 1.23 % for the interior specimens and from 0.57 to 1.38 % for the edge specimens. The yield strength of the column reinforcing bars was 486 MPa. Slab reinforcement yield strength varied from 500 MPa (No. 4 bars) to 533 MPa (No. 3 bars).

Load was applied only to the columns. Strain measurements were taken by means of electrical resistance foil type strain gauges. These were attached to the column and the slab rebar. Column gauges were attached at the joint mid-height and at levels above and below the concrete slab segment. Slab gauges were attached to the top reinforcing bars passing through the joint about 50 mm outside the column.

For the interior specimens, cracks formed in the slab near the column and radiated toward the slab boundaries. Because the slabs were reinforced with more top steel than bottom steel, the slab underside was pushed out more than the top, resulting in the slab curling upwards. At failure, cracks extended into the lower column stub and the specimen failed explosively.

For the edge specimens, vertical cracks formed first on the free face of the joint. Next, cracks appeared in the slab along the outline of the column. Vertical splitting cracks then formed in the columns. The specimen failed explosively at the joint region, with the joint concrete at the free face spalling off and the column reinforcement buckling at that location.

Test results reported by Gamble and Klinar are reported in a similar way to that adopted by Bianchini et al. An important conclusion drawn by Gamble and Klinar is that the ratio f'_{cc}/f'_{cs} appears to be generally applicable across the range of concrete strengths that were used. This means that similar test results for a connection specimen with f'_{cc}/f'_{cs} of 3.0 are reached with either a 60 MPa column concrete and a 20 MPa slab concrete or with a 90 MPa column concrete and a 30 MPa slab concrete. Gamble and Klinar also suggested that the column width-to-slab thickness ratio, c/h, affects the effective strength of the joint concrete. However, no tests were carried out to demonstrate this hypothesis.

For f'_{cc}/f'_{cs} values less than 1.4, Gamble and Klinar concluded that the column effective strength, f'_{ce}, is equal to the column cylinder strength, f'_{cc}. For higher ratios, the column effective compressive strength is evaluated as follows:

For interior columns,

$$f'_{ce} = 0.67 f'_{cs} + 0.47 f'_{cs} \geq 1.4 f'_{cs} \qquad [2.5]$$

For edge columns,

$$f'_{ce} = 0.85 f'_{cs} + 0.32 f'_{cc} \geq 1.4 f'_{cs} \qquad [2.6]$$

9

Gamble and Klinar found that design provisions in ACI 318 overestimate the strength of joints in which the ratio of column concrete strength to slab concrete strength is large.

2.2.2.4 Shu and Hawkins (1992)

Shu and Hawkins reported test results from 54 sandwich column specimens. This particular specimen shape was adopted to study the behaviour of joints restrained solely at the top and the bottom levels by two column ends.

Major variables in this investigation were the ratio of the slab thickness to the column width, h/c, and the ratio of the column concrete compressive strength to the slab concrete compressive strength, f'_{cc}/f'_{cs}.

Dimensions of the specimens are reported in Table 2.1. For the sandwich columns referred to as Group II specimens, the h/c ratio ranged from 0.17 to 3.00 and f'_{cc}/f'_{cs} varied between 1.0 to 5.6. Joint concrete compressive strength varied from 6.9 to 39.2 MPa. The size of the aggregate utilized in both the column and joint concrete was 19 mm (3/4 in). The amount of column longitudinal and transverse reinforcement was systematically varied to study the effect of this variable on the interaction of column and slab concrete. Axial compressive load was applied to the sandwich column specimens. The duration of each test was reported to be about one hour.

For specimens with small h/c values and a slab concrete strength close to that in the column stubs, vertical cracks appeared in the column. Such cracks widened enough so that column longitudinal reinforcing bars buckled and then the column core concrete crushed. For specimens with intermediate h/c values, cracks formed first in the sandwiched joint and then extended into the upper column stub. For test specimens with high values of h/c, failure was limited to the joint region. Specimens showed some ductility prior to failure.

Test results were not affected by the amount of column reinforcement. As in Bianchini et al., and Gamble and Klinar, the effective compressive strength was evaluated according to Eqs. 2.1 and 2.2. The main conclusion was that h/c is a significant variable affecting the effective compressive strength of columns intersected by layers of weaker concrete. Test results were reported as a function of this ratio. As h/c increases, the column effective compressive strength decreases.

Shu and Hawkins found the ACI 318 provisions to be unconservative for values of f'_{cc}/f'_{cs} equal to or less than 1.4. They also concluded that design provisions for f'_{cc}/f'_{cs} values greater than 1.4 were unduly conservative for edge and corner columns. With regards to interior columns, they inferred that for certain h/c and f'_{cc}/f'_{cs} values, ACI design provisions may be unsafe. They proposed the following design equation to evaluate the effective strength of edge and corner columns:

$$f'_{ce} = f'_{cs} + A\left(f'_{cc} - f'_{cs}\right) \qquad\qquad [2.7]$$

10

where

$$A = \frac{1}{(0.4 + 2.66\,h/c)} \qquad\qquad [2.8]$$

2.2.2.5 Kayani (1992)

Kayani tested 2 edge sandwich plates and 4 sandwich columns. Dimensions of these specimens are shown in Table 2.1. The column location and the ratio of the column compressive strength to the slab compressive strength, f'_{cc}/f'_{cs}, were the only parameters investigated. Column dimensions and slab thickness were kept constant, being equivalent to those of the specimens tested by Gamble and Klinar. Concrete strength for the columns ranged from 92.2 to 104.6 MPa. The slab concrete varied from 25.3 to 39.6 MPa.

The amount of column reinforcement varied according to the type of specimen. Two of the sandwich columns were provided with a steel hoop at the joint region. This consisted of a set of double No. 2 ties. For these columns, eight No. 6 longitudinal bars with single No. 2 ties spaced at 254 mm were provided. For the columns without hoop at the joint region, four No. 6 deformed bars were placed, along with double No. 2 ties spaced at 254 mm.

For the edge specimens, columns had similar reinforcement than those with the double stirrup at mid-height. The top slab reinforcement consisted of No. 3 and No. 4 bars spaced at 100 mm running in both directions. Two reinforcing bars passing between the vertical column bars running parallel to the free edge of the specimen were placed at the bottom of the slab. The slab flexural reinforcement ratio varied approximately from 0.43 to 1.23 %. Grade 60 ksi bars were used for both the column and the slab reinforcement.

Specimens were instrumented with electrical resistance foil type strain gauges attached to the column vertical and lateral reinforcement. Gauges in the column vertical reinforcement were attached at the joint mid-height and outside the joint region. Specimens were tested at ages between 42 and 99 days.

Only column load was applied to the specimens. Duration of tests ranged from 40 to 60 minutes.

For the sandwich column specimens without ties at the joint region, splitting cracks formed at the joint region at the very end of the test. Then, the specimens failed suddenly due to crushing of the joint concrete and buckling of the column longitudinal reinforcement at the joint region. Once the peak load was reached, the joint cross-section was destroyed.

For the sandwich columns with steel ties acting as lateral confinement in the joint, concrete spalling was also observed at the joint region. Spalling of joint concrete was

followed by a 32 to 46 % drop in the applied column load rather than by the sudden failure of the specimen. No indication of buckling of column vertical reinforcement was observed. Further attempts to increase the column load resulted in failure of the sandwich columns by crushing of joint concrete and buckling and rupture of the column longitudinal bars at the joint region.

For the edge specimens, vertical splitting cracks formed at the visible face of the joint region at a load much less than the maximum column load. These splitting cracks continued to form throughout the test and later extended into the column stubs. First cracks on the slab top face were observed only at the end of the tests. These formed throughout the slab surface. On reaching the maximum column load the joint concrete cover spalled off and the column load dropped by 16 to 37 %. Immediately after the loading was resumed the specimens failed due to crushing of the joint concrete and buckling of the outer column steel bars at the joint region.

Kayani re-processed the test results from Bianchini et al. and from Gamble and Klinar. He suggested that sandwich column specimens adequately model corner slab-column connections. He also inferred that the addition of hoops in the joint region results in increased ductility rather than in increased axial load capacity.

With regard to the existing code provisions, Kayani not only questioned the 1.4 ratio given in ACI 318 but also concluded that these provisions overestimate the effective strength of interior and edge columns intersected by floors made of weaker concrete, particularly when high values of f'_{cc}/f'_{cs} are considered.

Kayani reported the test results in a manner slightly different to that adopted by Bianchini et al. and by Gamble and Klinar. The effective strength of the column was found to be proportional to the ratio of the product of the column and slab concrete strengths to the sum of the column and slab concrete strengths, as indicated in Eq. 2.10.

$$f'_{ce} = 2.0 \lambda_G \frac{f'_{cc} f'_{cs}}{f'_{cc} + f'_{cs}}$$

[2.9]

Where λ_G is a constant that depends on the type of connection. The values of this constant are given as follows.

i. Interior columns   1.25
ii. Edge columns   1.00
iii. Corner columns   0.90

2.2.2.6 CSA A23.3-94

Section 10.12 of the 1994 Canadian standard refers to the transmissibility of column loads through concrete floors. This Standard presents significant modifications to the design provisions given in CSA A23.3-M84.

12

There is a significant re-wording of the 1984 CSA design guidelines. The concrete puddling procedure is retained, but the distance to which column concrete must extend from the face of the column is reduced to 500 mm. The equation to evaluate the effective compressive strength of an interior column is substantially modified. For corner columns, the limiting value for f'_{cc}/f'_{cs} beyond which the compressive strength of the corner column is affected by the presence of the weaker floor concrete is reduced from 1.4 to 1.0. Finally, the use of dowels and spirals is considered to augment the effective compressive strength of the connection rather than the slab concrete compressive strength.

The design recommendations to evaluate the effective compressive strength of columns intersected by concrete floors, f'_{ce}, are as follows.

For interior columns,

$$f'_{ce} = 1.05 f'_{cs} + 0.25 f'_{cc} \quad \leq f'_{cc} \qquad [2.10]$$

For edge columns,

$$f'_{ce} = 1.4 f'_{cs} \quad \leq f'_{cc} \qquad [2.11]$$

For corner columns,

$$f'_{ce} = f'_{cs} \qquad [2.12]$$

For interior columns, Eq. 2.10 results in column effective strengths equal to the column concrete cylinder strength for f'_{cc}/f'_{cs} values less or equal than 1.4. For edge columns, the effective compressive strength of the column is equal to the column concrete strength, for f'_{cc}/f'_{cs} values less or equal than 1.4.

2.3 Discussion of Available Test Results and Code Design Provisions

2.3.1 Effect of Slab Loading

For specimens with unloaded slab, the following behaviour may be predicted. Under the sole action of column loading, the joint concrete expands laterally due to Poisson's ratio. This expansion sets both top and bottom slab reinforcing bars near the column region under tension. Since no slab loads are applied, the only static requirement to be fulfilled is that the tensile stresses in the slab reinforcement be equilibrated by compression stresses from the surrounding slab concrete. The compressive character of these forces plus that of the load applied on the column allow us to assume that the joint is being subjected to a triaxial compressive state of stress. In light of this observation, the joint may be assumed to be confined across its full depth. Illustration of the system of forces acting on the joint region of a specimen without slab loads is provided in Fig. 2.5.

For specimens with loaded slab, the slab-column connection is subjected to negative flexural moments. As a result, the top level of the slab near the column undergoes tension. Even in the absence of slab loading, significant tension of the top slab reinforcement crossing the column was reported by Gamble and Klinar for their specimens tested without slab loads. Under slab loading, it may be conjectured that the top slab bars are subjected to much higher tensile strains, i.e. high transverse tension, at the upper part of the joint. For equilibrium of forces, the biaxial transverse tension applied at the joint top region is counteracted by compressive stresses acting at the bottom. The couple produced by the top tension and the bottom compression forces equilibrates the applied moment.

It follows then that an interior prototype sandwich plate joint may be viewed as a reinforced concrete prism subjected to two triaxial states of stress rather than one. At the top, the joint is subjected to vertical compression from the column load and to biaxial transverse tension from the slab bending. In this region, the joint concrete is pulled apart by the slab reinforcing bars traversing the joint rather than being confined. Conversely, the bottom joint region is subjected to a triaxial state of compressive stresses similar to that predicted for the full depth of joints under no slab loading. Accordingly, full confinement of the joint only takes place at the joint bottom half. Figure 2.6 illustrates this behaviour.

The effect of transverse tension on the compressive strength of reinforced concrete was examined by Chen and MacGregor (1993). They found that transverse tension reduces the compressive strength of reinforced concrete panels subjected to combined in-plane compression and tension loads. Their experimental program included results of 40 reinforced concrete panels. Panels were 420 mm wide, 640 mm high and 70 mm thick. For specimens in which the axial compression and the transverse tension were applied simultaneously, the maximum reduction in the concrete compressive strength was 59 %. The corresponding transverse strain was 3.4 %.

The detrimental effect of transverse tensile strain applies to the upper half of slab-column joints under column and slab loading. Since such portion of the joint region is subjected to transverse tension from the slab reinforcement due to the slab bending, one would expect a significant reduction in the joint axial compressive strength.

Figures 2.7 to 2.9 illustrate the existing design provisions found in the literature for the calculation of the effective compressive strength of interior, edge and corner columns intersected by concrete floors. For completeness, the figures include the test results published in the past. Ratios of column effective strength to slab concrete strength, f'_{ce}/f'_{cs}, are plotted as the ordinates whereas ratios of column concrete strength to slab concrete strength, f'_{cc}/f'_{cs}, are plotted as the abcisses. The design equation proposed by Shu and Hawkins is not shown since this expression also depends on the slab thickness to column width ratio, h/c. Discussion of this design equation will be presented in Chapter 5.

The design curves presented in ACI 318-95 and CSA A23.3-M84 are based on the results reported by Bianchini et al. The design equations proposed by Gamble and Klinar are a

14

lower bound for the tests reported by them and those reported by Bianchini et al. Kayani's equations are a lower bound for the results reported by Bianchini et al., Gamble and Klinar and by Kayani. In addition to test results of connection specimens with unloaded slabs, the design procedure given in CSA A23.3-94 also accounted for a limited number of test results of interior connection specimens subjected to slab loads. In general, a significant variation between all of these design curves is observed.

It is worth repeating that no slab loads were applied to the specimens tested by Bianchini et al. (1960), Gamble and Klinar (1991), and Kayani (1992). Any result from tests on specimens subjected only to column load tends to overestimate the strength of the joint concrete. It can hence be inferred that any design provision based solely on these tests is also likely to overestimate the strength of a connection.

2.3.2 Effect of the Aspect Ratio, h/c

The effect of h/c on the joint strength may be anticipated based on a parallel between the test of a sandwich plate or column and the test of a concrete prism, cube or cylinder.

In a sandwich plate or column, the joint concrete is loaded in a manner similar to that experienced by a concrete specimen loaded by the heads of a testing machine. The confining effect provided to the joint concrete by the upper and lower column ends may be similar to that provided to a concrete prism, cube or cylinder by the platens of a testing machine. In a concrete cylinder test, the frictional forces at the interface between the concrete specimen ends and the testing machine plates restrain the transverse strain in the specimen. For high cylinder aspect ratios this restraint is reduced thereby resulting in a reduction of the specimen compressive strength.

The selection of realistic h/c values is desirable for the test of sandwich plate and sandwich column specimens. In multistorey buildings, higher concrete strengths are usually specified for the lower level columns. The slab thickness usually remains constant throughout the building. According to this, higher connection aspect ratios, h/c, are found at higher levels of the structure. Aspect ratios varying from 0.3 to 0.5 may be expected at lower levels of flat plate structures. Higher ratios may be found for waffle slabs or slabs with drop panels. For buildings whose first stories are utilized as parking levels, h/c values ranging from 0.6 to 1.0 may also be found. Taking into consideration the minimum column cross sectional dimensions recommended by current codes, h/c values greater than 1.0 may be unlikely to be found in real life structures.

Thus far, the variable h/c has not been rigorously examined in the testing of reinforced concrete sandwich plate specimens. Gamble and Klinar suggested the ratio of the column side to the slab thickness, c/h, as an important variable to evaluate the effective strength of columns intersected by concrete floors but they did not significantly pursue this line of research in their test program.

Shu and Hawkins accounted for the effect of this variable in the test of sandwich column specimens. They concluded that the effective compressive strength of unconfined joints increases as h/c decreases. This reduction is more appreciable for large differentials between the column concrete strength, f'_{cc}, and the slab concrete strength, f'_{cs}. In their experimental program, Shu and Hawkins considered h/c values varying from 0.17 to 3.0. Test results of specimens with aspect ratios greater than the unity may be considered unrealistic since it is unlikely to find such connection aspect ratios in real life structures.

For lower h/c values, the effective compressive strength of the unconfined joints is conservatively predicted by the equation for interior slab-column joints given either in CSA A23.3-M84 or ACI 318-95. This suggests that, as long as h/c is small enough, the lateral confinement of the joint is not required.

Shu and Hawkins reported the use of 19 mm size aggregate for the concrete in all their specimens. For the sandwich columns with h/c equal to 0.17 the layer of the joint concrete was approximately 25 mm thick. This means that the coarse aggregate was practically bridging the joint region from the bottom high-strength column to the top column. This results in an undue significant increase of the column compressive strength since aggregates are stronger than the cement paste in lower strength concretes.

Considering the analogy to cylinder testing, the use of 19 mm size aggregate in 25 mm thick concrete joints may be debatable according to the following observations. Avram et al. (1981) remark that the effect of the aspect ratio cannot be separated from that of the maximum aggregate size. They suggest a maximum ratio of aggregate size to cube specimen side between 1/3 and 1/4. According to Troxell et al. (1968) the diameter of a concrete cylinder should be not less than three or four times the maximum size of the aggregate in order to avoid undue influence of boundary conditions and other irregularities. Tests by Price (1951) show that for cylinders with an aspect ratio of two and maximum aggregate size greater than one-fourth times the cylinder diameter, the strength of a 100 mm diameter cylinder exceeds by more than four percent of the strength of a 150 mm diameter cylinder. It may be assumed that an strength enhancement will occur when testing a sandwich column whose joint concrete is made with aggregates larger than recommended.

Design provisions in ACI 318-95, CSA A23.3-M84 and CSA A23.3-94 do not account for the h/c parameter in evaluating the strength of sandwich connections. Adequacy of the American and the 1984 CSA provisions was already debated in the previous section. As far as to h/c is concerned, CSA A23.3-94 provisions may be unduly conservative when low values of h/c intervene in the connection.

Research found in the literature does not account either for the effect of the column rectangularity on the strength of columns intersected by concrete floors. Based on the recognition of the aspect ratio, h/c, as a significant variable to assess the effective strength of columns intersected by weaker slabs, it is important to determine what column

16

dimension in the case of a rectangular column should be used to determine the h/c value to evaluate the column effective compressive strength.

2.3.3 Discussion of Other Provisions Found in the Codes

In addition to providing design expressions to evaluate the effective strength of columns, both ACI 318-95 and CSA A23.3-M84 provide some other guidelines for the design of high-strength concrete columns intersected by concrete floors.

One of them is to puddle concrete of the strength specified for the column within the joint region. A detailed description of this process was already given in Section 2.1. Though puddling has become common in modern multistorey building construction, it may lead to serious logistical and quality assurance problems. These arise from the fact that two concretes of different strengths must be on site for the casting of the slab. These inconveniences were recognized in the construction planning of the 311 South Wacker Drive tower in Chicago, as reported by Robison (1988). Since the specified compressive strength for the lower level columns of this building was around 82 MPa, the slab decks were cast with 62 MPa concrete in order to avoid concrete puddling. At the end, the chosen solution proved being economically sound.

A second code provision included in ACI 318-95 and in the 1984 edition of the Canadian Standard refers to the calculation of the effective compressive strength of interior, edge and corner columns. This provision recommends that the design the column be based on the concrete cylinder strength of the intervening weaker concrete, with the addition of dowels and spirals in the joint region, as required. The addition of the proposed reinforcement may be difficult since joint regions are usually congested zones. Furthermore, a proper vibration of the joint concrete may not be guaranteed.

		Dimensions (mm)					Approx. Reinforcement Ratios (%)	
Reference	Type	a	b	c	e	h	ρ_{col}	ρ_{slab}
Bianchini et al.	ISP	788	788	279	635	178	1.46	0.67
	ESP	533	788	279	635	178	1.46	0.67~0.74
	CSP	533	533	279	635	178	1.46	0.74
	SC	-	-	279	635	178	1.46	-
Gamble & Klinar	ISP	1067	1067	254	610	127 178	1.76	1.11~1.23
	ESP	762	1067	254	610	127	1.76	0.57~1.38
Shu and Hawkins	SC	-	-	152	305	25~458	1.23	-
Kayani	ESP	762	1067	254	610	178	1.76~3.52	0.43~1.23
	SC	-	-	254	610	178	1.82	-

Nomenclature: ISP : Interior Sandwich Plate
ESP : Edge Sandwich Plate
CSP : Corner Sandwich Plate
SC : Sandwich Column

Table 2.1   Description of Test Specimens Found in the Literature
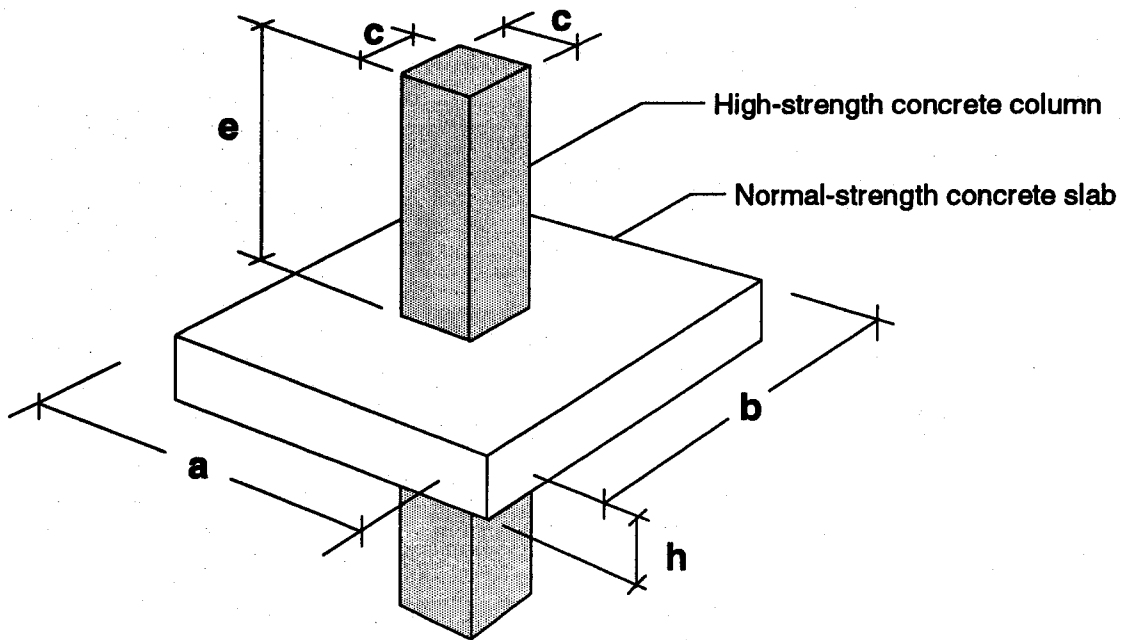
Figure 2.1   Interior Sandwich Plate Specimen
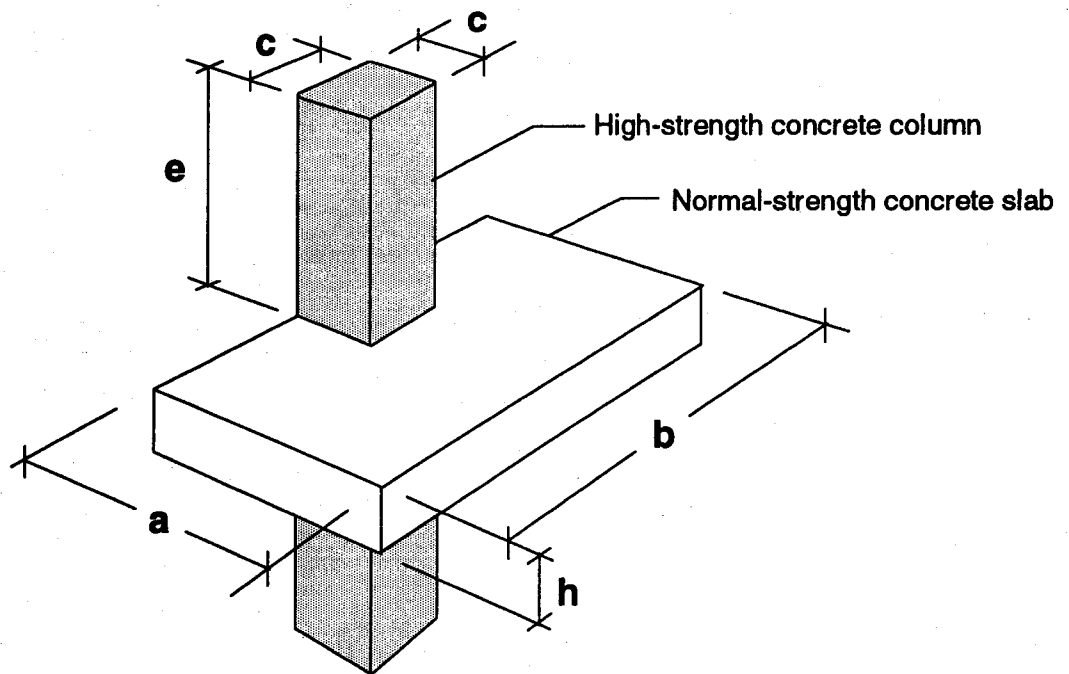
Figure 2.2   Edge Sandwich Plate Specimen

19
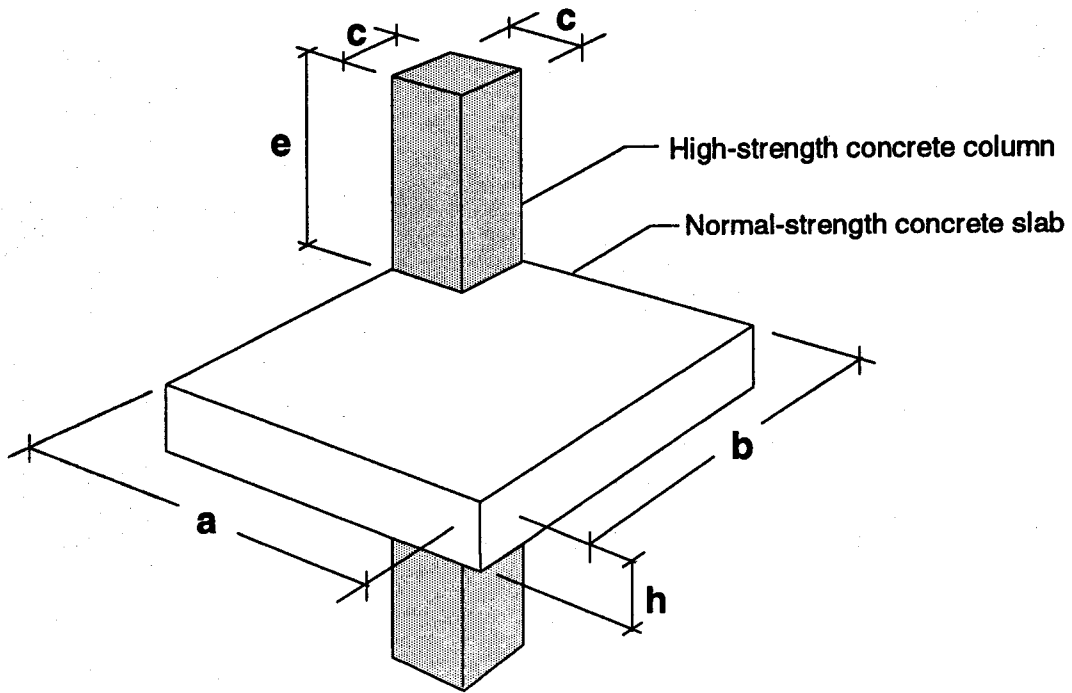
Figure 2.3   Corner Sandwich Plate Specimen
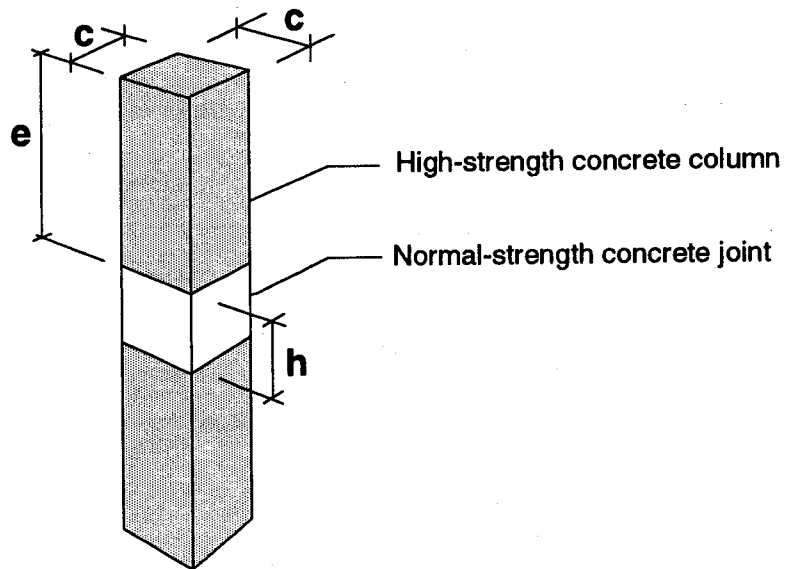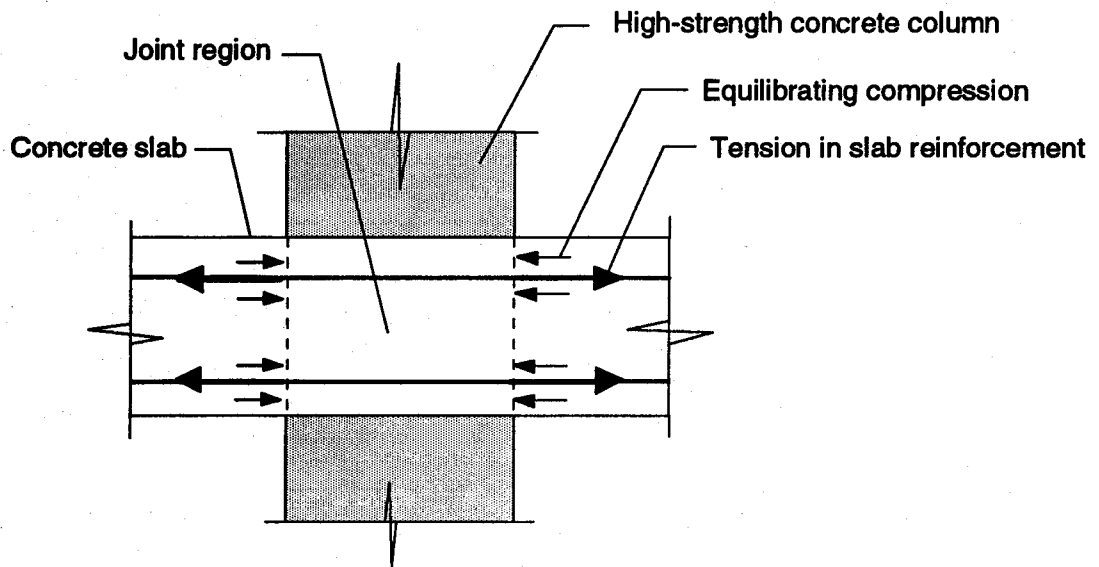

Figure 2.4   Sandwich Column Specimen

20

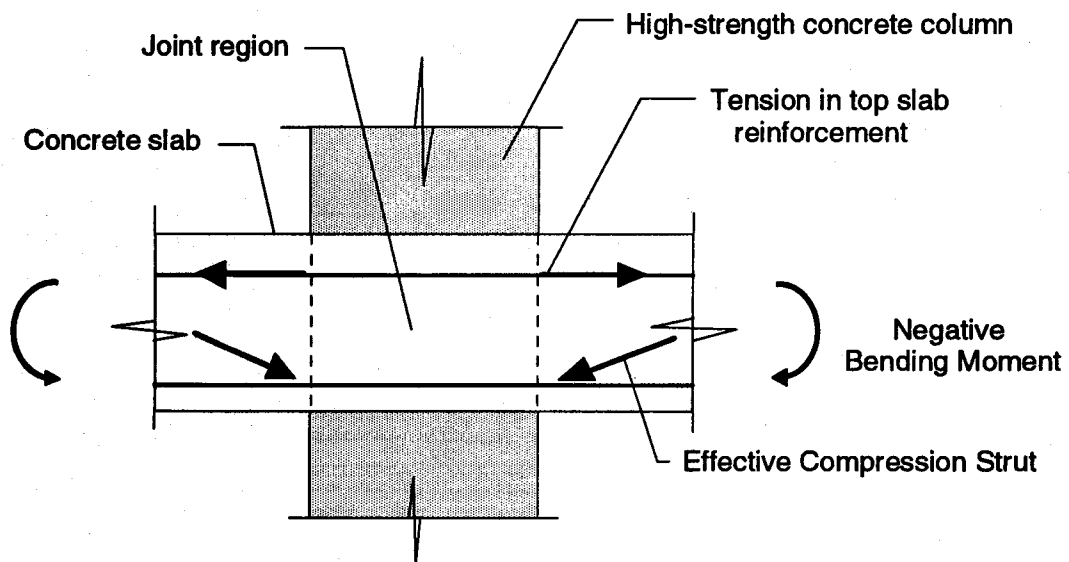**Figure 2.5 Stresses at Joint Region (Specimens with Unloaded Slabs)**

Figure 2.6 Stresses at Joint Region (Specimens with Loaded Slabs)

21
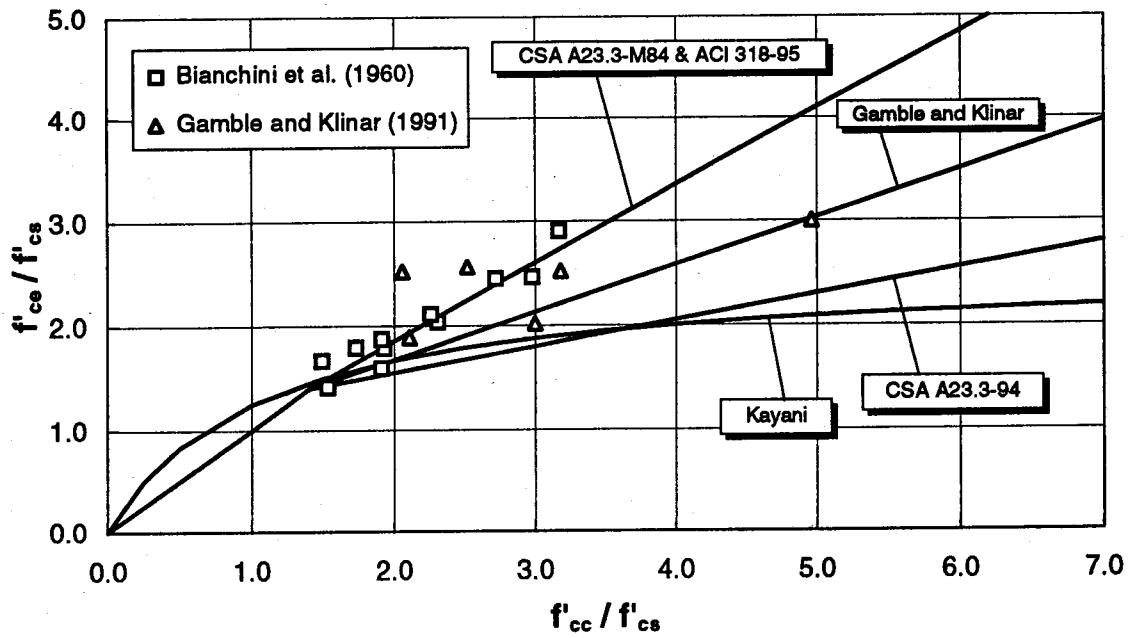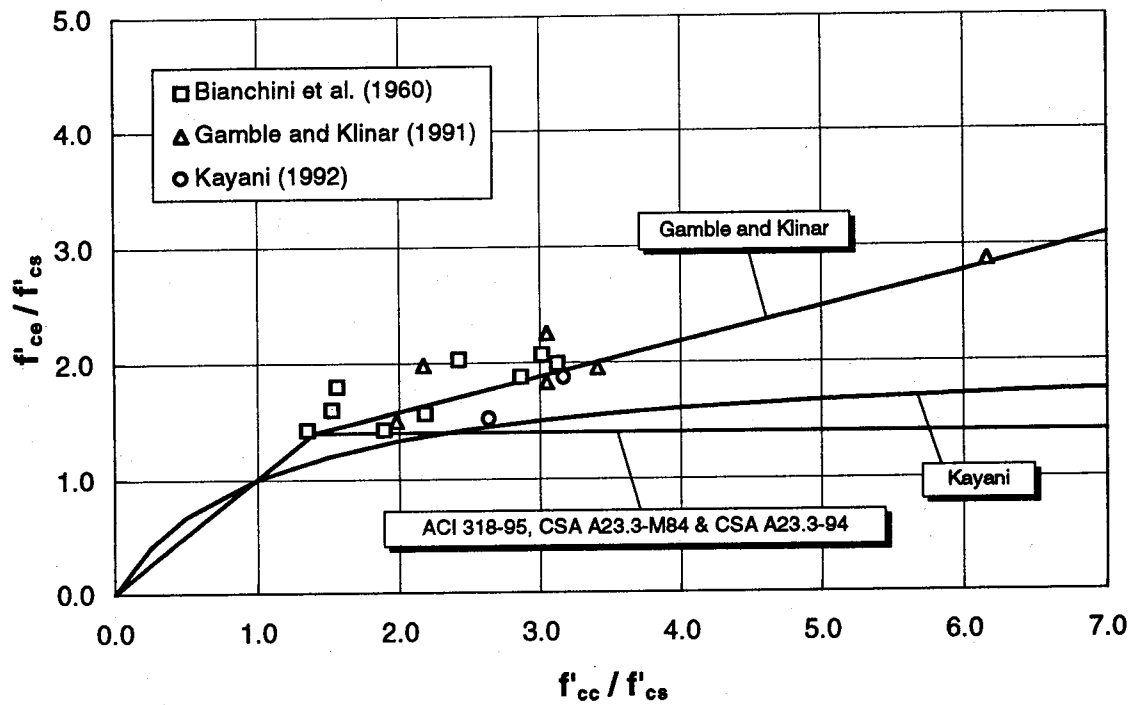
**Figure 2.7   Existing Design Provisions
for Interior Columns**

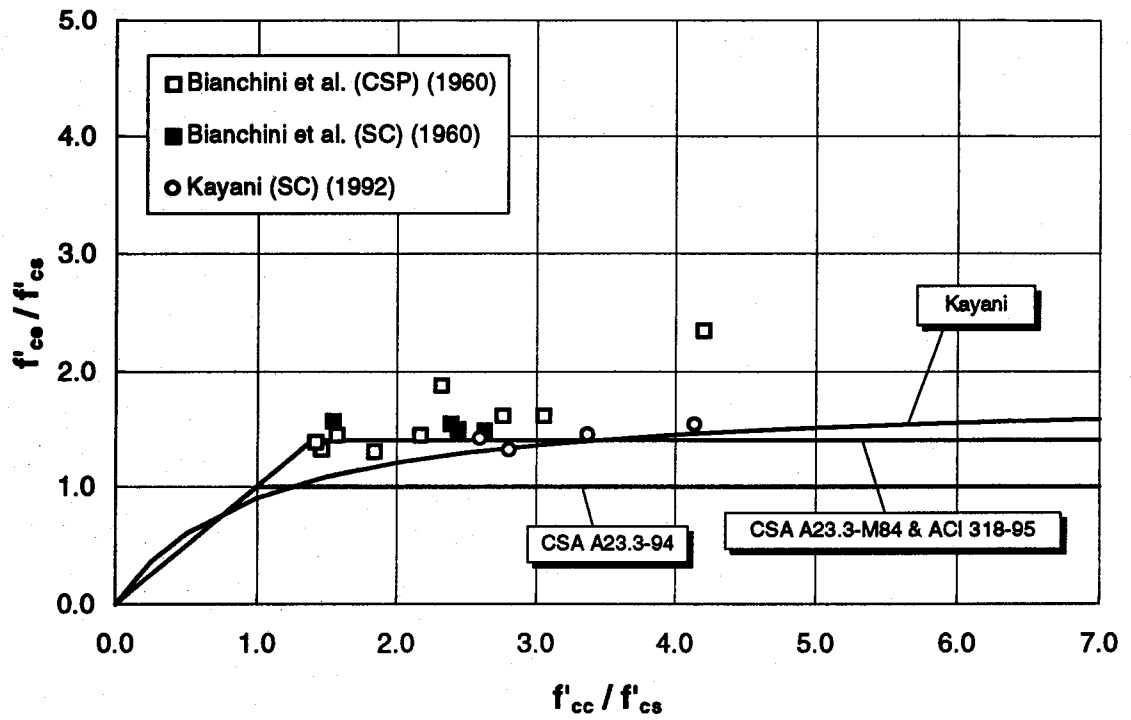**Figure 2.8   Existing Design Provisions for Edge Columns**

Figure 2.9   Existing Design Provision for Corner Columns

23

3. EXPERIMENTAL PROGRAM

3.1 Objectives of Testing

The primary objective of this project is to determine the appropriate concrete compressive strength to be used in the design of high-strength concrete columns intersected by floors made of lower strength concrete. Two variables that so far have been unaccounted for in the development of design guidelines are expected to have an effect on the strength of slab-column joints. These are the amount of slab loading and the ratio of the slab thickness to column width, h/c.

3.2 Experimental Program

A total of thirty specimens, in four separate series, were built to model reinforced concrete slab-column connections representative of flat plate and flat slab multistorey buildings. Of these, 20 were interior sandwich plates, six edge sandwich plates and four sandwich columns. Geometry of these specimens is described in Table 3.1 and in Figs. 3.1 to 3.3.

Dimensions of the slab segments were selected in such a way that the magnitude and location of the applied slab loading resulted in moments and shears at the column face matching those in a prototype connection. However, the geometry of the connection specimens was constrained by the capacity and the dimensions of the lab universal testing machine. Column dimensions were limited by the maximum capacity of the testing machine and the slab segment dimensions were also limited by the lateral clearance between the testing machine uprights.

3.3 Design of the Experiments

3.3.1 Series A Specimens (Interior Sandwich Plates)

The main purpose of this experimental series was to study the effect of slab loading on the joint compressive strength. Series A consisted of 12 interior sandwich plate specimens. Four sets of specimens were built and tested. Each set consisted of three specimens with equal f'_{cc}/f'_{cs} and h/c values. Three different slab load intensities were applied to each set. These correspond to high, medium and zero load levels. Loads which produced an initial average 2000 microstrain in the slab top reinforcement at the face of the column simulated high slab loads. Loads which produced a strain level of 1000 microstrain simulated medium slab load levels. The remaining specimen of each subset had no slab load applied on it. This was done not only to evaluate the effect of the amount of slab loading but also to establish some parallels with the tests results reported by Bianchini et al. and by Gamble and Klinar.

The level of slab load was set based on measured strain in the slab reinforcement. Readings were taken from strain gauges attached to the top slab reinforcing bars passing through the joint just 25 mm away from the column face. The slab load was increased until

the gauge readings averaged the target level of slab strain (1000 or 2000 $\mu\varepsilon$). This established the target level of slab load to be maintained throughout the test.

The test region extended approximately 300 mm above and below the slab. The height of the high-strength concrete column stubs was selected so that the axial compressive load could distribute uniformly throughout the test region. Height of the column ends was also determined accounting for the need of taking strain measurements along the columns. The overall height of series A interior sandwich plates varied according to the slab thickness.

Figure 3.1 illustrates the geometric dimensions of series A interior sandwich plates. Columns were square 200 mm wide. Slab thicknesses were either 100 or 150 mm. Specimens were reinforced according to reinforcement ratios likely to be provided in a prototype connection. Table 3.1 shows the concrete cylinder strengths of series A specimens. The cylinder compressive strength of the column was determined from the strength of the two column stubs, whichever was lower. Cylinder strengths correspond to those at the time of testing. High-strength concrete for the columns varied from 89 to 112 MPa. Slab cylinder compressive strengths ranged from 23 to 46 MPa. The ratio of column concrete strength to slab concrete strength, f'_{cc}/f'_{cs}, ranged from 2.43 to 4.61. The slab thickness-to-column width ratio, h/c, varied from 0.5 to 0.75. Table 3.3 shows the slab load intensities applied to the slab segments.

3.3.2 Series B Specimens (Interior Sandwich Plates)

The main purpose of this series was to study the effect of the aspect ratio, h/c, on the strength of interior slab-column connections subjected to specified slab loads. One of the specimens (B-3) had a high-strength concrete core embedded in the joint region. This was done to study the behaviour of slab-column joints when strong concrete rather than weak concrete was placed at the joint region. The test procedure for this series differed from that of series A in that target slab loads were based on a finite element analysis rather than a strain criteria.

Connection specimens were intended to simulate slab-column connections in a prototype structure. A plan view of the prototype flat plate is shown in Fig 3.4. Columns were spaced 4.45 m on centre. Column maximum side dimensions were set equal to 250 mm for the square column specimens, and 175 by 350 mm for the rectangular column specimens.

In this series, two different slab thickness were selected. Slabs 150 mm thick were intended to model a conventional flat plate structure whereas slabs 250 mm thick were selected to model connections in either flat slab or waffle-slab structures. This results in values of the slab thickness-to-column width ratio, h/c, of 0.6 and 1.0 for the specimens with square columns. The effect of column rectangularity is also studied in this specimen series as an special case of the h/c effect. The main objective of these tests was to determine what column dimension should be used in the evaluation of h/c.

Specified dead and live load intensities were defined according to code provisions. Dead load included the structure self weight as well as the weight of partitions and finishing work. The specific weight of reinforced concrete was assumed as 24 kN/m^3. Live load was set equal to 2.4 kPa whereas partitions and finishing work were assumed equal to 0.9 kPa.

3.3.2.1 Analysis of Prototype Connections and Test Specimens

Analyses were performed using a fully licensed educational version of the SAP90 program (Wilson and Habibullah (1992)). The purpose of these analyses was to ensure that the load and strain conditions in a joint test specimen were reasonably close to those in a prototype joint.

The finite element mesh modeling of an interior prototype slab-column connection is shown in Appendix A. The input data files are also shown in Appendix A. For convenience, the input data have been arranged in two columns. The level of applied slab load accounted for in the analyses along with the moment values at the face of the prototype column are reported in Table 3.2.

Based on the results from the analysis of the prototype connections, the analyses of the slab-column specimens were carried out. Appendix A also includes the input data files used for these analyses. Table 3.2 reports the amount of applied slab accounted for in the analyses of the test specimens together with the resulting moments at the face of the column.

Comparisons of the bending moment diagrams between the prototype connections and the specimen connections are shown in Figs. 3.5 and 3.6. These correspond to prototype and specimen connections with h/c ratios equal to 0.6 and 1.0, respectively. Good agreement is observed between moments at the face of the specimen columns and those at the face of the prototype columns.

Based on the analysis results, the expected level of strain at the slab top reinforcing bars crossing the column was calculated for each of the analyzed slab-column specimens. The strains were calculated at the face of the column. Evaluation of the strains was done to confirm the validity of the test results. Strain predictions proved to be more accurate for the specimens with thinner slabs (h/c value of 0.6). For the specimens with thicker slab segments (h/c value of 1.0), the predicted strains exceeded in up to 40 % those measured in the tests by means of the strain gauges.

Dimensions and cylinder compressive strengths of the series B sandwich plate specimens are reported in Table 3.1. Concrete cylinder strengths correspond to those at the time of testing. Cylinder compressive strengths for the slab concretes varied from 15 to 44 MPa. The ratio of column concrete strength to slab concrete strength, f'_{cc}/f'_{cs}, ranged from 2.48 to 6.33. Levels of slab load applied to the slab segments are reported in Table 3.3.

27

3.3.3 Series C Specimens (Edge Sandwich Plates)

This series consists of six test specimens simulating edge connections in flat-plate structures. The main variable was the level of slab load applied to each slab segment. Two sets of three edge specimens were built and tested. Each set had similar f'_{cc}/f'_{cs} and h/c values. Each specimen was subjected to a different slab load intensity. Slab loads sufficient to cause 0, 1000 or 2000 microstrain in the slab top reinforcement around the column were applied. The specimens with slab loads established a comparison with the test results reported by Bianchini et al., Gamble and Klinar, and Kayani.

Series C specimens were loaded following the same procedure used for series A. Unlike series A, the strain target averages included strain measurements away from the column face. The slab loads were applied and increased until the readings from eight top gauges located around the column periphery averaged 1000 or 2000 microstrain. This average included readings from three strain gauges located at the face of the column and from five gauges located outside the column region. Strain readings at the face of the column were considerably higher than those located outside the column outline.

In general, the applied slab loads were similar to those calculated from the tributary area of an edge slab-column connection, shown as the shaded region in the prototype slab illustrated in Fig. 3.7. The slab thickness was either 170 or 230 mm. For the edge specimens with 170 mm thick slabs, the prototype columns were assumed to be spaced four metres on centre. For the edge specimens with 230 mm thick slabs, the column spacing was increased up to 4.5 metres. Columns were square with 230 mm side dimensions. As a result, the h/c ratio was either 0.74 or 1.0.

For the edge plates the column concrete strength was either 107 or 108 MPa. For the slab segments the concrete compressive strength varied from 31 to 35 MPa. This led to column -to-slab concrete ratios, f'_{cc}/f'_{cs}, varying from 3.06 to 3.48.

Geometry of an edge sandwich plate specimen is illustrated in Fig. 3.2. Nomenclature and location of the point slab loads are also illustrated in this figure. Dimension of the edge sandwich plate specimens along with the corresponding concrete cylinder strengths are reported in Table 3.1. Table 3.3 shows the slab load intensities applied to the edge specimens.

3.3.4 Series D Specimens (Sandwich Columns)

Sandwich columns were tested to model unconfined slab-column joints in an attempt to reproduce test observations and conclusions reported by Bianchini et al., Kayani, and Shu and Hawkins. The main variable was the ratio of the slab concrete layer to the column side, h/c. Four specimens with similar f'_{cc}/f'_{cs} values were tested.

Columns were square with 250 mm side dimensions. Height-to-width ratios for each high-strength concrete column stub were selected to provide a test region of at least 375 mm

above and below the concrete joint. Thickness of the layer of floor concrete ranged from 75 to 250 mm. The joint thickness-to-column width ratios, h/c, varied from 0.3 to 1.0. The overall height of all the specimens was equal to 1.5 m.

Column concrete compressive strength varied from 105 to 107 MPa. Floor concrete strength was 17 MPa. Cylinder strengths correspond to those at the time of specimen testing. Values of f'_{cc}/f'_{cs} varied from 6.18 to 6.29. Geometric description and concrete strengths of the sandwich column specimens are provided in Table 3.1 and Fig. 3.3.

3.4 Materials

3.4.1 High-Strength Concrete

Bagged type 10 Portland cement was used in the high-strength concrete mixtures. Local coarse aggregates were used. They were washed and crushed gravel composed primarily of highquartzite sandstone, quartzite and hard sandstone with 14 mm maximum size chips. Locally available washed sand was utilized.

Use of silica fume has become almost mandatory if mixture strengths higher than 100 MPa are to be achieved. The product used for this purpose was condensed silica fume dissolved in a water slurry. The water content of this product was 51 % by weight. Specific gravity of this product was taken as 1.36. The specific gravity of the solid silica fume was assumed as 2.2. Percentage by weight of Portland cement substituted by Silica fume varied from 8 to 12 percent. Superplasticizer was used for the column concrete mixtures. The product used was a polynaphtalene sulfonate base mix. Dosage of superplasticizer ranged approximately from 1.0 to 2.0 % weight of solids by weight of cement and silica fume. Typical mix proportions for a high-strength concrete mixture are shown in Table 3.4.

In order to evaluate the concrete compressive strengths, a minimum of 4 control cylinders were cast from each batch of concrete. Cylinders were 100 mm in diameter and 200 mm in height. Cylinders were cured for 7 days and tested at the time each specimen was tested. Cylinders were ground and tested dry in a 2600 kN capacity rock testing machine. Load in the cylinder test was applied at a rate ranging from 0.3 to 0.35 MPa/sec. The overall column concrete compressive strength of a determined specimen was taken as the least compressive strength of the two column portions. A typical stress-strain curve for a high-strength concrete control cylinder under compression is shown in Fig. 3.15.

3.4.2 Normal-Strength Concrete

The same cement and aggregates used in casting the high-strength concrete columns were used to manufacture the slab concrete. No additives nor silica fume were added. Table 3.4 shows the mix proportions for a normal-strength concrete mixture.

A minimum of four cylinders were cast from each concrete batch. Cylinders were 100 mm in diameter and 200 mm high for series A and 150 mm in diameter and 300 mm high for

29

series B, C and D. Cylinders were cured for 7 days. After drying, cylinders were capped with a sulfur-based compound. Cylinders were tested at the time of testing the connection specimen. Slab compressive strengths were obtained as an average of the cylinder test results linked to every specimen slab. A typical stress-strain curve for a slab concrete cylinder tested in compression is presented in Fig. 3.16.

3.4.3 Reinforcement

Columns were reinforced longitudinally with grade G30.12 M400 No. 15 M deformed bars. Tie diameter used for series A and C specimens was 6 mm. In series B and D, No. 10 M ties were provided. The amount of column longitudinal reinforcement and the tie spacing varied from series to series.

All of the intervening slabs have top and bottom layers of reinforcement running in both directions. Deformed bars with 3/8" diameter were used in series A and C specimens. Grade G30.12 M400 No. 10 M bars were used in the slab segments of series B specimens. Spacing of slab top reinforcement varied throughout the experimental program. Following an anchorage failure in specimen A3-C, top reinforcing bars were anchored with 180° hooks at each end.

Integrity steel was only provided for series B specimens. These bars were placed at the bottom of the slab and crossed the joint between the column longitudinal reinforcement. Two No. 15 M deformed bars running in each direction were placed for this purpose. Tension tests were performed on three coupons taken from the same source. Typical stress-strain curves for No. 15 M and No. 10 M bars are shown in Figs. 3.17 and 3.18, respectively. Table 3.5 shows the properties of the steel reinforcing bars used in this investigation.

Figures 3.8 through 3.11 show the column reinforcement layouts for the sandwich plate and sandwich column specimens. Slab reinforcement layouts are shown in Figs. 3.12 through 3.14. Column and slab reinforcement ratios for all of the specimens are shown in Table 3.1.

3.5 Fabrication of Specimens

3.5.1 Mixing, Casting and Curing Procedures

3.5.1.1 Interior and Edge Sandwich Plates

Specimens were cast in three stages. Before casting the lower column, the column steel reinforcing cage was placed and aligned into wooden forms. Then, the high-strength concrete mixture for the lower column was mixed and placed in the forms. Control cylinders were filled and vibrated. The next step was to cast the slab concrete. To do this, the lower column forms were stripped and the slab forms installed so that the slab soffit coincided with the top level of the lower column stub. Slab forms were supported on the

30

floor by a metal frame system. Next, the slab reinforcement was placed and the slab concrete was mixed and cast. The slab concrete was placed so that a single batch of concrete was located at the slab-column joint to guarantee uniformity of the joint concrete strength. Slab concrete control cylinders were then cast and vibrated. Finally, the upper column forms were placed. Particular care was required to align the upper column with respect to the lower column. After the high-strength concrete was mixed the top column was cast. Control cylinders for the upper column were cast and vibrated. Following the form stripping, specimens were cured for a period of 7 days.

3.5.1.2 Sandwich Column Specimens

For the sandwich column specimens, the column steel reinforcing cage was placed and aligned into the lower column forms. Stirrups were tied up along the lower column region. The high-strength concrete was mixed and then placed in the forms. The next day, the slab concrete was mixed and cast. The following day, forms were stripped and stirrups were tied up along the top column stub. Upper column stub forms were then mounted. High-strength concrete was mixed and cast in the upper column forms. Finally, the column top forms were stripped and the specimens were cured for a week.

3.6 Testing

3.6.1 Test Set-up

3.6.1.1 Sandwich Plate Specimens

Set-ups for interior and edge sandwich plates are given in Figs. 3.19 and 3.20, respectively. The primary load, P_{col}, was applied to the column by the stroke control system of a 6600 kN universal testing machine. The load on the slab was applied to the slab segments by jacking against four 19 mm diameter steel load rods. The rods passed through the slab near the corners and were tied down to the lab strong floor. Locations at which the slab loads were applied are shown in Figs. 3.1 and 3.2.

For series A and B specimens (interior sandwich plates) subjected to slab loading, jacks were placed symmetrically with respect to the concentric column stub. All of the jacks were connected to a common manifold. Level of loading was controlled by a single hand pump. Jacking loads were approximately equal to each other throughout the test. The slab edges were unrestrained.

For series C specimens (edge sandwich plates), symmetric load conditions did not take place. Jacks were placed asymmetrically with respect to the column axis parallel to the slab free edge and symmetrically with respect to the column axis perpendicular to the slab free edge. Two hand pumps were used since two different slab load intensities were applied over the slab segments. For this reason, the slab loads in this series will be referred to as P_{s1} and P_{s2}, as illustrated in Fig. 3.2. Jacks located near the slab free edge closer to the column applied less load than those located farther from the column.

3.6.1.2 Sandwich Column Specimens

Since this type of specimen does not involve any slab concrete surrounding the sandwiched concrete layer, the primary load was a compressive-type load applied by the stroke control system of a 6600 kN universal testing machine. The test set up of a sandwich column specimen is shown in Fig. 3.21.

3.6.2 Instrumentation

3.6.2.1 Linear Variable-Differential Transformers (LVDTs)

These devices were used to measure the column axial longitudinal shortening inside and outside the joint region. The LVDTs were mounted on aluminum frames attached at three different locations along the column. LVDTs attached outside the slab region provided information on the shortening of both top and bottom high-strength concrete column stubs. Either single or coupled LVDTs were used for this purpose. LVDTs attached at the specimen mid-region provided information on column shortening at that location. This included the longitudinal shortening of the column through the floor and a small fraction of the high-strength column shortening.

Each of the three LVDT frames consisted of two extension aluminum arms. These were supported by 8 mm diameter threaded rods that traversed the column stubs. In all of the specimen series, each lower arm was fixed to the column. Fixed upper arms were used in series B, series C square column, and series D specimens. Pivoting arms were utilized in series A and series C rectangular column specimens. Use of fixed upper arms implies that the measurement of the column shortening is based on the average of two LVDTs. When using pivoting upper arms the calculation of the column shortening reduces to the readings from only one LVDT mounted at one end of the rack. Sketches describing each of the LVDT set-ups throughout the experimental program are shown in Figs. 3.22 to 3.26.

3.6.2.2 Strain Gauges

Electrical resistance foil-type strain gauges were used in all of the specimens. At each gauge location, steel bar ribs were ground smooth. Grinding was minimized so that the impact of the strain gauge on the bond characteristics of the reinforcement was reduced. Each gauge was glued to the bar with an epoxy adhesive and waterproofed.

To corroborate the LVDT readings at low levels of strain, gauges were attached to the column longitudinal reinforcement for series B (interior sandwich plates) and series D specimens (sandwich columns). Such gauges were attached at the middle of the joint and at levels about 235 mm above and below the slab concrete. Column gauge layouts corresponding to these specimen series are illustrated in Figs. 3.9 and 3.11.

32

Gauges were attached to the slab top reinforcement for all of the specimen series. Strain gauges attached at the bottom reinforcing bars were only installed in C series specimens. Slab gauges were placed in different patterns as shown in Figs. 3.12 through 3.14.

For series A specimens (interior sandwich plates) gauges were attached to the slab top reinforcing bars crossing through the joint 20 mm outside the column face. For series B specimens (interior sandwich plates), gauges were attached both at the face of the column and at the centre of the joint. Strain readings of the slab top steel reinforcing bars passing through the joint provides significant information about confinement conditions at the joint above the neutral axis of bending. For series C specimens (edge sandwich plates), a similar gauge layout as used in the A series was adopted. Some additional slab gauges were attached outside the column region as well as at the slab bottom reinforcement.

3.6.2.3 Load Cells

The column load was measured with the universal testing machine load cell. Each of the slab jacking loads was measured with a 89 kN (20 kips) load cell placed in between a system of steel plates.

3.6.3 Calculation of the Column Strain through the Slab Thickness

The average column strain through the slab thickness, ε_{tt}, was calculated using the readings from LVDTs mounted at three different locations along the column. In series B and D, this average strain was also estimated using the readings from strain gauges attached to the column reinforcement. Prior to yielding, the gauge readings were in reasonable agreement with strains calculated from LVDT measurements. Beyond this level, the strain gauges were not reliable due to strain localization and damage.

The middle LVDT measurement includes the column deformation through the slab thickness plus deformations of short segments of high-strength column above and below the joint, as shown in Figs. 3.27 and 3.28. To estimate the column strain through the slab thickness it is necessary to deduct those deformations attributed to the short segments above and below the slab. The shortening of the high-strength column segments is based on the average strains from top and bottom LVDT readings.

This procedure leads to the following equations to calculate the column longitudinal strain through the slab thickness, ε_{tt}.

$$\varepsilon_{col} = \frac{\varepsilon_{top\,col} + \varepsilon_{bot\,col}}{2} \qquad [3.1]$$

$$\varepsilon_{tt} = \frac{\varepsilon_{mid}(2m + h) - \varepsilon_{col}(2m)}{h} \qquad [3.2]$$

33

where

$\varepsilon_{top\,col}$: Column longitudinal strain measured along top column stub

$\varepsilon_{bot\,col}$: Column longitudinal strain measured along bottom column stub

ε_{col} : Average column longitudinal strain measured outside joint region

ε_{mid} : Column longitudinal strain measured at specimen mid-height (includes strain along high-strength column stubs and column strain through slab thickness)

ε_{tt} : Column longitudinal strain through slab thickness

h : Slab thickness

m : Distance between slab top and bottom levels and location of threaded rods supporting middle LVDT frame

3.6.4 Test Procedure

3.6.4.1 Interior and Edge Sandwich Plate Specimens

Specimens were installed in the 6600 kN capacity universal testing machine. Column stubs were aligned with respect to the machine axes. The column top surface was ground in order to prevent the tips of the column reinforcing bars from sticking out. To prevent crushing of concrete at both top and bottom column ends, both ends were capped with steel confining shoes. A layer of plaster was placed between each column end and its protective metal box to ensure a smooth bearing surface. All electrical connections were made and checked.

For the specimens with unloaded slabs, the ramp function controlling the primary load, P_{col}, was started and the specimen was loaded to failure.

For the specimens with slab loads, the loading procedure was intended to mimic the loading sequence of a prototype structure and to allow some comparisons with the tests reported in the past, wherein columns where brought to failure.

First, a small column preload was applied. This ranged from 200 to 400 kN for the A and B series specimens. This column seating load was increased to 500 kN for the edge plates with 170 mm thick slabs and to 700 kN for the edge sandwich plates with slabs 230 mm thick. This was done to prevent these specimens from overturning once the slab loads were applied. Then, the full load was applied to the slab by means of the four jacks traversing the overhanging slab segment. Jacking loads were controlled with one manual pump (interior specimens) or two manual pumps (edge specimens). The jacks were continually adjusted to maintain a relatively constant slab load throughout the test. Without this adjustment, the slab load decreased. Test duration ranged from 2 to 3.5 hours. Cracking patterns and structural behaviour of the specimens were recorded throughout the tests.

hours. Cracking patterns and structural behaviour of the specimens were recorded throughout the tests.

3.6.4.2 Sandwich Column Specimens

Sandwich column specimens were seated and aligned in the testing machine. Column ends were also capped using re-usable metal shoes to prevent the column ends from crushing. A layer of plaster was placed between the column ends and the steel shoes. Electrical connections were made and the specimen was carefully checked. Then, a compressive-type column pre-loading was applied over the specimen. This seating load varied between 100 and 200 kN. Then, the stroke control system of the universal testing machine was started and the specimen brought to failure. Duration of the tests varied from 1 to 1.5 hours. Cracking patterns and observations were recorded.

Specimen	Dimensions (mm)					Concrete Strength (MPa)		Approx. Reinf. Ratios (%)	
Mark	a	b	c	e	h	f'_{cc}	f'_{cs}	ρ_{col}	ρ_{slab}
A1-A,B,C	1380	1380	200	500	100	105 (27)	40 (28)	4.00	0.55
A2-A,B,C	1380	1380	200	500	100	112 (29)	46 (28)	4.00	0.41
A3-A,B,C	1380	1380	200	500	150	89 (27)	25 (28)	4.00	0.33
A4-A,B,C	1380	1380	200	500	150	106 (29)	23 (28)	4.00	0.33
B-1	1350	1350	250	625	250	104 (51)	42 (49)	1.28	0.26
B-2	1350	1350	250	675	150	104 (56)	42 (54)	1.28	0.47
B-3	1350	1350	250	625	250	113 (44)	44 (42)	1.28	0.26
B-4	1350	1350	250	675	150	113 (45)	44 (43)	1.28	0.47
B-5	1350	1350	250	625	250	95 (17)	15 (20)	1.28	0.26
B-6	1350	1350	250	675	150	95 (18)	15 (21)	1.28	0.47
B-7	1350	1350	175x350	625	250	120 (21)	19 (23)	1.28	0.26
B-8	1350	1350	175x350	675	150	120 (22)	19 (24)	1.28	0.47
C1-A	680	1220	230	465	170	107 (34)	32 (33)	3.02	0.27~0.32
C1-B	680	1220	230	465	170	107 (34)	35 (33)	3.02	0.27~0.32
C1-C	680	1220	230	465	170	107 (34)	34 (33)	3.02	0.27~0.32
C2-A	680	1220	230	435	230	108 (29)	31 (28)	3.02	0.20~0.22
C2-B	680	1220	230	435	230	108 (29)	34 (28)	3.02	0.20~0.22
C2-C	680	1220	230	435	230	108 (29)	33 (28)	3.02	0.20~0.22
D-SC1	-	-	250	712.5	75	105 (24)	17 (27)	1.28	-
D-SC2	-	-	250	687.5	125	105 (24)	17 (27)	1.28	-
D-SC3	-	-	250	675	150	107 (22)	17 (25)	1.28	-
D-SC4	-	-	250	625	250	105 (23)	17 (26)	1.28	-

Notes: 1. Concrete strengths correspond to those at the time of testing. Numbers in parentheses indicate column and slab concrete age in days at time of testing.

2. Column strengths are those from upper or lower column end, whichever is lower.

Table 3.1 Description of Test Specimens

Case	h	c	Dimensions	Load	M col face (kN.m)
Specimen	150	250	1.35m x 1.35m slab segment	4 point loads, 32.5 kN each	26.46
Prototype flat plate	150	250	4.45m x 4.45m flat plate	D.L.=3.6 kPa L.L.=3.3 kPa	26.22
Specimen	250	250	1.35m x 1.35m slab segment	4 point loads, 43.3 kN each	35.52
Prototype flat plate	250	250	4.45m x 4.45m flat plate	D.L.=6.0 kPa L.L.=3.3 kPa	35.34

Notes: D.L.: Dead Load
          L.L. : Live Load

Table 3.2 Dimensions and Analysis Results of Specimen and Prototype Slabs

Series	Mark	Slab Point Loads (kN)		Total Slab Load (kN)
		P_{s1}	P_{s2}	
A	A1-A	0	-	0
	A1-B	12	-	48
	A1-C	23.5	-	94
	A2-A	0	-	0
	A2-B	8.3	-	33.2
	A2-C	21.5	-	86
	A3-A	0	-	0
	A3-B	25	-	100
	A3-C	39.3	-	157.2
	A4-A	0	-	0
	A4-B	23.3	-	93.2
	A4-C	33.8	-	135.2
B	B-1	43.3	-	173.2
	B-2	32.5	-	130
	B-3	43.3	-	173.2
	B-4	0	-	0
	B-5	43.3	-	173.2
	B-6	32.5	-	130
	B-7	43.3	-	173.2
	B-8	32.5	-	130
C	C1-A	0	0	0
	C1-B	25.3	5.1	60.8
	C1-C	36.4	7.1	87
	C2-A	0	0	0
	C2-B	35.5	3.6	78.2
	C2-C	52.4	5.7	116.2

Notes: 1. Location of slab loads is illustrated in Figs. 3.1 and 3.2
      2. For interior plates: Total slab load = $4P_{s1}$
      3. For edge plates: Total slab load = $2P_{s1} + 2P_{s2}$

Table 3.3 Slab Loads

Constituents	Mix Proportions	
	Column Concrete Mix (120 MPa)	Slab Concrete Mix (15 MPa)
Cement (kg/m^3)	470	235
Water (kg/m^3)	110	188
Coarse aggregate (kg/m^3)	1040	1000
Sand (kg/m^3)	650	878
Silica fume (solid) (kg/m3)	48	-
SPN * (l/m^3)	16	-
W/(C+SF)	0.23	0.80

Mixes were designed based on 2 % air content.

* SPN had 70 % by weight water. This amount was subtracted from the total amount of mixing water required.

Table 3.4   Concrete Mix Proportions

Bar Designation	Modulus of Elasticity (MPa)	Static Yield Strength (MPa)	Static Ultimate Strength (MPa)
No. 15M	190320	400	632
No. 10M	208530	424	638

Table 3.5   Properties of Reinforcement Steel

140 mm (Series A)
100 mm (Series B)

140 mm (Series A)
100 mm (Series B)

Ps1

c

c

b

Ps1

100mm x 100 mm
blockout (typ.)

a
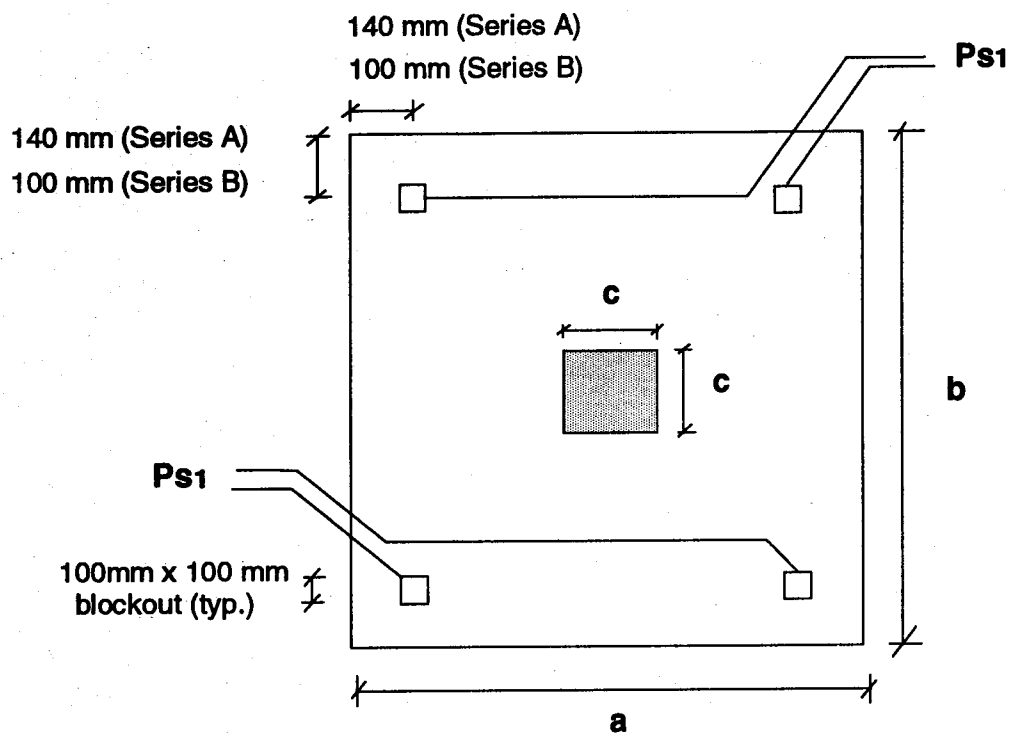
Note: Specimens B-7 and B-8 had a 175 by 350 mm rectangular column

c

e

h

a
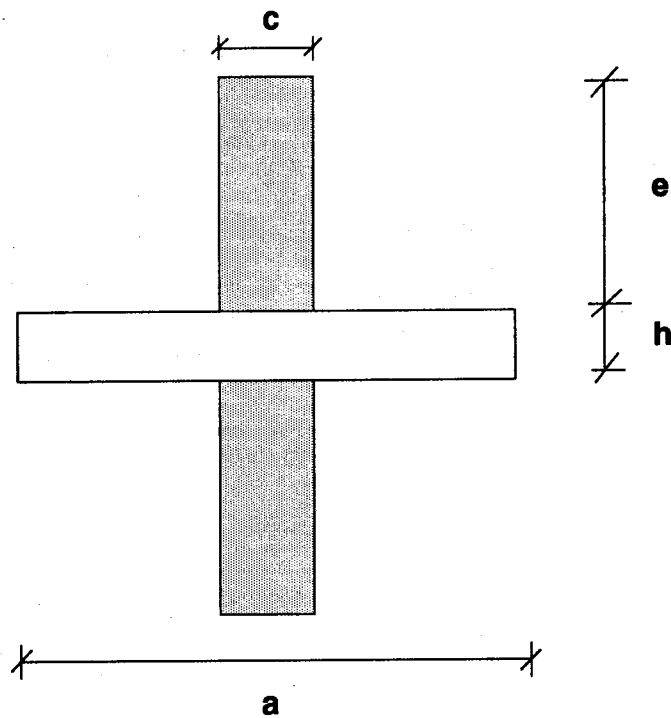
Figure 3.1 Geometry of Interior Sandwich Plate Specimens
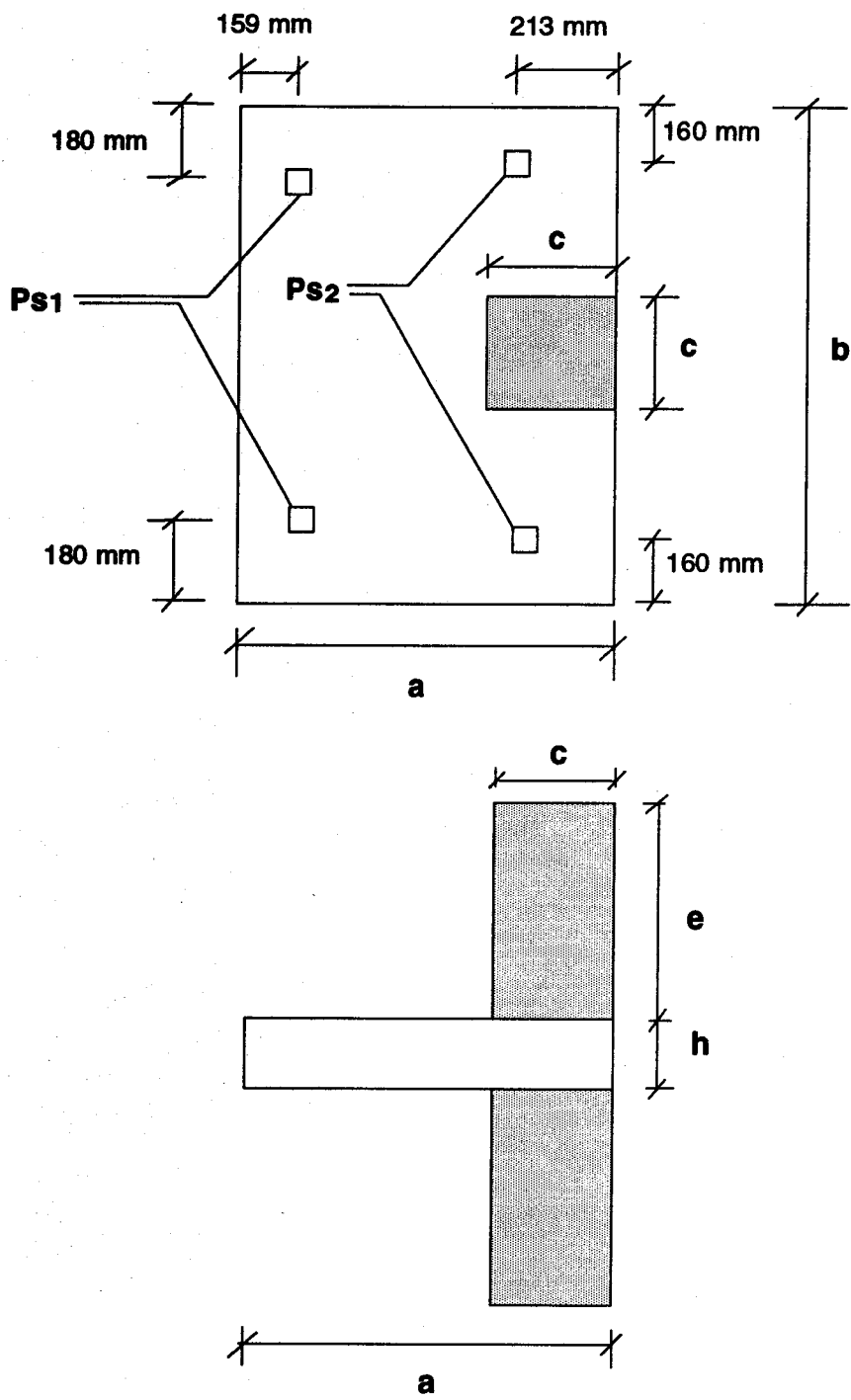
Figure 3.2 Geometry of Edge Sandwich Plate Specimens

41
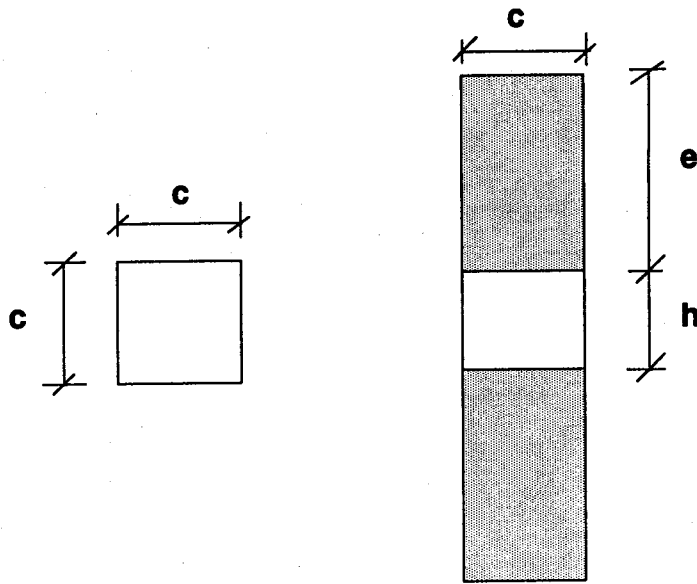
Figure 3.3   Geometry of Sandwich Column Specimens
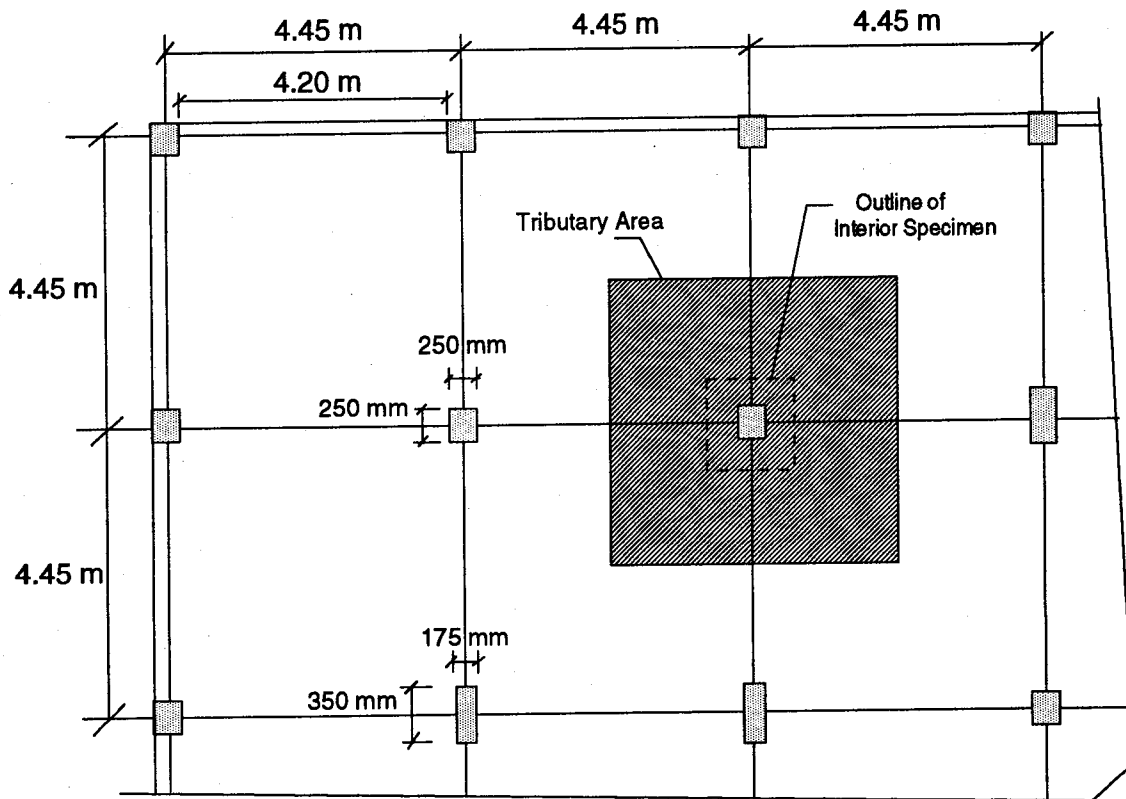
Note: Columns not drawn to scale

Figure 3.4   Prototype Flat Plate Structure (Series B Specimens)

42
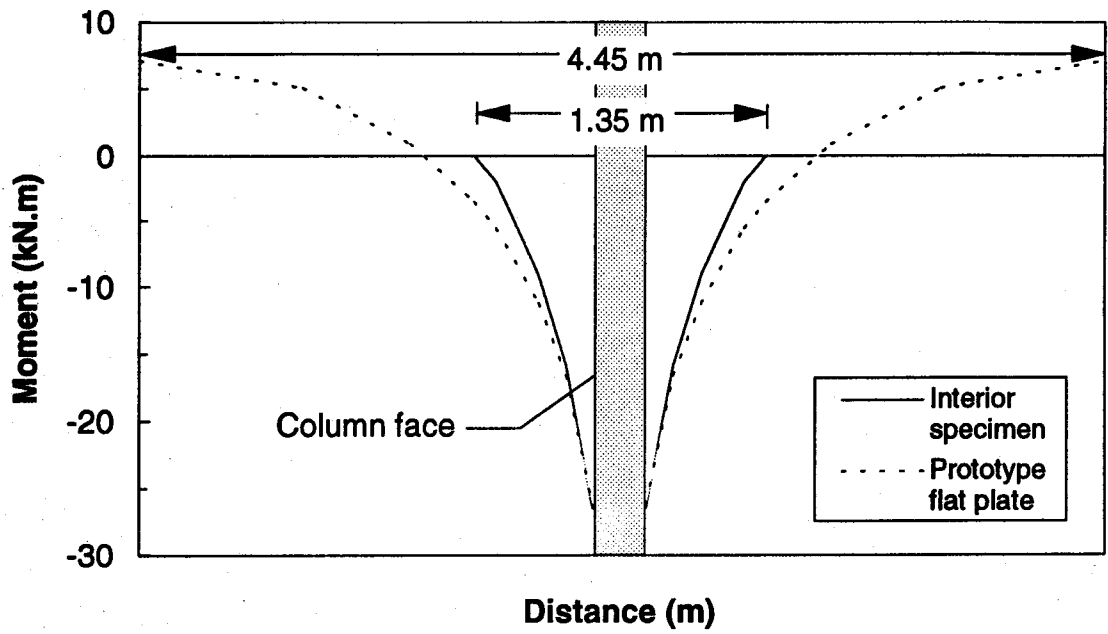
Figure 3.5   Bending Moments from SAP 90 Analyses
(h/c=0.6)
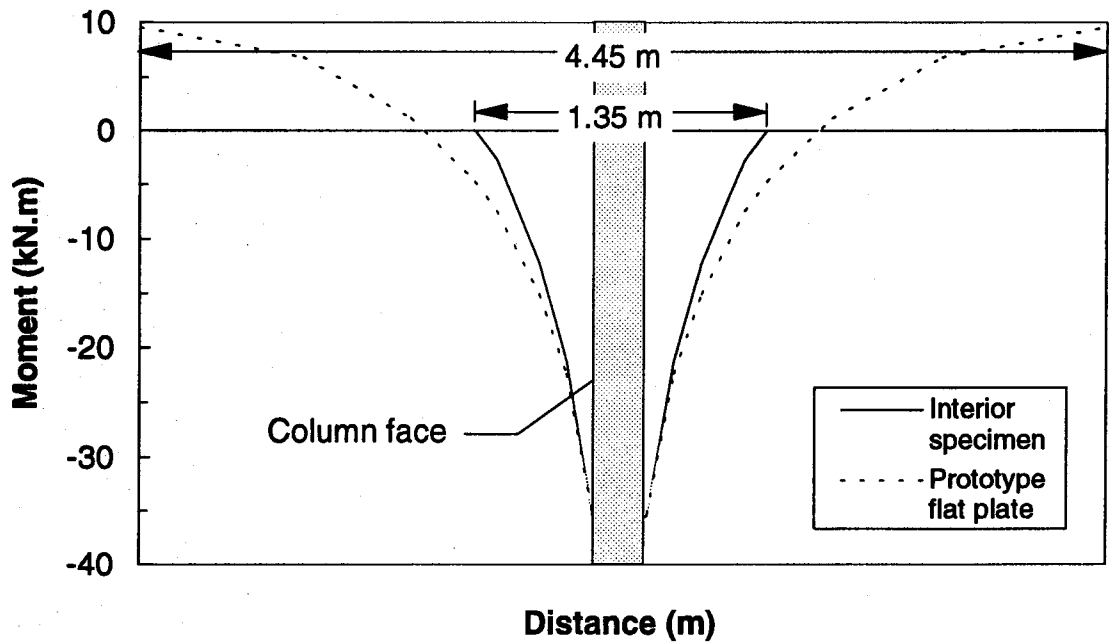
Figure 3.6   Bending Moments from SAP 90 Analyses
(h/c=1.0)
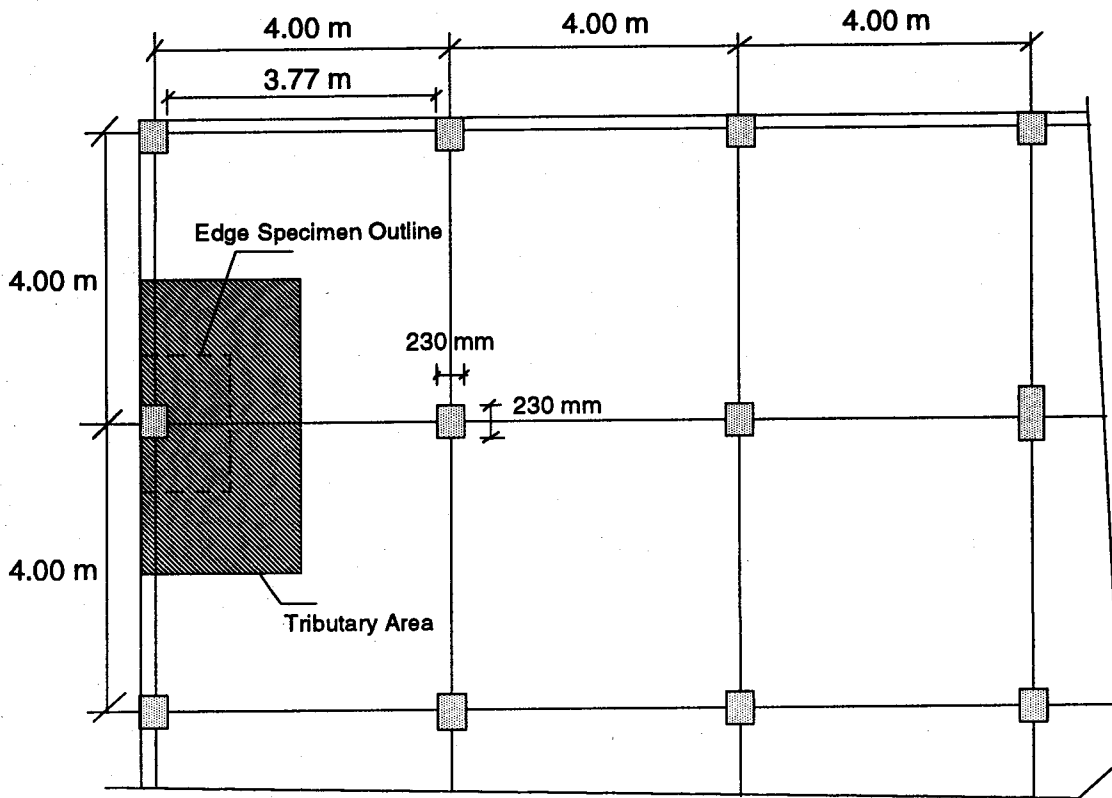
Note: Columns not drawn to scale

Figure 3.7 Prototype Flat Plate Structure (Series C Specimens)
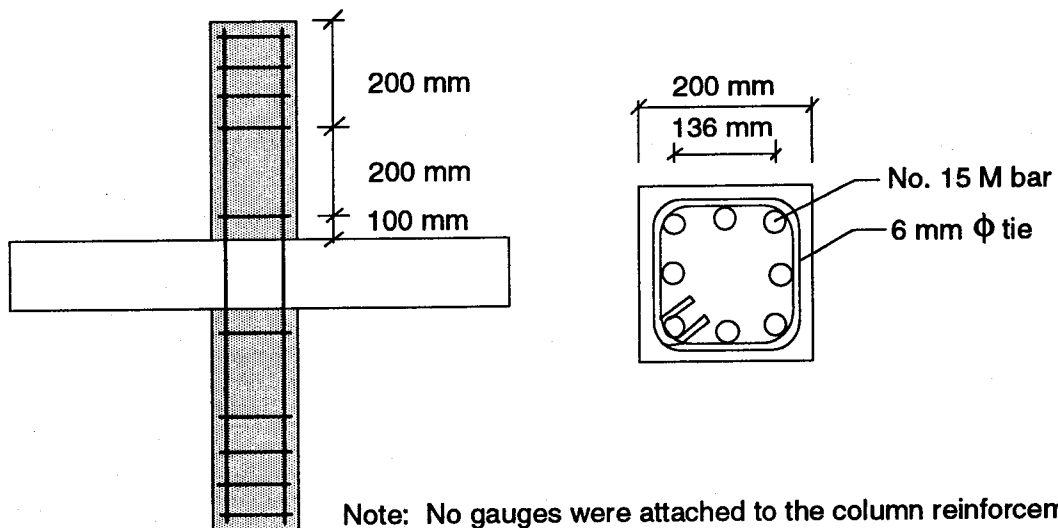
Note: No gauges were attached to the column reinforcement

Figure 3.8 Column Reinforcement Layout (Series A Specimens)

44
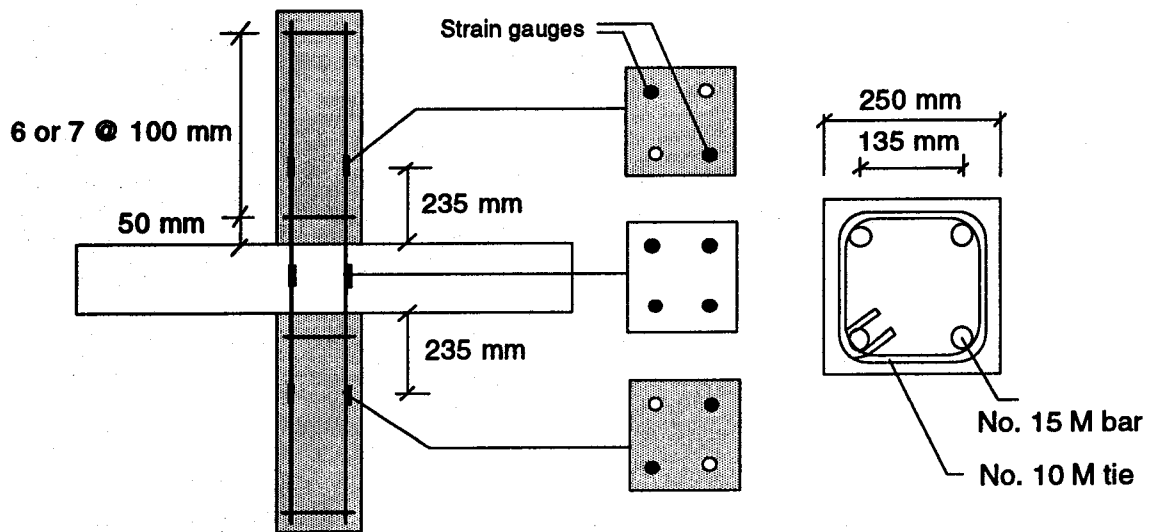
Figure 3.9 Column Reinforcement and Strain Gauge Layout (Series B Specimens)

Note: No gauges were attached to the column reinforcement
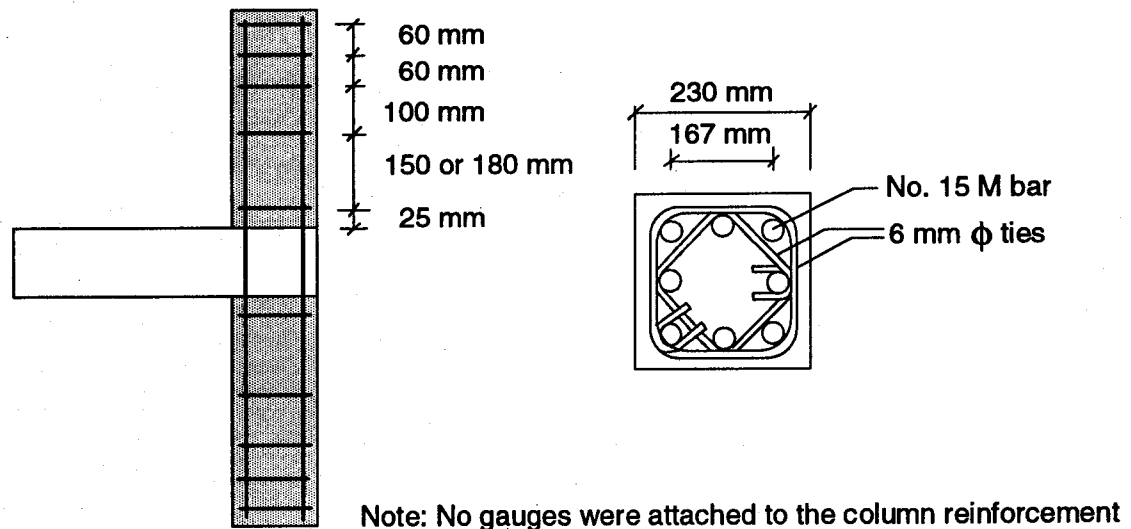
Figure 3.10 Column Reinforcement Layout (Series C Specimens)

45
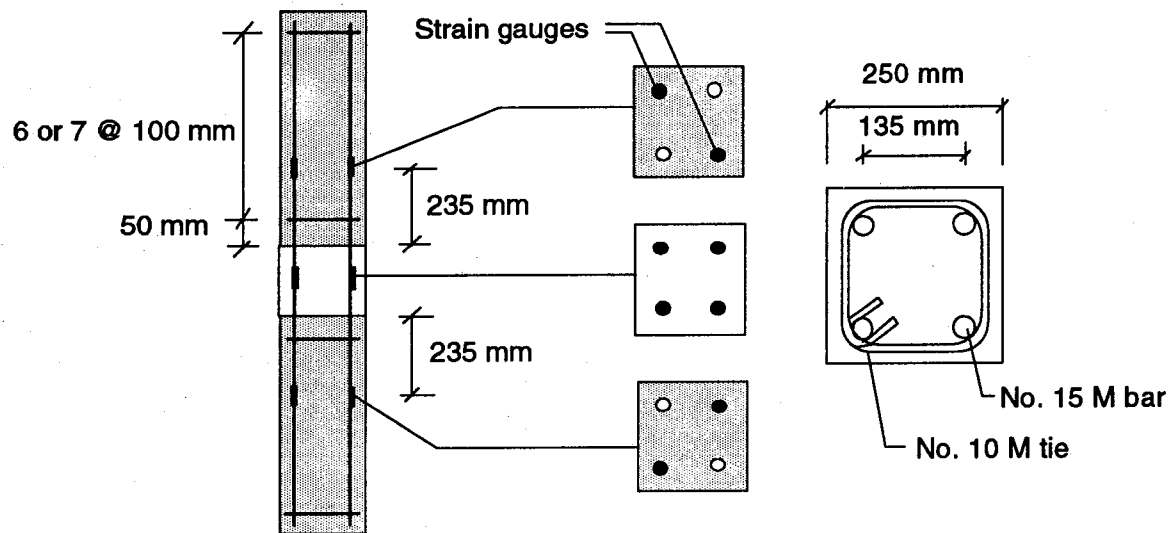
**Figure 3.11 Column Reinforcement and Strain Gauge Layout
(Series D Specimens)**

1 @ 600 (A2)
2 @ 300 (A1, A3, A4)

Strain gauges

Top Mat

1 @ 600

1 @ 600
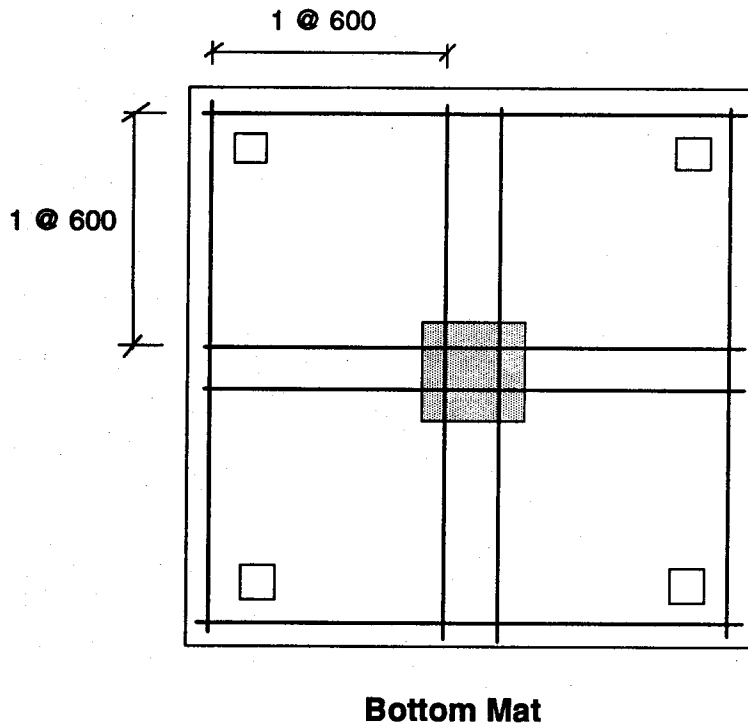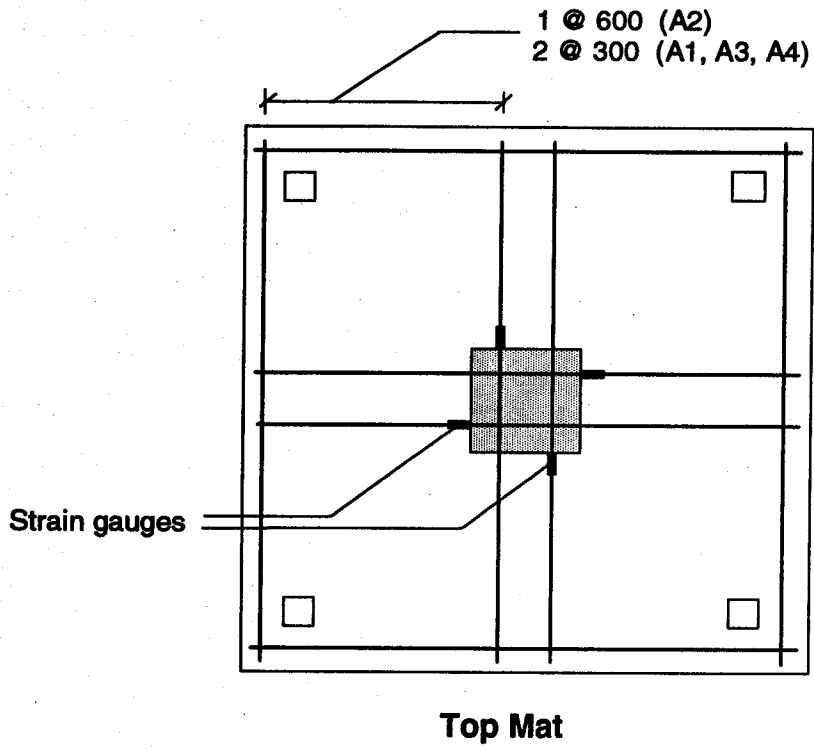
Bottom Mat

**Figure 3.12   Slab Reinforcement and Strain Gauge Layouts
(Series A Specimens)**

3 @ 150 (150 mm Slabs)
2 @ 200 (250 mm Slabs)

3 @ 150 (150 mm Slabs)
2 @ 200 (250 mm Slabs)

1 @ 150 (150 mm Slabs)
1 @ 200 (250 mm Slabs)

Strain Gauges

Top Mat

1 @ 300 (150 mm Slabs)
2 @ 200 (250 mm Slabs)

1 @ 300 (150 mm Slabs)
2 @ 200 (250 mm Slabs)

1 @ 300 (150 mm Slabs)
1 @ 200 (250 mm Slabs)

2 No. 15 M
(Integrity Steel Bars)
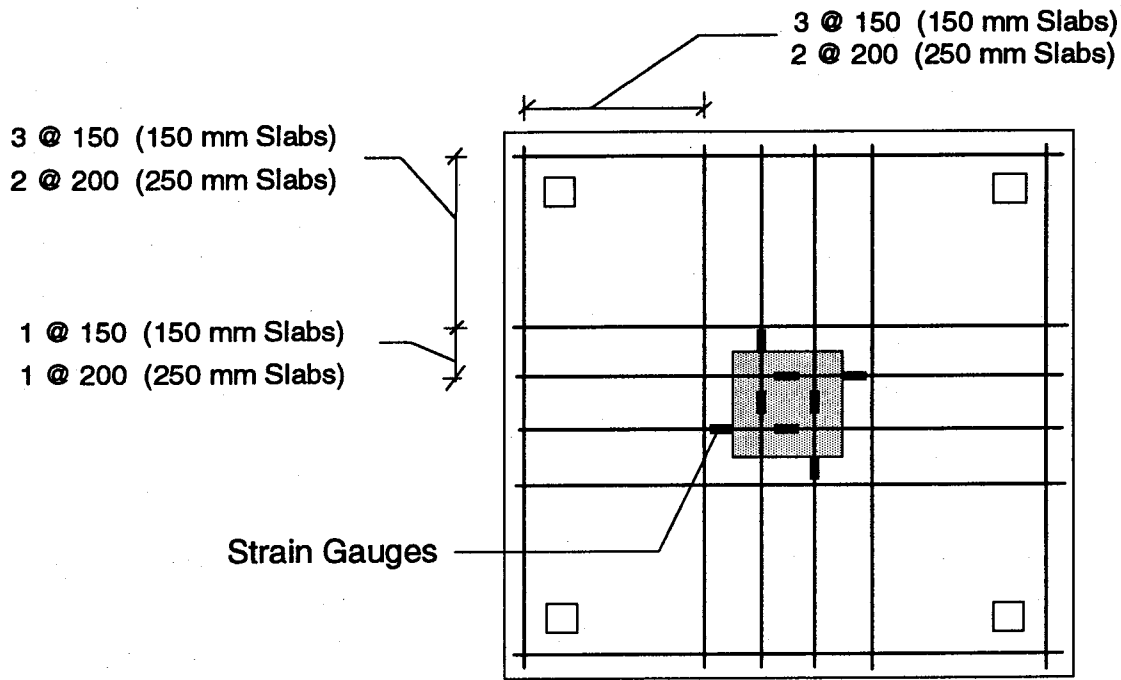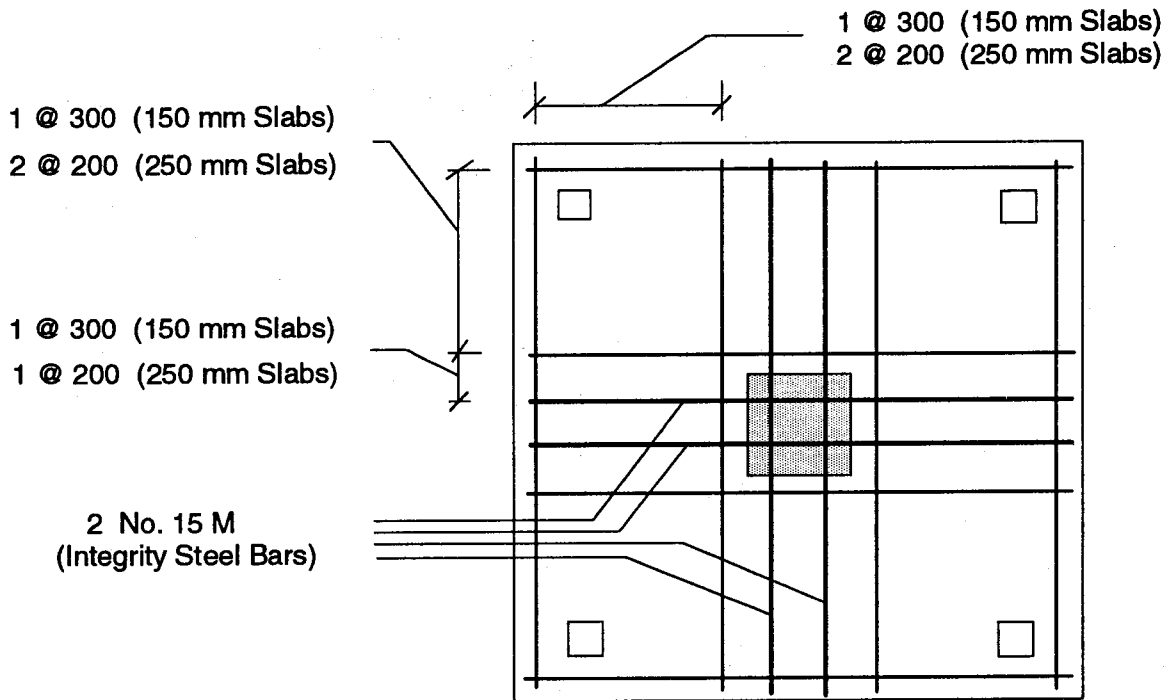
Bottom Mat

**Figure 3.13 Slab Reinforcement and Strain Gauge Layouts
(Series B Specimens)**
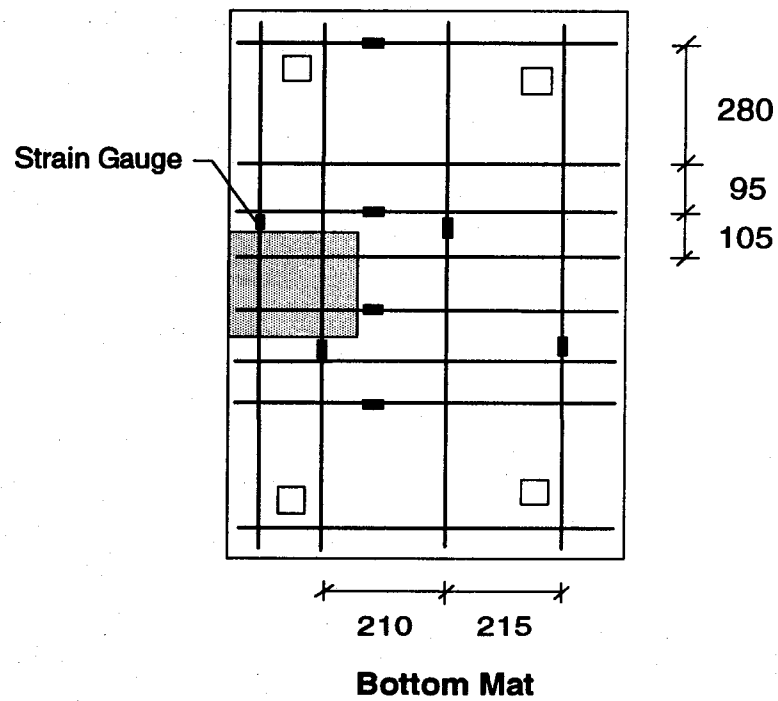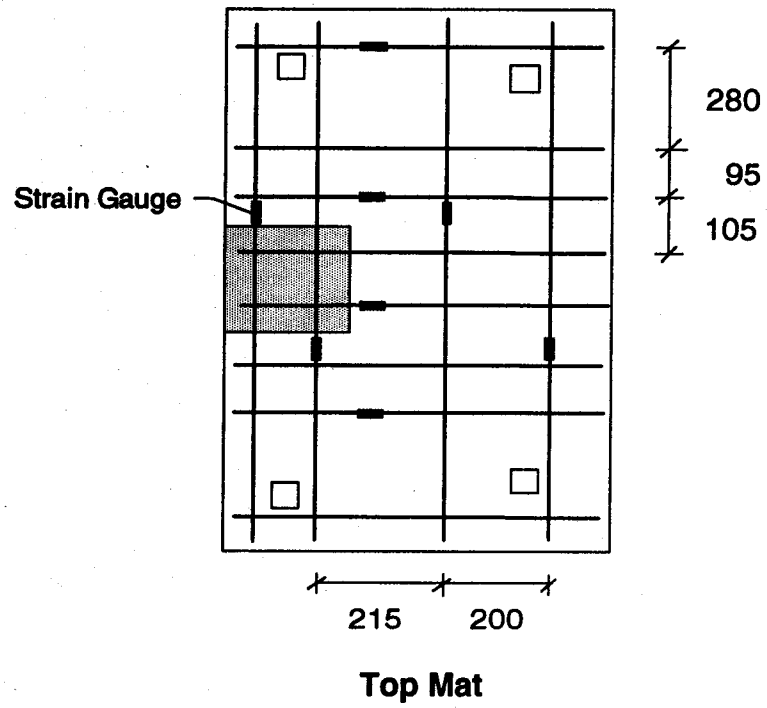
**Figure 3.14   Slab Reinforcement and Strain Gauge Layouts
(Series C Specimens)**
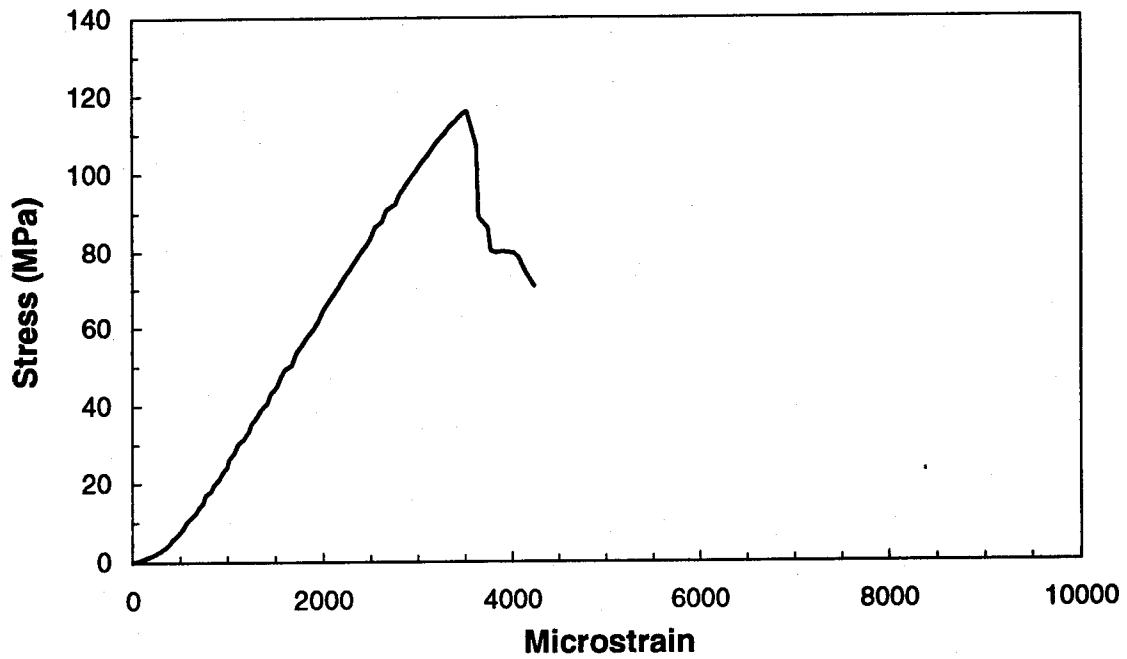
**Figure 3.15 Stress-Strain Curve for High Strength
Concrete Cylinder**
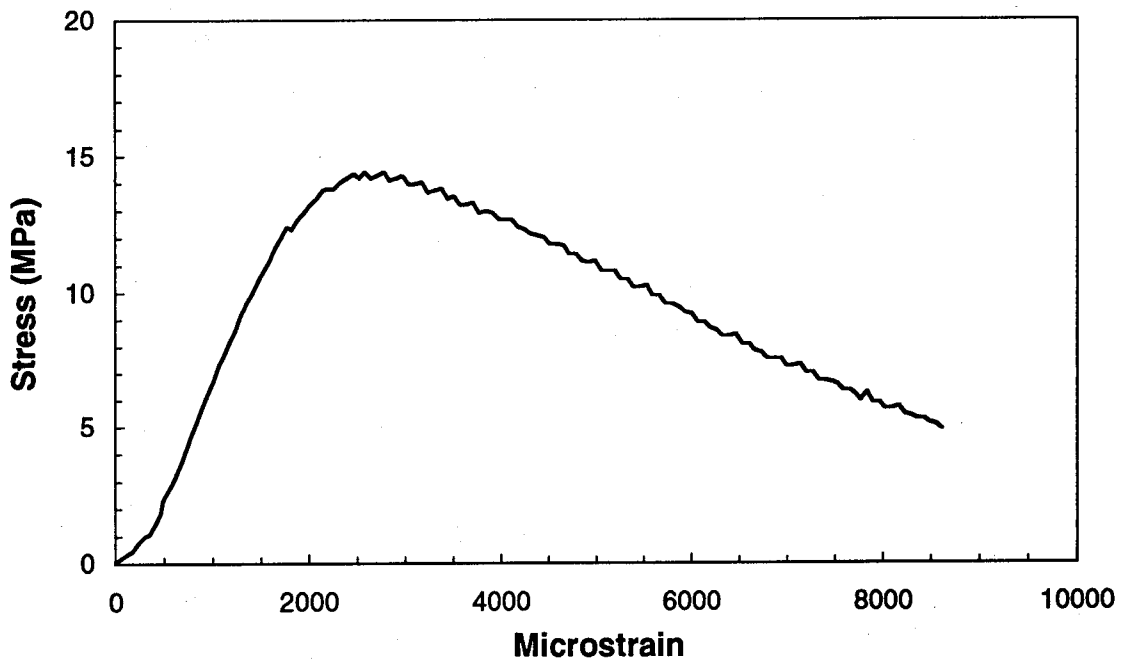
**Figure 3.16 Stress-Strain Curve for Normal Strength
Concrete Cylinder**
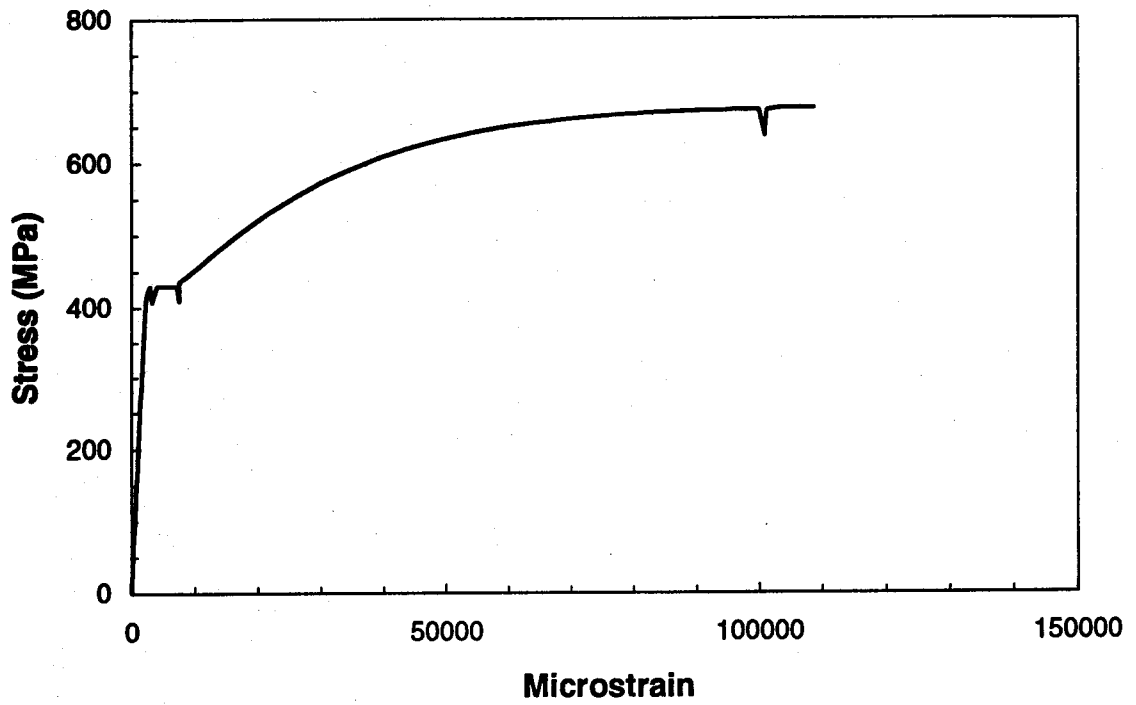
Figure 3.17 Stress-Strain Curve for No. 15 M Bar
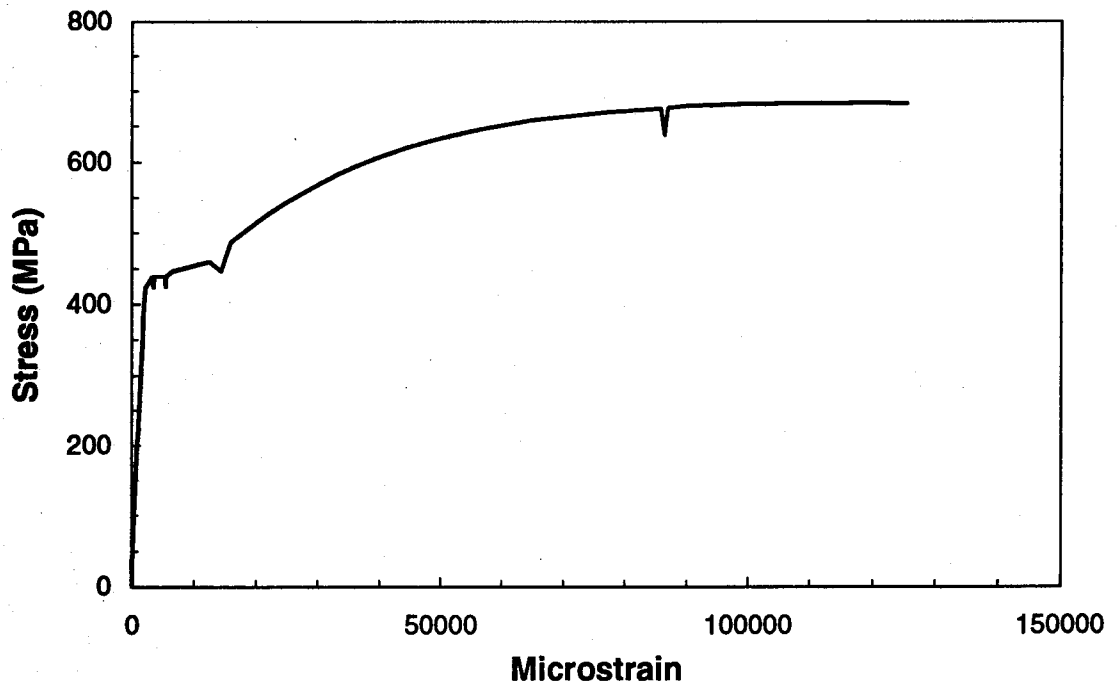
Figure 3.18 Stress-Strain Curve for No. 10 M Bar

51
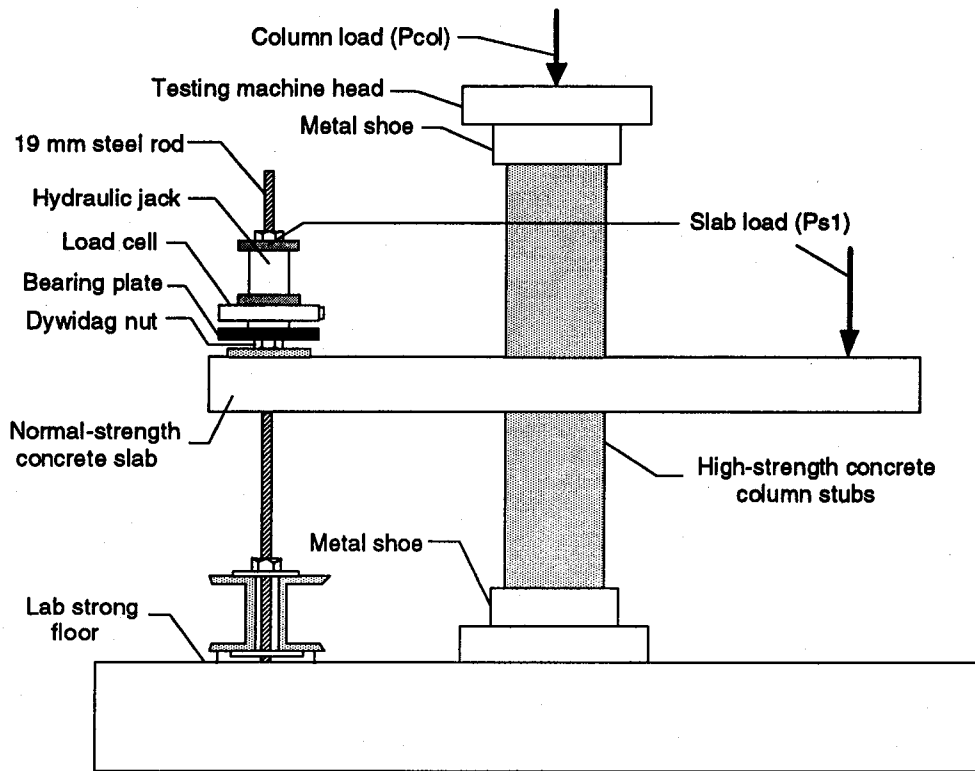
Figure 3.19   Test Set-up for Interior Sandwich Plate Specimens
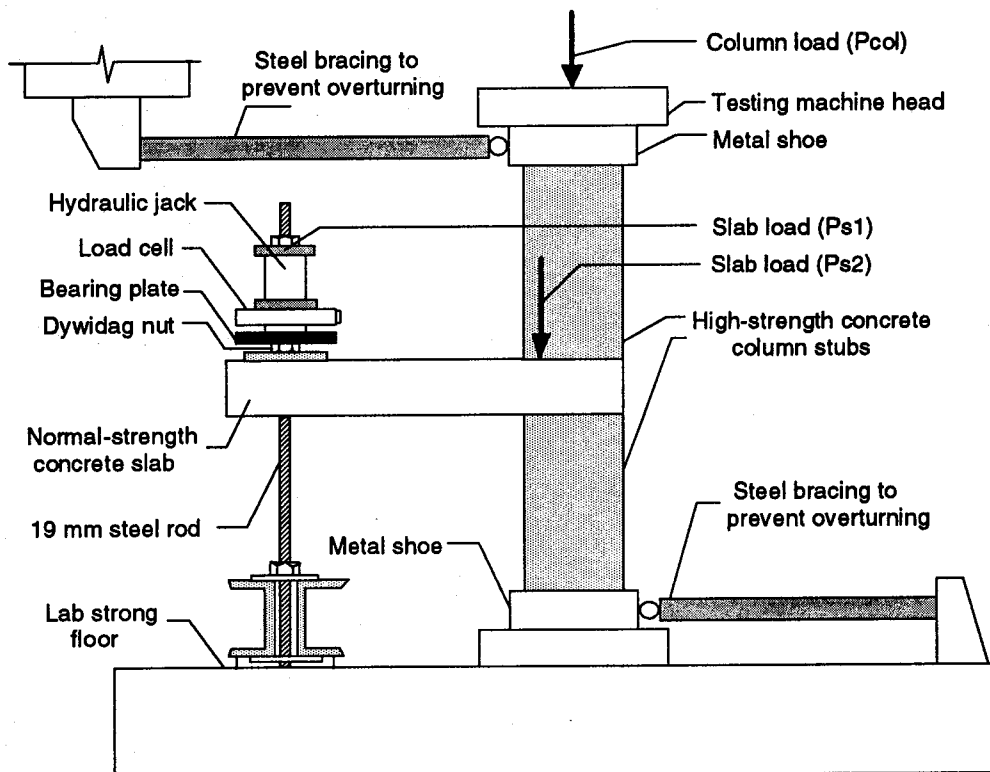
Figure 3.20   Test Set-up for Edge Sandwich Plate Specimens
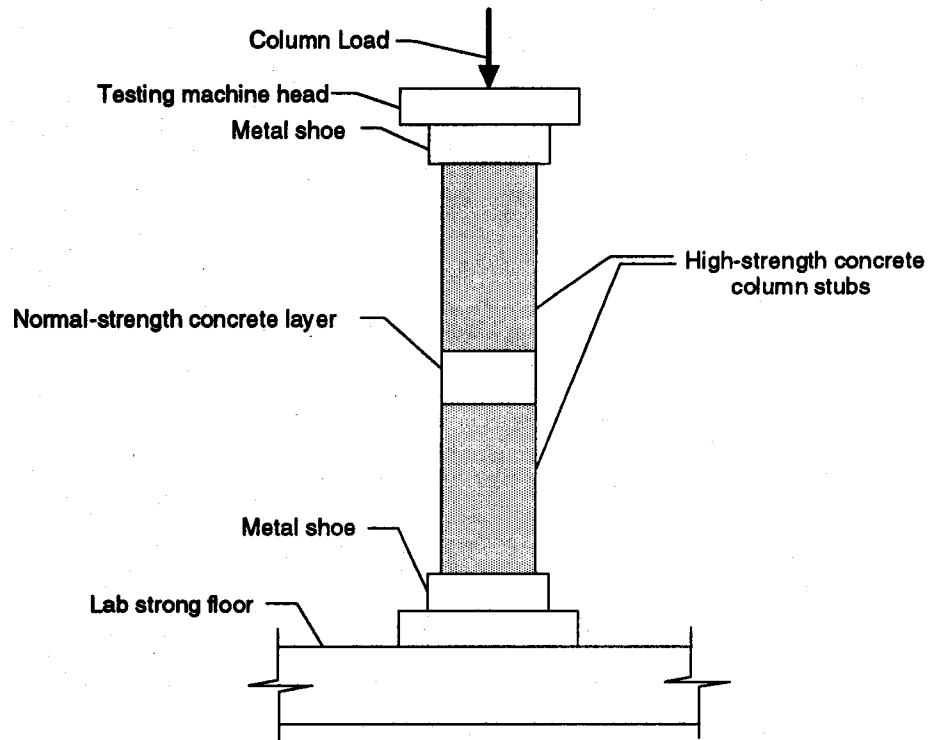
Figure 3.21 Test Set-up for Sandwich Column Specimens

53
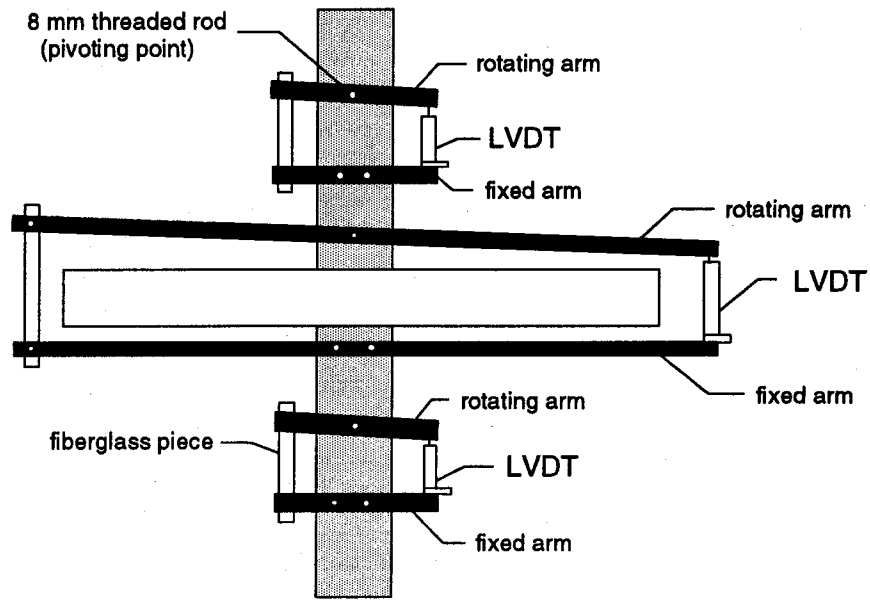
Figure 3.22   LVDT Set-up for Series A Specimens
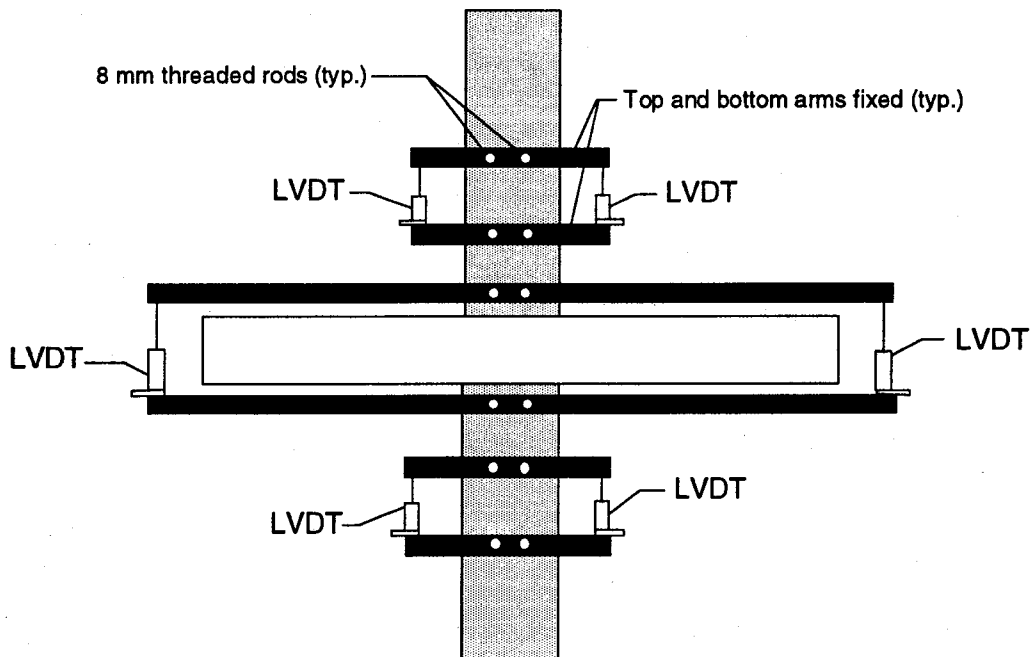
Figure 3.23   LVDT Set-up for Series B Square Column Specimens
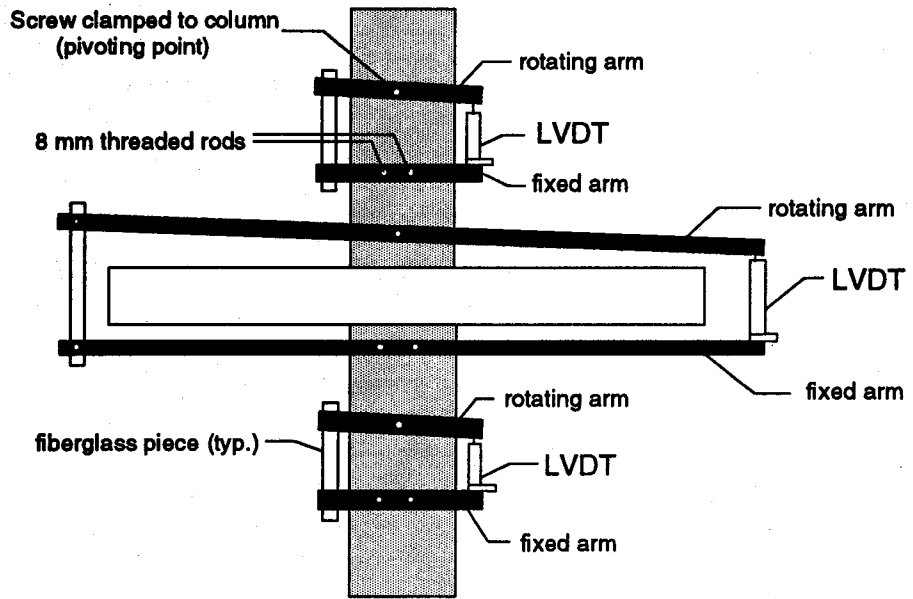
Figure 3.24   LVDT Set-up for Series B Rectangular Column Specimens
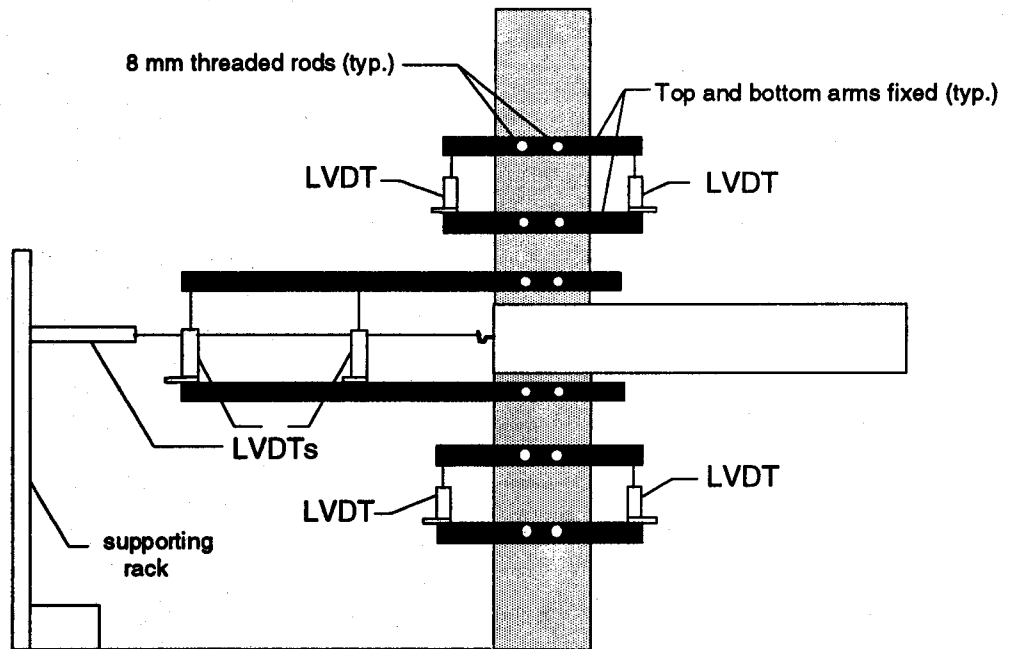
Figure 3.25   LVDT Set-up for Series C Specimens
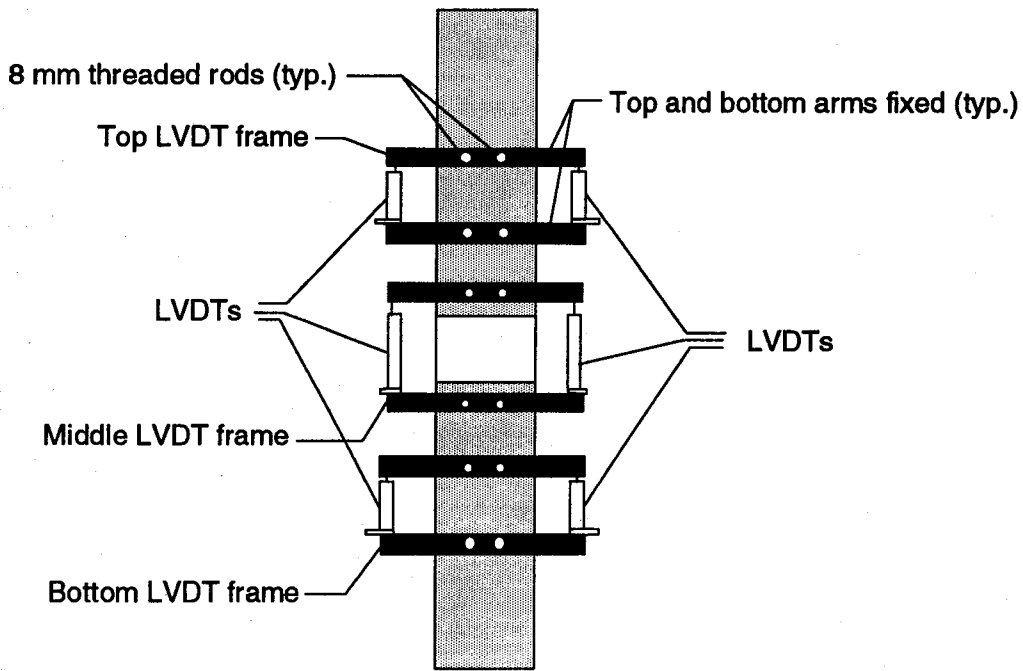
Figure 3.26   LVDT Set-up for Series D Specimens

Notes: m varied from 25 to 35 mm
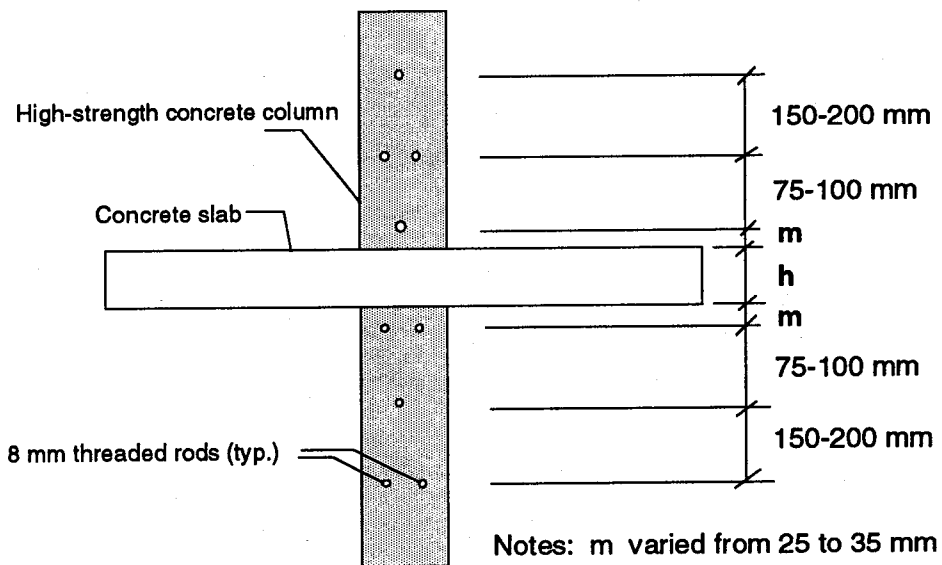
**Figure 3.27   Parameters to Calculate Column Strain
through Slab Thickness**

56
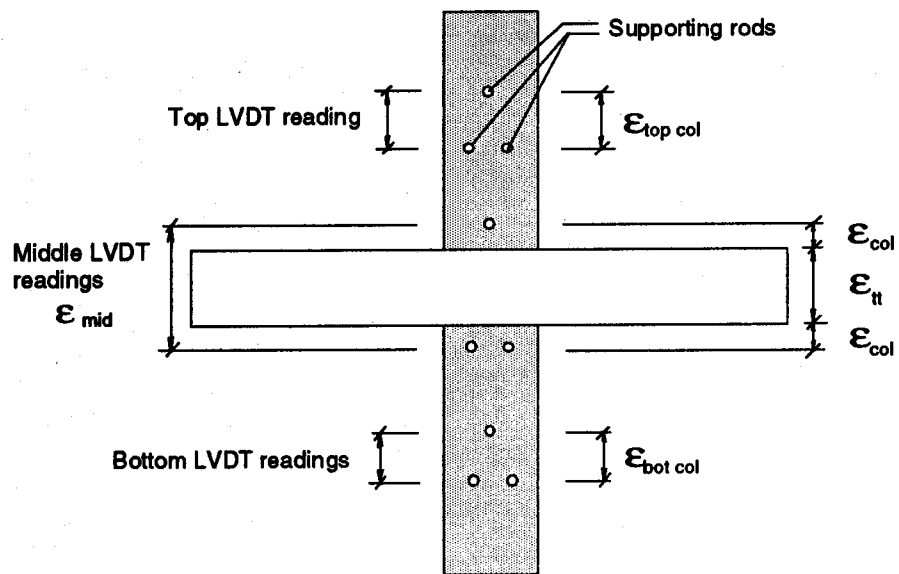
Figure 3.28 Relationship Between Column Strain through Slab Thickness and LVDT Strain Readings

4. TEST RESULTS AND OBSERVATIONS

4.1 General

Test results are summarized in Table 4.1. This table shows the ratios of slab thickness to column width, h/c, the ratios of column concrete cylinder strength to slab concrete cylinder strength, f'_{cc}/f'_{cs}, the maximum applied column loads, the effective compressive strengths, f'_{ce}, and the ratios of column effective compressive strength to slab concrete cylinder strength, f'_{ce}/f'_{cs}, for all of the specimens tested in this investigation. Unless stated otherwise, values of f'_{ce} reported in Table 4.1 were calculated based on Eq. 2.2. Table 4.1 also includes strain readings in the slab top reinforcement measured at the column face immediately after imposing the slab loads. The test results are presented according to the type of specimen, namely interior sandwich plate, edge sandwich plate or sandwich column. This chapter also reports the observed conditions through the tests along with sketches of crack patterns and pictures of the specimens during and after testing.

Stress-strain relationships for each of the test specimens are shown in Appendix B. Stress-strain plots constitute a useful way to identify the different carrying load mechanisms and to qualify the different cracking stages throughout a test. Appendix B includes plots of the applied compressive stress in the column, f_c, against the column longitudinal strain through the slab thickness, and against the longitudinal strain of both column and slab reinforcing bars. The average compressive stress applied on the column was calculated as

$$f_c = \frac{P_{col} - f_y A_{st}}{(A_g - A_{st})} \qquad [4.1]$$

where P_{col} corresponds to the column load applied on the tests, A_g represents the gross section of the column, A_{st} is the area of column longitudinal reinforcement, and f_y is the yield strength of the column longitudinal reinforcing bars.

4.2 General Behaviour of the Test Specimens

Figure 4.1 shows schematic relationships between the average compressive stress applied on the column, f_c, and the column longitudinal strain through the slab thickness, ε_{tt}, for the specimens tested in this investigation.

Three distinct stages of behaviour are identified. Stage I illustrates the behaviour of the specimen at the beginning of the test. During this phase, the stress-strain curve exhibits a linear-elastic behaviour. The end of stage I and the beginning of stage II is marked by a decrease in the slope of the stress-strain curve. This results from slab concrete crushing at the joint region as the applied stress on the column reaches the cylinder strength of the slab concrete, f'_{cs}. This coincides with yielding of the column longitudinal reinforcement at the joint region.

Throughout stage II, the specimen undergoes a continuous loss of stiffness. The softening of the joint concrete results in a gradual decrease in the slope of the stress-strain curve. Along this stage, there is a significant increase in the slab deflections for the specimens with loaded slabs. The peak stress marks the boundary between stage II and III. The strain corresponding to the peak stress is defined as the ultimate strain. Stage III covers the post-peak behaviour of the specimen. The shape of the stress-strain curve through stages II and III varied according to the type of the specimen, the load conditions and the compressive strength of both column and slab concrete.

4.2.1 Interior Sandwich Plate Specimens

4.2.1.1 Interior Specimens with Loaded Slabs

The schematic stress-strain behaviour of an interior sandwich plate with loaded slab is shown in Fig. 4.1.

Cracks in the slab top level were first noticed after 50 to 60 % the slab load was imposed. These cracks are believed to form from shrinkage cracks that widened as a result of the imposition of the slab loads. The cracks extended from the column to the slab boundaries directly on top of the slab reinforcement mat. This was accompanied by a downward deflection of the slab segment. No further slab cracking was noticed during stage I.

Crushing of the joint concrete and yielding of the column reinforcement at the slab portion occurred almost simultaneously. Direct observation of joint crushing was not possible since the joint was covered by the surrounding slab. Joint crushing coincided with the slab strains at the joint centreline overtaking those at the column face. Strain readings for the column longitudinal reinforcement are shown in Appendix B. It can be seen that column strains in the joint are always higher than those outside the joint.

Yielding of the slab reinforcement at both column face and joint centre was observed at the beginning of stage II. Yielding of the slab steel was recorded at higher stresses for specimens with stronger slabs. Yielding of the column reinforcement outside the joint region was only observed for specimens B-2, B-3 and B-6.

When the applied column effective stress reached 70 to 85 % the maximum column strength, the existing slab cracks began to widen and the slab deflected further downwards. At this level, additional cracks formed around the top column outline and within the slab corner around the jacks. Cracks along the column outline opened wide rather than closing. This suggests that the slab concrete provided little or no restraint to the upper portion of the joint. No cracks were observed on the slab underside at the end of stage II.

It is worth noting that throughout stage II it was necessary to pump the jacks at very short time intervals to keep the slab load constant. Failure to do so resulted in not only a

decrease in the level of slab load but also in an increase of the column strength. This may be observed from the stress-strain curve of specimen B-5 shown in Appendix B.

Immediately before reaching the maximum column load, splitting cracks extended from the joint into the top column stub. Spalling of column concrete was noticed in the corners of the column above the slab. This behaviour suggests that more restraint was provided to the lower half of the joint than to the upper portion. At this level, cracks formed on the slab underside. These cracks formed along the diagonals of the slab segment, extending from the column corners towards the slab edges. Once the maximum column load was reached, additional spalling of concrete at the corners of the top column stub was observed. Column cracks widened and penetrated further into the column. Stage II covered approximately 70 to 80 % of the ultimate strain.

Specimens with loaded slabs displayed ductile behaviour, as it can be seen through stages II and III. Cracking of concrete at the top column progressed rapidly with concrete chunks frequently falling off. Spalling of column concrete below the slab was rarely observed. Tests were suspended when significant reduction of the axial load capacity was attained. However, it is worth mentioning that the specimens continued carrying load when the tests were terminated. Buckling of the column reinforcement at the slab region was not observed for these specimens. At final stages of the tests, deflections of at least 50 mm were measured at the slab corners.

Pictures of interior sandwich plates under testing are presented in Figs. 4.2 and 4.3. These correspond to interior sandwich plates with h/c values of 1.0 and 0.6, respectively. Figure 4.4 shows the typical crack pattern of an interior sandwich plate with a slab thickness-to-column width ratio, h/c, of 1.0. A crack pattern of an interior specimen with h/c of 0.6 is illustrated in Fig. 4.5.

4.2.1.2 Interior Specimens with Unloaded Slabs

Figure 4.1 illustrates a typical stress-strain relationship for interior sandwich plates tested in absence of slab loads.

As with the specimens subjected to slab loading, specimens with no slab loads displayed linear elastic behaviour through stage I. No cracks were observed during this phase. Crushing of the joint concrete coincided with yielding of the column longitudinal bars at the joint region.

First cracks in the slab top level were noticed when the applied column stress was approximately 60 % the maximum column strength. These cracks formed along the slab diagonals, starting at the column corners and extending towards the slab corners. These cracks result from the lateral expansion of the joint concrete because of the Poisson's ratio effect. Cracks formed approximately at 45° to the slab reinforcement since this is the direction of minimum stiffness for a reinforcement mesh with equally spaced bars running at each direction.

The observed cracking pattern suggests the formation of diagonal compression struts along the slab diagonals interacting with tension rings acting along the slab segment periphery. These tension ties resemble the behaviour of a square hoop, as shown in Fig. 4.6.

As the column load further increased, existing cracks widened and extended towards the slab corners. At this level, yielding of the column longitudinal reinforcement outside the joint region was observed. Later, cracks formed at the slab mid-edges right in between the cracks along the slab diagonals and progressed towards the column. These cracks formed through the full slab thickness. For this reason, top and bottom cracking patterns were similar.

As illustrated in Fig. 4.7, this cracking behaviour resembles that of a deep beam lying in the plane of the slab. The joint lateral expansion is equilibrated by tensile stresses in the top and bottom slab reinforcing steel.

Before the maximum column load was attained, the lateral expansion of the joint concrete caused splitting cracks to penetrate into the upper column stub. Because the slabs were more reinforced at the bottom portion of the joint, more restraint was applied to the lower portion of the joint than at the upper portion. Stage II spanned approximately 80 to 90 % the ultimate column strain through the slab thickness.

Following the formation of splitting cracks in the upper column, failure of the specimen was imminent. The observed failure was explosive and violent. Large portions of column concrete spalled off violently above the slab and the column longitudinal reinforcement buckled.

The sole specimen with an unloaded slab that exhibited ductile behaviour across stage III was specimen A4-A. For this specimen, the effective compressive strength of the column was significantly less than the column concrete strength, mainly because of the low strength of the concrete placed in the slab. This behaviour opposes to that displayed by specimen B-4. This specimen failed explosively in the upper column region when the stress applied on the column reached the in-place compressive strength of the column concrete.

A picture of specimen B-4 under testing is shown in Fig. 4.8. Figure 4.9 illustrates the failure at the specimen top column stub. A sketch of the typical crack pattern of an interior sandwich plate with unloaded slab is shown in Fig. 4.10.

4.2.2 Edge Sandwich Plate Specimens

4.2.2.1 Edge Specimens with Loaded Slabs

The stress-strain behaviour of edge specimens under slab loading follows the schematic path shown in Fig. 4.1.

After imposing the slab loads, cracks formed on top of the slab in the direction perpendicular to the slab free edge. These cracks may have resulted from existing shrinkage cracks that became visible due to the imposition of the jacking loads. As a result of the slab loads, the slab segment deflected downwards. Average strain readings at the face of the column are included in Appendix B.

At the beginning of stage II, vertical splitting cracks formed at the visible face of the joint. Cracks in the slab widened and progressed from the column towards the slab edge, parallel to the free edge, forming directly over the slab top reinforcement. It became difficult to keep the jack loads at the desired level. As was the case for the interior sandwich plates, a decrease in the jacking loads resulted in an increase in the column strength.

As the column load increased, torsional cracks formed at the free face of the joint starting at the corners of the slab-top column interface. This was followed by the formation of diagonal cracks on the slab top level close to the column. These cracks propagated from the interior corners of the upper column outline and spread apart until reaching the slab free edge. Based on these observations and also on the strain readings from gauges attached at both top and slab bottom reinforcing bars crossing the joint, the system of forces acting on the edge joints is illustrated in Fig. 4.11.

Following the formation of the torsional cracks, splitting cracks in the joint extended into the top column. Significant loss of stiffness during stage II was observed compared to that for the interior plates. Stage II covered approximately 90 % of the ultimate strain. At the onset of stage III, spalling of concrete was observed in the top column close to the slab top level. This was followed by buckling of the column longitudinal reinforcement at the same location. Spalling of column concrete limited to upper column stub. Cracks in the slab underside were not observed. When tests were stopped, the column still was carrying a significant amount of load.

A picture of an edge specimen under testing is shown in Fig. 4.12. Figure 4.13 illustrates the typical crack pattern for an edge sandwich plate with slab heavily loaded.

4.2.2.2 Edge Specimens with Unloaded Slabs

The stress-strain behaviour of an edge plate not subjected to slab loading is shown in Fig. 4.1.

Specimens remained intact until stage II began. At this level, vertical splitting cracks formed at the joint free face. These cracks are attributed to the lateral expansion of the joint because of the Poisson's ratio effect. Cracks then formed on the slab top level. These cracks radiated from the column region towards the slab boundaries in a similar way than that exhibited by the interior plates with unloaded slabs.

As the column load increased, splitting cracks extended from the joint into the upper and lower column stubs. At the joint region, the concrete spalled resulting in the loss of readings of the joint lateral expansion. Later, column cracks widened and lengthened. This was followed by spalling of concrete in the corners of the upper column right above the slab. Splitting cracks were observed in much less degree at the bottom column stub. The larger confinement at the joint lower region results from more reinforcement placed at the joint bottom zone than at the top.

Through stage II, edge specimens with unloaded slabs displayed additional loss of stiffness compared to the edge plates with loaded slabs. Ultimate strains for the edge plates tested in absence of slab loads exceeded those recorded for the specimens with loaded slab segments. Stage II covered approximately 90 % of the ultimate strain.

Shortly after the maximum column load was applied buckling of the column vertical bars was observed at the joint region. This was accompanied by the opening of joint concrete along the path of these bars. Unlike the majority of interior plates without slab loads, the slab-unloaded edge specimens exhibited a ductile behaviour. Tests were stopped with the column concrete still carrying load.

Picture of an edge plate specimen without slab loads after conclusion of test is shown in Fig. 4.14. A representative crack pattern of this specimen is shown in Fig. 4.15.

4.2.3 Sandwich Column Specimens

The schematic shape of the stress-strain curve for the sandwich column specimens is similar to that recorded for the interior sandwich plates. However, significant reduction in strength and ultimate strain are observed for the sandwich columns. The schematic stress-strain relationship is shown in Fig. 4.1.

No visible column cracking was observed until the applied effective stress in the column was close to the maximum column compressive strength. Specimens remained intact along stage I. First cracks to be observed corresponded to vertical splitting cracks forming at the joint region at approximately 90 % of the failure load. This was followed by concrete spalling off at the joint region and splitting cracks extending into both top and bottom column portions. Spalling of concrete was observed in both top and bottom column concrete ends.

The maximum column strength was reached shortly after the cylinder strength of the joint concrete was reached. At the end of stage III, buckling of the column longitudinal

reinforcement was observed along with significant widening of cracks within the column stubs. Specimens displayed some ductility and when tests were suspended the columns were still carrying load.

Figure 4.16 shows a sandwich column under testing. A picture of the four sandwich columns after failure is given in Fig. 4.17. A typical cracking of a sandwich column is illustrated in Fig. 4.18.

4.3 Effect of Slab Loading

Figures 4.19 and 4.20 show the effect of slab loading on the strength of interior sandwich plate specimens. Figure 4.21 illustrates the same effect for edge sandwich plates.

Figures 4.19 and 4.20 compare the stress-strain curves of selected specimens from series A and B. With all other factors being equal, different levels of slab load were applied. The consistent effect of the slab load is to reduce both the ultimate strength and strain. For the set of specimens from series A, the ultimate strain values ranged approximately from 2 to 4 %. These values are ten to twenty times greater than that associated with unconfined compression, which is typically equal to 0.2 %. This shows that even when high slab load intensities are applied, the joint benefits from some transverse confinement. For the specimens from series B, the effect of the slab load was consistent with that of series A but not as large.

Figure 4.21 compares the stress-strain behaviour of three edge plates with similar column and slab concrete strengths and equal h/c values, tested under three different levels of slab loading. An increase in the slab load intensity leads to a reduction in both the ultimate stress and strain. The ultimate strain for the edge plate with unloaded slab was 2.5 %. This strain value reduced to 1.4 % for the specimen with heavy slab loads. These values are less than those displayed by the interior plates, but still greater than 0.2 %. As was the case for interior columns, the effect of slab load is to reduce the effective compressive strength of the column. However, comparing the values of f'_{ce}/f'_{cs} given in Table 4.1 suggests that the compressive strength reduction is less significant for edge columns.

The stress-strain curves of Fig. 4.21 also illustrate that the edge plates exhibited a marked reduction in stage II stiffness compared to the interior plates. This is explained by the geometry of edge connections since one face of the joint does not receive any confinement from the surrounding floor.

Figure 4.22 compares the joint transverse strain at the column face and at the column centreline of two interior sandwich plate specimens, B-2 (loaded slab) and B-4 (unloaded slab). At early stages of the test, strains at both the column face and the column centreline indicate that the slab top level is subjected to tension. For specimen B-2, the tensile strains at the face of the joint through stage I are higher than those at the joint centre. It should be mentioned that this difference was larger for other specimens with thinner slabs (see Appendix B). After the imposition of slab loads, the strains at the joint centreline increased

at a faster rate than at the joint face. Strains at the joint face remained almost constant throughout stage I. Strains at the joint centreline overtake those at the column face when the joint concrete crushes and the column vertical bars yield within the joint region. Beyond this level, both strain readings increase in tandem. For specimen B-4, the tensile strains at the face of the joint are less than the strains at the column centreline. This observation applies for the entire duration of the test.

It can be seen in Fig. 4. 22 that the stress-strain curves at the joint centreline and at the column face for specimen B-2 virtually parallel the corresponding stress-strain curves for specimen B-4. At the joint centreline the difference in strain between both curves is 1000 microstrain. At the column face this difference increases to 1500 microstrain. The fact that strains at the column face are higher than those at the column centreline implies that under column and slab loading, the upper half of the joint is not only unconfined, it is also pulled apart by the slab bending action.

At the top, the joint may be viewed as a concrete prism subjected to a triaxial state of stress consisting of longitudinal compression from the column load and biaxial transverse tension from the slab bending. This effect leads to a reduction in the column axial load capacity (Chen and MacGregor (1993)). Since it is required for equilibrium of forces and moments that the transverse tension at the top be equilibrated at the bottom by transverse compression, only the bottom portion of the joint is subjected to confinement from the surrounding slab concrete. At the bottom, the joint concrete is in triaxial compression from the combined effect of compressive column load and the bi-axial transverse compression due to bending. Figure 4.23 illustrates this behaviour.

For the specimens with no slab loads, the tension of the top and bottom slab reinforcing bars crossing the column is equilibrated by compression from the surrounding slab concrete since no flexural moment is applied. In this case, a compressive triaxial state of stress acts over the full depth of the joint, in other words, the joint is fully confined by the surrounding slab concrete. This is illustrated in Fig. 4.24. Since confinement acts over the full depth of the joint an enhancement of column effective compressive strength is expected in joints with unloaded slabs compared to that in joints with loaded slabs.

4.4 Effect of h/c

The effect of the ratio of slab thickness to column width, h/c, on the stress-strain behaviour of interior sandwich plates and sandwich columns is shown in Figs. 4.25 and 4.26, respectively.

Figure 4.25 shows the stress-strain behaviour of two sets of specimens with f'_{cc}/f'_{cs} varying from 2.48 to 6.33, with h/c values equal to 0.6 and 1.0. For both sets of specimens, the stress-strain curves are similar up to a stress level approximately equal to that of the cylinder strength of the floor concrete. Beyond this level, the curves diverge. The observed effect is that the ultimate strength of the connection decreases as h/c increases. The reduction is higher for the specimens with larger f'_{cc}/f'_{cs} value.

Figure 4.26 shows the stress-strain behaviour of series D sandwich columns. For these specimens, f'_{cc}/f'_{cs} varied from 6.18 to 6.29. The observed trend is that as h/c increases the ultimate strength and strain of the column decrease. This observation confirms that the effect of h/c on the compressive strength of unconfined joints is similar to that in a conventional cylinder or prism compression test. In a sandwich column specimen, the joint concrete may be viewed as a concrete prism compressed by two stronger column ends. These column ends act as the platens of a testing machine. These ends provide transverse restraint at the top and bottom levels of the sandwiched layer of concrete. For joints with lower h/c values, the benefits from the end restraint are larger.

4.5 Effect of Column Rectangularity

The effect of column rectangularity is presented in Fig. 4.27. This figure shows the stress-strain relationship of two interior sandwich plates built with similar column and slab concrete strengths and with columns of equal cross-section but different shapes. Specimen B-5 had a square column 250 mm wide whereas specimen B-7 had a rectangular column, 175 mm wide and 350 mm deep.

The stress-strain curves are virtually identical. This is attributed to the fact that the column area was almost equal for both specimens. However, it is worth mentioning that the column and slab concrete strengths used in specimen B-7 were slightly higher than those used in specimen B-5. This means that a higher strength was expected for specimen B-7, which in fact, did not occur. This suggests that the square column outperformed the rectangular column.

4.6 Effect of High-Strength Concrete Core at the Joint Region

Figure 4.28 shows the stress-strain behaviour of two interior sandwich plate specimens built with similar dimensions and concrete strengths. The only difference between these two is that specimen B-3 was provided with a high-strength concrete core at the joint region. This comparison was intended to evaluate the possible benefits of this construction technique.

During stage I, both specimens displayed similar behaviour. The onset of stage II occurred later for the specimen with the high-strength core. Moreover, through stage II, the stress-strain curve of the specimen with the core had a higher slope. A higher ultimate column strength was recorded for the specimen with the built-in core whereas a higher ultimate strain was reached for the conventionally-built specimen.

Series	Specimen	h/c	$P_{col,max}$ (kN)	f'_{ce} (MPa) **	Slab Strain (µε) †	$\dfrac{f'_{cc}}{f'_{cs}}$	$\dfrac{f'_{ce}}{f'_{cs}}$
A	A1-A	0.5	3914	100.31	0	2.63	2.51
	A1-B	0.5	3678	93.08	1000	2.63	2.33
	A1-C	0.5	3498	87.56	2000	2.63	2.19
	A2-A	0.5	3820	97.43	0	2.43	2.12
	A2-B	0.5	3807	97.03	1000	2.43	2.11
	A2-C	0.5	3591	90.41	2000	2.43	1.97
	A3-A	0.75	3437	85.69	0	3.56	3.43
	A3-B	0.75	3174	77.63	1000	3.56	3.11
	A3-C *	0.75	2275	50.09	2000	3.56	2.00
	A4-A	0.75	3272	80.64	0	4.61	3.51
	A4-B	0.75	2927	70.07	1000	4.61	3.05
	A4-C	0.75	2376	53.19	2000	4.61	2.31
B	B-1	1.0	4072	71.54	750	2.48	1.70
	B-2	0.6	5359	96.08	1600	2.48	2.29
	B-3	1.0	5078	90.72	600	2.57	2.06
	B-4	0.6	6298	113.99	0	2.57	2.59
	B-5	1.0	2703	45.44	1500	6.33	3.03
	B-6	0.6	3720	64.83	2000	6.33	4.32
	B-7 ‡	0.7	2758	47.45	1200	6.32	2.50
	B-8 ‡	1.17	4032	72.25	1800	6.32	3.80
C	C1-A	0.74	3246	59.76	0	3.34	1.87
	C1-B	0.74	3049	55.25	2800	3.06	1.58
	C1-C	0.74	2959	53.18	3200	3.15	1.56
	C2-A	1.0	2936	52.65	0	3.48	1.70
	C2-B	1.0	2736	48.69	1500	3.18	1.43
	C2-C	1.0	2564	44.12	3300	3.27	1.34
D	D-SC1	1.0	1421	21.00	-	6.18	1.24
	D-SC2	0.6	1716	26.61	-	6.18	1.57
	D-SC3	0.5	1991	31.87	-	6.29	1.87
	D-SC4	0.3	2279	37.35	-	6.18	2.20

Handwritten annotations in right margin: "← 26%" (near B-1/B-2 rows), "← 30%" (near B-5/B-6 rows).

* Specimen exhibited anchorage failure in slab.

** Calculated according to Eq. 2.2 ($\alpha_1 = 0.85$).

† Average slab strain measured at column face immediately after slab loads were applied.

‡ The h/c ratio was calculated based on the shorter column dimension.

Table 4.1   Test Results
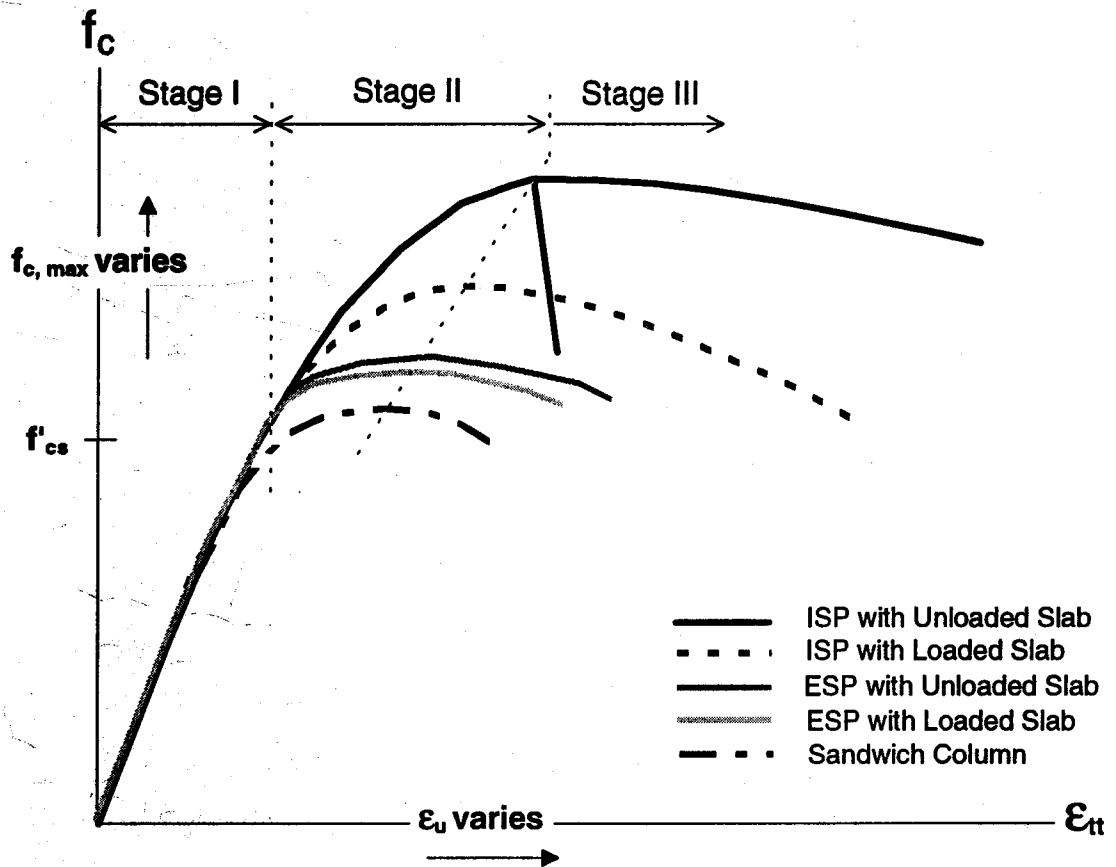
Figure 4.1   Schematic Stress-Strain Curve

69

Figure 4.3   Test of Interior Sandwich Plate
with Loaded Slab (h/c=0.6)

Figure 4.2   Test of Interior Sandwich Plate
with Loaded Slab (h/c=1.0)

70
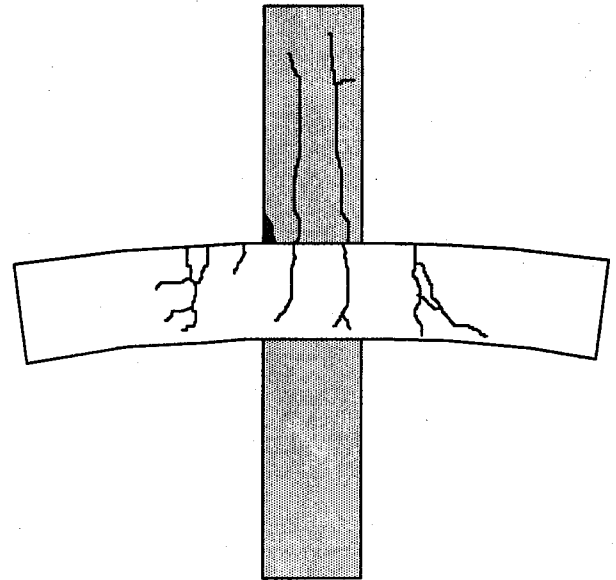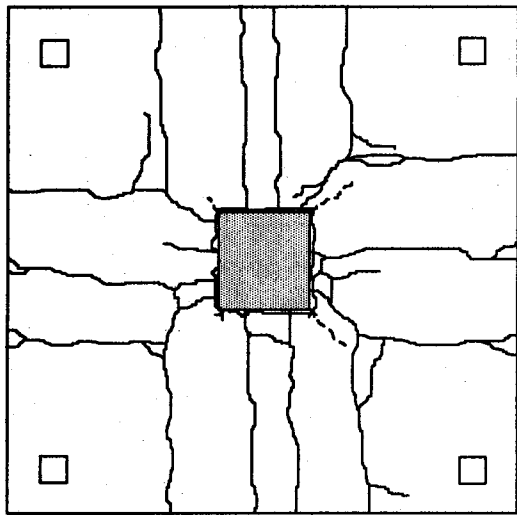
— Top slab cracks

⌐‾ ⌐‾ Bottom slab cracks

Spalling of column concrete

Figure 4.4   Cracking Pattern (Specimen B-1)
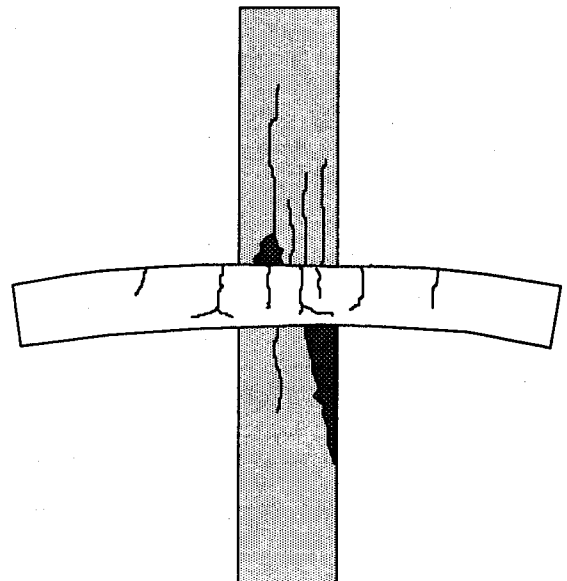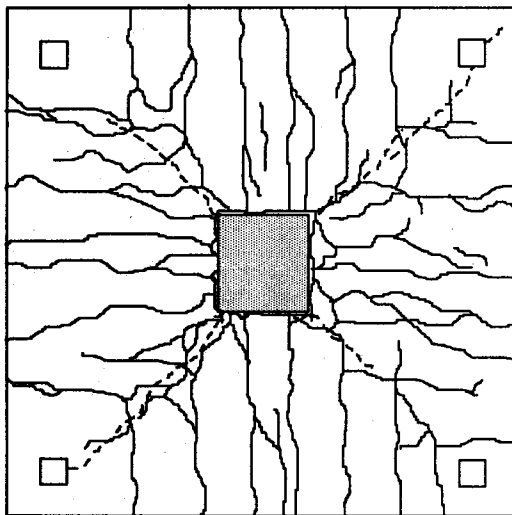
— Top slab cracks

⌐‾ ⌐‾ Bottom slab cracks

Spalling of column concrete

Figure 4.5   Cracking Pattern (Specimen B-2)

71
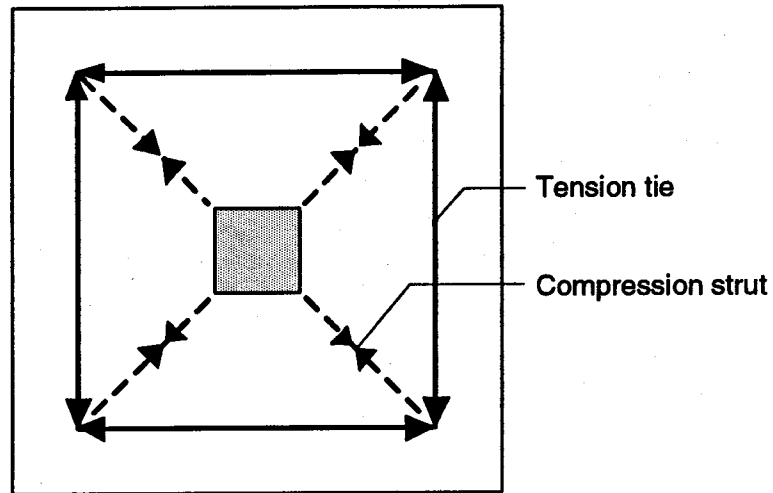
Figure 4.6   Square Hoop Behaviour of Interior Sandwich Plate with Unloaded Slab
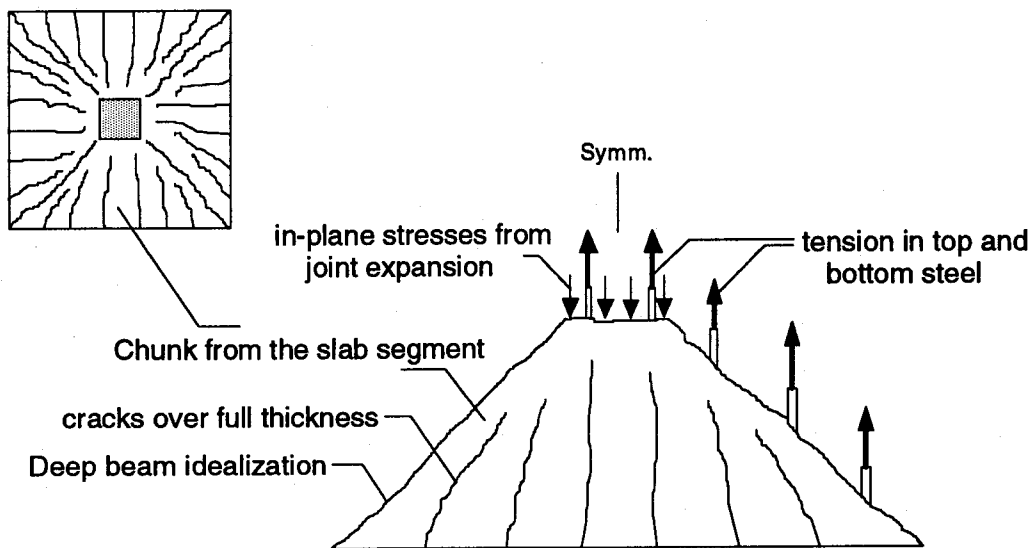
Figure 4.7   Deep Beam Behaviour of Interior Sandwich Plate with Unloaded Slab

Figure 4.9 Detail of Specimen B-4 After Failure

Figure 4.8 Test of Interior Sandwich Plate
with Unloaded Slab (h/c=0.6)
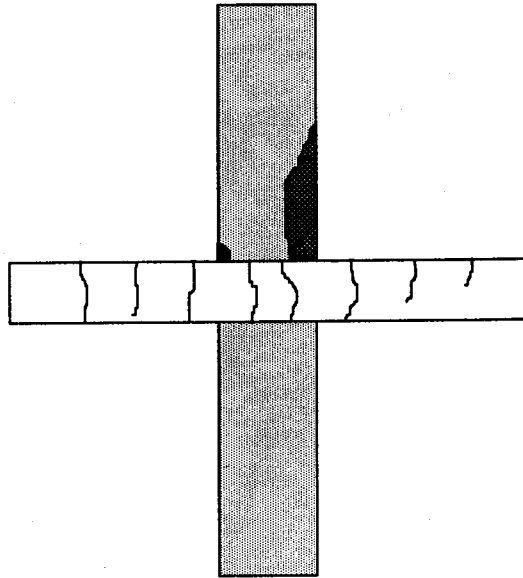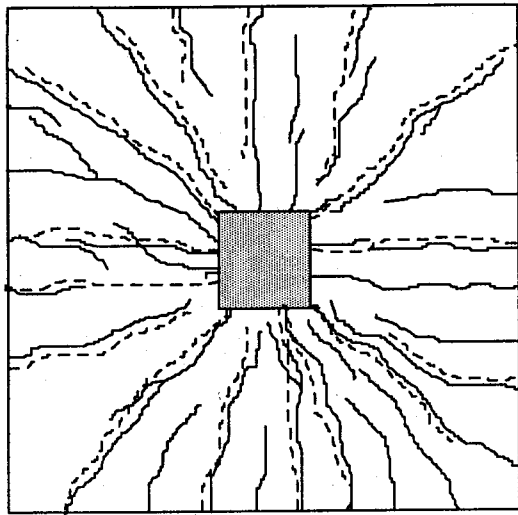
_____∿_ Top slab cracks

‾ヽ_ r‾¬ Bottom slab cracks

Spalling of column concrete

Figure 4.10   Cracking Pattern (Specimen B-4)

Top slab level

Column load

Slab load

Joint free face
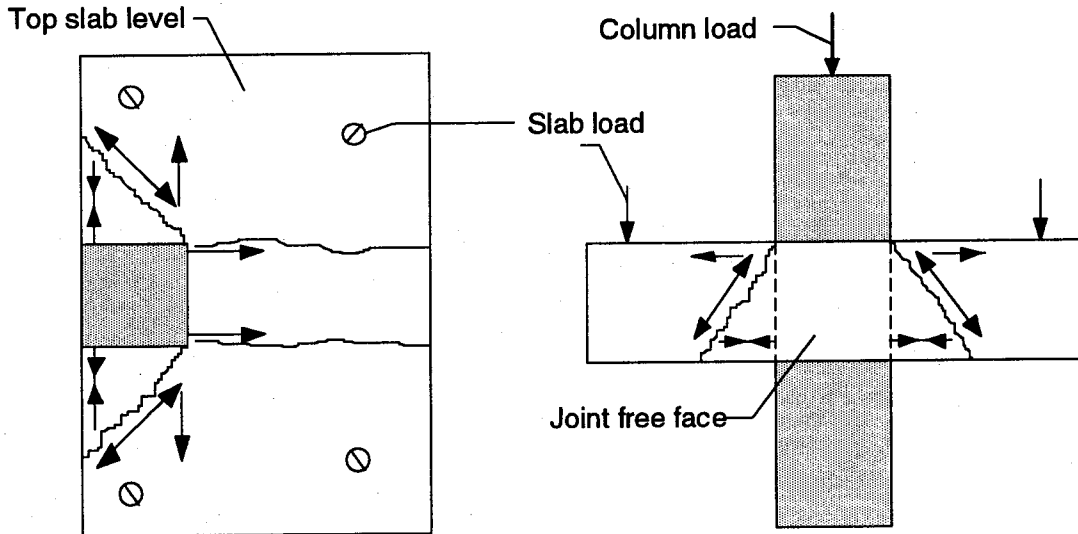
**Figure 4.11   Forces Acting over an Edge Slab-Column Joint
with Slab Loads**
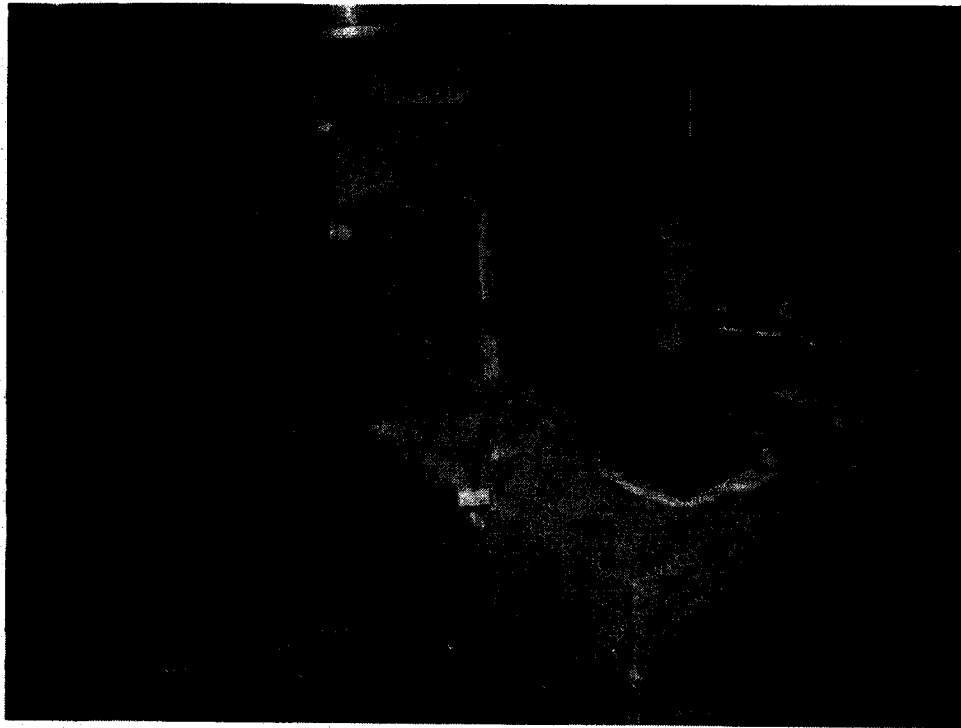
**Figure 4.12   Test of Edge Sandwich Plate
with Loaded Slab**

Section 1-1

⌐‿‿⌐ Top slab cracks

⌐‿⌐‿⌐ Bottom slab cracks

◆◆ Spalling of concrete
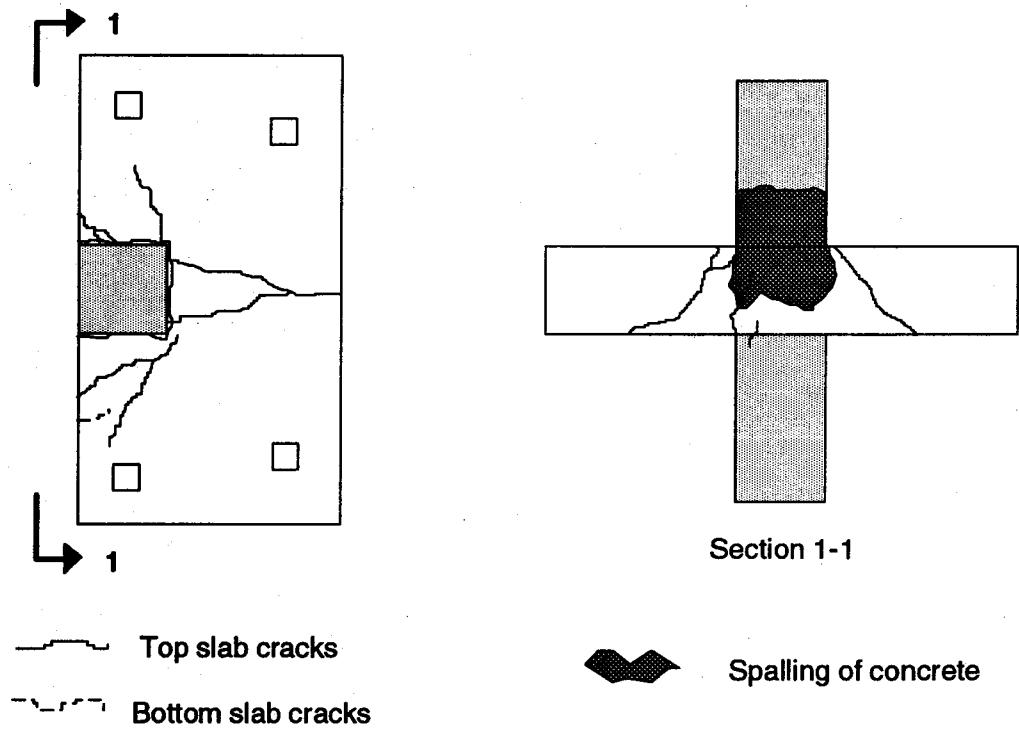
Figure 4.13   Cracking pattern (Specimen C2-C)

75
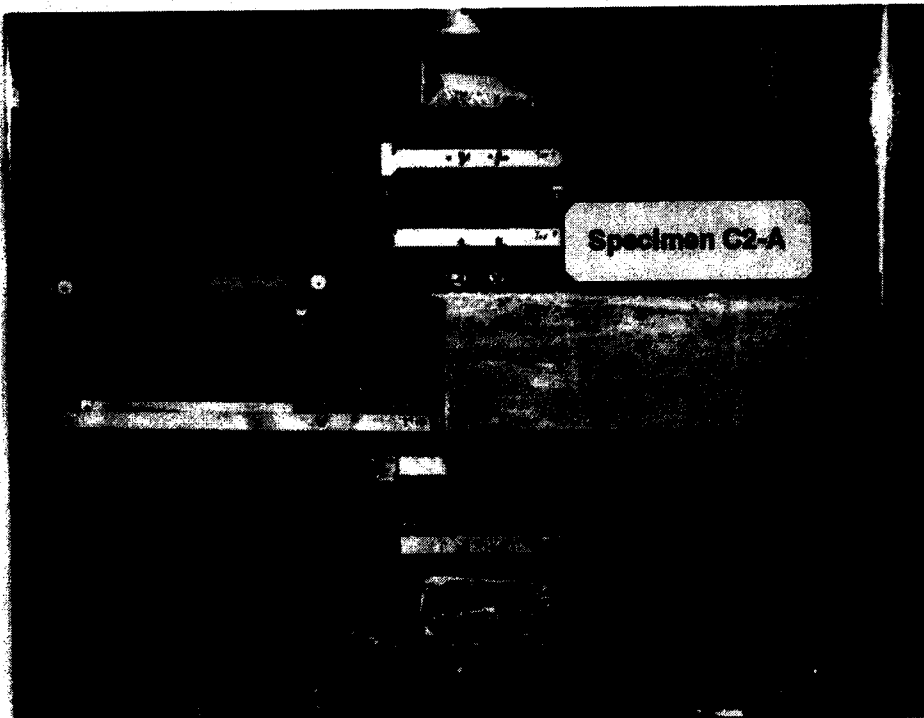
**Figure 4.14   Test of Edge Sandwich Plate
with Unloaded Slab**

1

1

Section 1-1

⌐‿⌐   Top slab cracks

▬▬   Spalling of concrete

⌐‿⌐   Bottom slab cracks
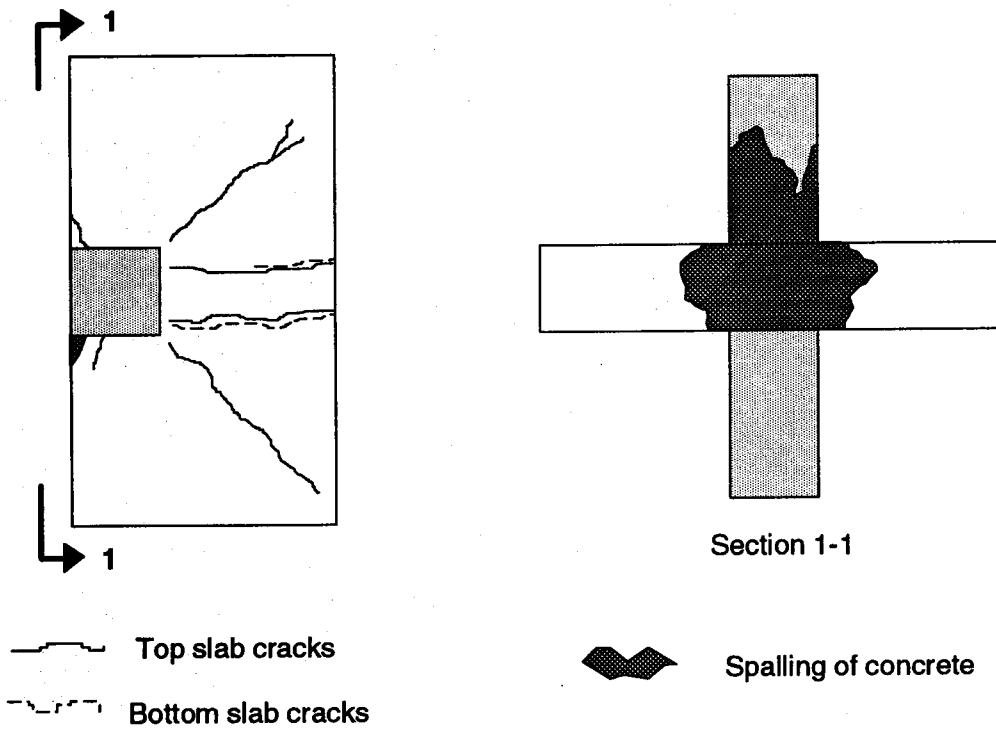
Figure 4.15   Cracking pattern (Specimen C2-A)
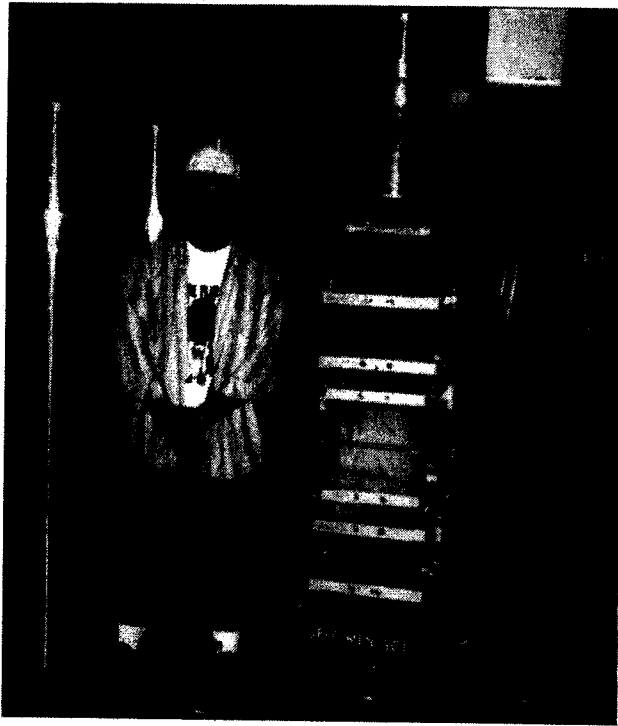
Figure 4.16   Test of Sandwich Column
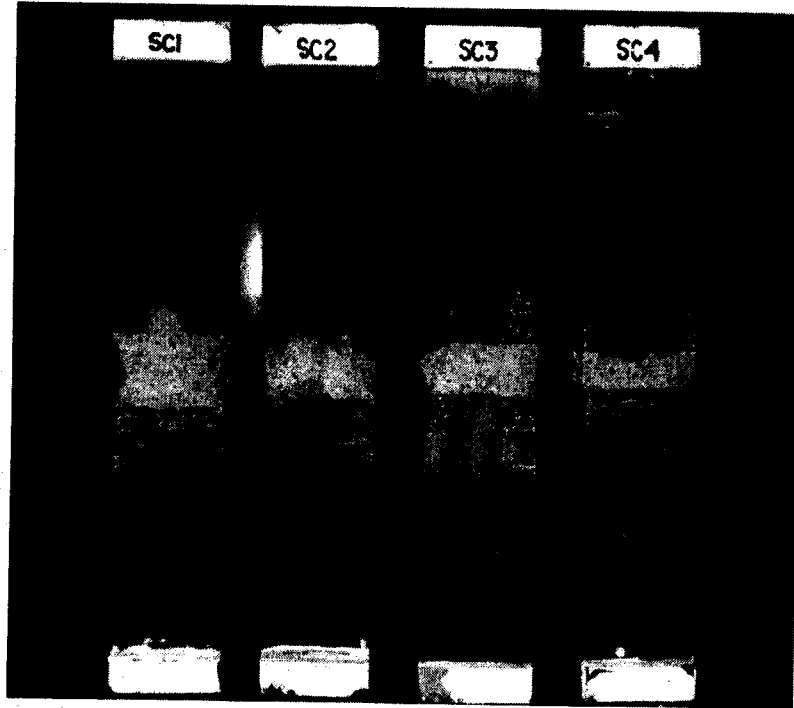
Figure 4.17   Sandwich Columns after Failure

Spalling of column concrete

Figure 4.18   Cracking pattern (Specimen D-SC1)
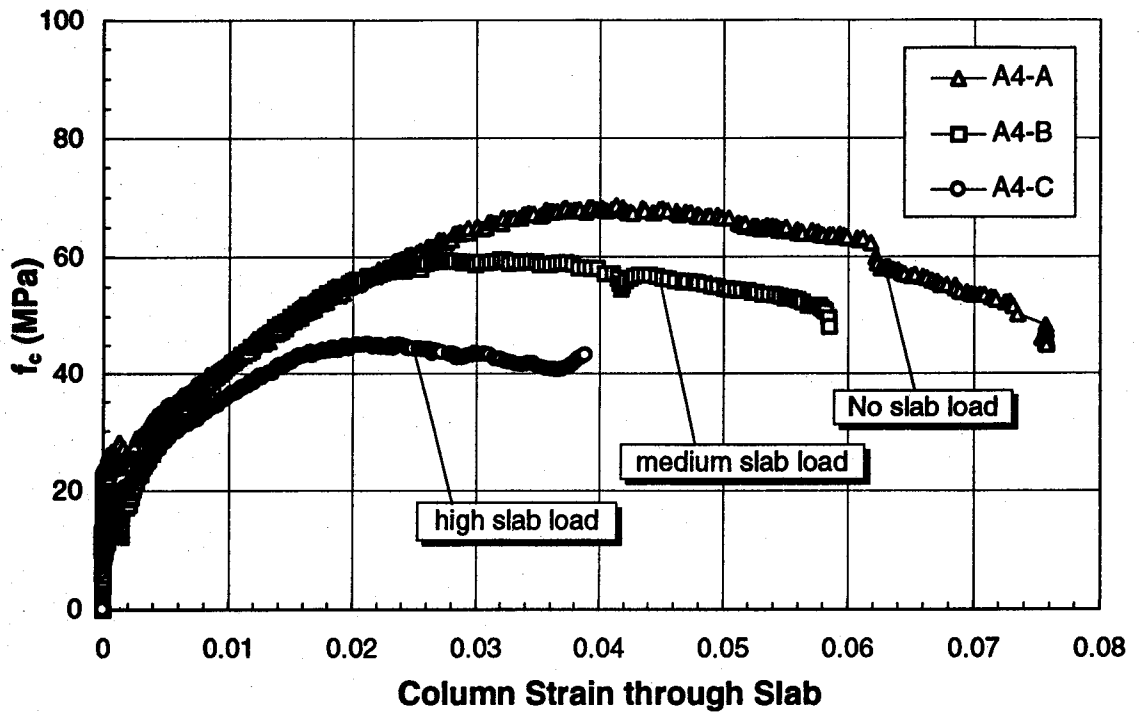
Figure 4.19   Slab Load Effect on Interior Joint Strength
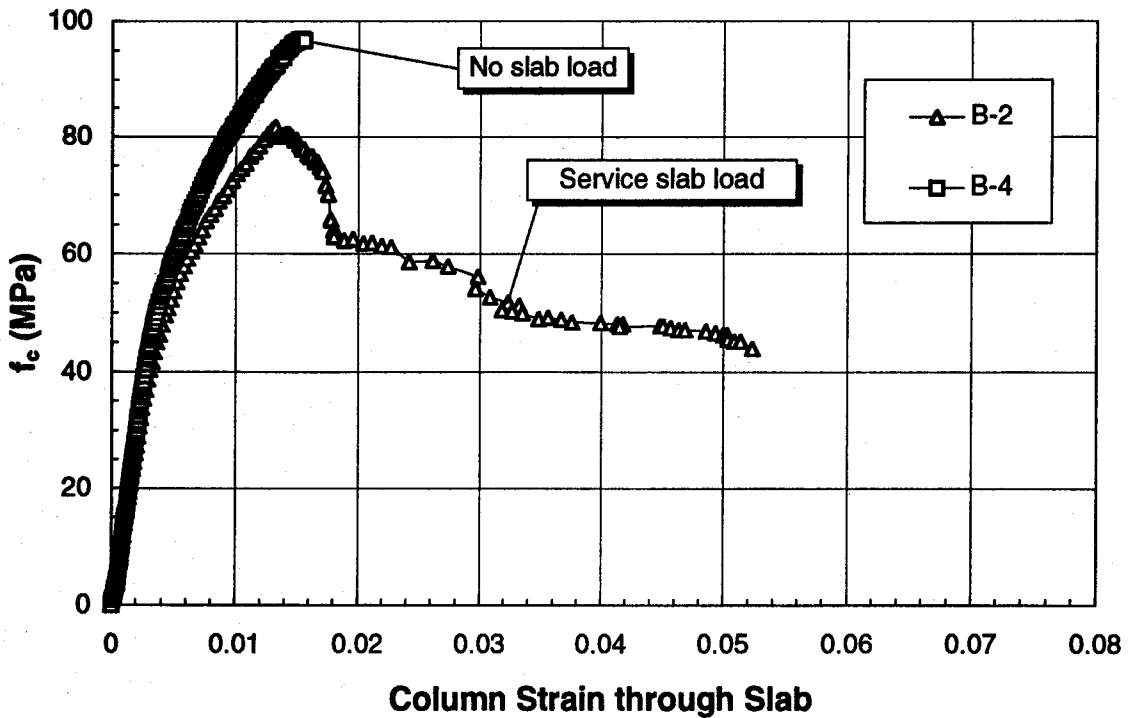
Figure 4.20   Slab Load Effect on Interior Joint Strength

79
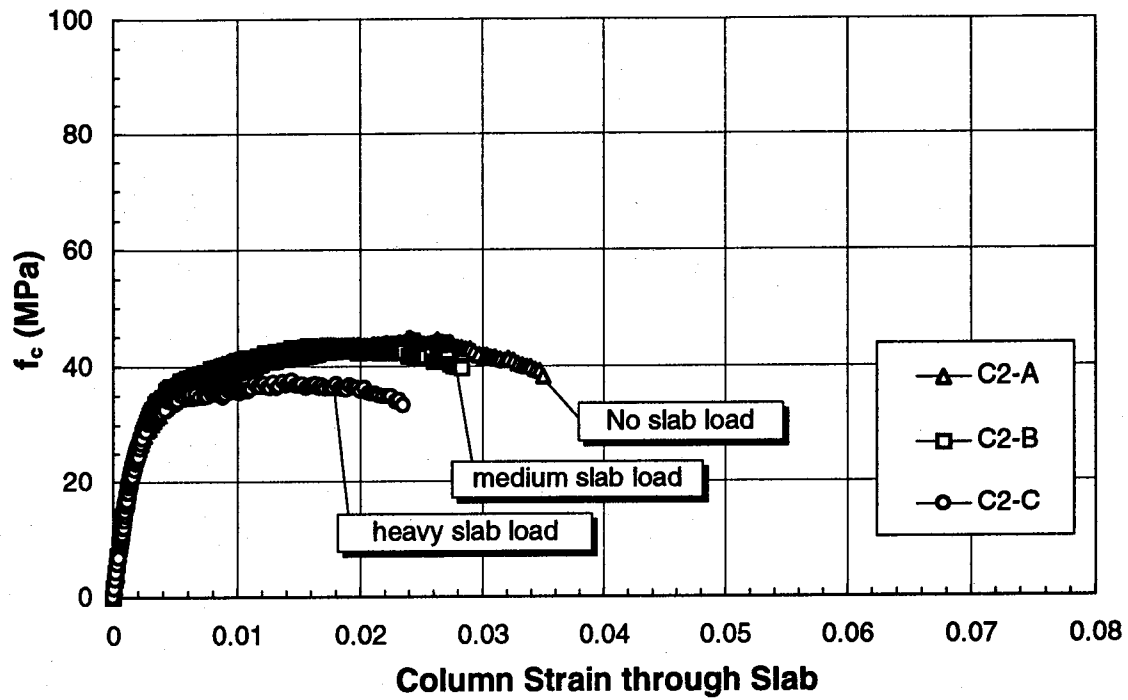
Figure 4.21   Slab Load Effect on Edge Joint Strength
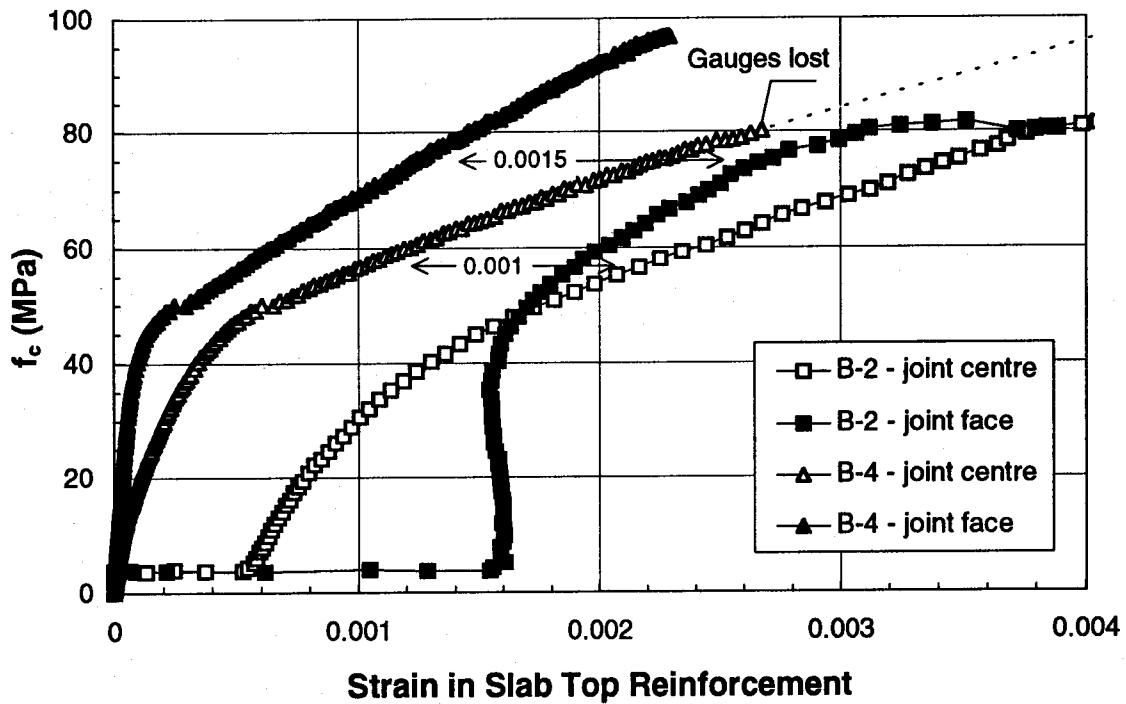
Figure 4.22   Slab Load Effect on Joint Transverse Strain
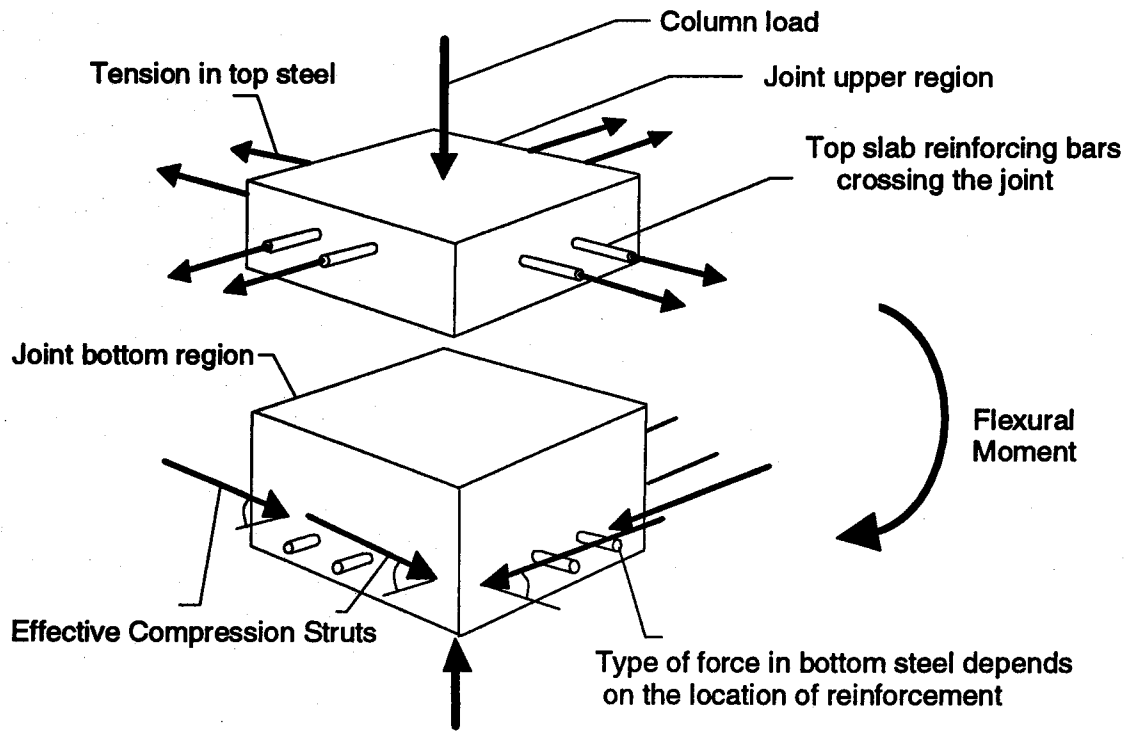
**Figure 4.23   Triaxial State of Stresses at Joint Region
(Interior Plates with Loaded Slab)**
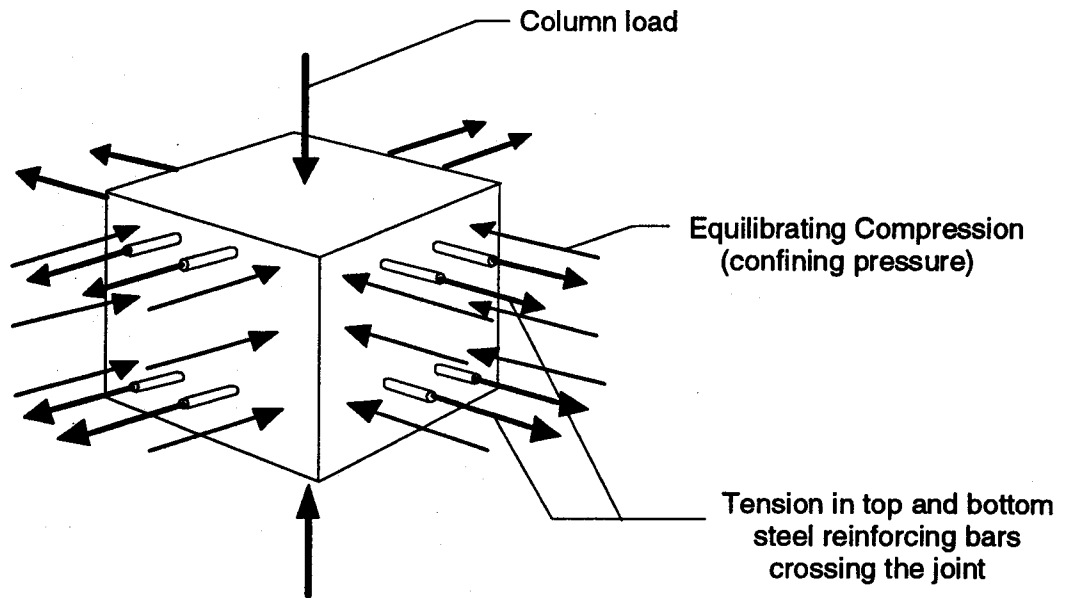
**Figure 4.24   Triaxial State of Stresses at Joint Region
(Interior Plates with Unloaded Slab)**

81
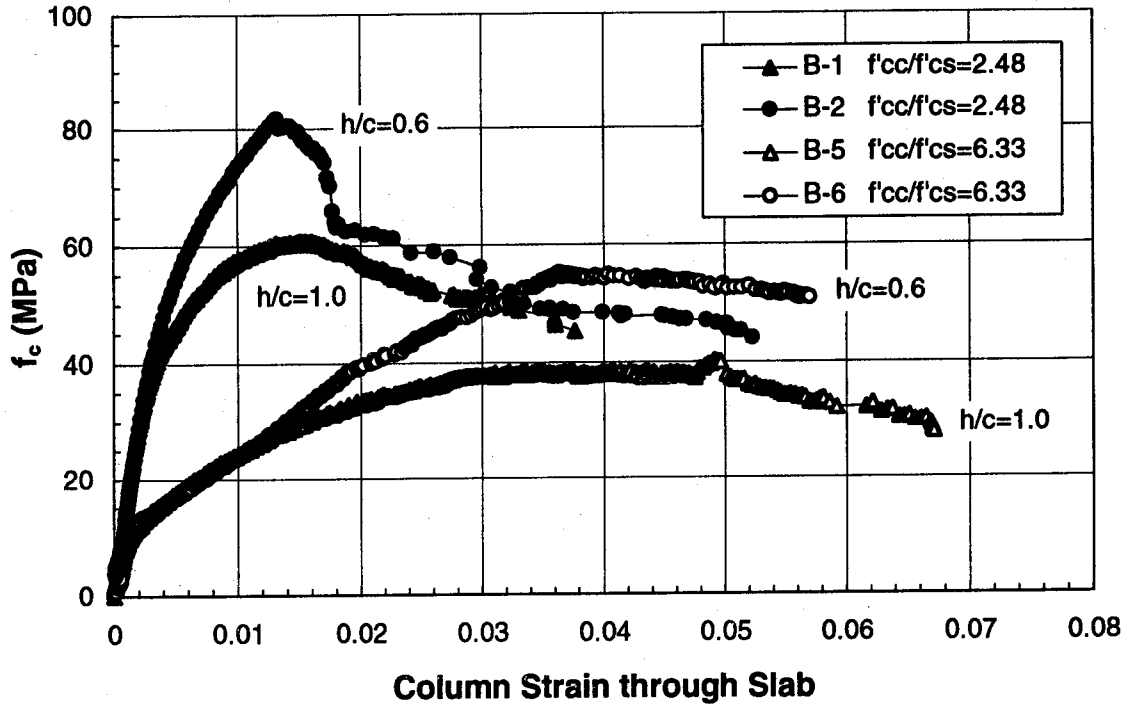
Figure 4.25   Effect of h/c on Interior Joint Strength
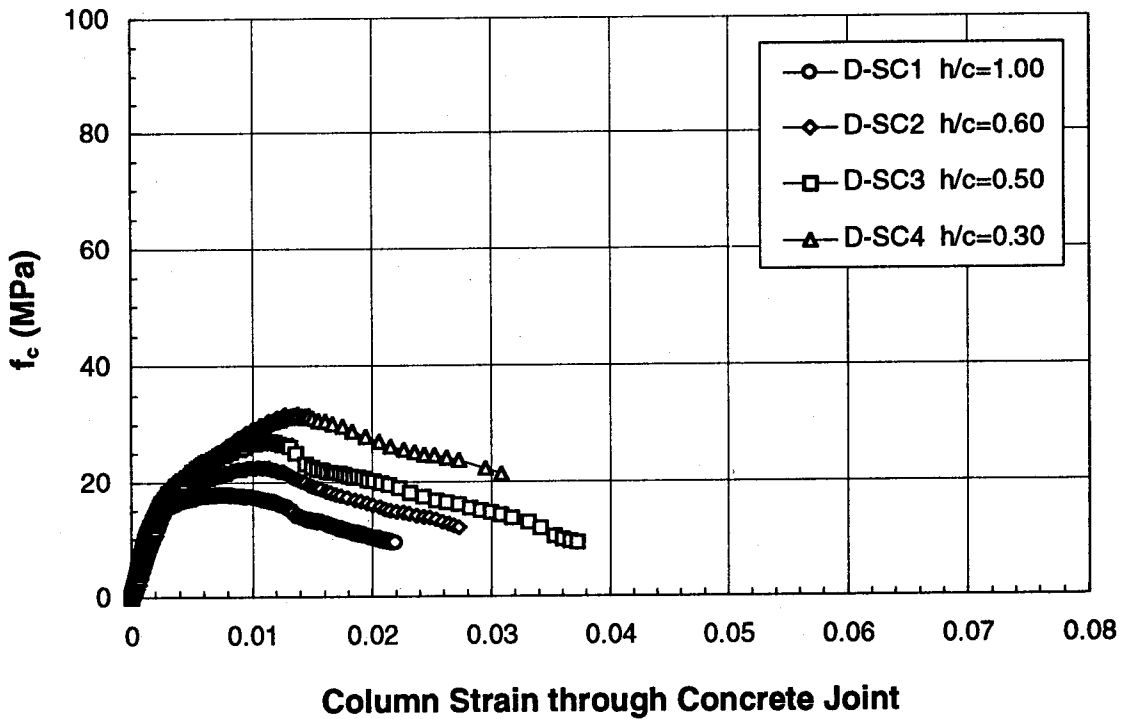
Figure 4.26   Effect of h/c on Sandwich Column Strength

82
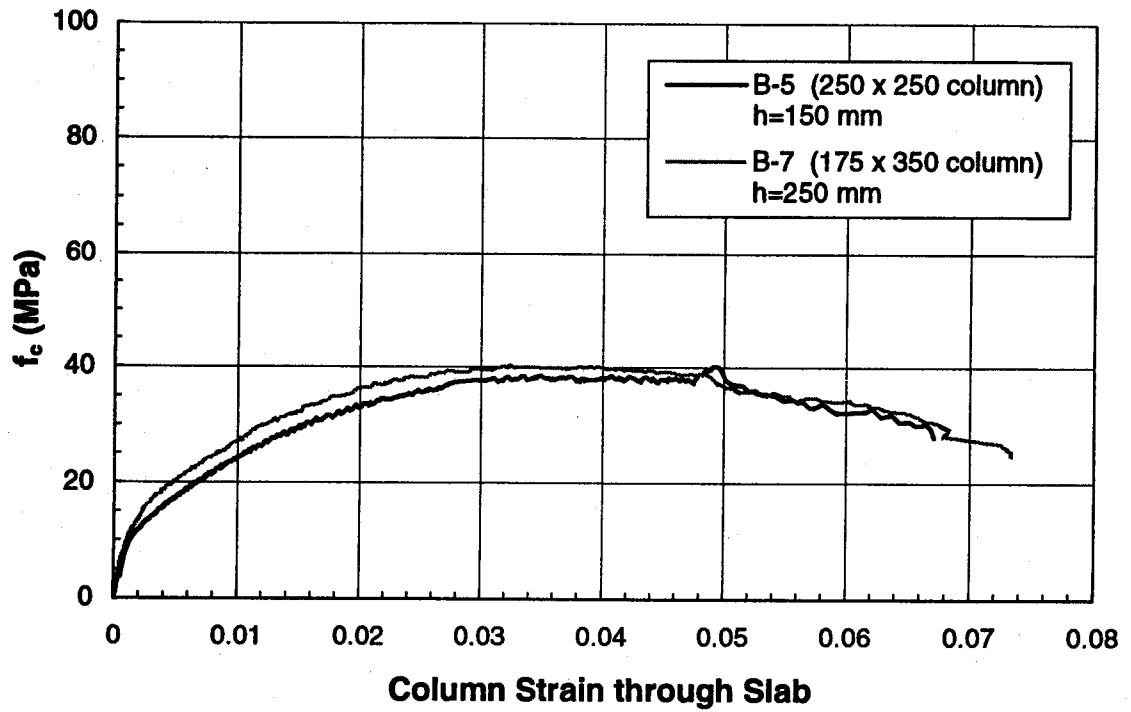
Figure 4.27   Effect of Column Rectangularity
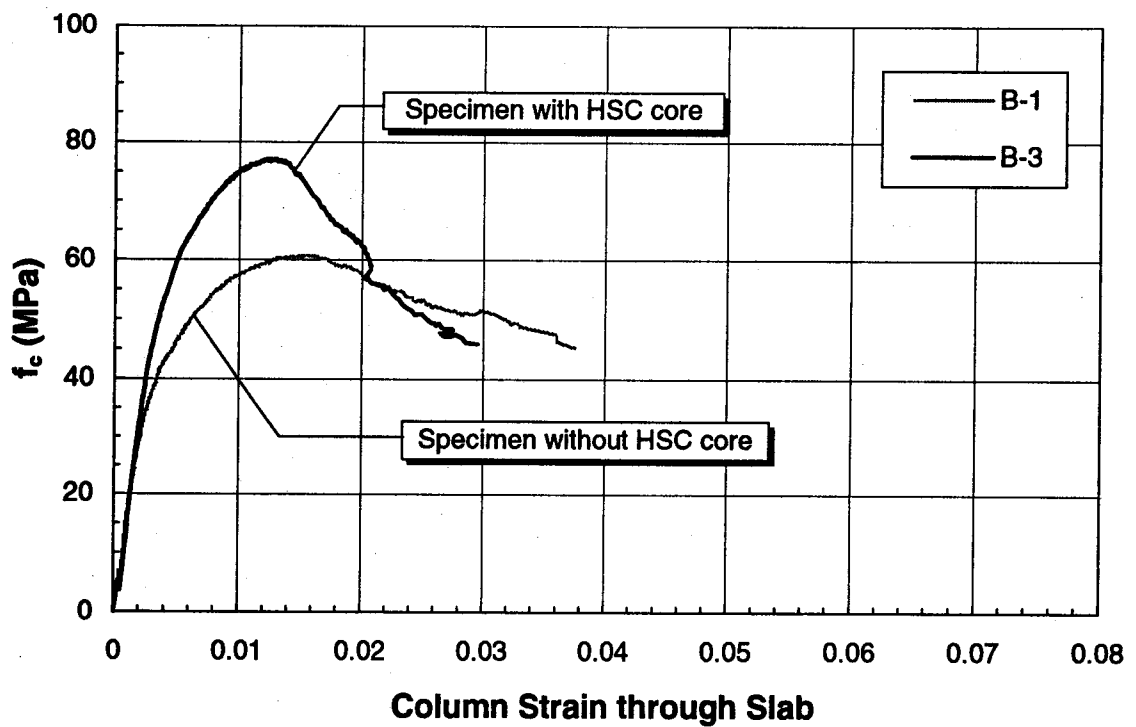
Figure 4.28   Effect of HSC Core on Joint Strength

5. EFFECT OF TEST VARIABLES

5.1 General

This chapter presents an evaluation of the variables that affect the compressive strength of reinforced concrete columns intersected by concrete slabs. Test results from this experimental program are compared with those reported in the literature. Unless noted otherwise, all column effective compressive strength values, f'_{ce}, reported in this chapter are calculated using Eq. 2.2. Existing design provisions are evaluated . Results of tests conducted in this experimental program are shown in Figs. 5.1 , 5.2 and 5.3.

5.2 Effect of Slab Loading

Values of f'_{ce}/f'_{cs} for interior and edge sandwich plates with unloaded slabs are shown in Figs. 5.4 and 5.5, respectively. These include results from this experimental program along with those presented by researchers in the past. To establish some useful comparisons, the design curves given by ACI 318-95/CSA A23.3-M84, CSA A23.3-94, Gamble and Klinar, and Kayani, are reported.

For the case of interior columns, Fig. 5.4 shows that the ACI 318-95/CSA A23.3-M84 design curve tends to overestimate the strength of columns with high f'_{cc}/f'_{cs} values. In contrast, the 1994 Canadian provisions appear to be conservative. The design equation proposed by Gamble and Klinar falls between the ACI 318-95 and the CSA A23.3-94 design curves. This equation appears to be a reasonable lower bound for the results shown. The design curve proposed by Kayani has been rearranged and expressed as a function of f'_{cc}/f'_{cs}. This design curve also represents a lower limit for the results reported. Kayani did not specify limits of applicability for his design equation. Presumably, values of f'_{ce} in excess of f'_{cc} indicate that the column will fail outside the joint.

As to edge columns, both ACI and CSA provisions are a suitable lower bound for reported tests on edge sandwich plate specimens without slab loads. Gamble and Klinar propose a more liberal equation than do the design codes. As was the case for interior columns, their design provision is an adequate lower limit for the results reported by them and by Bianchini et al. However, test results reported by Kayani and by the author fall below the design curve proposed by Gamble and Klinar. The equation proposed by Kayani is also a safe limit for the results reported. As was the case for interior columns, it may lead to column effective compressive strengths greater than the column concrete cylinder strength, for connections with f'_{cc}/f'_{cs} values less than unity.

The effect of slab loading on interior and edge sandwich plates is presented in Figs. 5.6 and 5.7. These figures show plots of f'_{ce}/f'_{cs} versus f'_{cc}/f'_{cs} for interior and edge sandwich plates subjected to three different slab load intensities. It can be concluded from these figures that as the slab load intensity increases the column strength decreases. The reduction in column strength due to slab loading is more significant for edge than for interior columns. The column strength reduction varied from 7 to 42 % for the interior

columns, and from 17 to 21 % for the edge columns. The higher reduction took place for the set of specimens with higher values of f'_{cc}/f'_{cs} and h/c.

Based on these observations, any realistic amount of slab loading would reduce the strength of the specimens tested by Bianchini et al., by Gamble and Klinar, and by Kayani. Consequently, any design provisions based solely on these test results may be unsafe. In effect, the ACI 318-95/CSA A23.3-M84 design provision appears to be unconservative, particularly for slab-column connections with high f'_{cc}/f'_{cs} values. For example, the calculated effective strength for specimen A-4C (with heavy slab load) is 39 % lower than that predicted by ACI 318-95 and the 1984 CSA standard. For f'_{cc}/f'_{cs} varying from 2.0 to 3.0, the difference between test results and the ACI 318-95/CSA A23.3-M84 predictions is not as dramatic as in the cited case. However, the results for these specimens still lie below the design curves.

In contrast, the design equation for interior columns given in the 1994 CSA standard appears to be conservative for the vast majority of tests herein reported. This design provision overestimates the strength of only one specimen (B-7), as shown in Fig. 5.1. However, this apparent unconservatism is due to setting α_1 to 0.85 rather than using the expression given in the 1994 CSA standard. Evaluation of the column effective compressive strength based on a variable α_1 will take place later in this chapter.

As far as the edge specimens are concerned, both ACI 318-95 and the 1984 and 1994 CSA provisions are identical. The design limit appears to be a reasonable lower bound for the majority of specimens tested with slab loads. Only one test result, (on specimen C2-C) falls below these design curves. This specimen was subjected to a very high slab load level that may be considered unrealistic in buildings.

The only tests on corner sandwich plates known to the authors were carried out by Bianchini et al. These specimens had no loads applied on the slabs. Noting that the compressive strength reduction due to slab loading was less significant for edge columns than for interior columns, it may then be extrapolated that slab loading will have an even smaller effect on corner columns. As a result, the imposition of slab load on the corner plates tested by Bianchini et al. would have led to a minimal decrease in the column compressive strength. This reasoning suggests that, whether loaded or not, the slab provides little confinement to a corner slab-column joint. Therefore, tests of sandwich column specimens should be representative of corner slab-column joints. As a result, tests from sandwich columns and corner sandwich plates are pooled and compared to design provisions in Fig. 5.8. It would appear that the effective compressive strength of either a sandwich column or a corner sandwich plate is independent of f'_{cc}/f'_{cs}. While the design limit given in CSA A23.3-94 is conservative for all test results, several fall below the ACI 318-95/CSA A23.3-M84 design curve. It should be noted that the sandwich column test results reported by Shu and Hawkins are not included in Fig. 5.8 for reasons that will be outlined in the following section.

5.3 Effect of h/c

The effect of h/c on the effective compressive strength of slab-column connections is related to the level of confinement provided to the joint concrete by the column ends framing into the connection. It is therefore presumed that the effect of h/c applies to both interior, edge and corner connections.

The effect of varying the ratio of the slab thickness to the column dimension, h/c, for interior sandwich plates with loaded slabs is shown in Fig. 5.9. It can be concluded that the effective compressive strength of the column decreases as the aspect ratio, h/c, increases. The column effective compressive strength dropped by 26 to 30 % for a variation in h/c from 0.6 to 1.0, and f'_{cc}/f'_{cs} from 2.48 to 6.33.

Tests specifically evaluating the effect of h/c on the compressive strength of edge columns were not carried out in this investigation. However, test results from series C specimens (reported in Table 4.1) show that as h/c increases, the effective compressive strength of an edge connection decreases.

The sandwich column test results from this investigation (series D), shown in Fig. 5.8, suggest that the effective compressive strength of corner sandwich plates is also influenced by h/c. A reduction of 21 % in the sandwich column strength was observed for a variation in h/c from 0.6 to 1.0. This reduction is similar to that observed for interior sandwich plates with similar values of f'_{cc}/f'_{cs} and h/c. This suggests that the reduction in interior column strength due to the aspect ratio effect may be eventually simulated with testing of sandwich columns, which are easier and cheaper to test.

Correction factors for the compressive strength of concrete cylinders varying with their aspect ratio have been reported in the past. Correction factors independent of the cylinder compressive strength are given in ASTM C42-90. Cylinder strength-dependent factors have been reported, among others, by Murdock and Kesler (1957). Avram et al. (1981) reported correction factors with respect to the cube strength for concrete prisms. A correction factor can be interpreted as an equivalent f'_{ce}/f'_{cs} ratio for a given h/c ratio. Figure 5.9 compares some of these correction factors with the results of sandwich column tests reported by the authors together with the results of sandwich columns with f'_{cc}/f'_{cs} of 5.6 reported by Shu and Hawkins. The reasonable agreement between the correction factor predictions and the results reported by the authors confirms the effect of h/c. However, though the results reported by Shu and Hawkins show a similar trend, the effective compressive strength of their specimens appears to be excessively high. This observation is also illustrated in Fig. 5.11.

Shu and Hawkins reported the use of 19 mm (3/4 in) size coarse aggregate in the fabrication of their sandwich columns. Moreover, the joint concrete compressive strength for the set of specimens with f'_{cc}/f'_{cs} equal to 5.6, was 6.9 MPa (1 ksi). According to their column dimensions, the joint portion of the specimens with h/c of 0.17 is as large as the coarse aggregate. This may suggest that the aggregate in the joint concrete could have

connected both upper and lower high-strength column ends, leading to an undue increase in compressive strength. However, even with this explanation, it is difficult to explain the surprising high values of f'_{ce} obtained for specimens with 6.9 MPa joint concrete and higher values of h/c. Certainly, the effective strengths reported by Shu and Hawkins are greater than those predicted by the ASTM C42 standard. However, to try to explain why the sandwich columns tested by Shu and Hawkins reached very high effective compressive strengths lies beyond the scope of this study. The fact that we were not able to reproduce their test results explains why these test data were not included in Fig. 5.8.

5.4 Effect of Column Rectangularity

The effect of column rectangularity is examined based on the comparison of two sets of interior sandwich plate specimens, each built with identical slab thicknesses and values of f'_{cc}/f'_{cs} but with different column shapes (B-5, B-6, B-7 and B-8). Results from these tests are compared in Fig. 5.12. As expected, the values of f'_{ce}/f'_{cs} were lower for the specimens with thicker slabs compared to those with thinner slabs. Moreover, the specimens with square columns outperformed the comparable rectangular column specimens by 14 to 21 %.

This suggests that one can account for the effect of column rectangularity by choosing an appropriate value of c to be used in the evaluation of the aspect ratio, h/c. This has the advantage of not introducing an additional parameter for the prediction of f'_{ce}. From Fig. 5.12 it is clear that defining the smallest column dimension will result in the appropriate decrease in predicted effective compressive strength.

The test result of one of the rectangular column specimens (B-7) falls below the design equation given by CSA A23.3-94. As discussed earlier, this is because data for Fig. 5.12 were processed using α_1 equal to 0.85 rather than the variable expression given in the 1994 CSA standard. As to ACI 318-95/CSA A23.3-M84, the design limit is unconservative for the two tests of rectangular column sandwich plate specimens reported in this investigation.

Thus far, the effect of column rectangularity has not been considered in the development of existing design provisions. It should be kept in mind that the evaluation of the column rectangularity effect herein reported is based on only four test results. Additional tests are required to confirm the validity of the conclusions.

5.5 Effect of High-Strength Concrete Core at the Joint Region

Figure 5.13 shows the effect of the inclusion of a high-strength concrete core in the joint region of a slab-column connection. According to this figure, the specimen with high-strength core (B-3) outperformed the conventionally built specimen by 21 %.

Use of high-strength cores in slab-column joints may be more effective in larger scale columns where a larger core area is available. This procedure is a possible alternative that

88

avoids the logistical problems associated with puddling and the congestion of reinforcement associated with the addition of dowels in the joint. Additional testing of sandwich plates with high-strength concrete cores is required to establish a more reliable conclusion.

5.6 Evaluation of the Effective Column Compressive Strength, f'_{ce}, with Variable α_1

Evaluation of the stress block factors in the 1994 Canadian code differs from ACI 318-95/CSA A23.3-M84. In ACI 318-95/CSA A23.3-M84 the α_1 factor is assumed constant and equal to 0.85. In CSA A23.3-94, the α_1 factor is defined in terms of the compressive strength of concrete, as indicated in Eq. 5.1.

$$\alpha_1 = 0.85 - 0.0015 f'_c \geq 0.67 \tag{5.1}$$

Re-writing Eq. 2.2 with the constant 0.85 replaced by α_1 results in:

$$f'_{ce} = \frac{P_{col,max} - f_y A_{st}}{\alpha_1 \left(A_g - A_{st} \right)} \tag{5.2}$$

Combining Eqs. 5.1 and 5.2 produces a quadratic expression in α_1 whose solution is given as follows:

$$\alpha_1 = \frac{0.85 + \sqrt{0.85^2 - 0.006k}}{2} \geq 0.67 \tag{5.3a}$$

$$\text{where} \quad k = \frac{P_{col,max} - f_y A_{st}}{\left(A_g - A_{st} \right)} \tag{5.3b}$$

Table 5.1 shows the values of the α_1 factor and the corresponding effective compressive strength, f'_{ce}, of the specimens tested in this investigation. In all cases, the calculated values are less than 0.85. Consequently, the values of the effective compressive strength, f'_{ce}, always exceed those calculated based on a constant α_1 factor equal to 0.85.

The effect of the non-constant α_1 is greatest where f'_{ce} is large. This usually occurs in cases with relatively high values of f'_{cs} and correspondingly modest values of f'_{cc}/f'_{cs}. The effect is minimal in cases that combine very high-strength column concrete and normal strength slab concrete. This means that the calculated effective strength of a connection with very high values of f'_{cc}/f'_{cs} is only slightly increased by using the variable α_1 in lieu of the constant α_1.

Series	Specimen	h/c	$\dfrac{f'_{cc}}{f'_{cs}}$	α_1	f'_{ce} (MPa)	$\dfrac{f'_{ce}}{f'_{cs}}$
A	A1-A	0.5	2.63	0.67	127.25	3.18
	A1-B	0.5	2.63	0.67	117.4	2.93
	A1-C	0.5	2.63	0.69	108.23	2.71
	A2-A	0.5	2.43	0.67	123.6	2.69
	A2-B	0.5	2.43	0.67	123.1	2.68
	A2-C	0.5	2.43	0.68	112.91	2.45
	A3-A	0.75	3.56	0.69	105.24	4.21
	A3-B	0.75	3.56	0.71	92.85	3.71
	A3-C	0.75	3.56	0.77	55.53	2.22
	A4-A	0.75	4.61	0.70	97.37	4.23
	A4-B	0.75	4.61	0.73	81.91	3.56
	A4-C	0.75	4.61	0.76	59.42	2.58
B	B-1	1.0	2.48	0.72	83.99	2.0
	B-2	0.6	2.48	0.67	121.89	2.9
	B-3	1.0	2.57	0.68	113.43	2.58
	B-4	0.6	2.57	0.67	144.61	3.29
	B-5	1.0	6.33	0.78	49.82	3.32
	B-6	0.6	6.33	0.74	74.67	4.98
	B-7	0.7	6.32	0.77	52.27	2.75
	B-8	1.17	6.32	0.72	84.99	4.47
C	C1-A	0.74	3.34	0.75	67.9	2.12
	C1-B	0.74	3.06	0.76	62.04	1.77
	C1-C	0.74	3.15	0.76	59.41	1.75
	C2-A	1.0	3.48	0.76	58.74	1.89
	C2-B	1.0	3.18	0.77	53.79	1.58
	C2-C	1.0	3.27	0.78	48.23	1.46
D	D-SC1	1.0	6.18	0.82	21.83	1.28
	D-SC2	0.6	6.18	0.81	28.0	1.65
	D-SC3	0.5	6.29	0.80	33.89	1.99
	D-SC4	0.3	6.18	0.79	40.21	2.37

Table 5.1   Evaluation of Column Effective Compressive Strength
Based on a Variable α_1
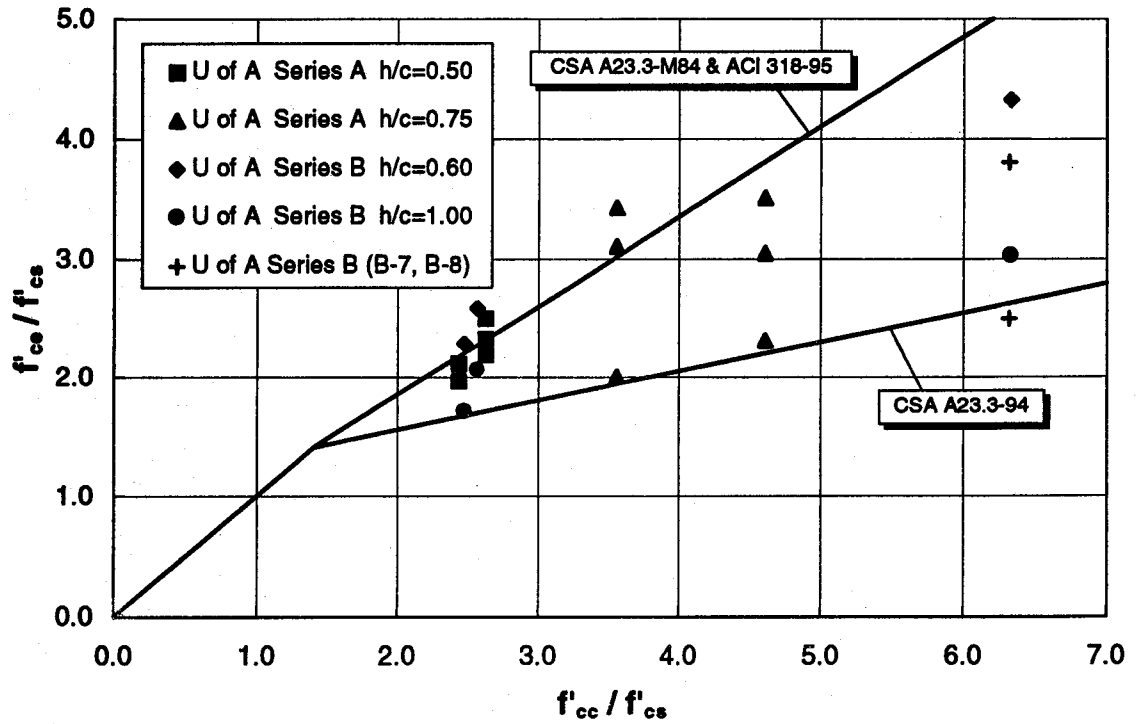
Figure 5.1   Test Results of Interior Sandwich Plates
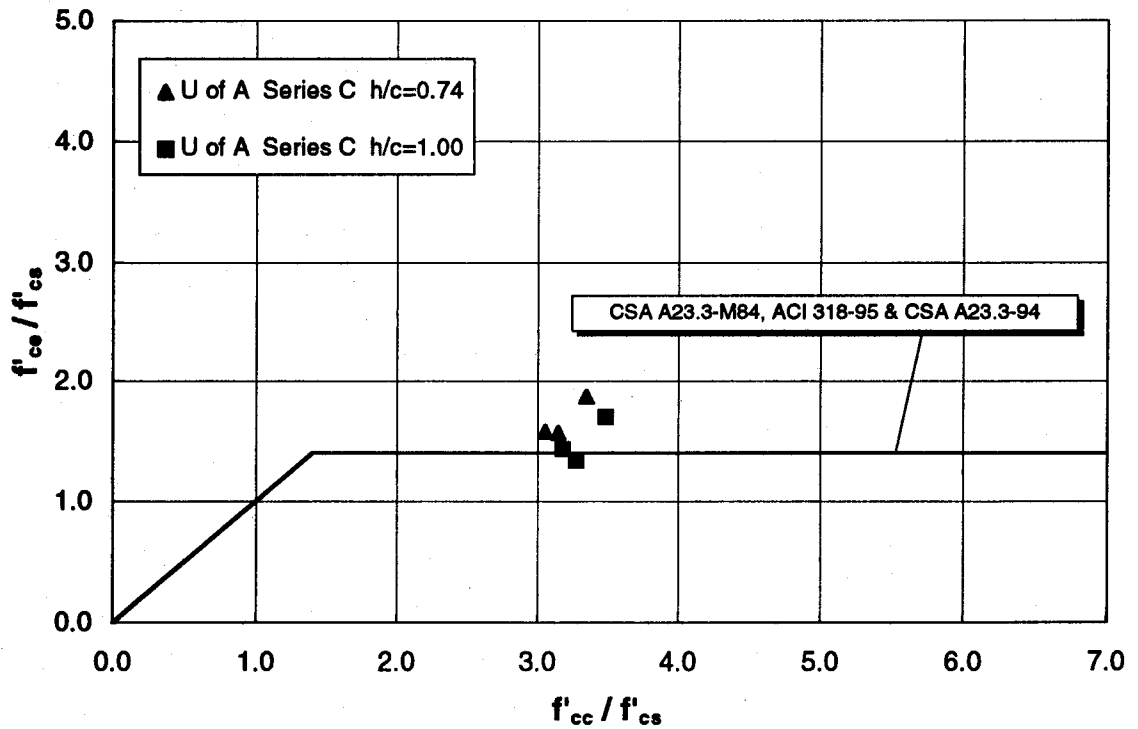
Figure 5.2   Test Results of Edge Sandwich Plates
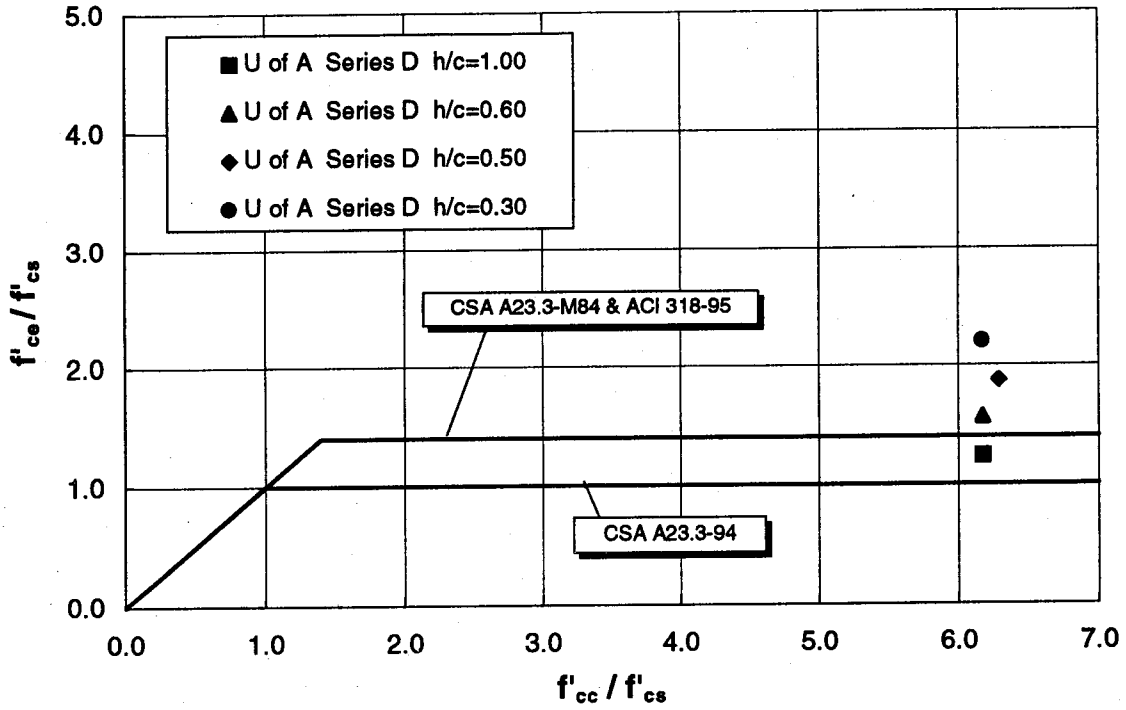
Figure 5.3 Test Results of Sandwich Columns
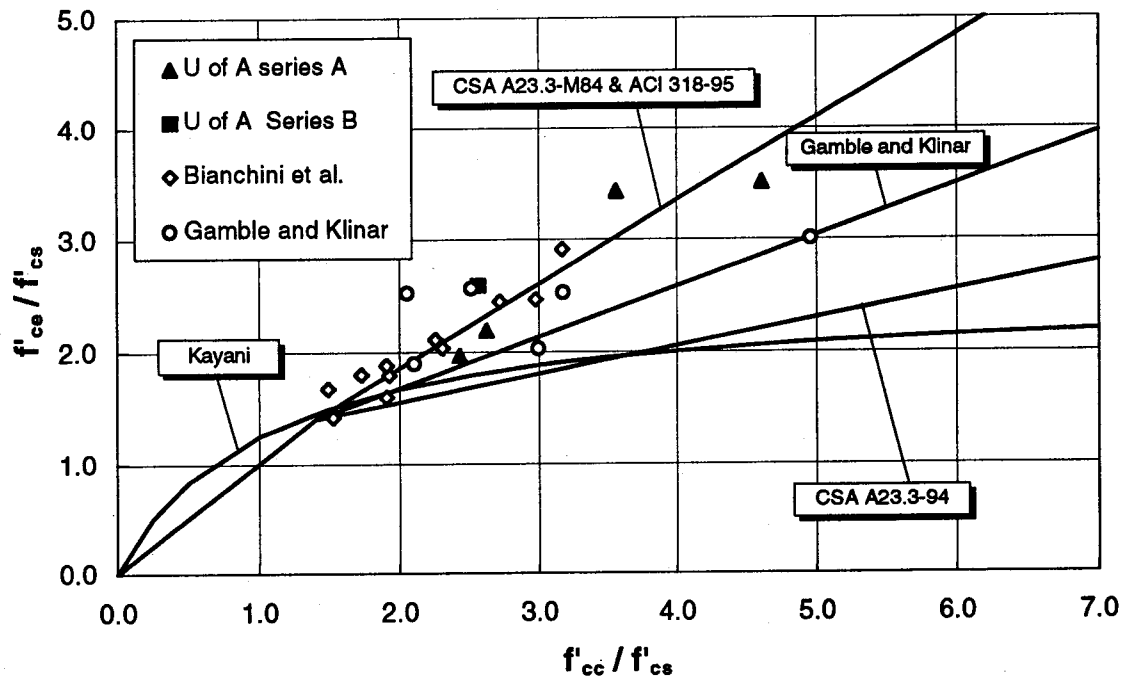
Figure 5.4 Tests of Interior Sandwich Plates
- Unloaded Slabs -
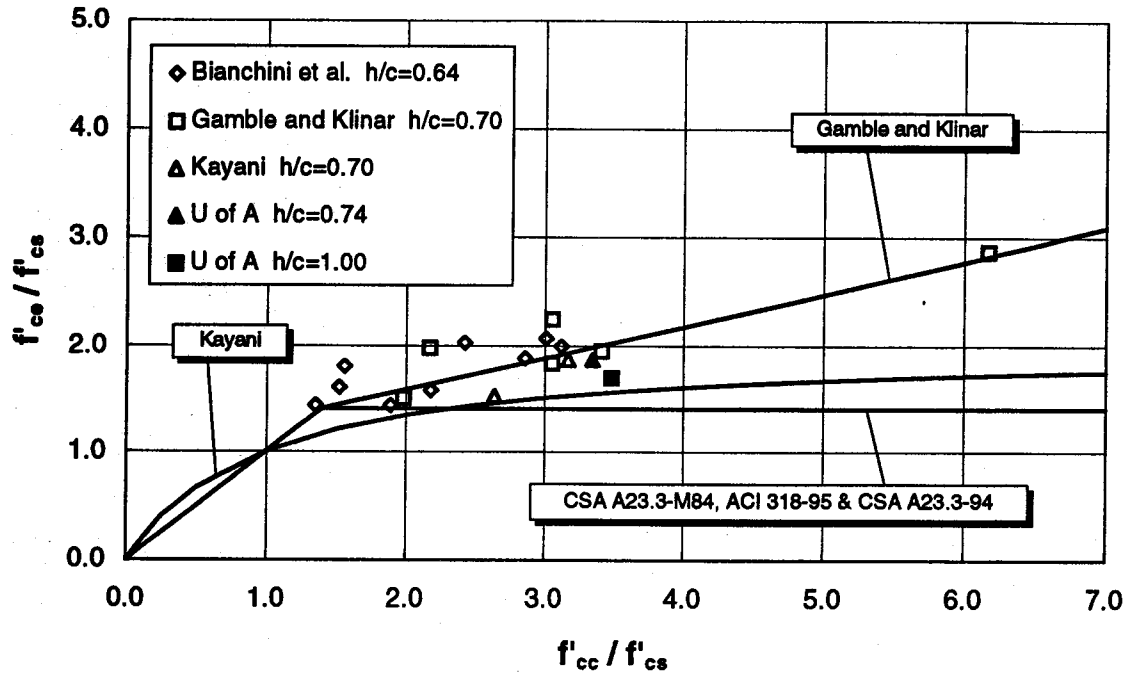
Figure 5.5   Tests of Edge Sandwich Plates
- Unloaded Slabs -
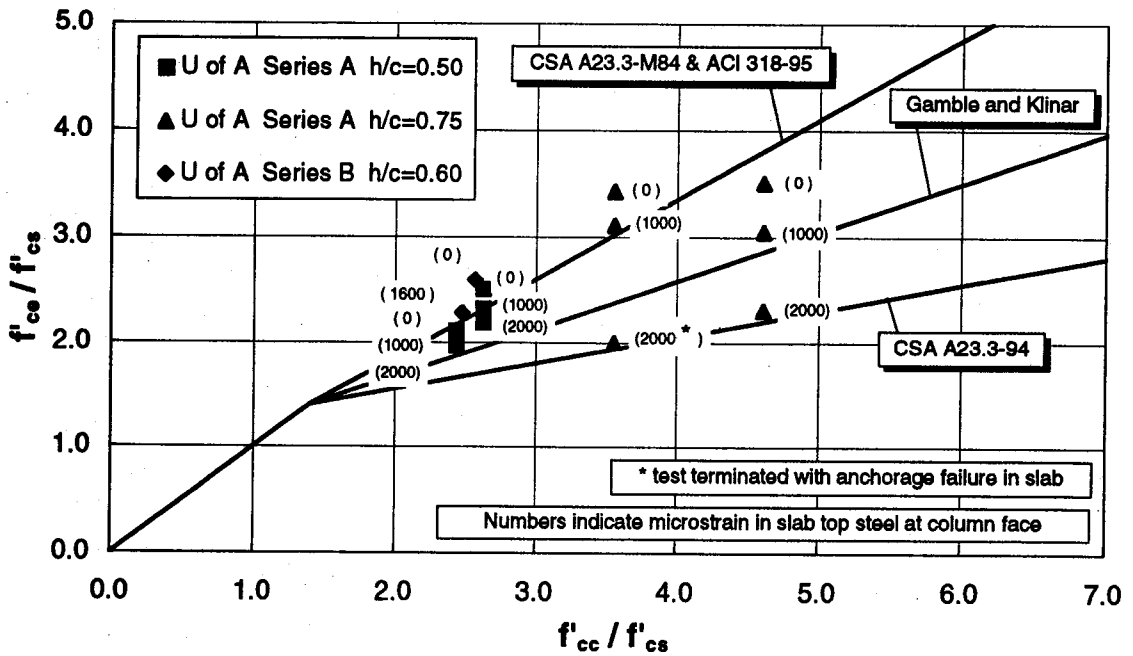
Figure 5.6   Interior Sandwich Plates : Slab Load Effect
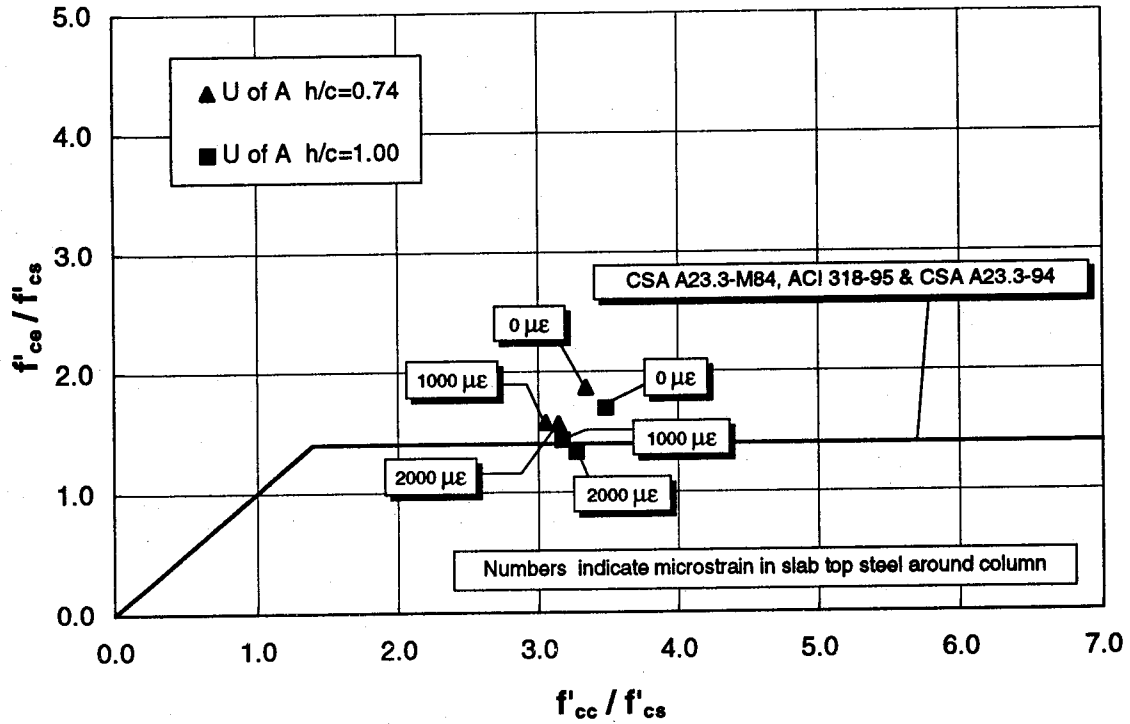
Figure 5.7   Edge Sandwich Plates : Slab Load Effect
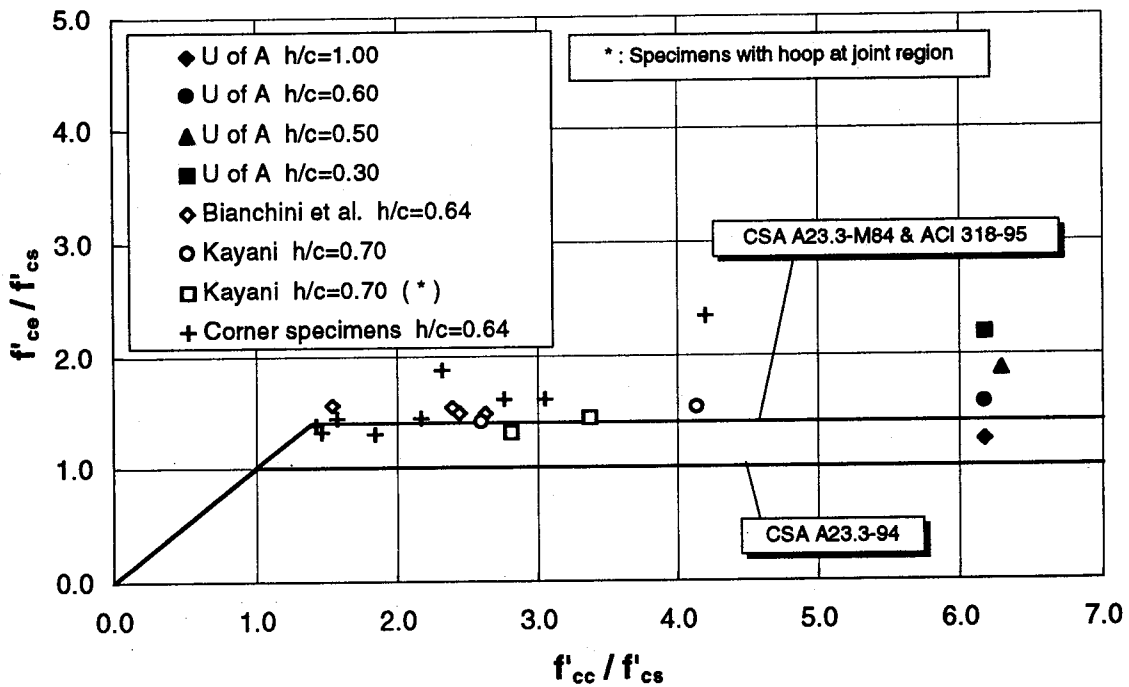
Figure 5.8   Test Results of Corner Sandwich Plates and Sandwich Columns

94
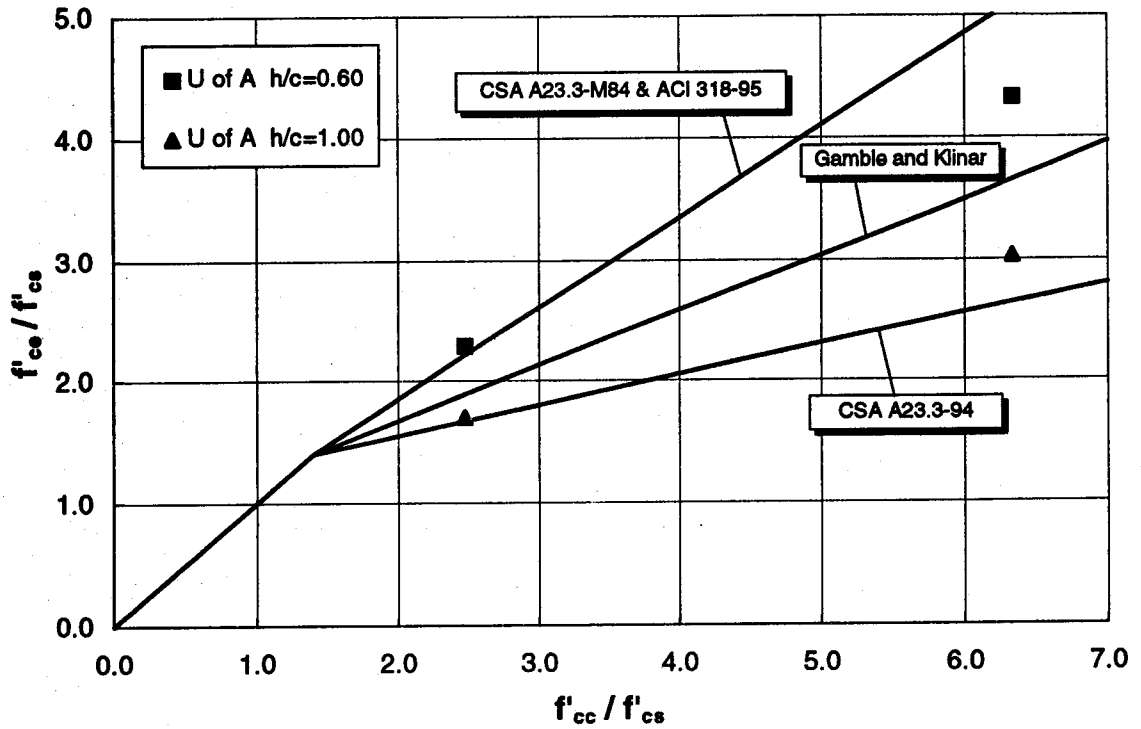
Figure 5.9 Interior Sandwich Plates : Effect of h/c
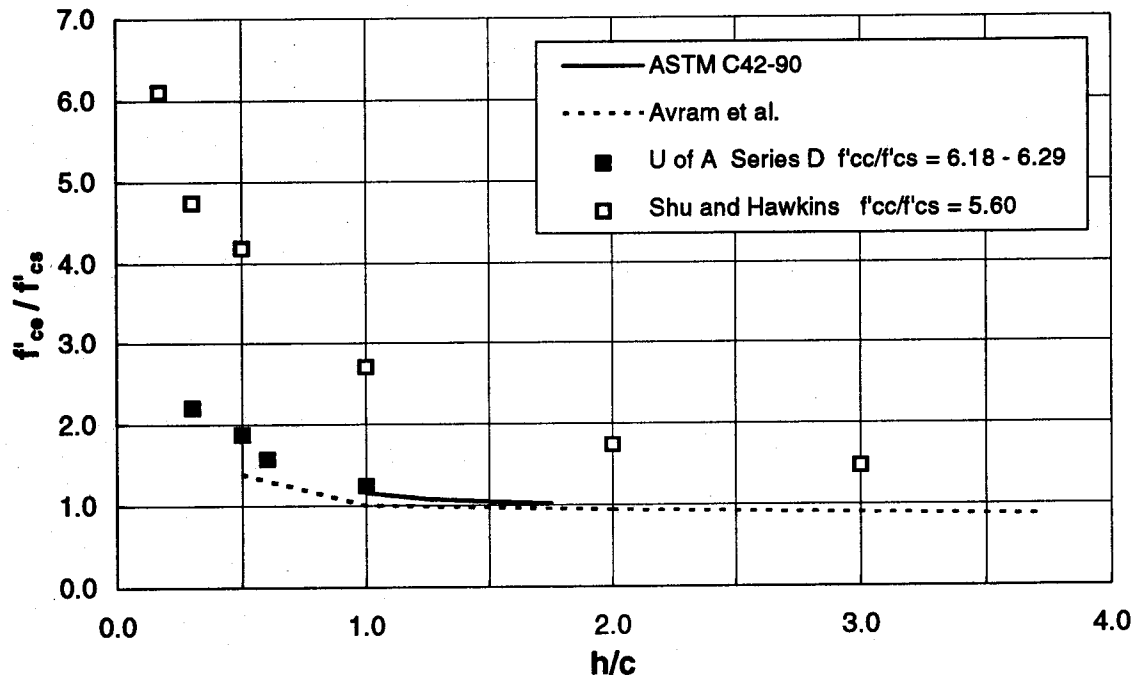
**Figure 5.10 Comparison between SC Tests and Correction
Factors for Cylinder and Cube Tests**
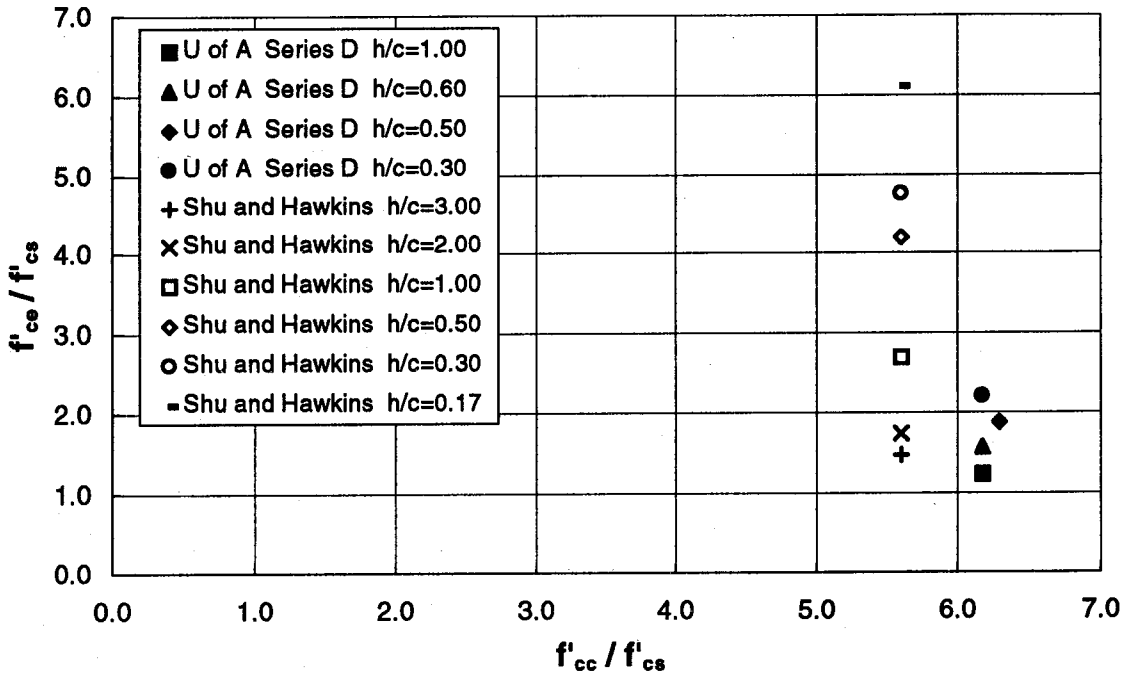
Figure 5.11   Comparison of Test Results of Sandwich Columns
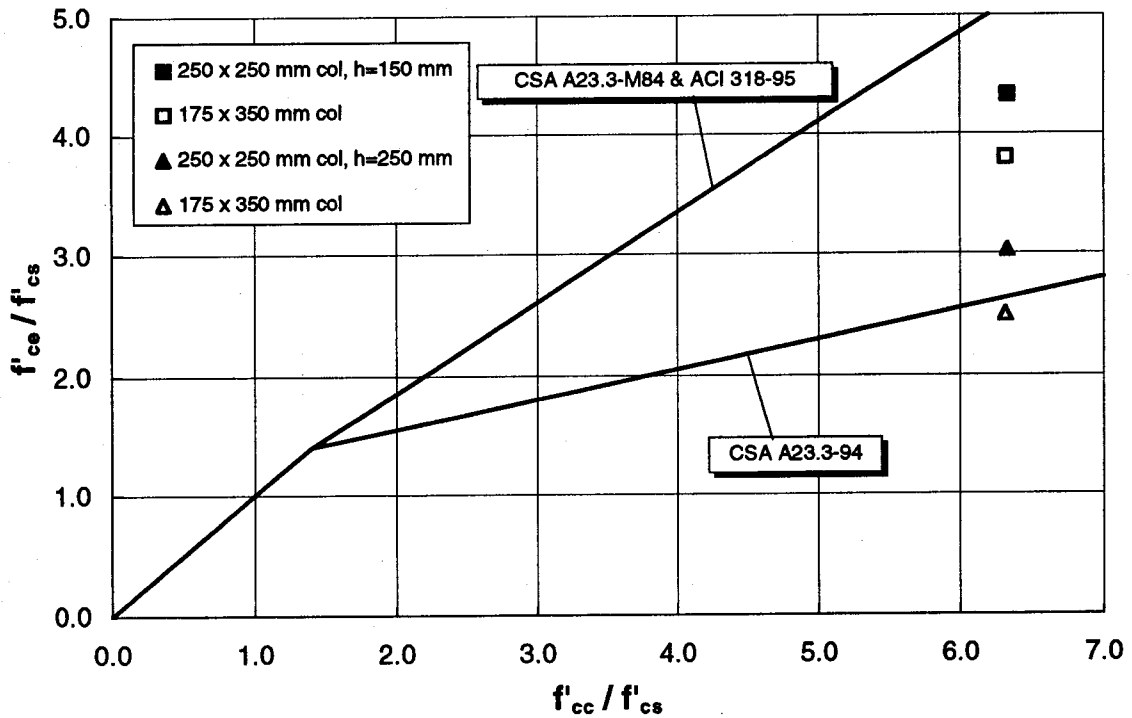
Figure 5.12   Effect of Column Rectangularity
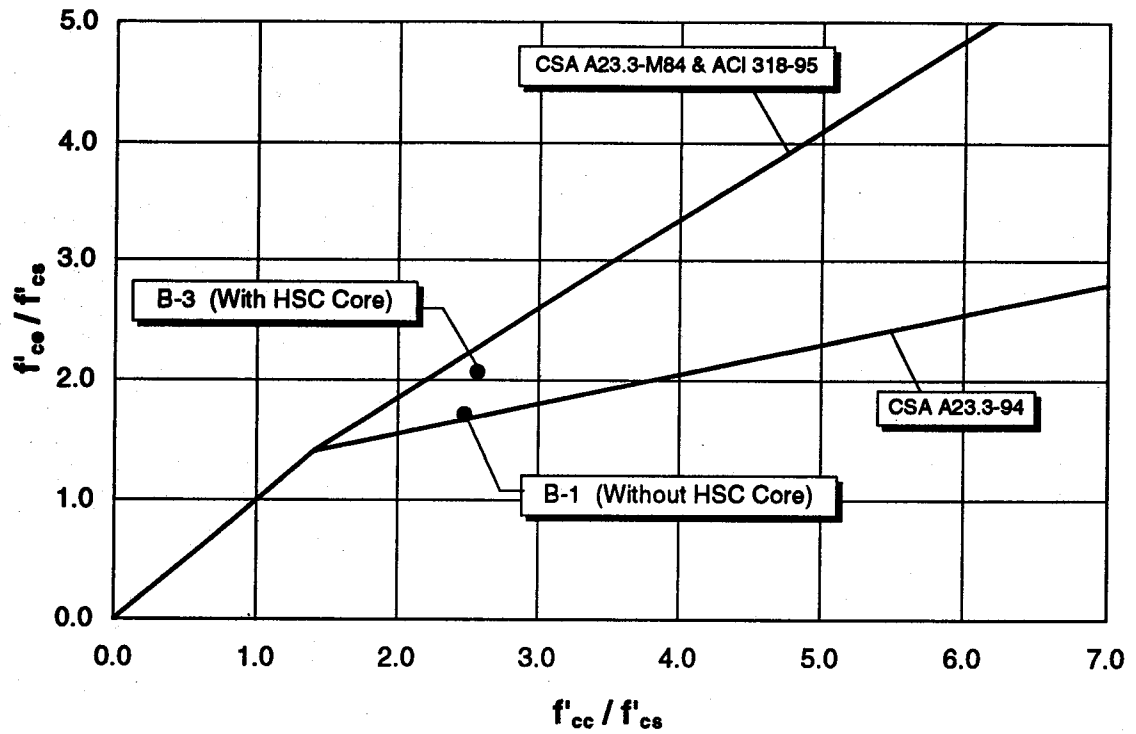
Figure 5.13   Effect of HSC Core on Interior Joint Strength
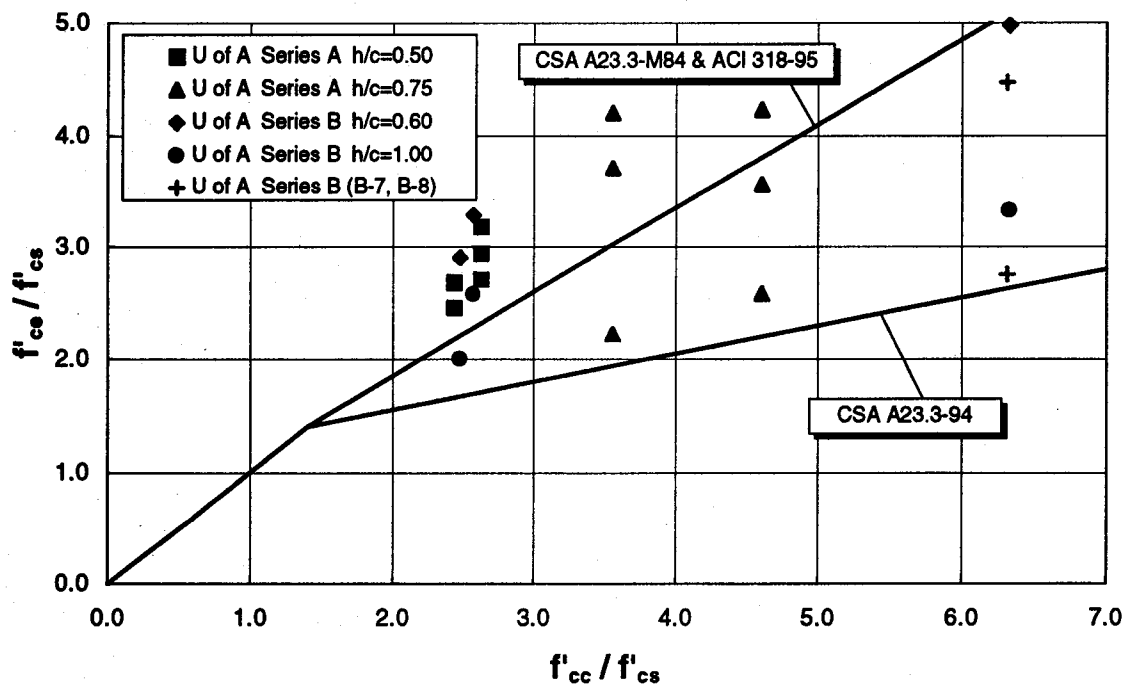
**Figure 5.14   Test Results of Interior Sandwich Plates
Evaluated with Variable α_1**
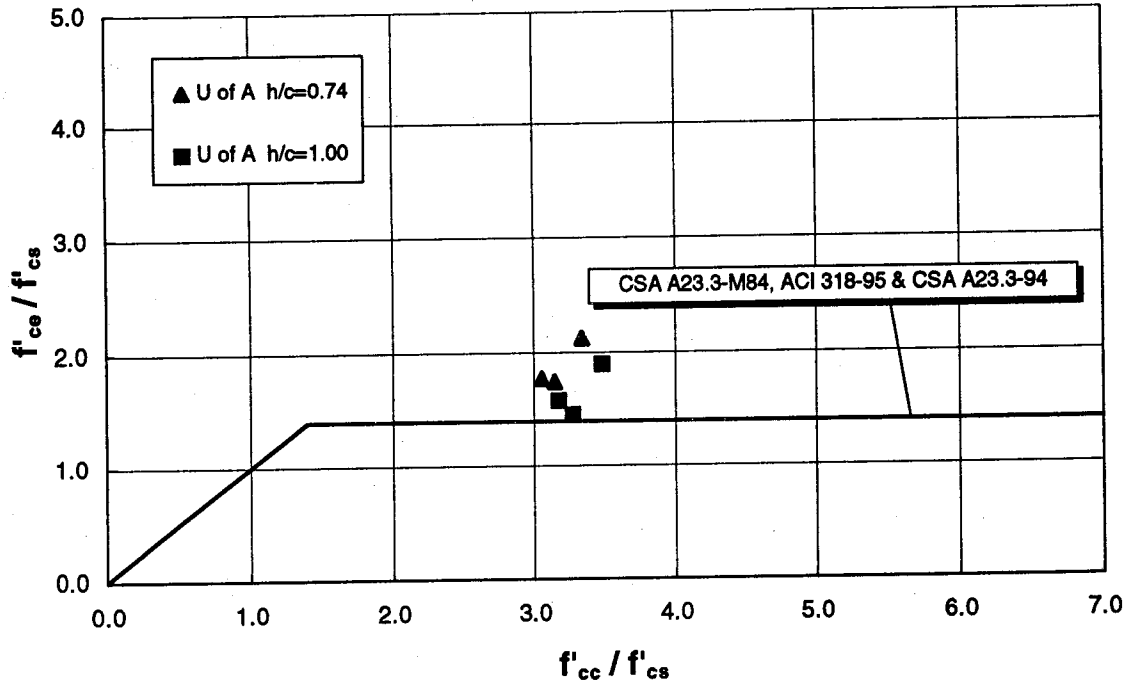
Figure 5.15   Test Results of Edge Sandwich Plates Evaluated with Variable α_1
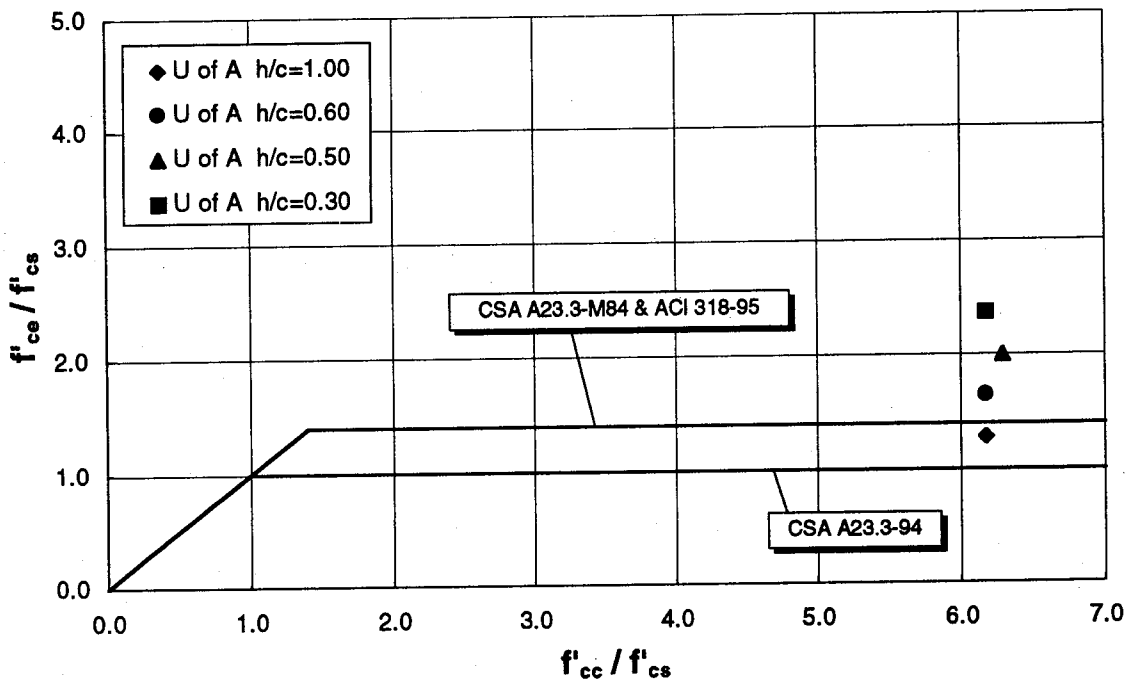
Figure 5.16   Test Results of Sandwich Columns Evaluated with Variable α_1

6. PROPOSED DESIGN PROVISIONS

6.1 Interior Columns

Design provisions in the current ACI and CSA codes define the effective column compressive strength as a weighted average of the slab and column concrete strengths. There is no experimental evidence to suggest anything wrong with this approach.

Both Standards use a value of f'_{cc}/f'_{cs} of 1.4 as the limit beyond which the compressive strength of an interior column is reduced by the intervening slab concrete. While the results of this investigation are not inconsistent with this limiting value, there are insufficient test data from connection specimens with loaded slabs to make a definitive statement.

Examination of current design provisions in light of the test results on interior sandwich plate specimens with loaded slabs infers that the design curve given by CSA A23.3-94 appears to be satisfactory for interior connections with h/c equal to 1.0. Conversely, the design curve given in ACI 318-95/CSA A23.3-M84 is very unconservative for h/c values equal to 1.0 while only slightly unconservative for h/c equal to 0.6.

In view of the preceding statements, Eq. 6.1 is proposed for the design of interior reinforced concrete columns intersected by concrete floors.

$$f'_{ce} = \left(1.4 - \frac{0.35}{h/c}\right)f'_{cs} + \frac{0.25}{h/c}f'_{cc} \quad \leq f'_{cc}$$

where h/c shall not to be taken less than one-third.   [6.1]

Equation 6.1 follows the same format as the existing design provisions. For h/c equal to one, it matches the expression given in CSA A23.3-94. For h/c equal to one-third, it matches the expression given in ACI 318-95/CSA A23.3-M84. To account for column rectangularity, c is defined as the shortest column dimension.

Figure 6.2 shows predictions using Eq. 6.1 for h/c ratios of 0.6 and 1.0 and the corresponding test results, based on a constant α_1 factor equal to 0.85. Test results show that effective compressive strength predictions are safe in all cases.

Table 6.1 shows the ratios of test-to-predicted effective compressive strength for the series B interior sandwich plate specimens subjected to slab loads. These ratios were calculated based on a constant α_1 of 0.85. Results using ACI 318-95/CSA A23.3-M84 and the proposed design equation are compared.

On average, ratios of test-to-predicted column effective strengths less than 1.0 were obtained with the ACI 318-95 design equation. In the worst case, the ACI design equation

99

overestimated the effective compressive strength of the connection by over 100 %. Using the CSA A23.3-94 provisions, the average ratio of test to predicted strength is in excess of unity. At its most conservative, the 1994 CSA procedure underestimated the effective strength by about 40 %.

Results using the proposed equation are on average closer to unity than those of either of the existing design Standards. Moreover, the scatter of the predicted results is markedly reduced as evidenced by a coefficient of variation of 9 % compared to 24 % and 19 % for the ACI 318-95 and CSA A23.3-94 equations, respectively.

6.2 Edge Columns

This investigation supports the design equation for edge columns given by CSA A23.3-94 and by ACI 318-95. This equation is given as

$$f'_{ce} = 1.4 f'_{cs} \leq f'_{cc} \qquad [6.2]$$

The limit set by this equation is shown in Fig. 6.3. For comparison, the results on edge sandwich plates with heavily loaded slabs are included. This design provision appears to be a reasonable lower bound for the majority of test results. Only one test result falls immediately below this design equation. However, this test result corresponds to an edge plate specimen loaded with very heavy slab loads. Slab load intensities close to the load level applied over this specimen may be unlikely to occur in a typical residential or office building.

6.3 Corner Columns and Unconfined Joints

All available results from corner sandwich plate and sandwich column tests are presented in Fig. 6.4. The design equation proposed in CSA A23.3-94 for the design of corner columns appears to be conservative for all results shown. Conversely, the design limit given by ACI 318-95 is unconservative in many cases. Based on the available test results, a f'_{cc}/f'_{cs} value of 1.2 appears also to be a safe lower bound. Beyond this limit, the value of f'_{ce}/f'_{cs} appears to be independent of f'_{cc}/f'_{cs}. Accordingly, the proposed design provision for the design of corner columns is given as follows.

$$f'_{ce} = 1.2 f'_{cs} \leq f'_{cc} \qquad [6.3]$$

100

Specimen		ACI 318-95		CSA A23.3-94		Authors	
Mark	$f'_{ce,test}$	$f'_{ce,calc}$	$\dfrac{f_{ce,test}}{f_{ce,calc}}$	$f'_{ce,calc}$	$\dfrac{f_{ce,test}}{f_{ce,calc}}$	$f'_{ce,calc}$	$\dfrac{f_{ce,test}}{f_{ce,calc}}$
B-1	71.54	92.70	0.77	70.10	1.02	72.10	1.02
B-2	96.08	92.70	1.04	70.10	1.37	77.63	1.24
B-3	90.72	100.15	0.91	74.45	1.22	74.45	1.22
B-5	45.44	76.50	0.59	39.50	1.15	39.50	1.15
B-6	64.83	76.50	0.85	39.50	1.64	51.83	1.25
B-7	47.45	96.65	0.49	49.95	0.95	42.93	1.11
B-8	72.25	96.65	0.75	49.95	1.45	53.75	1.34
Mean :			0.77		1.26		1.19
Standard Deviation :			0.1848		0.2448		0.1065
C.O.V. :			24 %		19 %		9 %

Notes: 1. $f'_{ce,test}$ values were calculated based on α_1 equal to 0.85.
2. Specimen B-4 was not subjected to slab loading.

Table 6.1   Ratios of Test-to-Predicted Column Effective Compressive Strength for Interior Slab-Column Connections
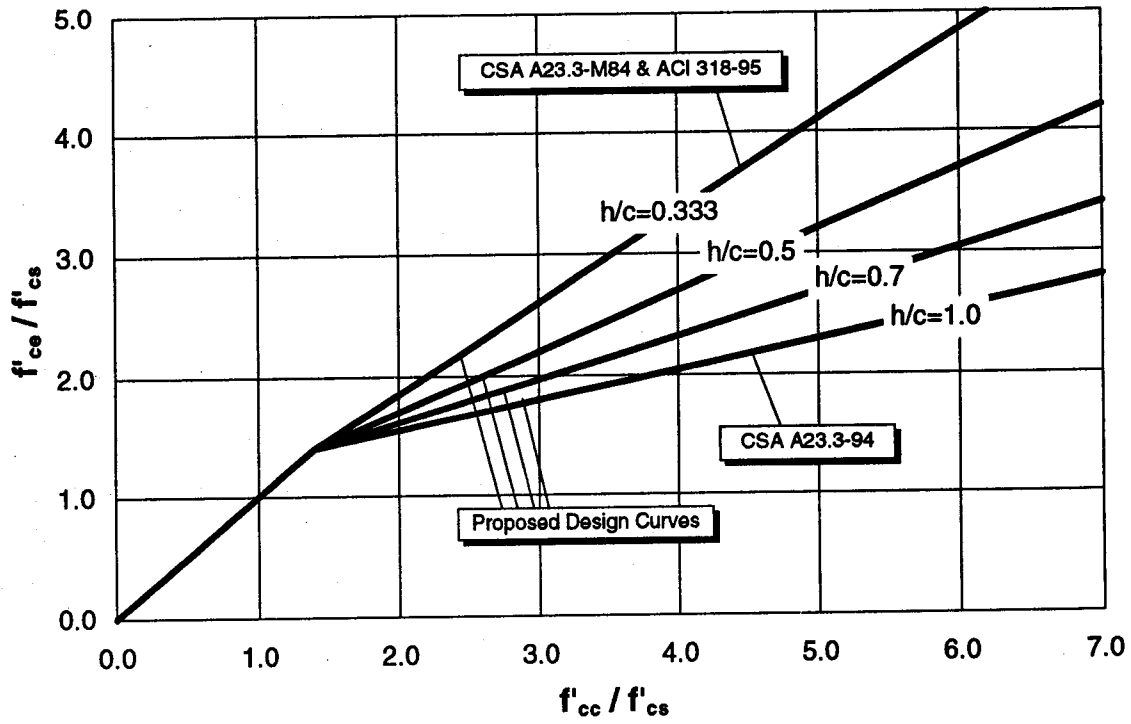
Figure 6.1 Proposed Design Curves for Interior Columns
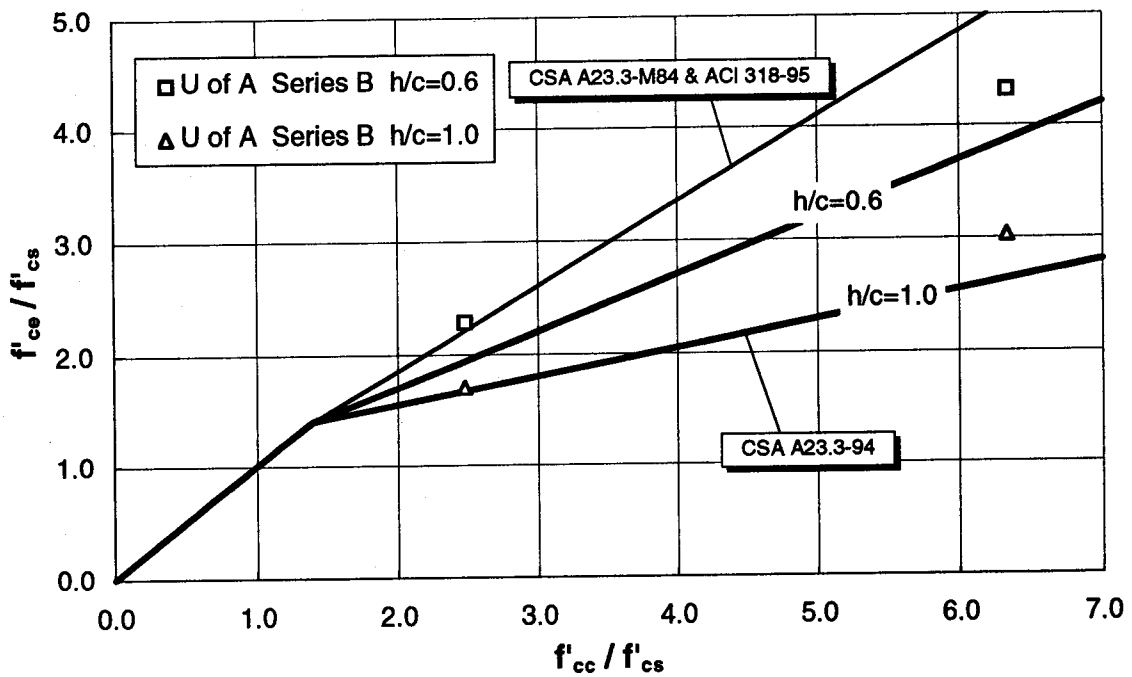
Figure 6.2 Comparison of Design Curve Predictions
with Interior Sandwich Plate Test Results
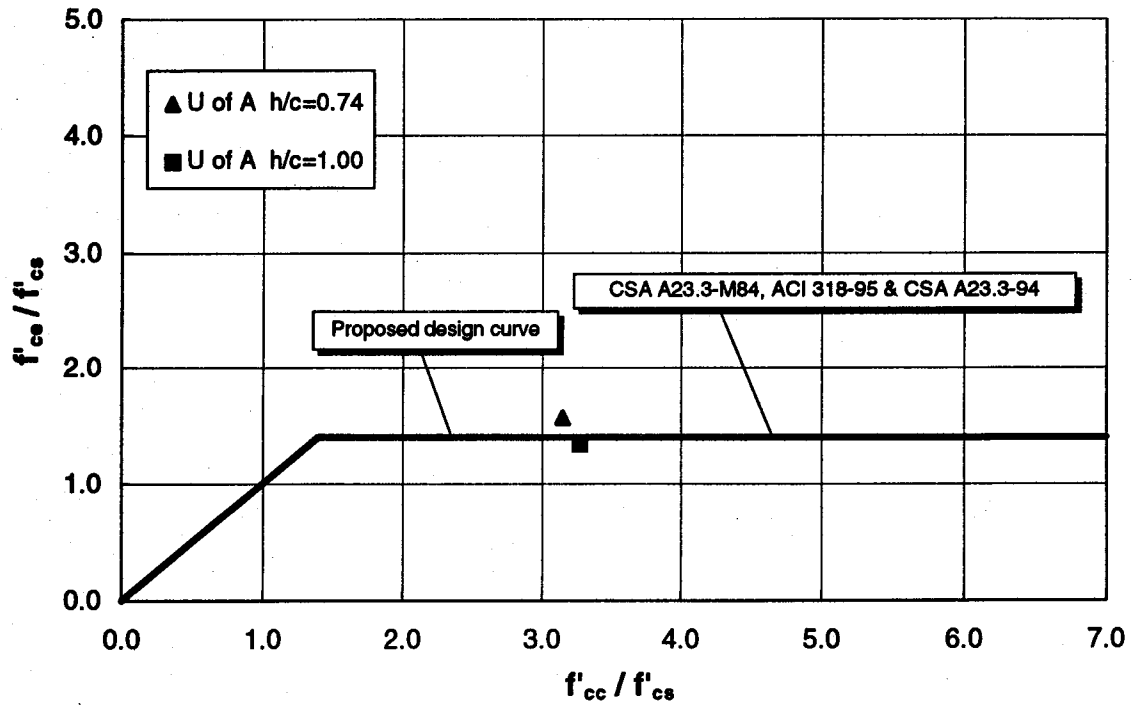
Figure 6.3   Proposed Design Curve for Edge Columns
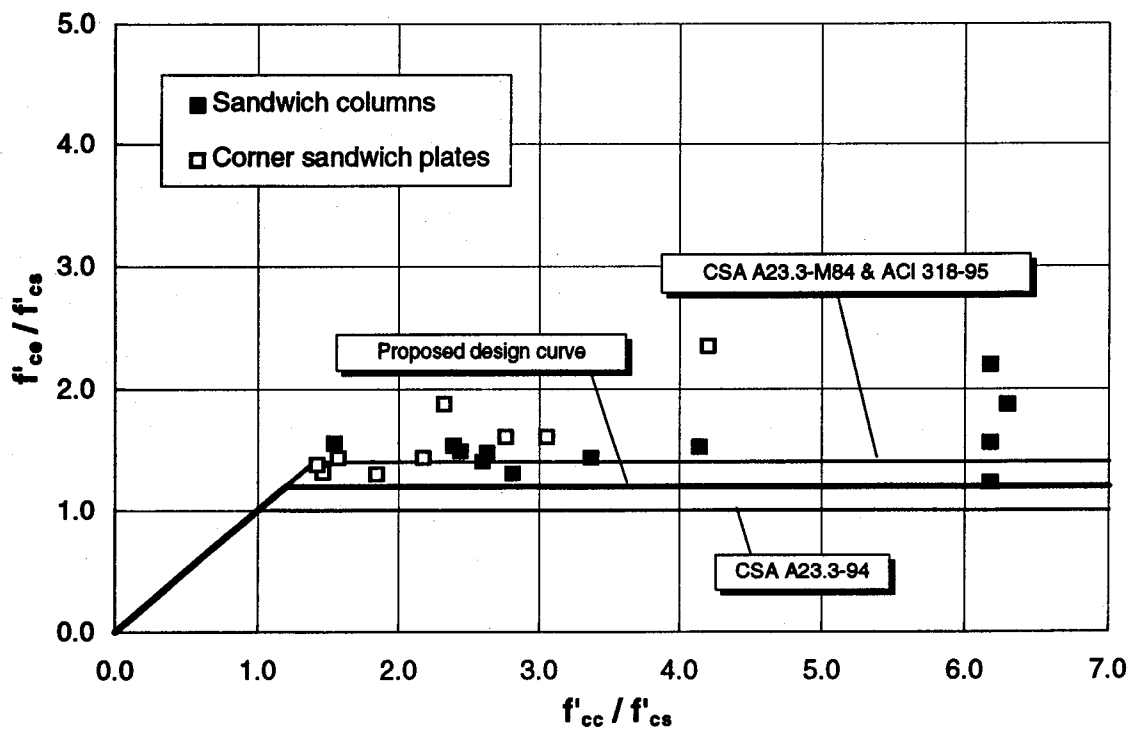
Figure 6.4   Proposed Design Curve for Corner Columns

7. SUMMARY, CONCLUSIONS AND RECOMMENDATIONS

7.1 Summary

Because columns in modern reinforced concrete buildings are often cast with concrete much stronger than that used in the floors, it is important to evaluate the effect that the weaker concrete will have on the compressive strength of the column. The main factor that determines the strength of the floor portion of a column is the amount of confinement applied over the joint region by the surrounding floor concrete. Two main variables that may substantially modify this confinement regime are the level of gravity load applied on the slab and the ratio of the slab thickness to column dimension, h/c.

A literature survey showed that the only variable thus far accounted for in the evaluation of the strength of the floor portion of a column has been the ratio of column to slab concrete strength, f'_{cc}/f'_{cs}. The literature review also showed that neither the slab loading nor the aspect ratio, h/c, have been considered. These observations led to the experimental program developed in this study.

Results from 30 specimens simulating slab-column joints are presented in this study. Of these, 26 were sandwich plate specimens and four were sandwich columns. Sandwich plate specimens consist of two high-strength concrete column stubs intersected by a slab segment. Sandwich column specimens consist of two high-strength concrete column ends intersected only by a layer of slab concrete.

The experimental program was divided into four series. Series A examined the effect of slab loading on interior slab-column connections. Twelve sandwich plate specimens were built and tested for this purpose. Series B examined the effect of aspect ratio, h/c, column rectangularity and the placement of high-strength core within the joint region, as well as the effect of slab loading on the column strength. Eight sandwich plates were built and tested. Series C consisted of six edge sandwich plate specimens that were tested to evaluate the effect of slab loading on edge slab-column connections. Series D consisted of four sandwich column specimens. The main objective of this series was to evaluate the effect of h/c on the compressive strength of unconfined joints.

Sandwich plate specimens were subjected to either column load or to column load plus slab loads. Sandwich column specimens were subjected to column load only. Column concrete strengths varied from 89 to 120 MPa. Slabs and unconfined joint concrete strengths varied from 15 to 46 MPa.

According to test results, three design provisions were developed to evaluate the effective compressive strength of interior, edge and corner reinforced concrete columns intersected by concrete slabs.

7.2 Conclusions

7.2.1 Conclusions from Testing

1. As the level of load applied on the slab increases the effective compressive strength of the column decreases. This decrease in strength is higher for specimens with columns built with concrete much stronger than that used in the floor.

2. The slab thickness-to-column width ratio, h/c, is important in determining the effective compressive strength of a column. As this ratio increases, the effective compressive strength of the column decreases. This reduction is greater for higher ratios of column concrete cylinder strength to slab concrete cylinder strength, f'_{cc}/f'_{cs}. The effect of h/c is greater for interior connections than for edge and corner connections.

3. For rectangular columns, it is the shortest column dimension that should be used in calculating the h/c ratio.

4. Placement of a high-strength concrete core within the joint region increases the strength of the column.

7.2.2 Conclusions Regarding Design Provisions

1. Design provisions should be based on results of connection specimens tested with slab loads. Omission of the slab load effect leads to unconservative designs. For this reason, the design equations contained in ACI 318-95 and CSA A23.3-M84 to evaluate the effective compressive strength of reinforced concrete columns intersected by concrete floors are not adequate. CSA A23.3-94 provides for a lower bound for available results on connection specimens with loaded slabs.

2. No existing code procedure accounts for the effect of h/c when evaluating the compressive strength of columns intersected by concrete floors. According to available test data, ACI 318-95 and CSA A23.3-M84 design provisions may become unconservative for slab-column connections with high h/c values. Conversely, CSA A23.3-94 provisions may become overly conservative for connections with low h/c values.

3. No special provision for the design of rectangular columns intersected by floors of weaker concrete strength is given in any code design provision.

4. A modification to CSA A23.3-94 and ACI 318-95 provisions for the design of interior columns is proposed in Chapter 6.

5. This investigation supports the design equation for edge columns presented by CSA A23.3-94 and by ACI 318-95.

106

6. For the design of corner columns, a modification to the CSA A23.3-94 design curve is also proposed. This equation is reported in Chapter 6.

7.3 Recommendations

The results herein reported constitute the only source of data from tests of slab-column connection specimens subjected to both column and slab loads. There is a need to reproduce and confirm these results. In view of the dramatic scarcity of such experimental results, the following recommendations are made.

1. Further testing of interior, edge and corner slab-column connections under realistic slab loading is required to extend the available data base. Selection of f'_{cc} / f'_{cs} values varying from 1.0 to 2.0 would be desirable in order to examine thoroughly the level beyond which the column concrete compressive strength is affected by the presence of the weaker slab concrete.

2. Test data herein reported resulted from experiments on slab-column connection specimens subjected to a constant level of slab load and to an incremental column loading. It would be important to produce results from a different loading regime. A recommended loading condition would be to keep the column load constant and to gradually increase the gravity load applied on the slab.

3. Tests need also be extended to slab/beam-column connections. Previous research on this type of specimen was carried out by Bianchini et al. and Siao (1994). There is a need to carry out tests on this specimen type with properly controlled load and boundary conditions.

4. Further evaluation of the effect the aspect ratio, h/c, is required to improve and refine the proposed design equations for interior columns. Further study of the effect of this variable on edge and corner columns is needed. Tests of specimens with low h/c values may be preferred since these are more likely to be found in modern buildings.

5. Tests further evaluating the effect of column shape (rectangular, circular, etc.) are also recommended.

6. Exhaustive assessment of the effect of placement of a high-strength concrete core within the joint region is suggested. This constructive technique offers an alternative solution to the problem of transmission of loads from high-strength concrete columns through normal-strength concrete floors. It is necessary to examine both the advantages and disadvantages of this procedure.

LIST OF REFERENCES

ACI Committee 318, 1995, "Building Code Requirements for Structural Concrete (ACI 318-95) and Commentary (ACI 318R-95)," American Concrete Institute, Detroit, 369 pp.

ASTM Committee C-9, 1992, "ASTM C42-90: Standard Test Method for Obtaining and Testing Drilled Cores and Sawed Beams of Concrete," Annual Book of ASTM Standards, Vol. 04.02, American Society for Testing and Materials, Philadelphia, pp. 27-29.

Avram, C., Facaoaru, I., Filimon, O. and Tertea, I., 1981, Concrete Strength and Strains, Elsevier Scientific Publishing Company, Amsterdam, 558 pp.

Bianchini, A. C., Woods, R. E. and Kesler, C. E., 1960, "Effect of Floor Concrete Strength on Column Strength," ACI Journal, Proceedings, Vol. 31, No. 11, pp. 1149-1169.

Canadian Standards Association, 1984, "Design of Concrete Structures for Buildings (CSA CAN3-A23.3-M84)," Canadian Standards Association, Rexdale, Ontario, 280 pp.

Canadian Standards Association, 1994, "Design of Concrete Structures for Buildings (CSA A23.3-94)," Canadian Standards Association, Rexdale, Ontario, 199 pp.

CEB/FIP, 1994, "Application of High Performance Concrete," CEB Bulletin d'Information No. 222, Comite Euro-International du Beton (CEB)/Federation Internationale de la Precontrainte (FIP), Lausanne, 65 pp.

Chen, S. A. and MacGregor, J. G., 1993, "A Shear-Friction Truss Model for Reinforced Concrete Beams subjected to Shear," Structural Engineering Report No. 188, Department of Civil Engineering, University of Alberta, Edmonton, 359 pp.

Gamble, W. L. and Klinar, J. D., 1991, "Tests of High-Strength Concrete Columns with Intervening Floor Slabs," Journal of Structural Engineering, ASCE, Vol. 117, No. 5, pp. 1462-1476.

Howard, N. L. and Leatham, D. M., 1992, "The Production and Delivery of High-Strength Concrete," ACI Compilation 17, pp. 20-24.

Kayani, M. K., 1992, "Load Transfer from High-Strength Concrete Columns through Lower Strength Concrete Slabs," Ph.D. Thesis, Department of Civil Engineering, University of Illinois, Urbana-Champaign, 111 pp.

Moreno, J., 1990, "225 W. Wacker Drive," Concrete International, Vol. 12, No. 1, pp. 35-39.

Murdock, J. W. and Kesler, C. E., 1957, "Effect of Length to Diameter Ratio of Specimen on the Apparent Compressive Strength of Concrete," ASTM bulletin, pp. 68-73.

Price, W. H., 1951, "Factors Influencing Concrete Strength," ACI Journal, Vol. 22, No. 6, pp. 417-432.

Randall, V. and Foot, K., 1992, "High-Strength Concrete for Pacific First Center," ACI Compilation 17, pp. 54-56.

Robison, R., 1988, "High Strength High Rise," Civil Engineering, ASCE, Vol. 58, No. 3, pp. 62-65.

Shu, Ch-Ch. and Hawkins, N. M., 1992, "Behavior of Columns Continuous through Concrete Floors," ACI Structural Journal, Vol. 89, No. 4, pp. 405-414.

Siao, W. B., 1994, "Reinforced Concrete Column Strength at Beam/Slab and Column Intersection," ACI Structural Journal, Vol. 91, No. 1, pp. 3-9.

Troxell, G. E., Davis, H. E. and Kelly, J. W., 1968, Composition and Properties of Concrete, McGraw-Hill Book Company, New York, 529 pp.

Wilson, E. L. and Habibullah, A., 1992, SAP90, A Series of Computer Programs for the Finite Element Analysis of Structures, Computers and Structures, Inc., Berkeley.

APPENDIX A

Finite Element Modeling of Prototype Slab-Column Connections and Connection Specimens

Finite Element Modeling of Prototype R/C Interior Connection (h=250mm, c=250mm)
SYSTEM
L=1 : Applied dead and live load

JOINTS

1	X=0.00 Y=0.00 Z=0.00		46	X=3.20	
2	X=0.75		47	X=3.70	
3	X=1.25		48	X=4.45	
4	X=1.55		C		
5	X=1.65		49	X=0.00 Y=1.55	
6	X=1.85		50	X=0.75	
7	X=1.975		51	X=1.25	
8	X=2.10		52	X=1.55	
9	X=2.35		53	X=1.65	
10	X=2.475		54	X=1.85	
11	X=2.60		55	X=1.975	
12	X=2.80		56	X=2.10	
13	X=2.90		57	X=2.35	
14	X=3.20		58	X=2.475	
15	X=3.70		59	X=2.60	
16	X=4.45		60	X=2.80	
C			61	X=2.90	
17	X=0.00 Y=0.75		62	X=3.20	
18	X=0.75		63	X=3.70	
19	X=1.25		64	X=4.45	
20	X=1.55		C		
21	X=1.65		65	X=0.00 Y=1.65	
22	X=1.85		66	X=0.75	
23	X=1.975		67	X=1.25	
24	X=2.10		68	X=1.55	
25	X=2.35		69	X=1.65	
26	X=2.475		70	X=1.85	
27	X=2.60		71	X=1.975	
28	X=2.80		72	X=2.10	
29	X=2.90		73	X=2.35	
30	X=3.20		74	X=2.475	
31	X=3.70		75	X=2.60	
32	X=4.45		76	X=2.80	
C			77	X=2.90	
33	X=0.00 Y=1.25		78	X=3.20	
34	X=0.75		79	X=3.70	
35	X=1.25		80	X=4.45	
36	X=1.55		C		
37	X=1.65		81	X=0.00 Y=1.85	
38	X=1.85		82	X=0.75	
39	X=1.975		83	X=1.25	
40	X=2.10		84	X=1.55	
41	X=2.35		85	X=1.65	
42	X=2.475		86	X=1.85	
43	X=2.60		87	X=1.975	
44	X=2.80		88	X=2.10	
45	X=2.90		89	X=2.35	

```
 90  X=2.475                      141  X=2.90
 91  X=2.60                       142  X=3.20
 92  X=2.80                       143  X=3.70
 93  X=2.90                       144  X=4.45
 94  X=3.20                    C
 95  X=3.70                       145  X=0.00  Y=2.475
 96  X=4.45                       146  X=0.75
C                                 147  X=1.25
 97  X=0.00  Y=1.975              148  X=1.55
 98  X=0.75                       149  X=1.65
 99  X=1.25                       150  X=1.85
100  X=1.55                       151  X=1.975
101  X=1.65                       152  X=2.10
102  X=1.85                       153  X=2.35
103  X=1.975                      154  X=2.475
104  X=2.10                       155  X=2.60
105  X=2.35                       156  X=2.80
106  X=2.475                      157  X=2.90
107  X=2.60                       158  X=3.20
108  X=2.80                       159  X=3.70
109  X=2.90                       160  X=4.45
110  X=3.20                    C
111  X=3.70                       161  X=0.00  Y=2.60
112  X=4.45                       162  X=0.75
C                                 163  X=1.25
113  X=0.00  Y=2.10               164  X=1.55
114  X=0.75                       165  X=1.65
115  X=1.25                       166  X=1.85
116  X=1.55                       167  X=1.975
117  X=1.65                       168  X=2.10
118  X=1.85                       169  X=2.35
119  X=1.975                      170  X=2.475
120  X=2.10                       171  X=2.60
121  X=2.35                       172  X=2.80
122  X=2.475                      173  X=2.90
123  X=2.60                       174  X=3.20
124  X=2.80                       175  X=3.70
125  X=2.90                       176  X=4.45
126  X=3.20                    C
127  X=3.70                       177  X=0.00  Y=2.80
128  X=4.45                       178  X=0.75
C                                 179  X=1.25
129  X=0.00  Y=2.35               180  X=1.55
130  X=0.75                       181  X=1.65
131  X=1.25                       182  X=1.85
132  X=1.55                       183  X=1.975
133  X=1.65                       184  X=2.10
134  X=1.85                       185  X=2.35
135  X=1.975                      186  X=2.475
136  X=2.10                       187  X=2.60
137  X=2.35                       188  X=2.80
138  X=2.475                      189  X=2.90
139  X=2.60                       190  X=3.20
140  X=2.80                       191  X=3.70
```

192 X=4.45
C
193 X=0.00 Y=2.90
194 X=0.75
195 X=1.25
196 X=1.55
197 X=1.65
198 X=1.85
199 X=1.975
200 X=2.10
201 X=2.35
202 X=2.475
203 X=2.60
204 X=2.80
205 X=2.90
206 X=3.20
207 X=3.70
208 X=4.45
C
209 X=0.00 Y=3.20
210 X=0.75
211 X=1.25
212 X=1.55
213 X=1.65
214 X=1.85
215 X=1.975
216 X=2.10
217 X=2.35
218 X=2.475
219 X=2.60
220 X=2.80
221 X=2.90
222 X=3.20
223 X=3.70
224 X=4.45
C
225 X=0.00 Y=3.70
226 X=0.75
227 X=1.25
228 X=1.55
229 X=1.65
230 X=1.85
231 X=1.975
232 X=2.10
233 X=2.35
234 X=2.475
235 X=2.60
236 X=2.80
237 X=2.90
238 X=3.20
239 X=3.70
240 X=4.45
C
241 X=0.00 Y=4.45

242 X=0.75
243 X=1.25
244 X=1.55
245 X=1.65
246 X=1.85
247 X=1.975
248 X=2.10
249 X=2.35
250 X=2.475
251 X=2.60
252 X=2.80
253 X=2.90
254 X=3.20
255 X=3.70
256 X=4.45
C

RESTRAINTS
C
 18 31 1 R=0,0,0,0,0,0
 34 47 1 R=0,0,0,0,0,0
 50 63 1 R=0,0,0,0,0,0
 66 79 1 R=0,0,0,0,0,0
 82 95 1 R=0,0,0,0,0,0
 98 111 1 R=0,0,0,0,0,0
114 119 1 R=0,0,0,0,0,0
122 127 1 R=0,0,0,0,0,0
130 135 1 R=0,0,0,0,0,0
138 143 1 R=0,0,0,0,0,0
146 159 1 R=0,0,0,0,0,0
162 175 1 R=0,0,0,0,0,0
178 191 1 R=0,0,0,0,0,0
194 207 1 R=0,0,0,0,0,0
210 223 1 R=0,0,0,0,0,0
226 239 1 R=0,0,0,0,0,0
C
C Joints at slab-column joint location
120 121 1 R=1,1,1,0,0,0
136 137 1 R=1,1,1,0,0,0
C
C Corner Joints
  1 16 15 R=0,0,0,1,1,1
241 256 15 R=0,0,0,1,1,1
C
C Edge joints along X direction
  2 15 1 R=0,0,0,1,0,1
242 255 1 R=0,0,0,1,0,1
C
C Edge joints along Y direction
 17 225 16 R=0,0,0,0,1,1
 32 240 16 R=0,0,0,0,1,1
C

SHELL
NM=1 Z=-1
C
1 E=1 U=0.20 W=37.2
C
C W includes applied dead and live load
C W (kN/m^3)
C
1 JQ=1,2,17,18 TH=0.25 M=1 G=15,15 LP=0 ETYPE=0

COMBO
1 C=1.0 : 1.0

Finite Element Modeling of Prototype R/C Interior Connection (h=150mm, c=250mm)
SYSTEM
L=1 : Applied dead and live load

JOINTS

1	X=0.00 Y=0.00 Z=0.00		31	X=3.70	
2	X=0.75		32	X=4.45	
3	X=1.25		C		
4	X=1.55		33	X=0.00	Y=1.25
5	X=1.65		34	X=0.75	
6	X=1.85		35	X=1.25	
7	X=1.975		36	X=1.55	
8	X=2.10		37	X=1.65	
9	X=2.35		38	X=1.85	
10	X=2.475		39	X=1.975	
11	X=2.60		40	X=2.10	
12	X=2.80		41	X=2.35	
13	X=2.90		42	X=2.475	
14	X=3.20		43	X=2.60	
15	X=3.70		44	X=2.80	
16	X=4.45		45	X=2.90	
C			46	X=3.20	
17	X=0.00 Y=0.75		47	X=3.70	
18	X=0.75		48	X=4.45	
19	X=1.25		C		
20	X=1.55		49	X=0.00	Y=1.55
21	X=1.65		50	X=0.75	
22	X=1.85		51	X=1.25	
23	X=1.975		52	X=1.55	
24	X=2.10		53	X=1.65	
25	X=2.35		54	X=1.85	
26	X=2.475		55	X=1.975	
27	X=2.60		56	X=2.10	
28	X=2.80		57	X=2.35	
29	X=2.90		58	X=2.475	
30	X=3.20		59	X=2.60	

60 X=2.80
61 X=2.90
62 X=3.20
63 X=3.70
64 X=4.45
C
65 X=0.00 Y=1.65
66 X=0.75
67 X=1.25
68 X=1.55
69 X=1.65
70 X=1.85
71 X=1.975
72 X=2.10
73 X=2.35
74 X=2.475
75 X=2.60
76 X=2.80
77 X=2.90
78 X=3.20
79 X=3.70
80 X=4.45
C
81 X=0.00 Y=1.85
82 X=0.75
83 X=1.25
84 X=1.55
85 X=1.65
86 X=1.85
87 X=1.975
88 X=2.10
89 X=2.35
90 X=2.475
91 X=2.60
92 X=2.80
93 X=2.90
94 X=3.20
95 X=3.70
96 X=4.45
C
97 X=0.00 Y=1.975
98 X=0.75
99 X=1.25
100 X=1.55
101 X=1.65
102 X=1.85
103 X=1.975
104 X=2.10
105 X=2.35
106 X=2.475
107 X=2.60
108 X=2.80
109 X=2.90
110 X=3.20

111 X=3.70
112 X=4.45
C
113 X=0.00 Y=2.10
114 X=0.75
115 X=1.25
116 X=1.55
117 X=1.65
118 X=1.85
119 X=1.975
120 X=2.10
121 X=2.35
122 X=2.475
123 X=2.60
124 X=2.80
125 X=2.90
126 X=3.20
127 X=3.70
128 X=4.45
C
129 X=0.00 Y=2.35
130 X=0.75
131 X=1.25
132 X=1.55
133 X=1.65
134 X=1.85
135 X=1.975
136 X=2.10
137 X=2.35
138 X=2.475
139 X=2.60
140 X=2.80
141 X=2.90
142 X=3.20
143 X=3.70
144 X=4.45
C
145 X=0.00 Y=2.475
146 X=0.75
147 X=1.25
148 X=1.55
149 X=1.65
150 X=1.85
151 X=1.975
152 X=2.10
153 X=2.35
154 X=2.475
155 X=2.60
156 X=2.80
157 X=2.90
158 X=3.20
159 X=3.70
160 X=4.45
C

```
161  X=0.00  Y=2.60          209  X=0.00  Y=3.20
162  X=0.75                  210  X=0.75
163  X=1.25                  211  X=1.25
164  X=1.55                  212  X=1.55
165  X=1.65                  213  X=1.65
166  X=1.85                  214  X=1.85
167  X=1.975                 215  X=1.975
168  X=2.10                  216  X=2.10
169  X=2.35                  217  X=2.35
170  X=2.475                 218  X=2.475
171  X=2.60                  219  X=2.60
172  X=2.80                  220  X=2.80
173  X=2.90                  221  X=2.90
174  X=3.20                  222  X=3.20
175  X=3.70                  223  X=3.70
176  X=4.45                  224  X=4.45
C                            C
177  X=0.00  Y=2.80          225  X=0.00  Y=3.70
178  X=0.75                  226  X=0.75
179  X=1.25                  227  X=1.25
180  X=1.55                  228  X=1.55
181  X=1.65                  229  X=1.65
182  X=1.85                  230  X=1.85
183  X=1.975                 231  X=1.975
184  X=2.10                  232  X=2.10
185  X=2.35                  233  X=2.35
186  X=2.475                 234  X=2.475
187  X=2.60                  235  X=2.60
188  X=2.80                  236  X=2.80
189  X=2.90                  237  X=2.90
190  X=3.20                  238  X=3.20
191  X=3.70                  239  X=3.70
192  X=4.45                  240  X=4.45
C                            C
193  X=0.00  Y=2.90          241  X=0.00  Y=4.45
194  X=0.75                  242  X=0.75
195  X=1.25                  243  X=1.25
196  X=1.55                  244  X=1.55
197  X=1.65                  245  X=1.65
198  X=1.85                  246  X=1.85
199  X=1.975                 247  X=1.975
200  X=2.10                  248  X=2.10
201  X=2.35                  249  X=2.35
202  X=2.475                 250  X=2.475
203  X=2.60                  251  X=2.60
204  X=2.80                  252  X=2.80
205  X=2.90                  253  X=2.90
206  X=3.20                  254  X=3.20
207  X=3.70                  255  X=3.70
208  X=4.45                  256  X=4.45
C                            C
```

117

RESTRAINTS
```
 18  31  1  R=0,0,0,0,0,0
 34  47  1  R=0,0,0,0,0,0
 50  63  1  R=0,0,0,0,0,0
 66  79  1  R=0,0,0,0,0,0
 82  95  1  R=0,0,0,0,0,0
 98 111  1  R=0,0,0,0,0,0
114 119  1  R=0,0,0,0,0,0
122 127  1  R=0,0,0,0,0,0
130 135  1  R=0,0,0,0,0,0
138 143  1  R=0,0,0,0,0,0
146 159  1  R=0,0,0,0,0,0
162 175  1  R=0,0,0,0,0,0
178 191  1  R=0,0,0,0,0,0
194 207  1  R=0,0,0,0,0,0
210 223  1  R=0,0,0,0,0,0
226 239  1  R=0,0,0,0,0,0
C
C Joints at slab-column joint location
120 121  1  R=1,1,1,0,0,0
136 137  1  R=1,1,1,0,0,0
C
C Corner joints
  1  16 15  R=0,0,0,1,1,1
241 256 15  R=0,0,0,1,1,1
C
C Edge joints along X direction
  2  15  1  R=0,0,0,1,0,1
242 255  1  R=0,0,0,1,0,1
C
C Edge joints along Y direction
 17 225  16  R=0,0,0,0,1,1
 32 240  16  R=0,0,0,0,1,1
C
```

SHELL
```
NM=1  Z=-1
C
1  E=1  U=0.20  W=46
C
C W includes applied dead and live load
C W (kN/m$^3$)
C
1  JQ=1,2,17,18  TH=0.15  M=1  G=15,15  LP=0  ETYPE=0
```

COMBO
```
1 C=1.0  : 1.0
```

118

SAP90

Z
X
Y

PROTSLAB
UNDEFORMED
SHAPE

OPTIONS
RESTRAINTS
WIRE FRAME
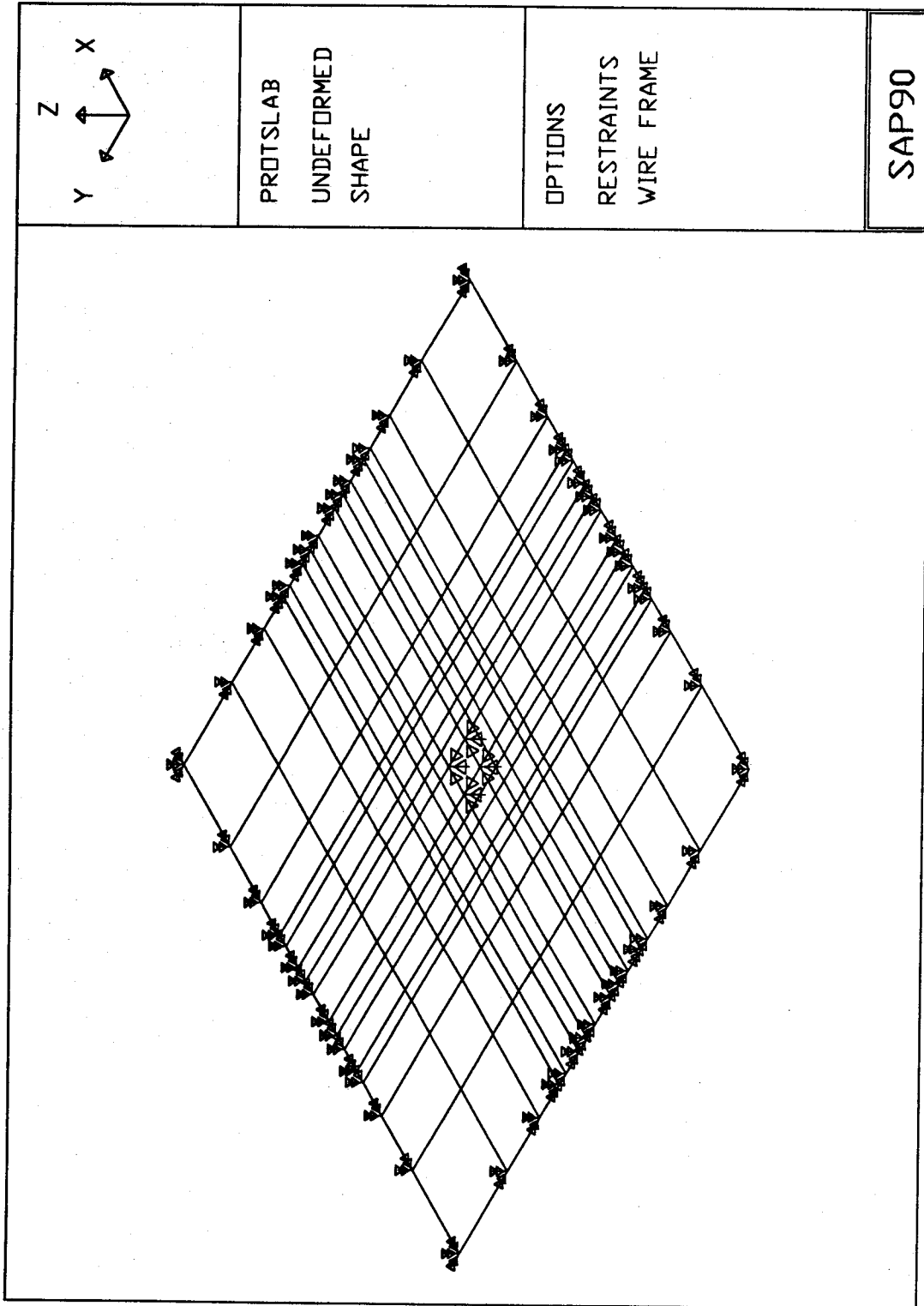
Figure A.1 3-D View of Finite Element Mesh of Prototype Connection

119
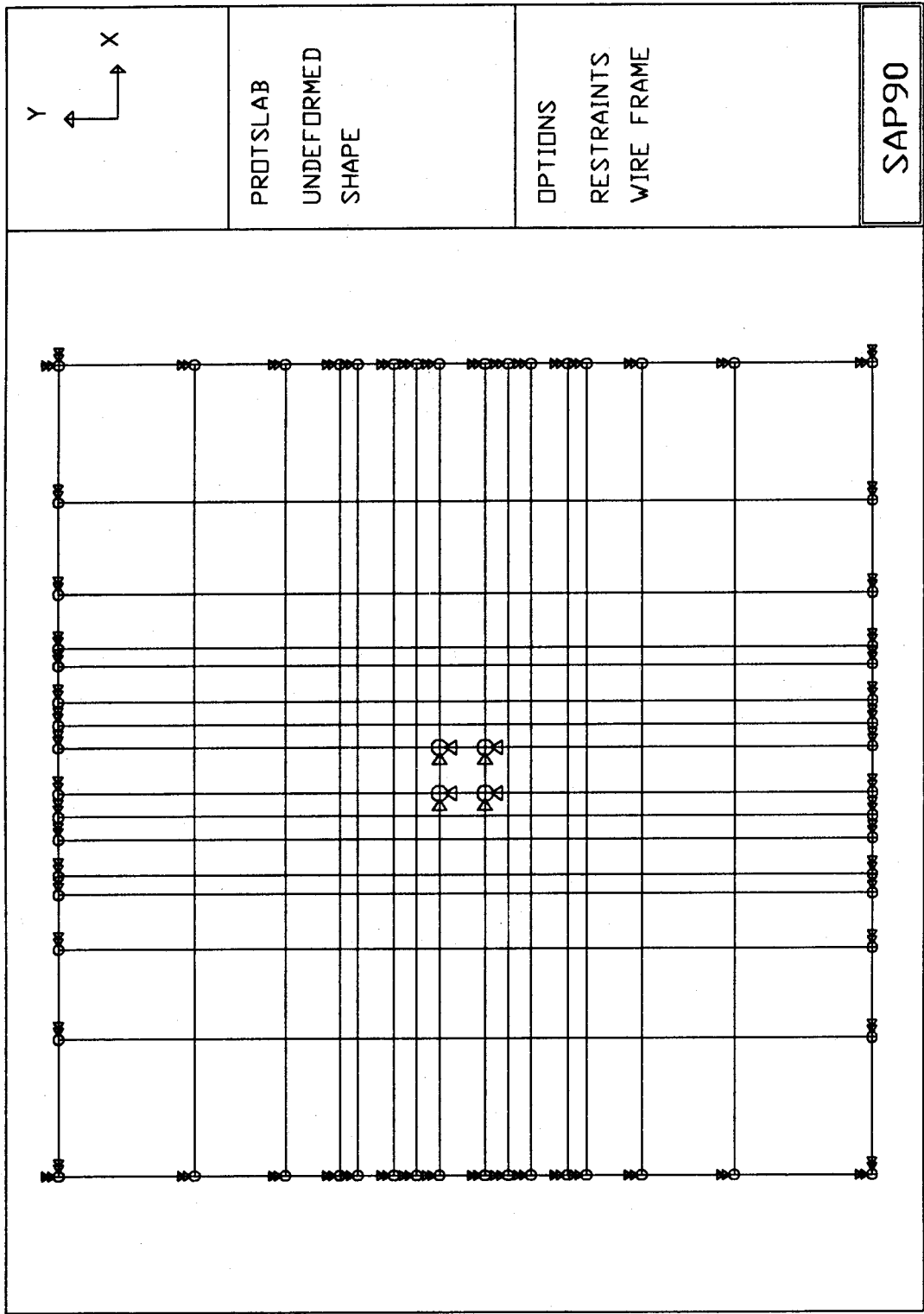
Figure A.2 Plan View of Finite Element Mesh of Prototype Connection

Finite Element Modeling of R/C Slab-Column Connection Specimen (h=250mm, c=250mm)
SYSTEM
L=1 : Jacking loads applied on the slab segment

JOINTS

1	X=0.00 Y=0.00 Z=0.00	46 X=0.80
2	X=0.10	47 X=0.925
3	X=0.30	48 X=1.05
4	X=0.425	49 X=1.25
5	X=0.55	50 X=1.35
6	X=0.80	C
7	X=0.925	51 X=0.00 Y=0.80
8	X=1.05	52 X=0.10
9	X=1.25	53 X=0.30
10	X=1.35	54 X=0.425
C		55 X=0.55
11	X=0.00 Y=0.10	56 X=0.80
12	X=0.10	57 X=0.925
13	X=0.30	58 X=1.05
14	X=0.425	59 X=1.25
15	X=0.55	60 X=1.35
16	X=0.80	C
17	X=0.925	61 X=0.00 Y=0.925
18	X=1.05	62 X=0.10
19	X=1.25	63 X=0.30
20	X=1.35	64 X=0.425
C		65 X=0.55
21	X=0.00 Y=0.30	66 X=0.80
22	X=0.10	67 X=0.925
23	X=0.30	68 X=1.05
24	X=0.425	69 X=1.25
25	X=0.55	70 X=1.35
26	X=0.80	C
27	X=0.925	71 X=0.00 Y=1.05
28	X=1.05	72 X=0.10
29	X=1.25	73 X=0.30
30	X=1.35	74 X=0.425
C		75 X=0.55
31	X=0.00 Y=0.425	76 X=0.80
32	X=0.10	77 X=0.925
33	X=0.30	78 X=1.05
34	X=0.425	79 X=1.25
35	X=0.55	80 X=1.35
36	X=0.80	C
37	X=0.925	81 X=0.00 Y=1.25
38	X=1.05	82 X=0.10
39	X=1.25	83 X=0.30
40	X=1.35	84 X=0.425
C		85 X=0.55
41	X=0.00 Y=0.55	86 X=0.80
42	X=0.10	87 X=0.925
43	X=0.30	88 X=1.05
44	X=0.425	89 X=1.25
45	X=0.55	

121

```
 90  X=1.35
C
 91  X=0.00  Y=1.35
 92  X=0.10
 93  X=0.30
 94  X=0.425
 95  X=0.55
 96  X=0.80
 97  X=0.925
 98  X=1.05
 99  X=1.25
100  X=1.35
C
```

RESTRAINTS
```
  1 44  1  R=0,0,0,0,0,0
 45 46  1  R=1,1,1,0,0,0  :Restraint at slab-column joint location
 47 54  1  R=0,0,0,0,0,0
 55 56  1  R=1,1,1,0,0,0  :Restraint at slab-column joint location
 57 100 1  R=0,0,0,0,0,0
```

SHELL
```
NM=1  Z=-1
C
1  E=1  U=0.20  W=24
C
C  W includes only the self-weight of the slab segment
C  W (kN/m³)
C
1  JQ=1,2,11,12  TH=0.25  M=1  G=9,9  LP=0  ETYPE=0
```

LOADS
```
C
 12 19  7  L=1  F=0,0,-43.3    :2 point loads, (43.3 kN each)
 82 89  7  L=1  F=0,0,-43.3    :2 point loads, (43.3 kN each)
```

COMBO
```
1 C=1.0
```

122

Finite Element Modeling of R/C Slab-column Connection Specimen (h=150mm, c= 250mm)
SYSTEM
L=1 :Jacking loads applied on the slab segment

JOINTS

  1 X=0.00 Y=0.00 Z=0.00
  2 X=0.10
  3 X=0.30
  4 X=0.425
  5 X=0.55
  6 X=0.80
  7 X=0.925
  8 X=1.05
  9 X=1.25
 10 X=1.35
C
 11 X=0.00 Y=0.10
 12 X=0.10
 13 X=0.30
 14 X=0.425
 15 X=0.55
 16 X=0.80
 17 X=0.925
 18 X=1.05
 19 X=1.25
 20 X=1.35
C
 21 X=0.00 Y=0.30
 22 X=0.10
 23 X=0.30
 24 X=0.425
 25 X=0.55
 26 X=0.80
 27 X=0.925
 28 X=1.05
 29 X=1.25
 30 X=1.35
C
 31 X=0.00 Y=0.425
 32 X=0.10
 33 X=0.30
 34 X=0.425
 35 X=0.55
 36 X=0.80
 37 X=0.925
 38 X=1.05
 39 X=1.25
 40 X=1.35
C
 41 X=0.00 Y=0.55
 42 X=0.10
 43 X=0.30
 44 X=0.425

 45 X=0.55
 46 X=0.80
 47 X=0.925
 48 X=1.05
 49 X=1.25
 50 X=1.35
C
 51 X=0.00 Y=0.80
 52 X=0.10
 53 X=0.30
 54 X=0.425
 55 X=0.55
 56 X=0.80
 57 X=0.925
 58 X=1.05
 59 X=1.25
 60 X=1.35
C
 61 X=0.00 Y=0.925
 62 X=0.10
 63 X=0.30
 64 X=0.425
 65 X=0.55
 66 X=0.80
 67 X=0.925
 68 X=1.05
 69 X=1.25
 70 X=1.35
C
 71 X=0.00 Y=1.05
 72 X=0.10
 73 X=0.30
 74 X=0.425
 75 X=0.55
 76 X=0.80
 77 X=0.925
 78 X=1.05
 79 X=1.25
 80 X=1.35
C
 81 X=0.00 Y=1.25
 82 X=0.10
 83 X=0.30
 84 X=0.425
 85 X=0.55
 86 X=0.80
 87 X=0.925
 88 X=1.05

```
 89  X=1.25
 90  X=1.35
C
 91  X=0.00 Y=1.35
 92  X=0.10
 93  X=0.30
 94  X=0.425
 95  X=0.55
 96  X=0.80
 97  X=0.925
 98  X=1.05
 99  X=1.25
100  X=1.35
```

RESTRAINTS
```
  1  44  1  R=0,0,0,0,0,0
 45  46  1  R=1,1,1,0,0,0  :Restraint at slab-column joint location
 47  54  1  R=0,0,0,0,0,0
 55  56  1  R=1,1,1,0,0,0  :Restraint at slab-column joint location
 57 100  1  R=0,0,0,0,0,0
```

SHELL
```
NM=1  Z=-1
C
1 E=1  U=0.20  W=24
C
C W includes only the self-weight of the slab segment
C W (kN/m³)
C
1 JQ=1,2,11,12  TH=0.15  M=1  G=9,9  LP=0  ETYPE=0
```

LOADS
```
C
 12 19  7  L=1  F=0,0,-32.5 :2 point loads, (32.5 kN each)
 82 89  7  L=1  F=0,0,-32.5 :2 point loads, (32.5 kN each)
```

COMBO
```
1 C=1.0
```
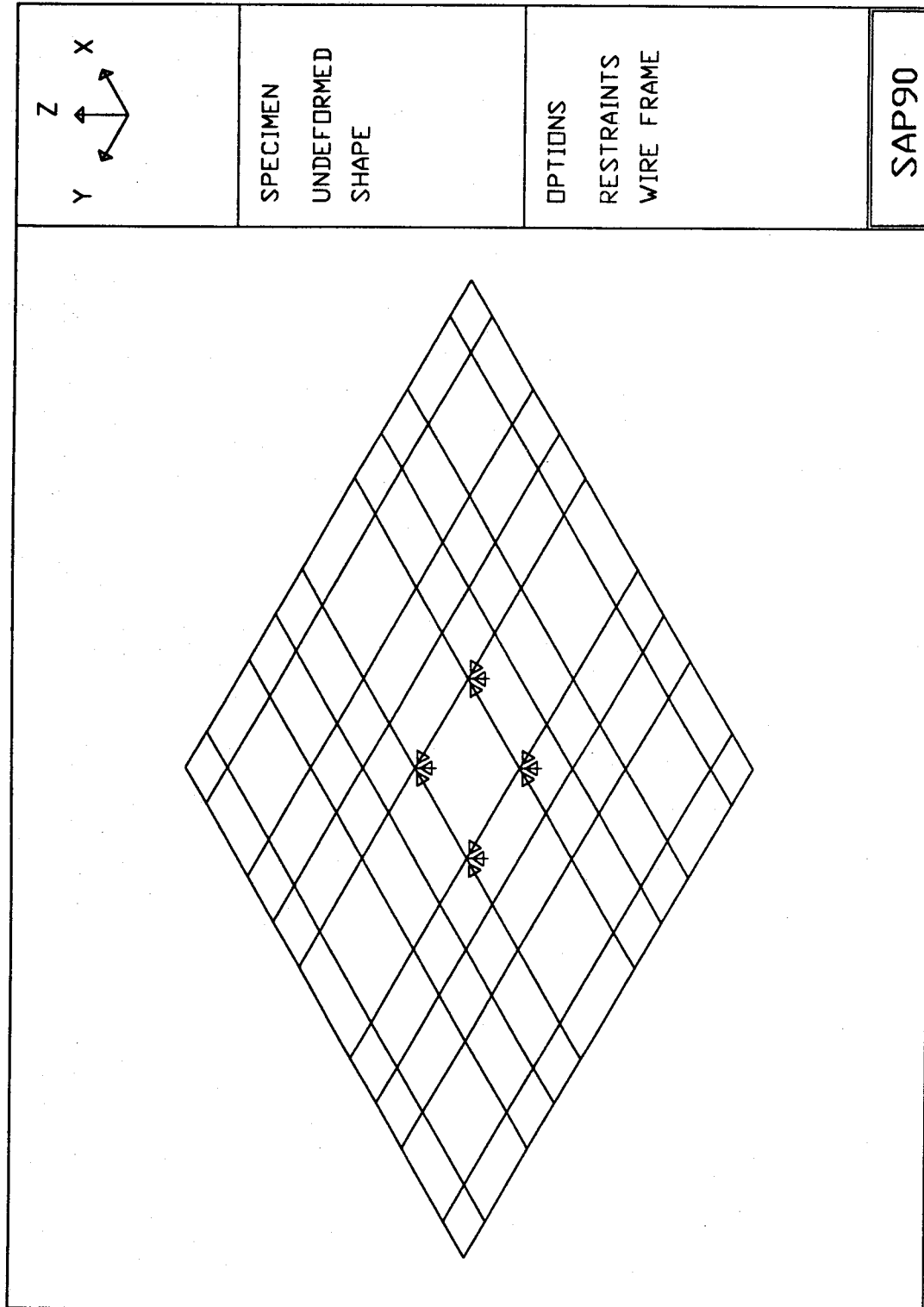
Figure A.3 3-D View of Finite Element Mesh of Connection Specimen
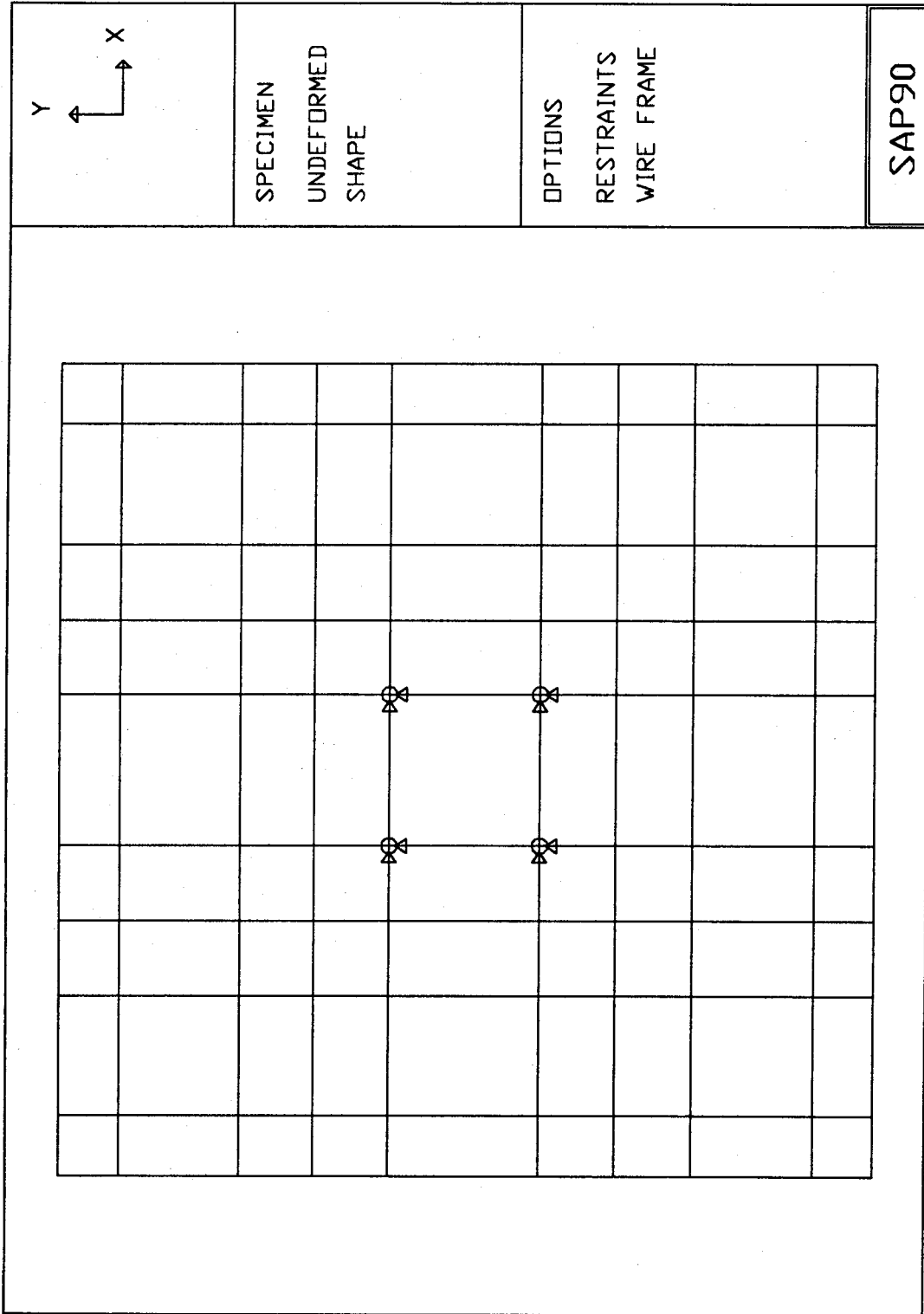
Figure A.4 Plan View of Finite Element Mesh of Connection Specimen

APPENDIX B

Strain Gauge and LVDT Readings

Series A Specimens

- Interior Sandwich Plates -
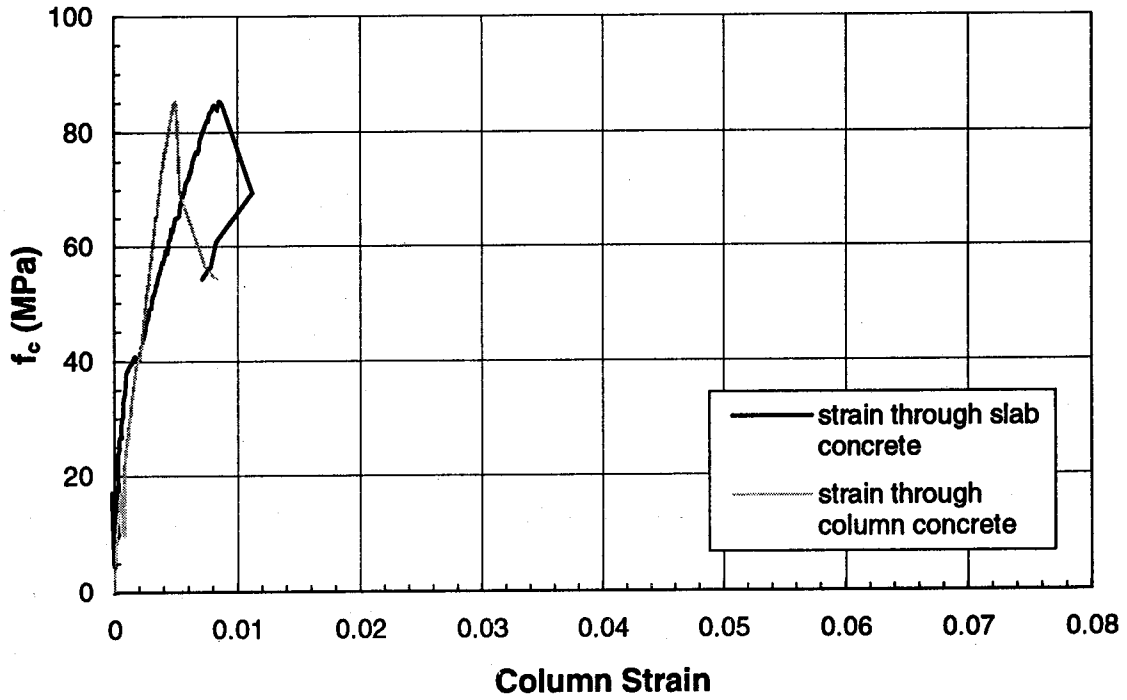
Figure B.1   Stress-Strain Behaviour (Specimen A1-A)
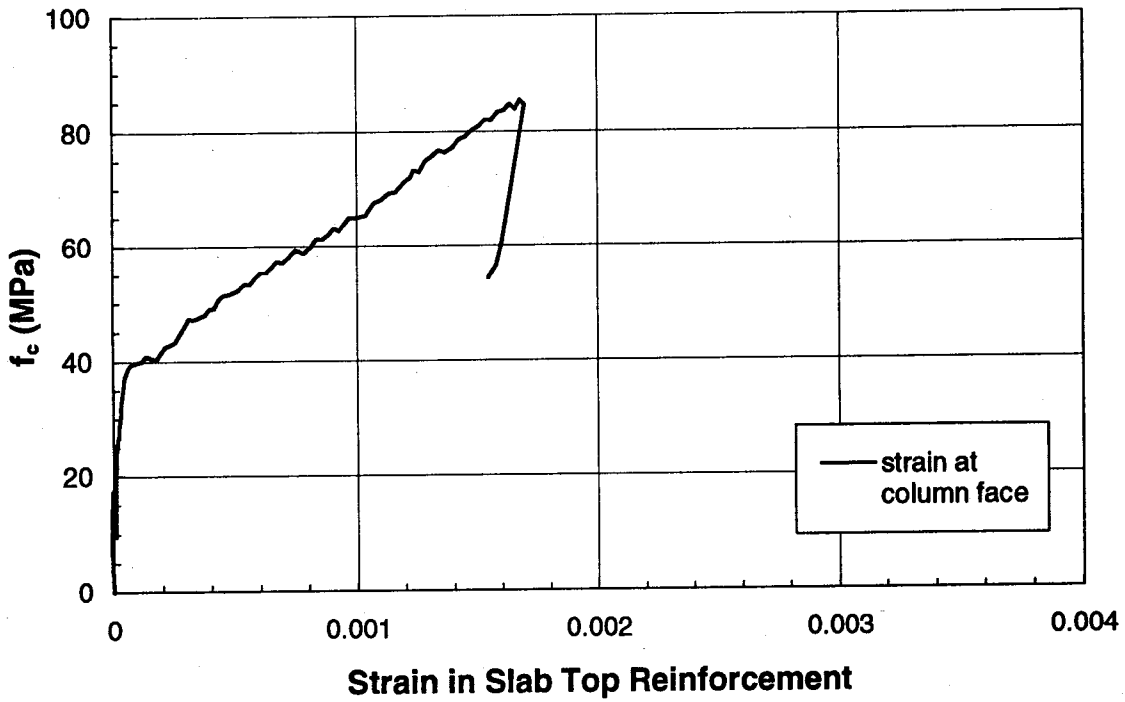
Figure B.2   Slab Transverse Strain (Specimen A1-A)

130
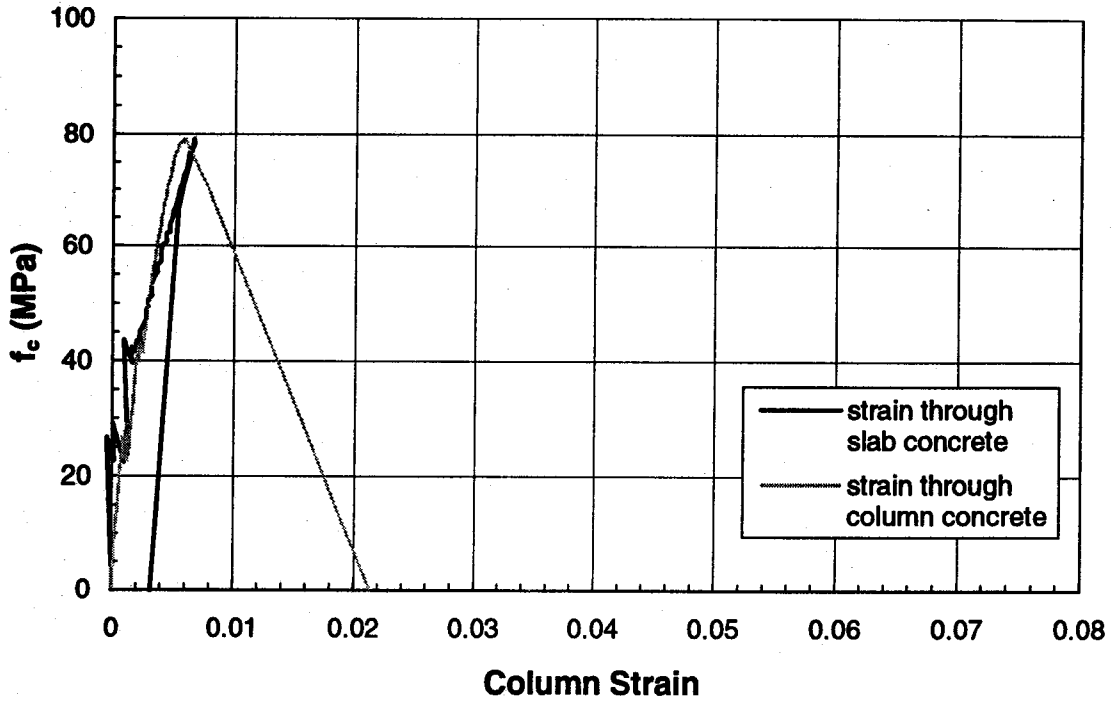
Figure B.3   Stress-Strain Behaviour (Specimen A1-B)
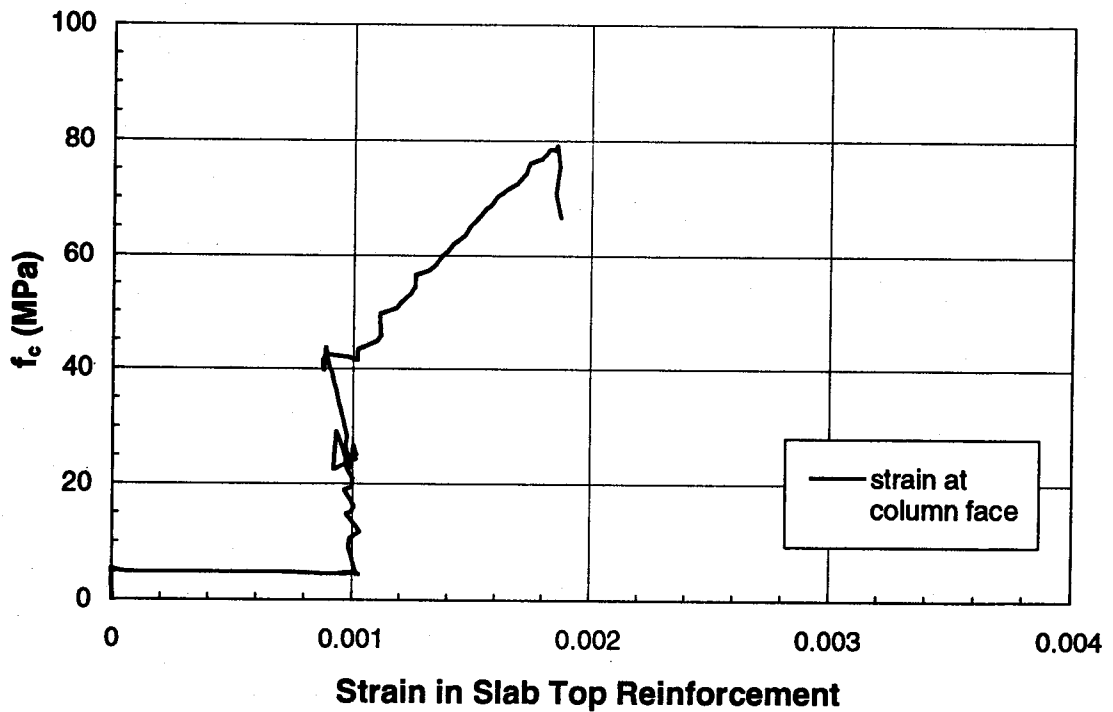
Figure B.4   Slab Transverse Strain (Specimen A1-B)
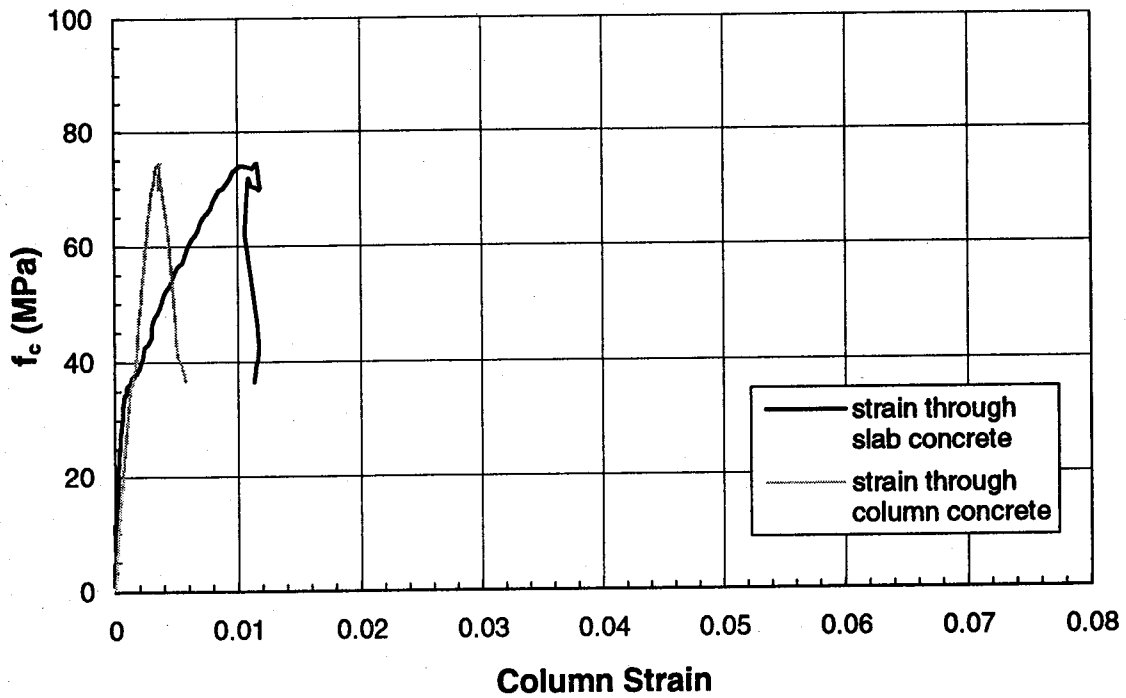
Figure B.5   Stress-Strain Behaviour (Specimen A1-C)
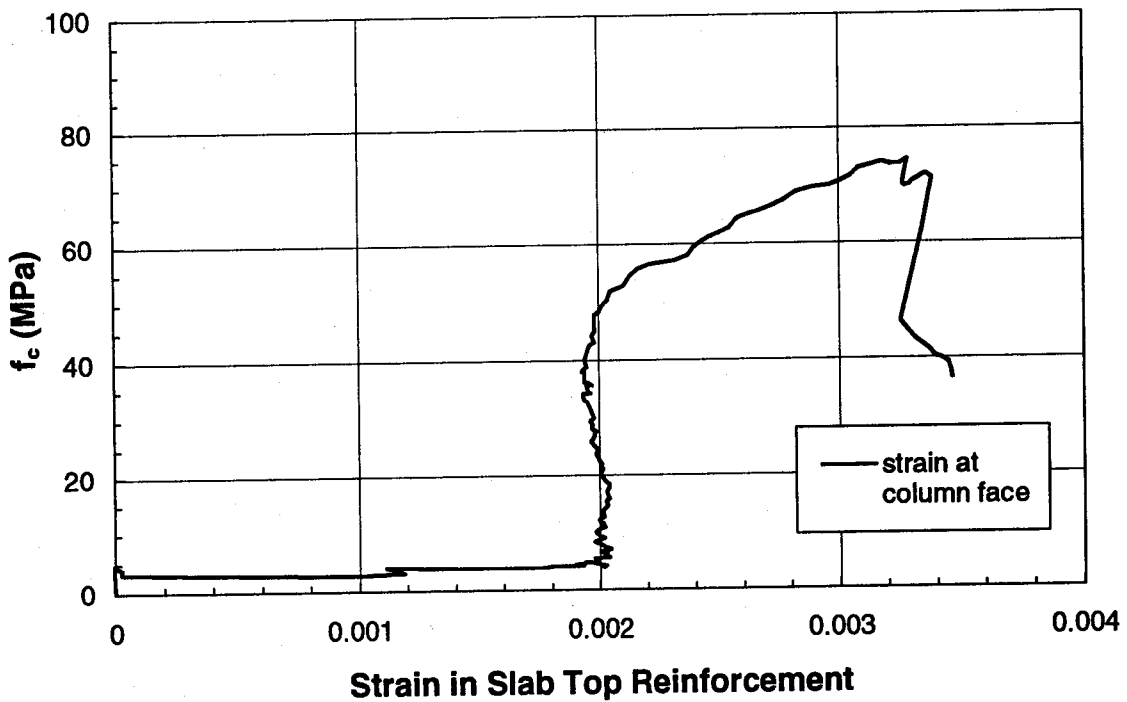
Figure B.6   Slab Transverse Strain (Specimen A1-C)

132
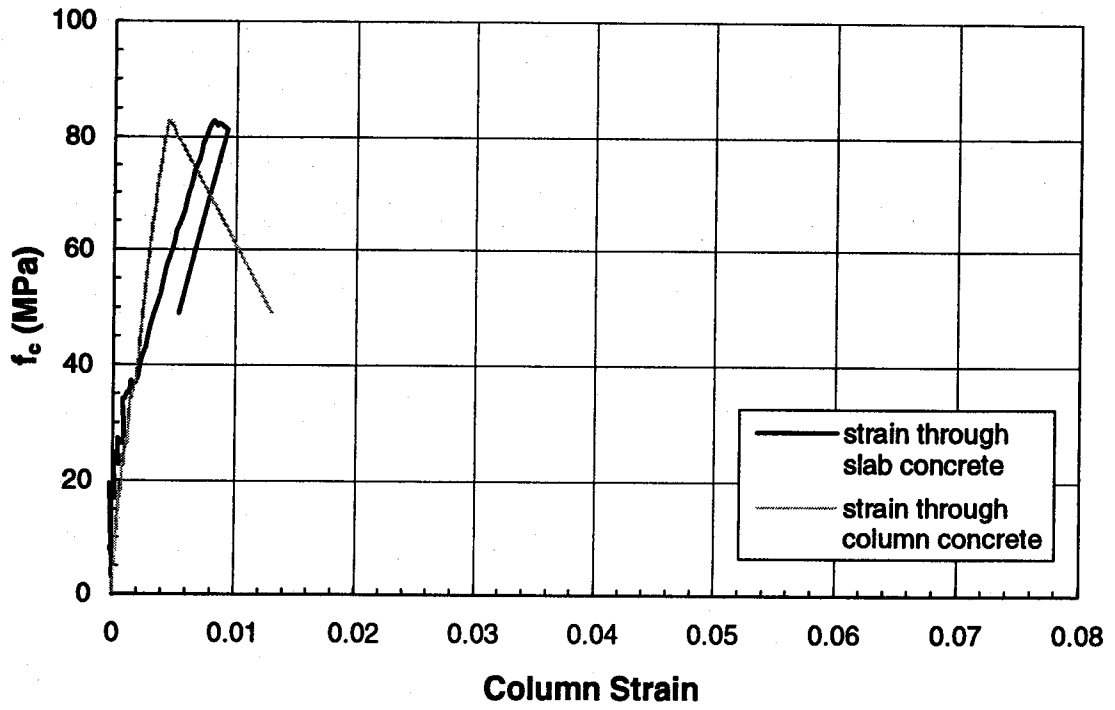
Figure B.7   Stress-Strain Behaviour (Specimen A2-A)
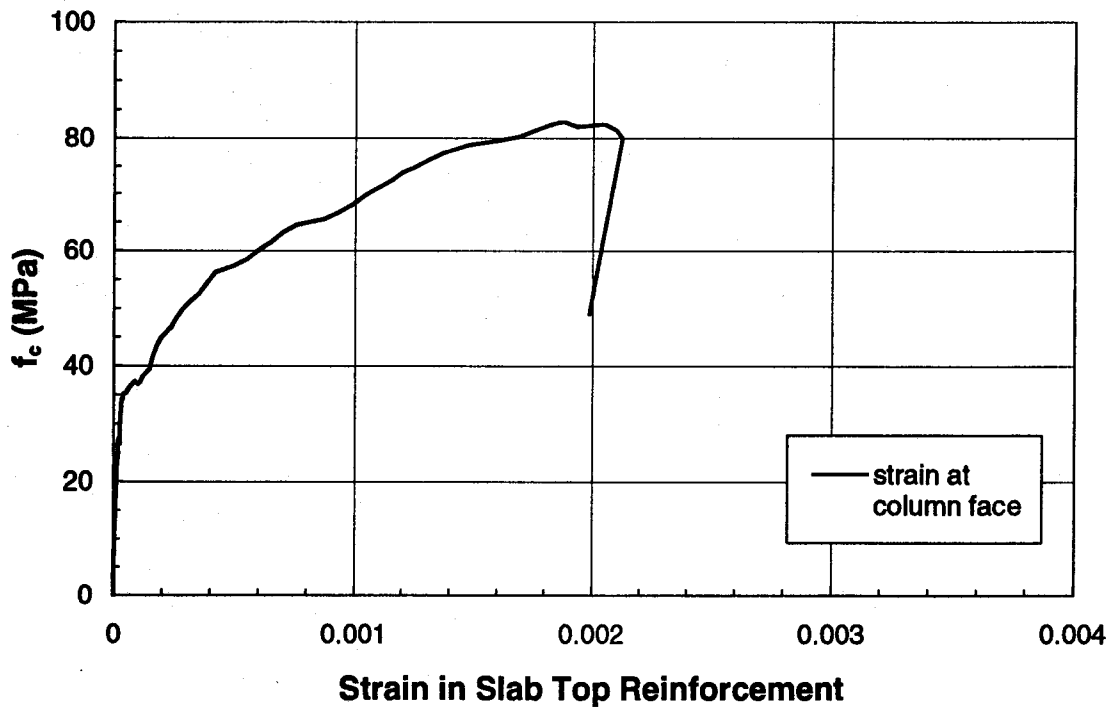
Figure B.8   Slab Transverse Strain (Specimen A2-A)
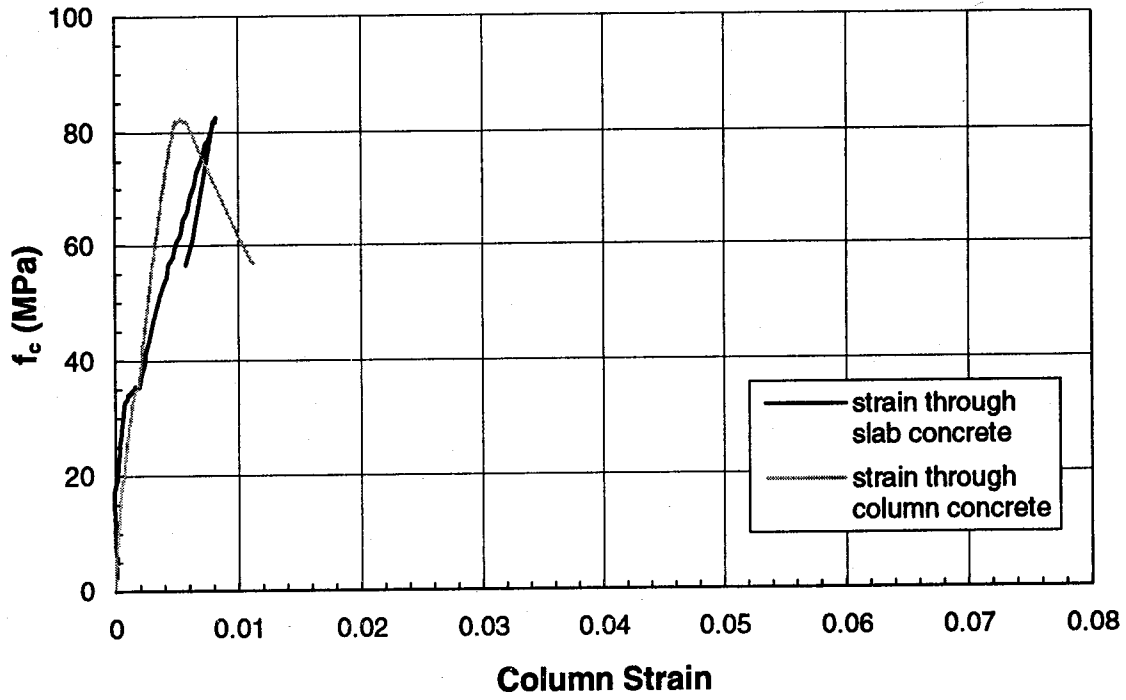
Figure B.9   Stress-Strain Behaviour (Specimen A2-B)
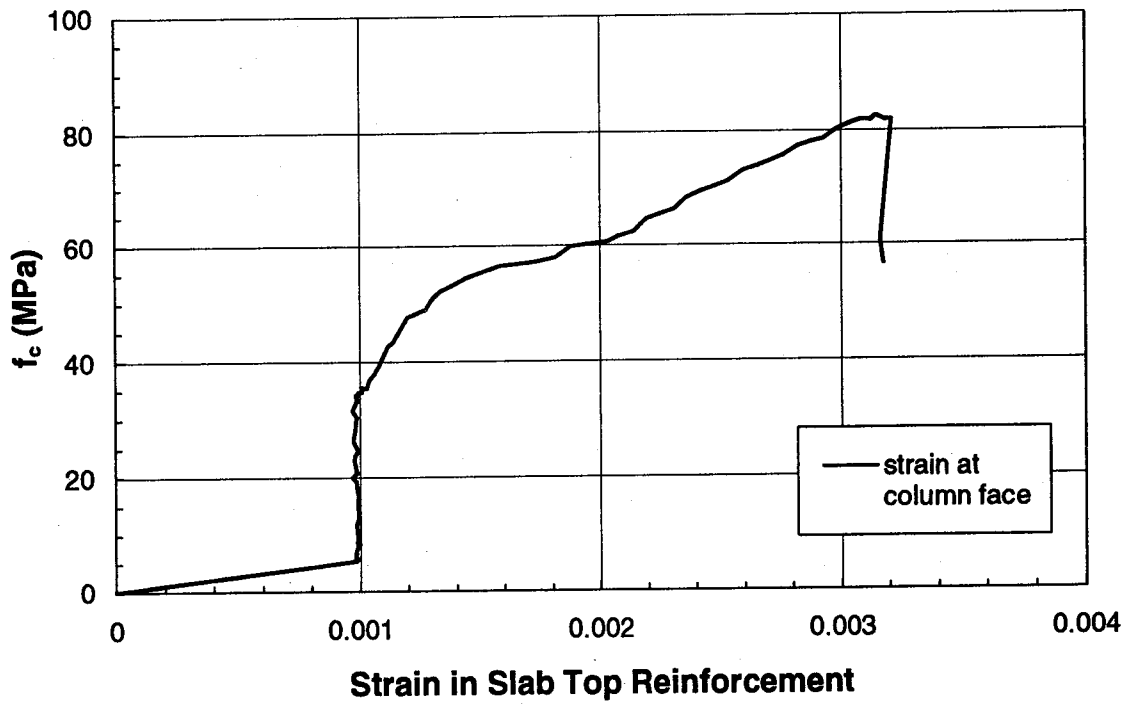
Figure B.10   Slab Transverse Strain (Specimen A2-B)

134
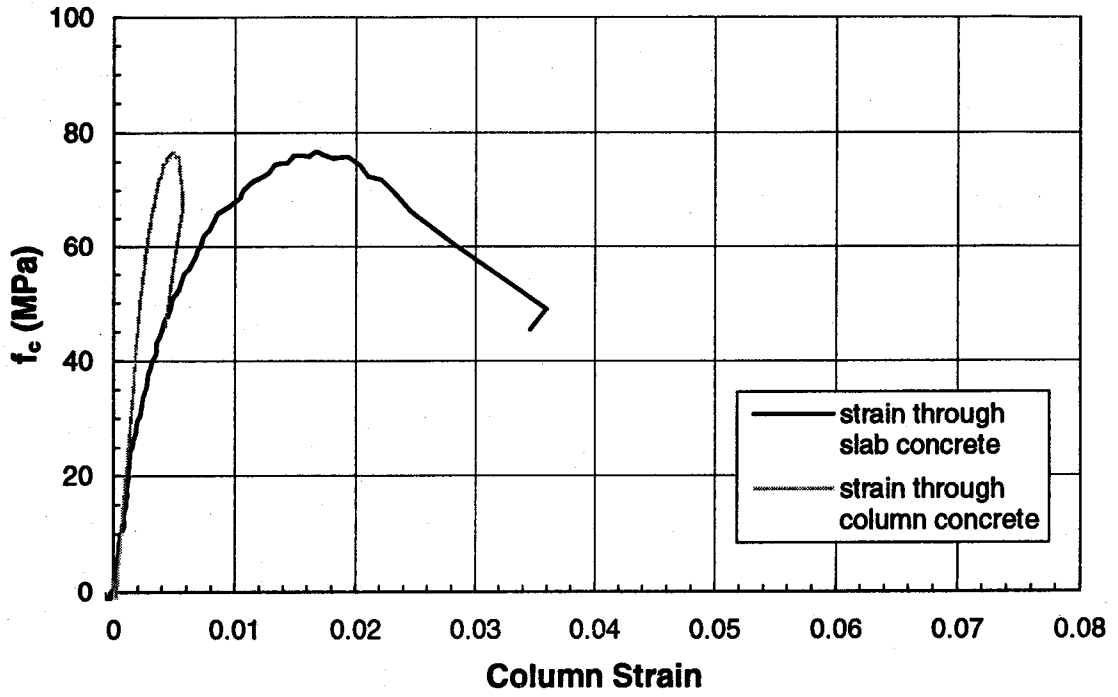
Figure B.11   Stress-Strain Behaviour (Specimen A2-C)
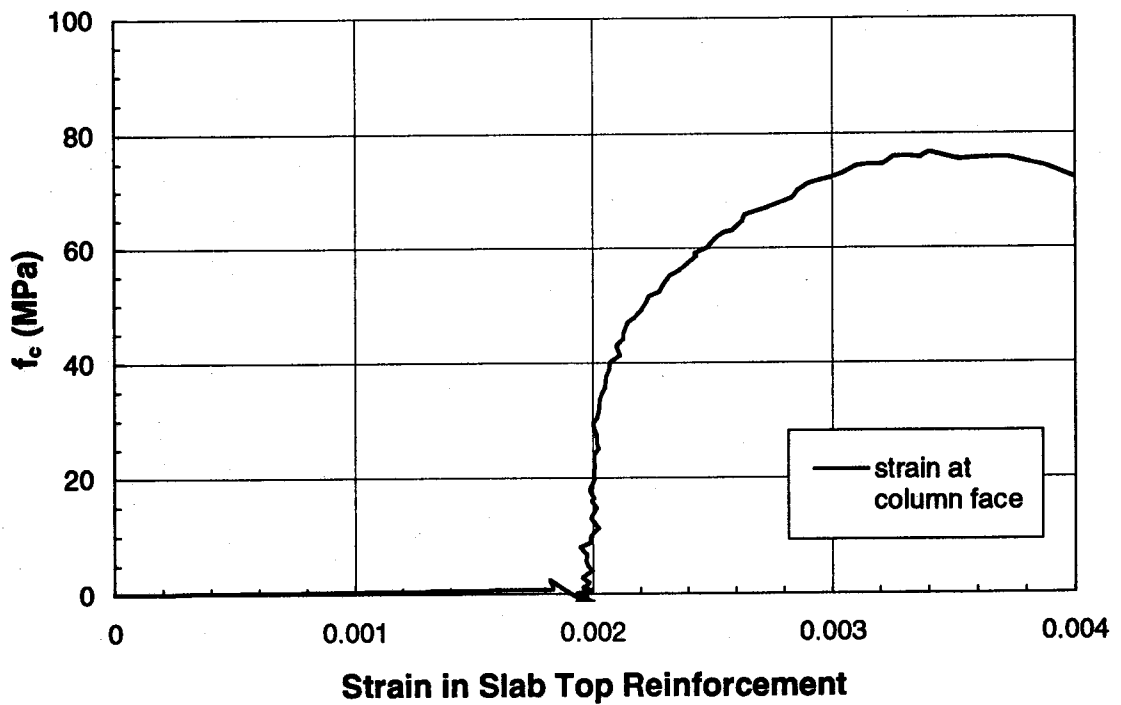
Figure B.12   Slab Transverse Strain (Specimen A2-C)

135
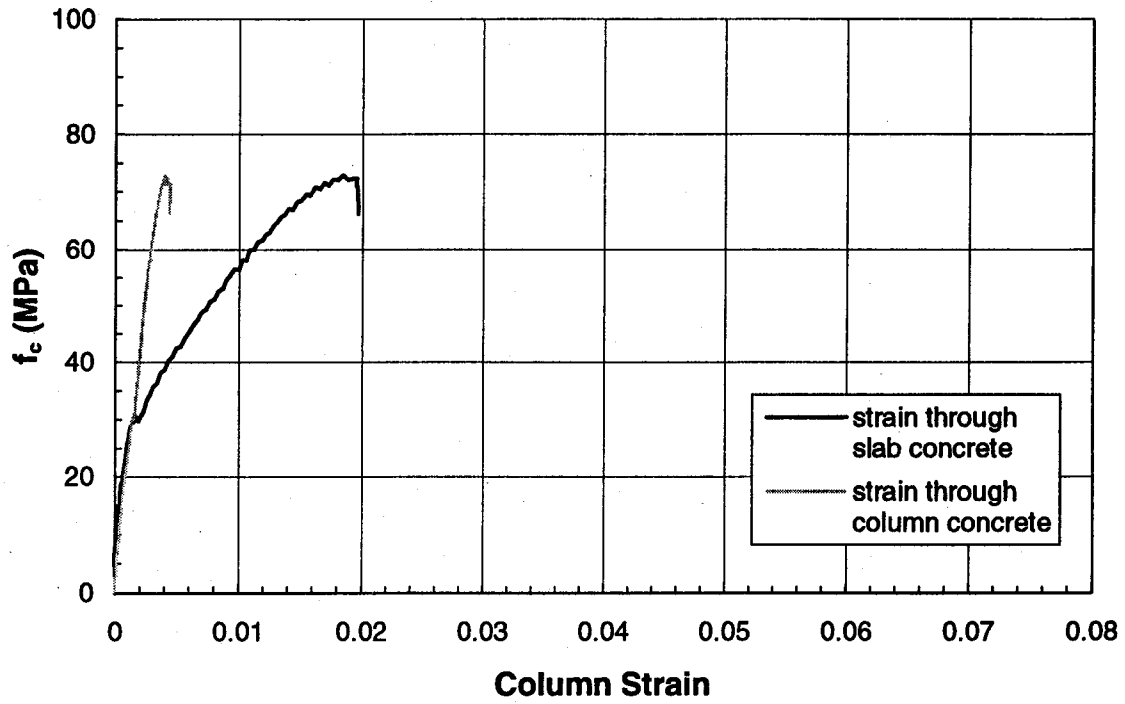
Figure B.13   Stress-Strain Behaviour (Specimen A3-A)
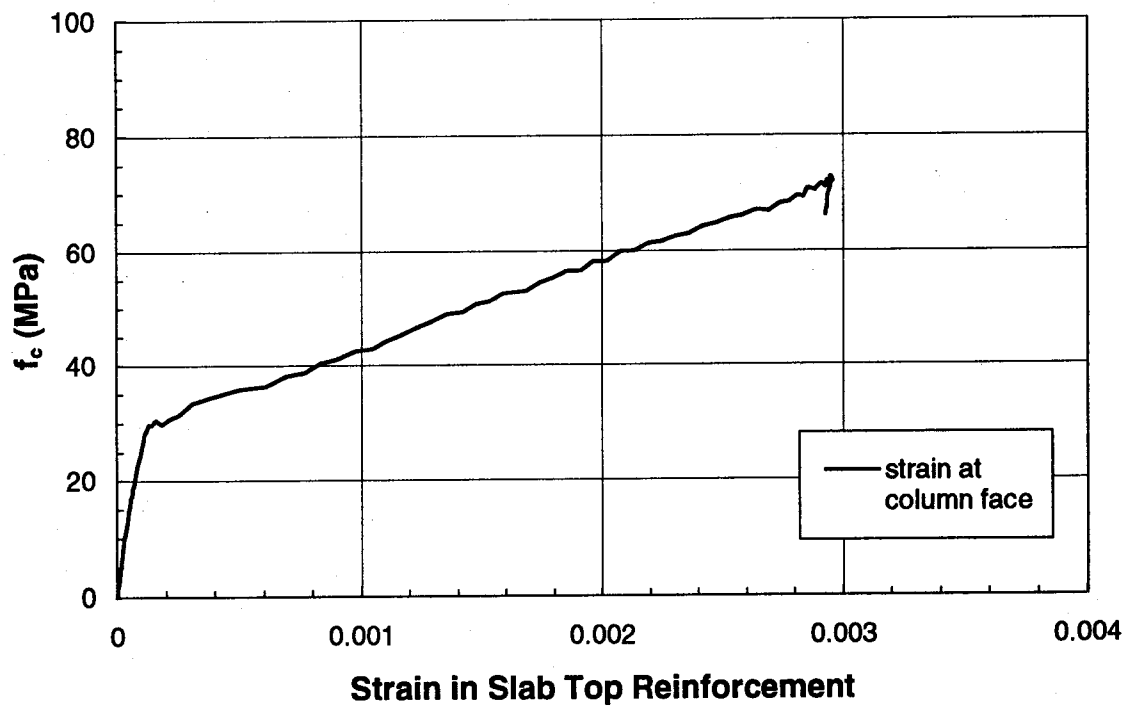
Figure B.14   Slab Transverse Strain (Specimen A3-A)

136
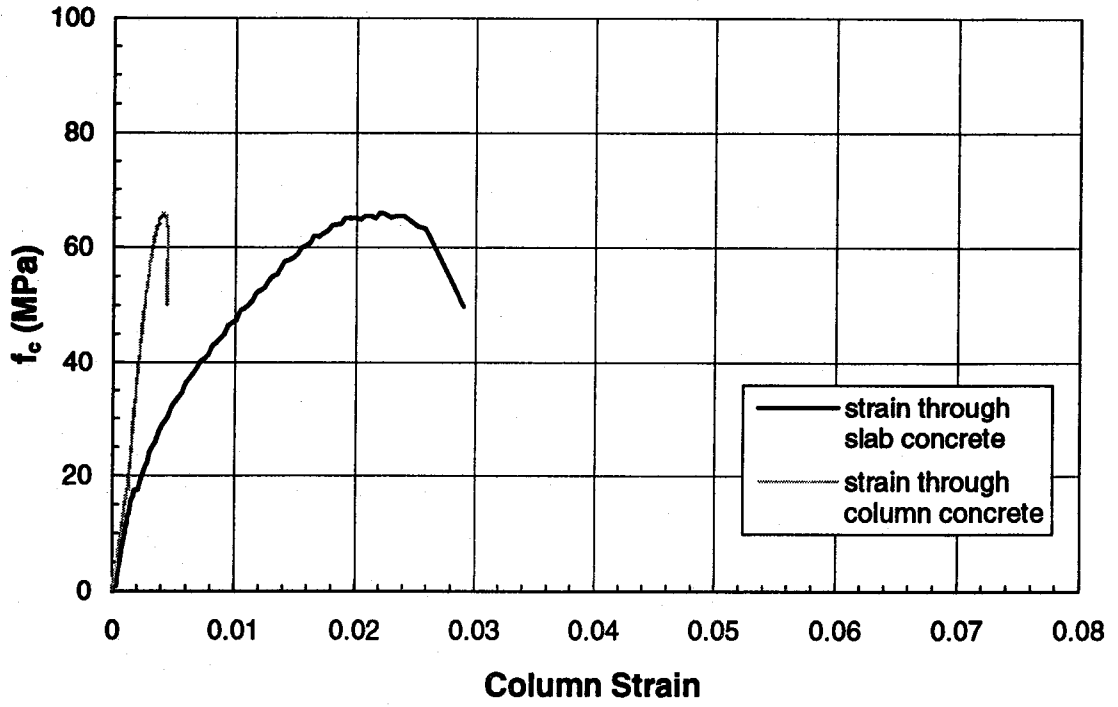
Figure B.15   Stress-Strain Behaviour (Specimen A3-B)
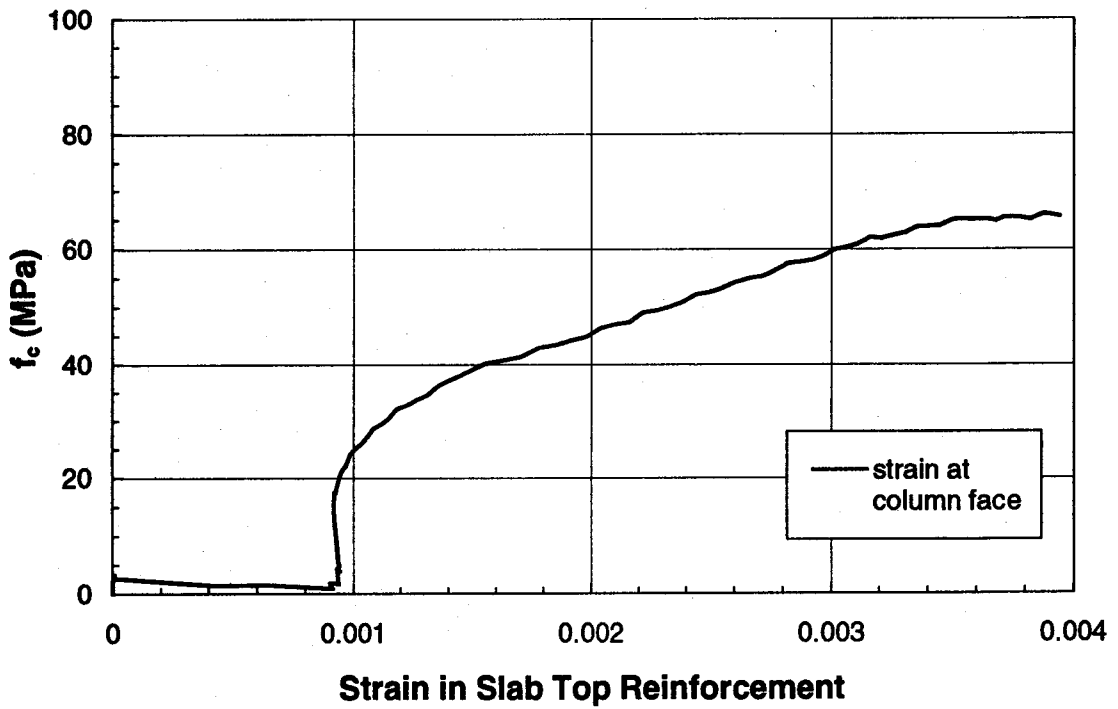
Figure B.16   Slab Transverse Strain (Specimen A3-B)
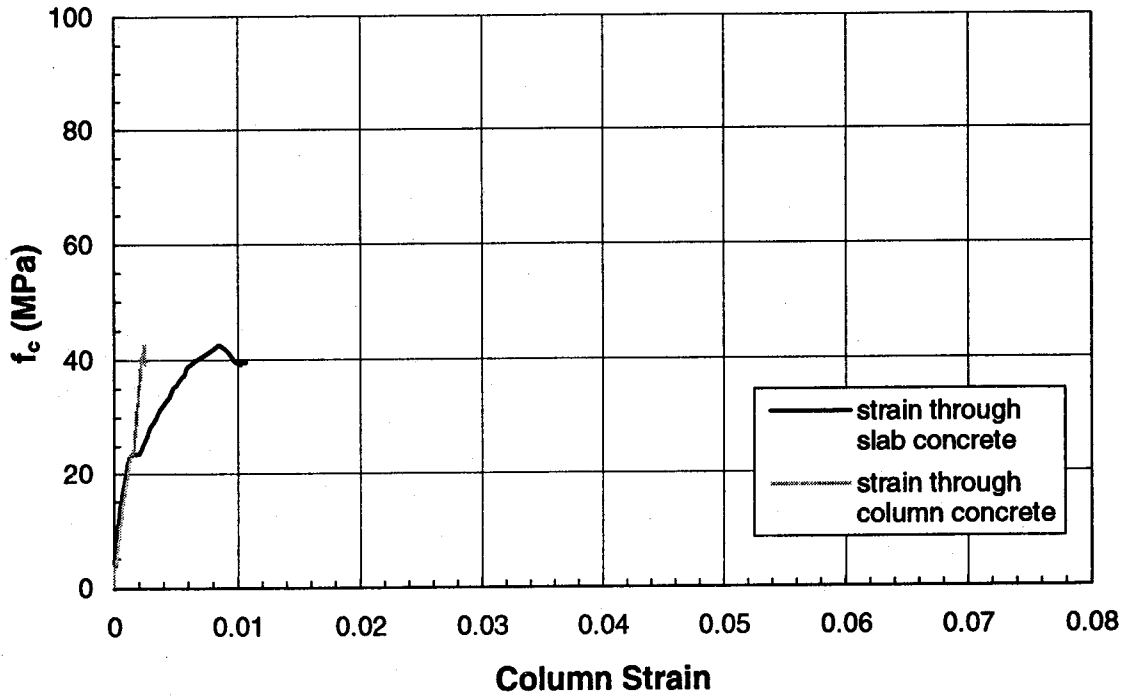
Figure B.17   Stress-Strain Behaviour (Specimen A3-C)
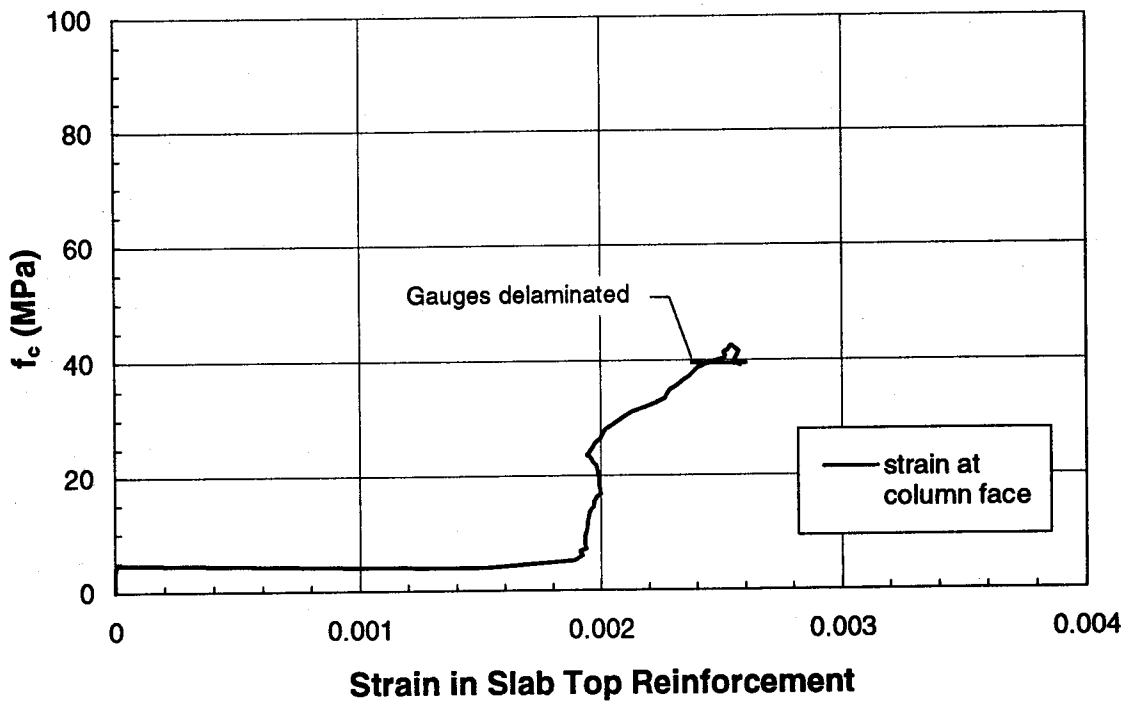
Figure B.18   Slab Transverse Strain (Specimen A3-C)

138
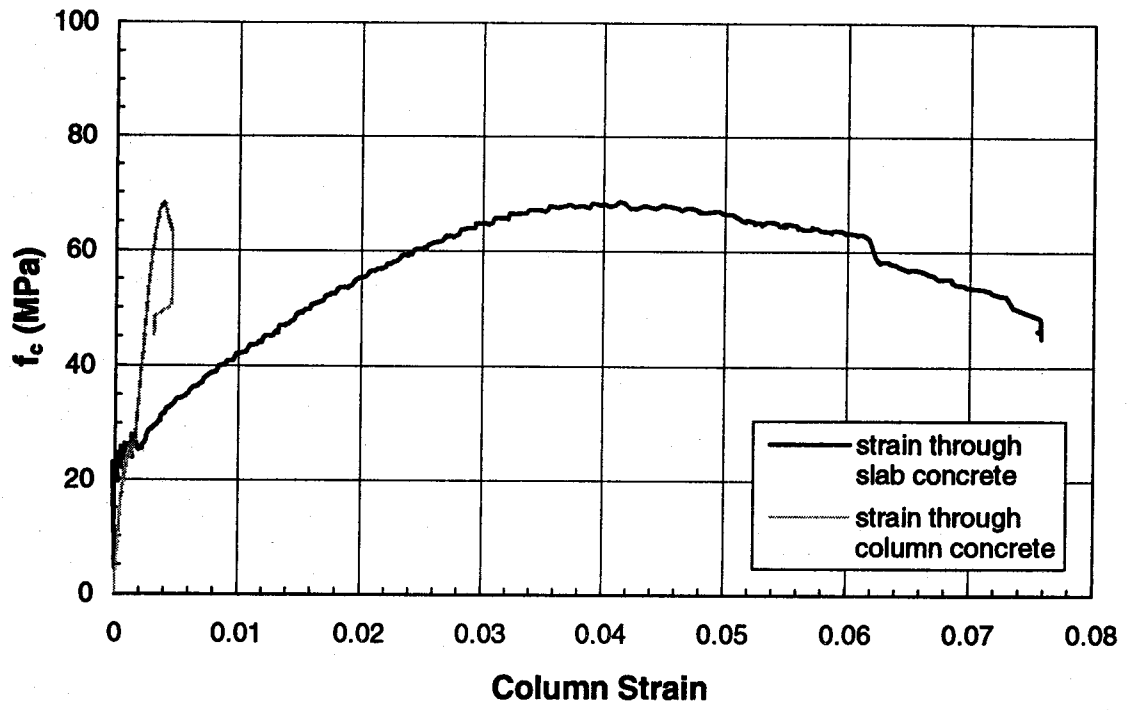
Figure B.19   Stress-Strain Behaviour (Specimen A4-A)
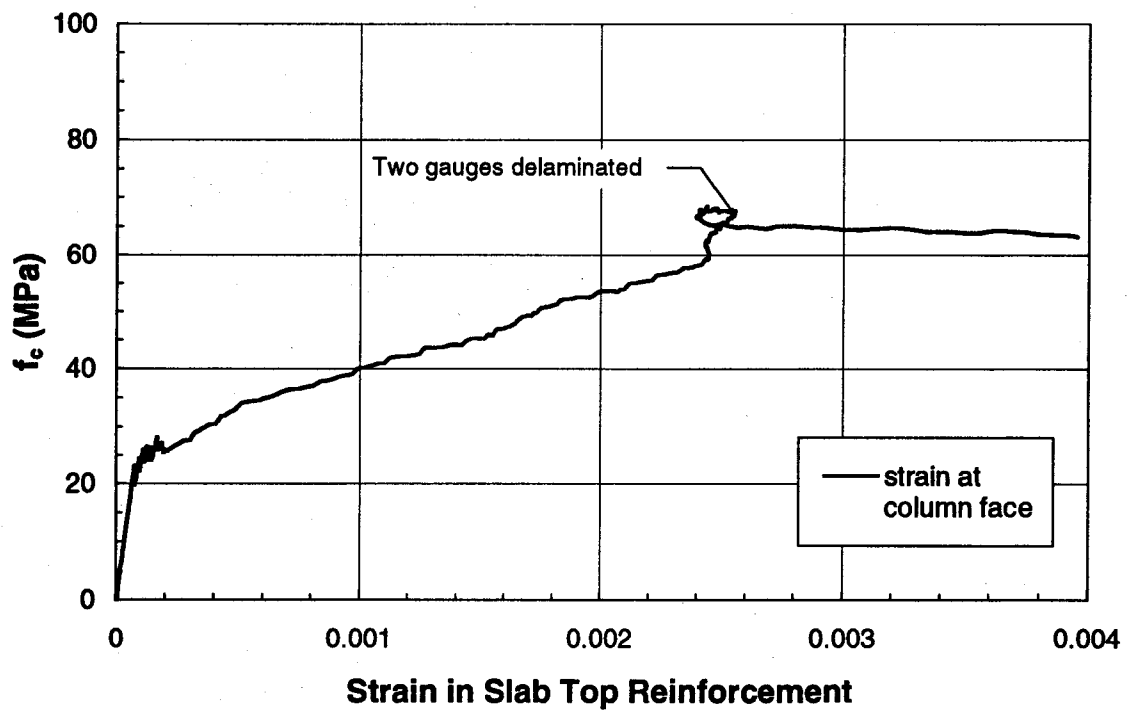
Figure B.20   Slab Transverse Strain (Specimen A4-A)
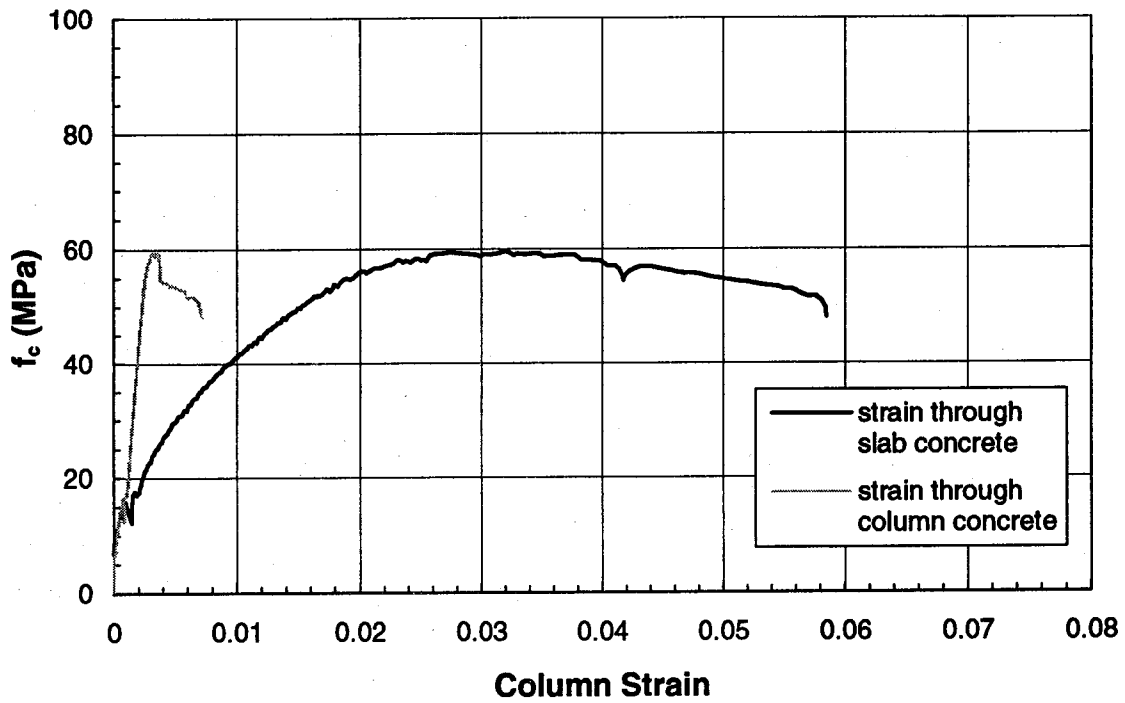
Figure B.21   Stress-Strain Behaviour (Specimen A4-B)
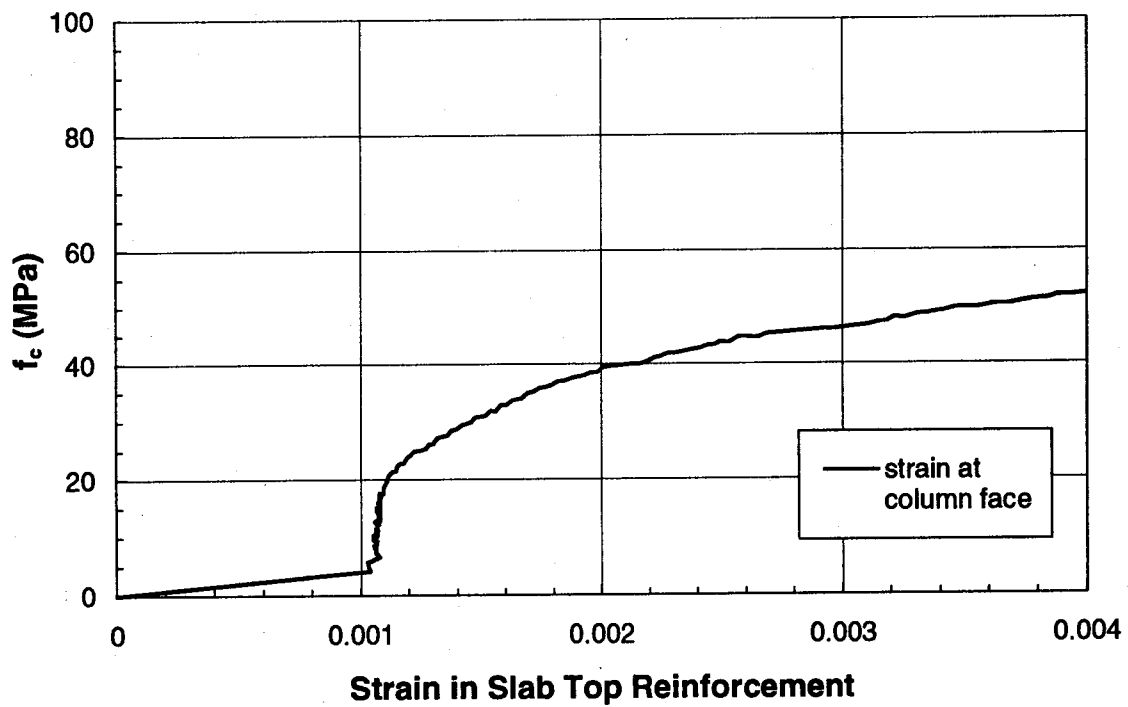
Figure B.22   Slab Transverse Strain (Specimen A4-B)

140
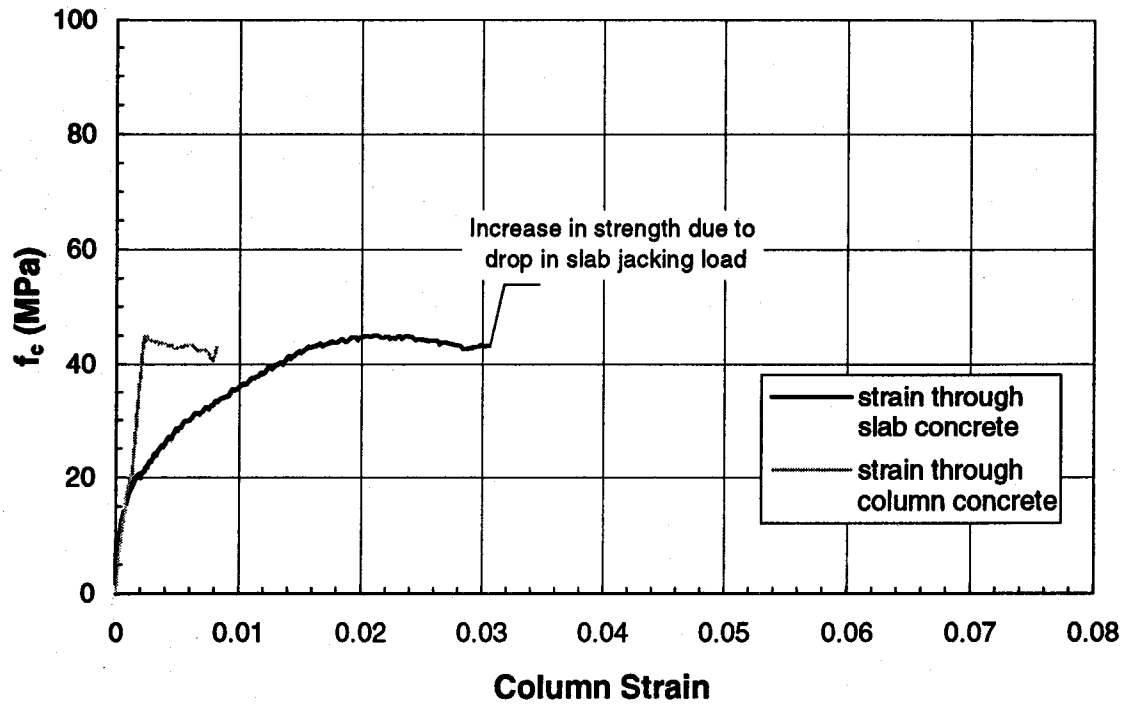
Figure B.23   Stress-Strain Behaviour (Specimen A4-C)
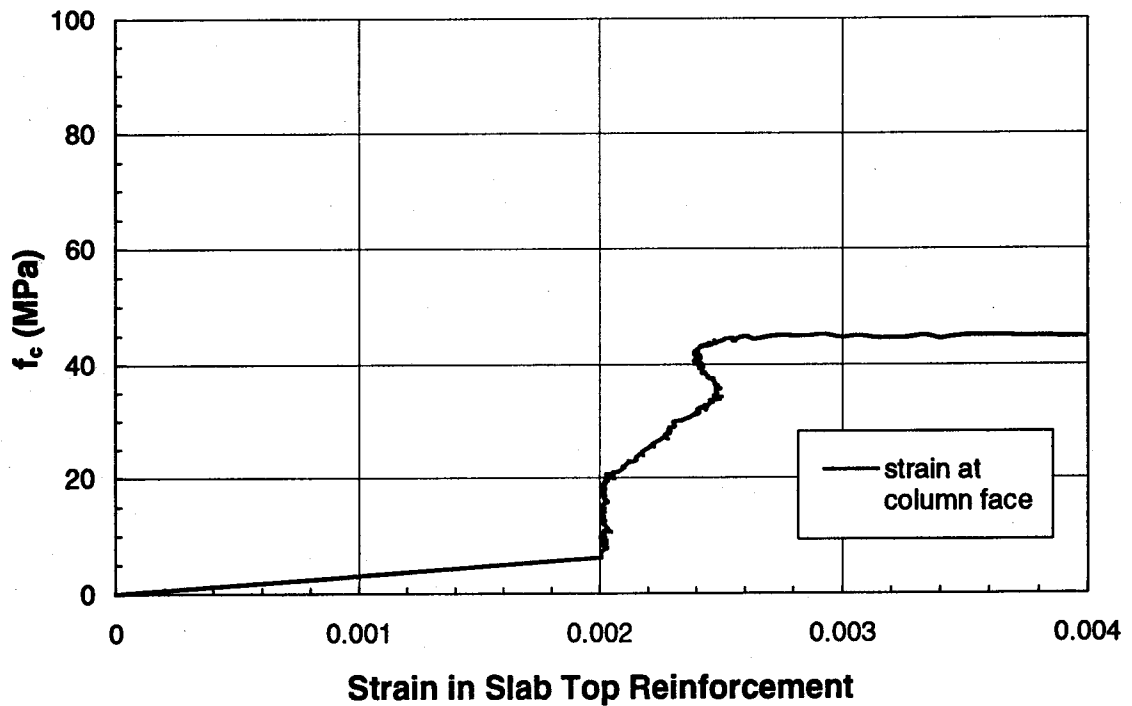
Figure B.24   Slab Transverse Strain (Specimen A4-C)

141

Series B Specimens

- Interior Sandwich Plates -
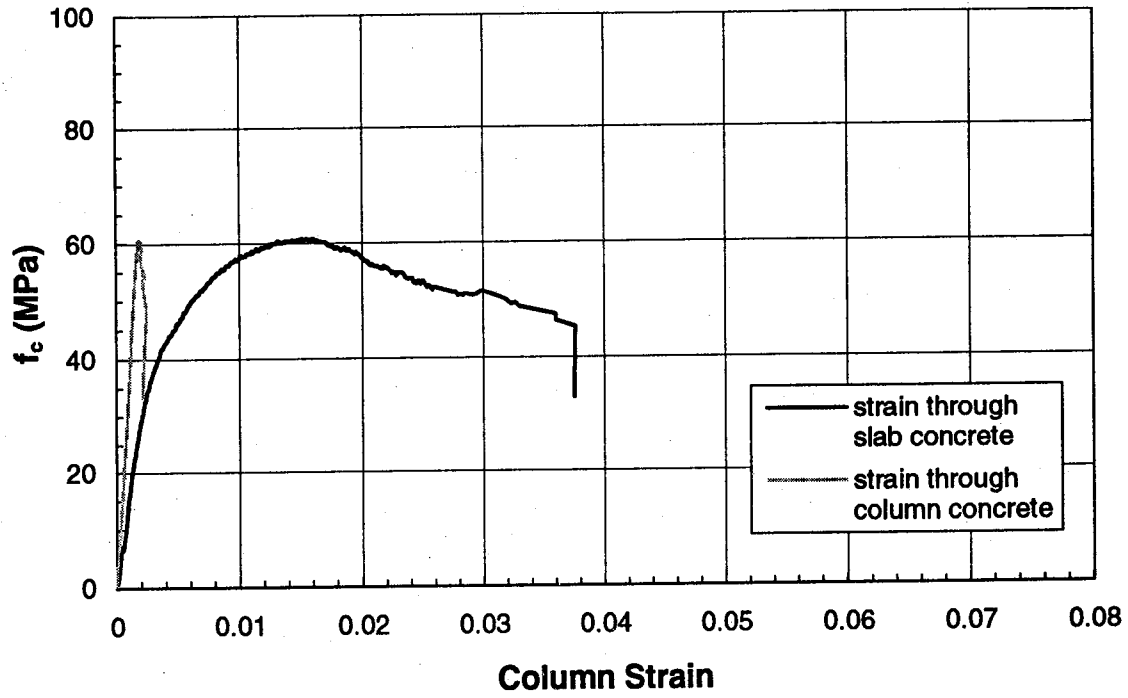
Figure B.25   Stress-Strain Behaviour (Specimen B-1)
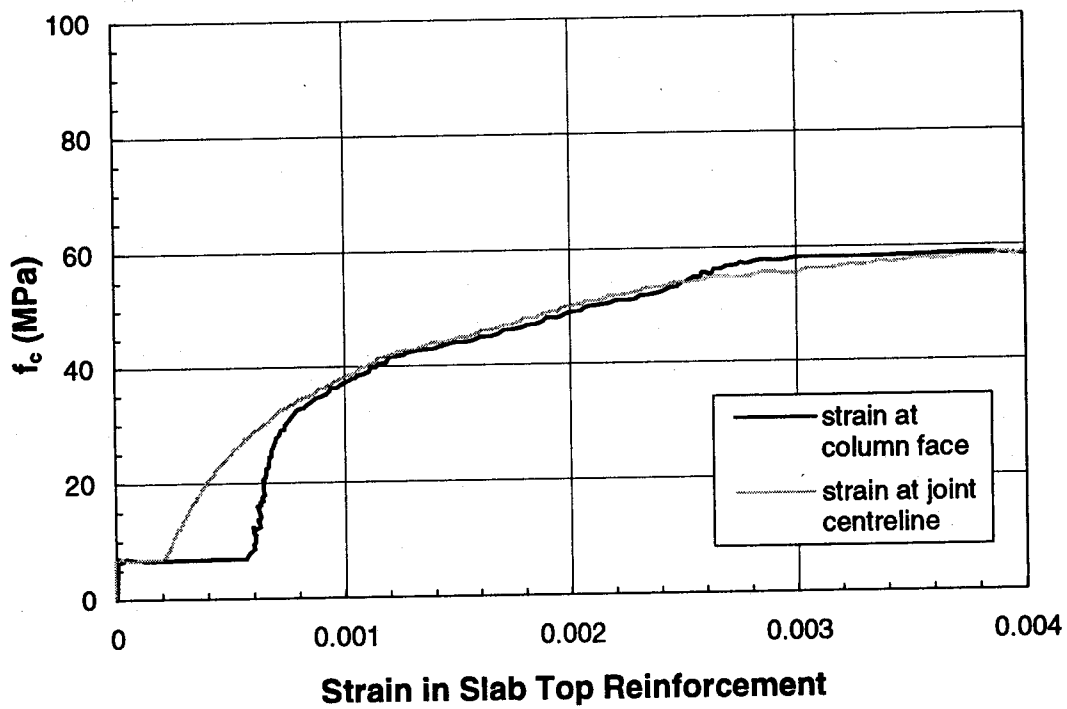
Figure B.26   Slab Transverse Strain (Specimen B-1)
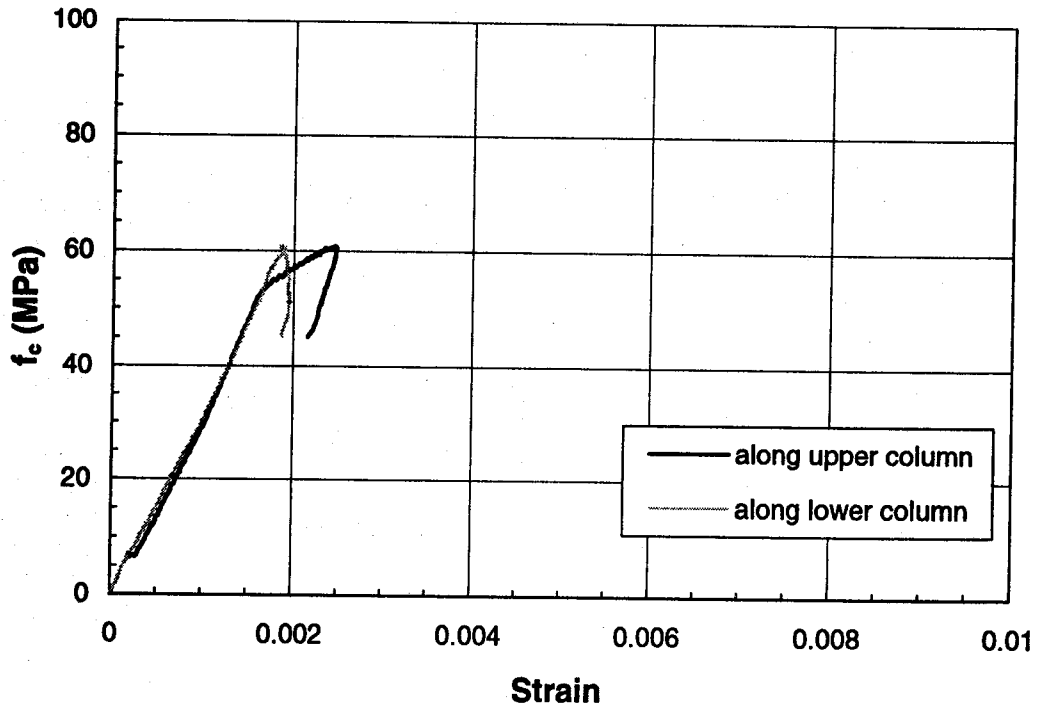
Figure B.27   Column Longitudinal Strain (Specimen B-1)
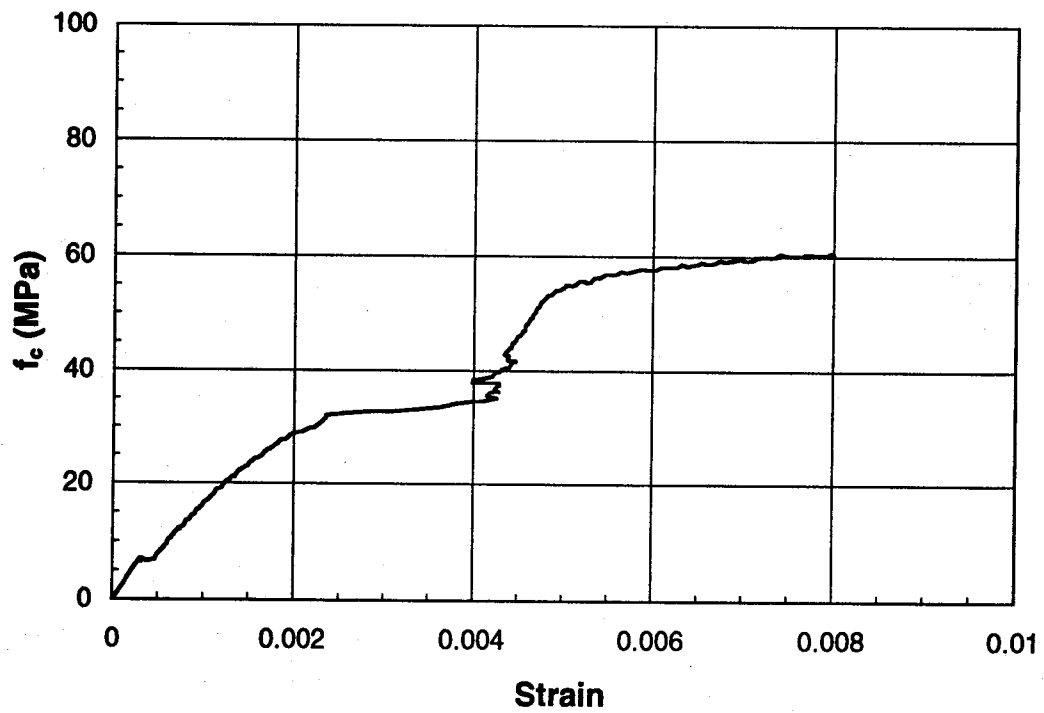
Figure B.28 Column Strain through Slab (Specimen B-1)

145
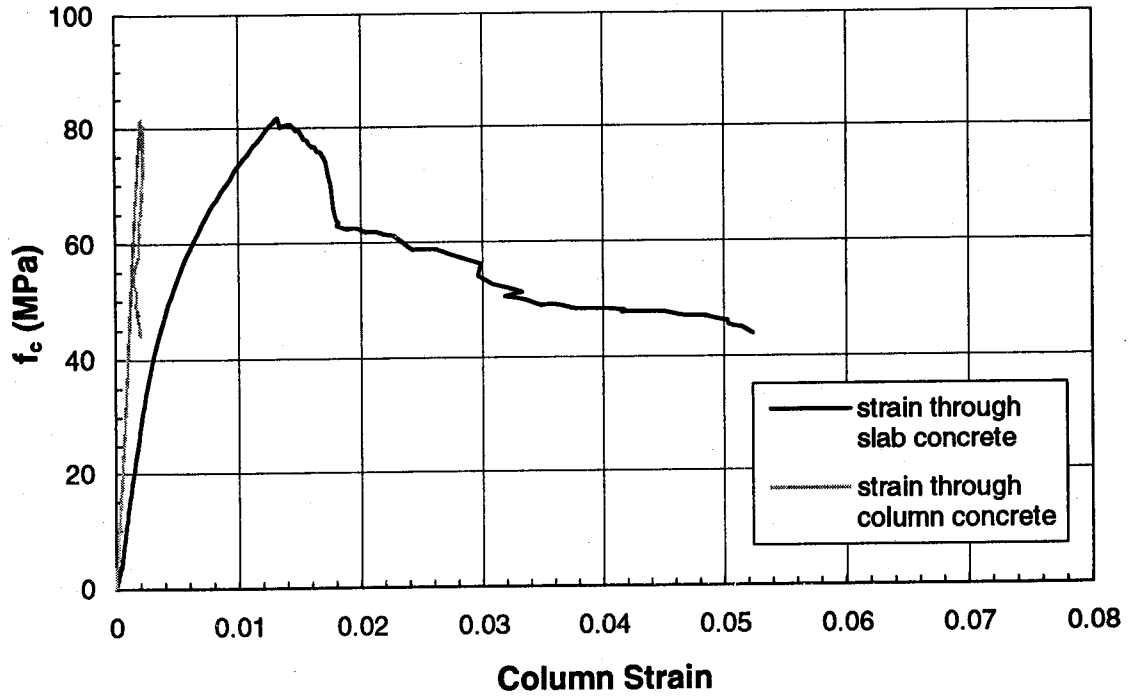
Figure B.29 Stress-Strain Behaviour (Specimen B-2)
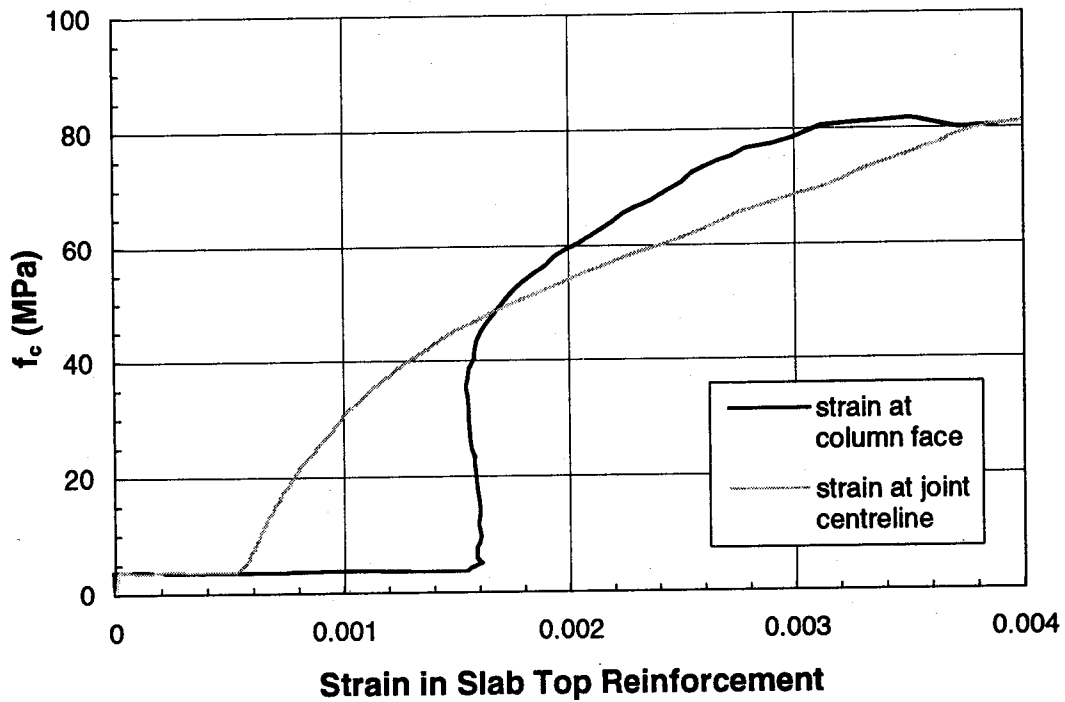
Figure B.30 Slab Transverse Strain (Specimen B-2)
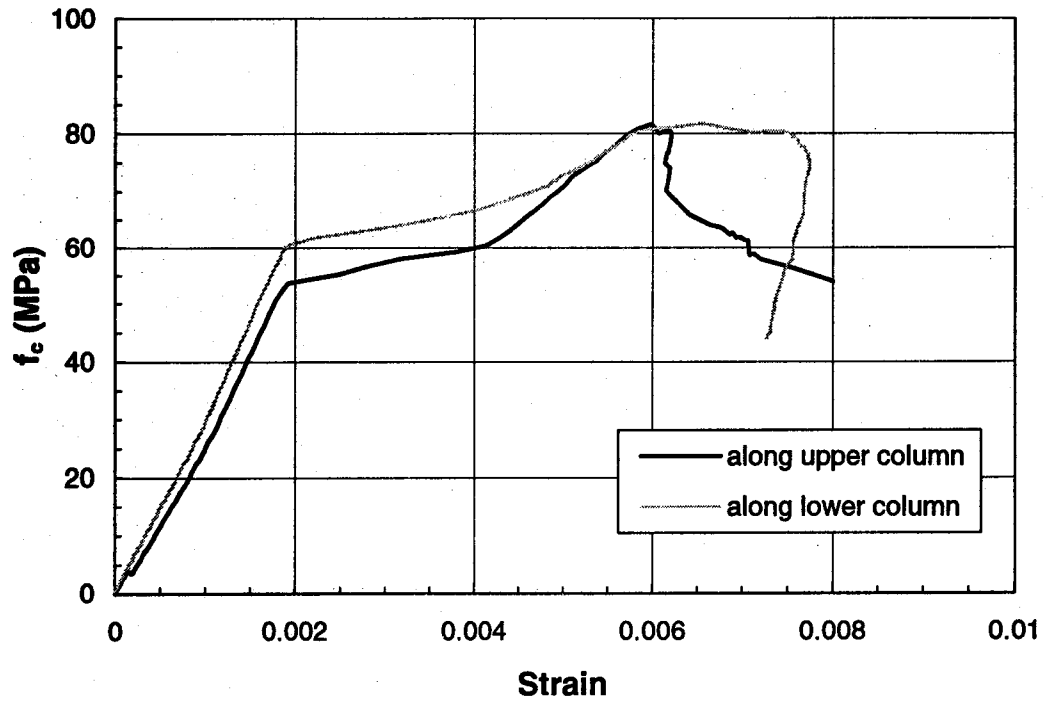
Figure B.31   Column Longitudinal Strain (Specimen B-2)
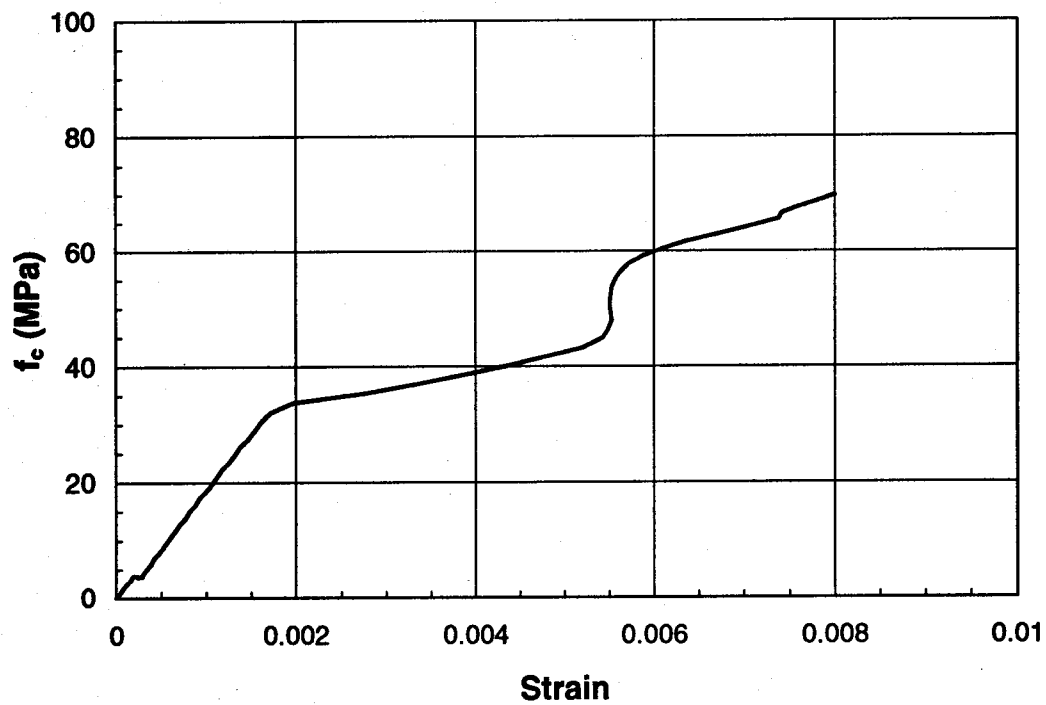
Figure B.32 Column Strain through Slab (Specimen B-2)

147
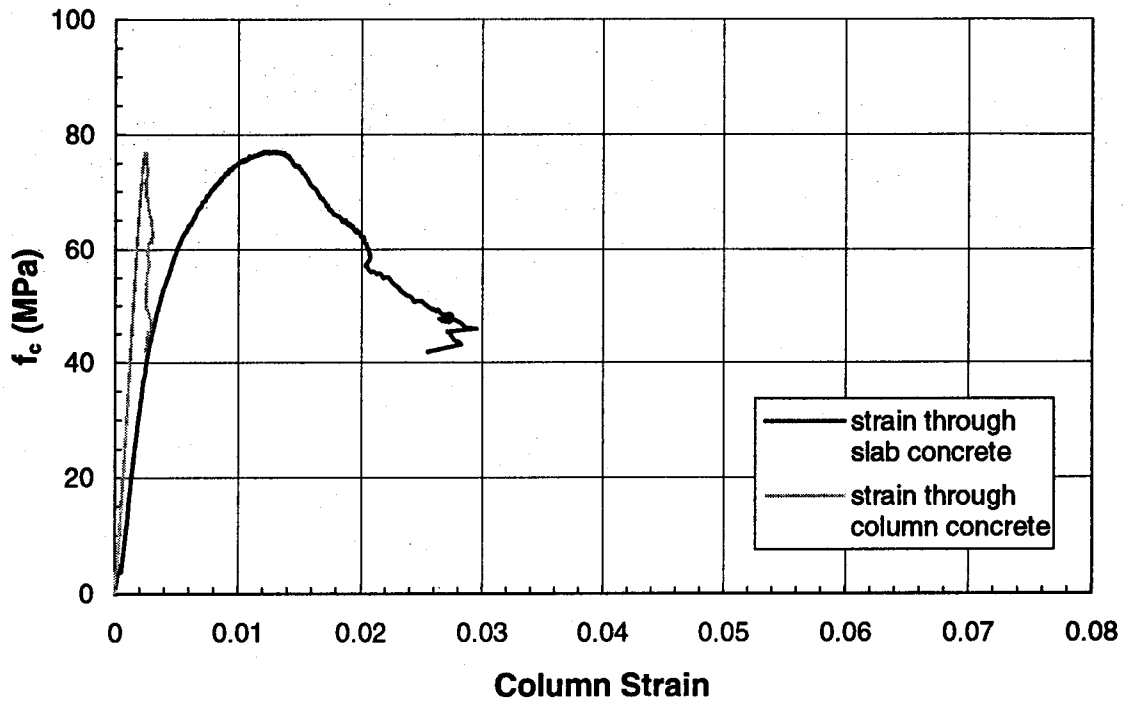
Figure B.33   Stress-Strain Behaviour (Specimen B-3)
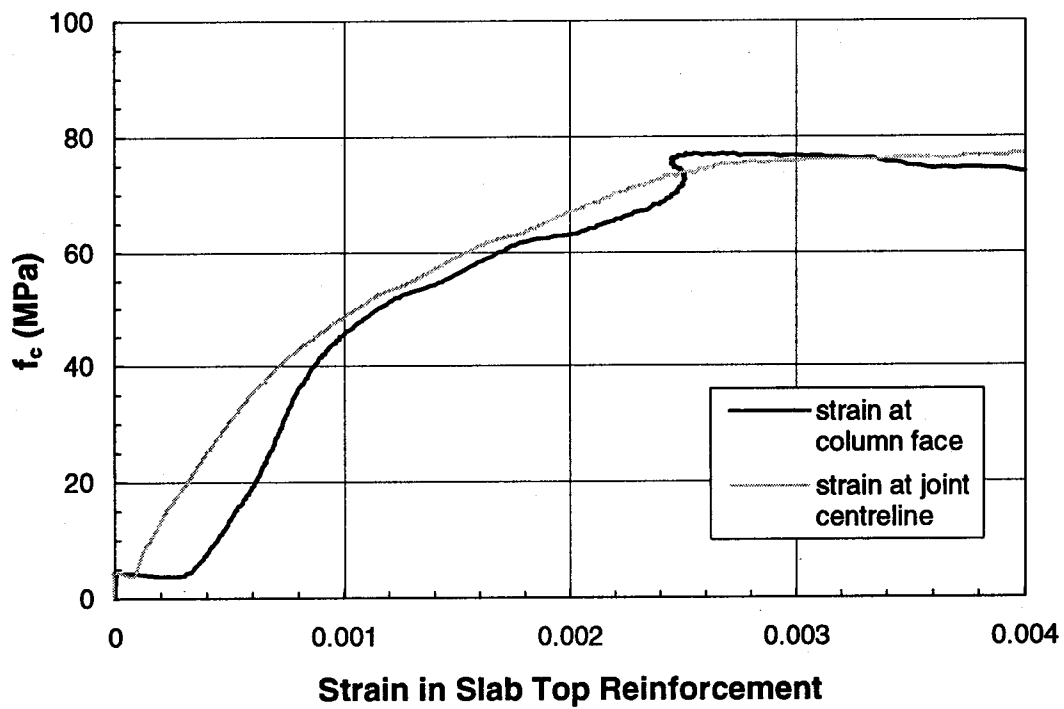
Figure B.34   Slab Transverse Strain (Specimen B-3)

148
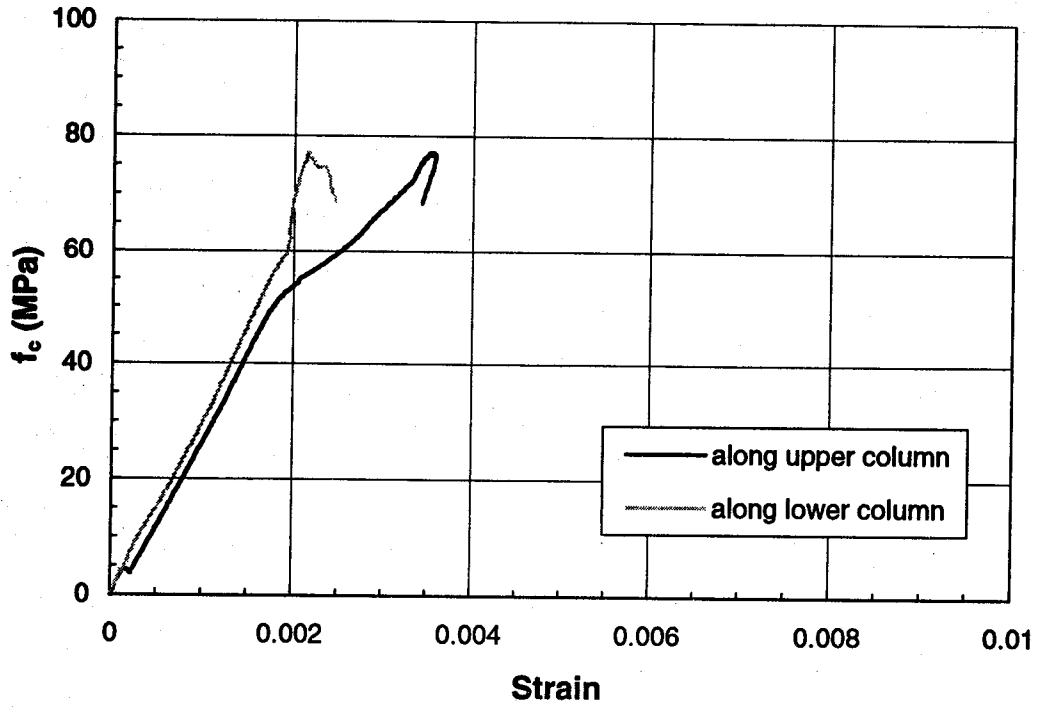
Figure B.35   Column Longitudinal Strain (Specimen B-3)
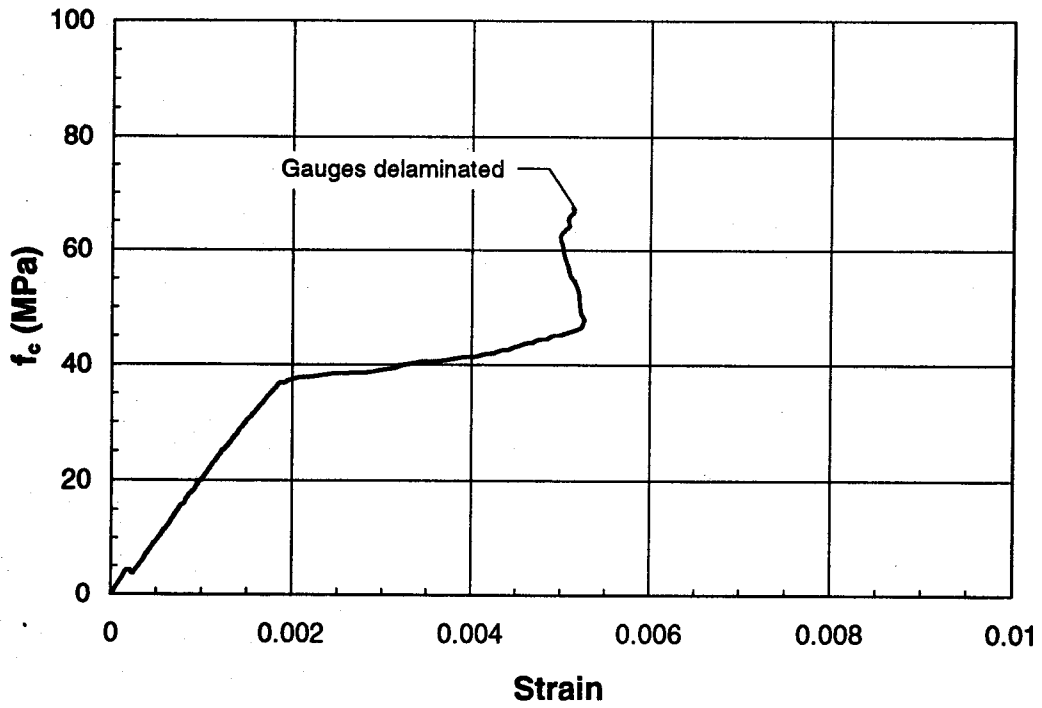
Figure B.36 Column Strain through Slab (Specimen B-3)
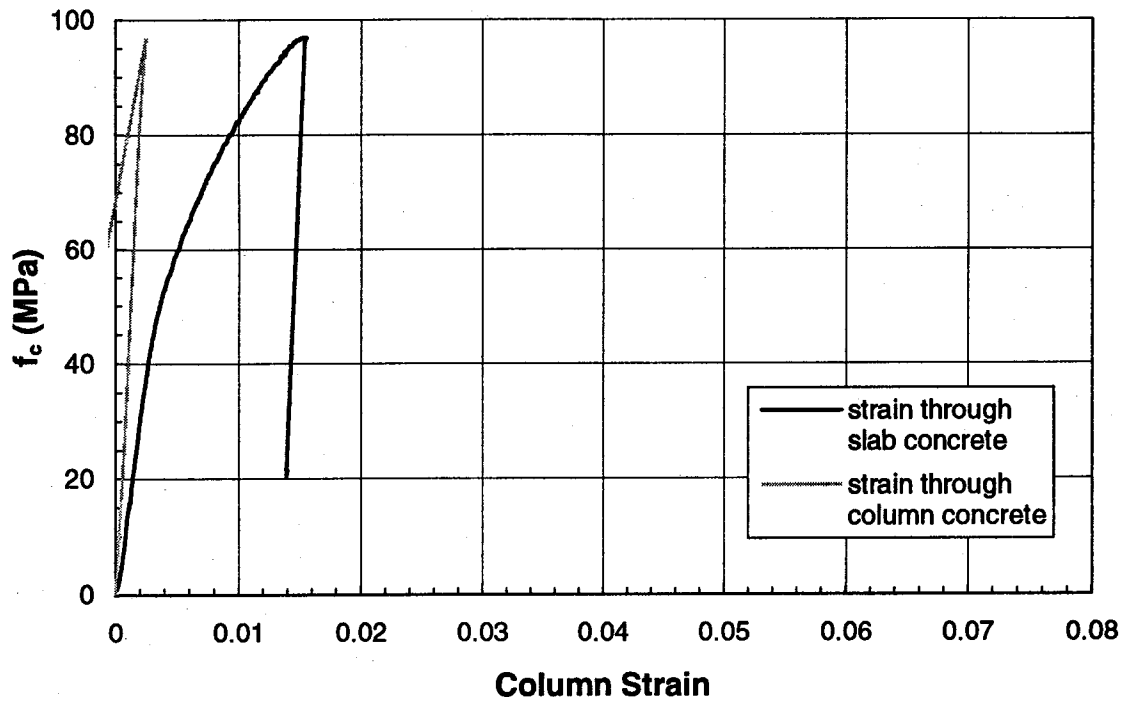
Figure B.37   Stress-Strain Behaviour (Specimen B-4)
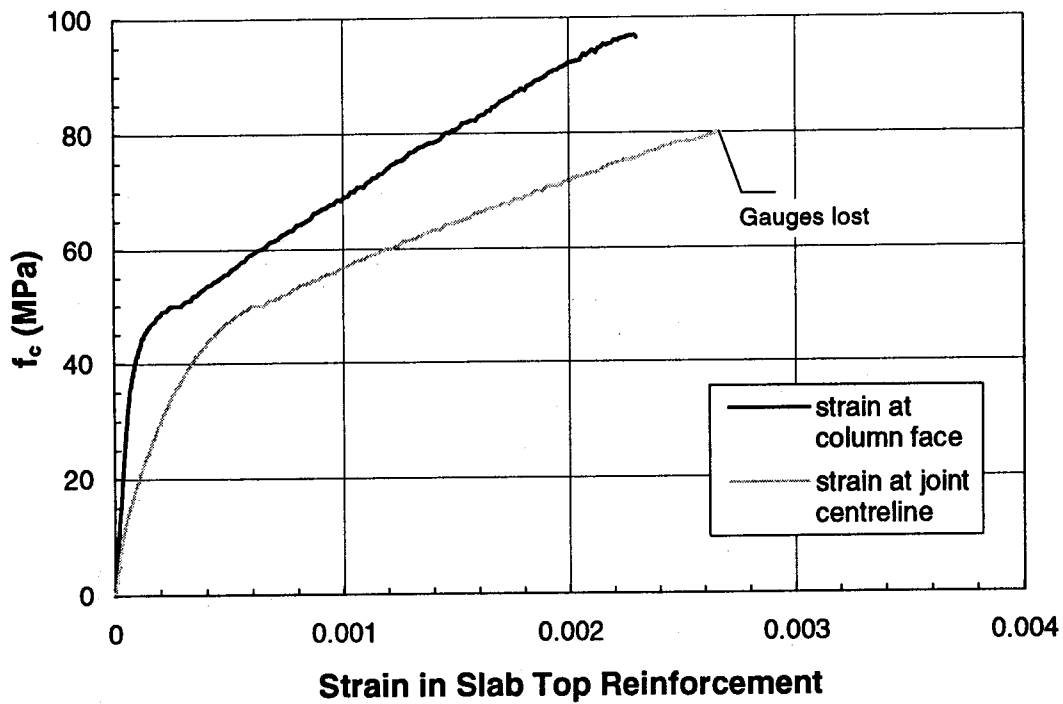
Figure B.38   Slab Transverse Strain (Specimen B-4)

150
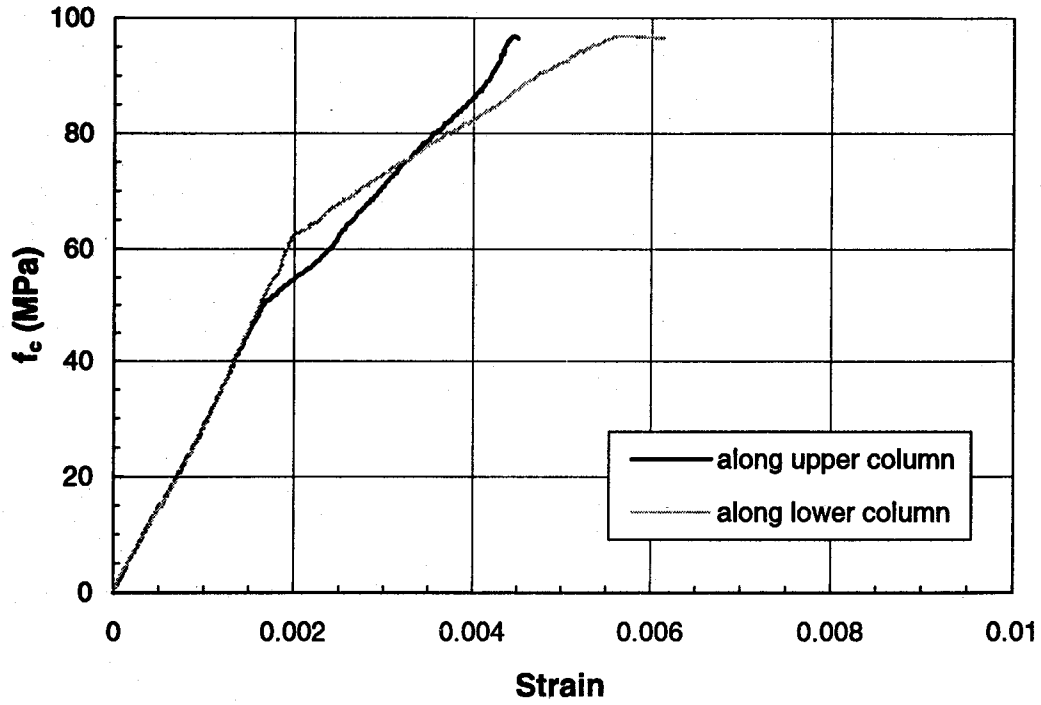
Figure B.39   Column Longitudinal Strain (Specimen B-4)
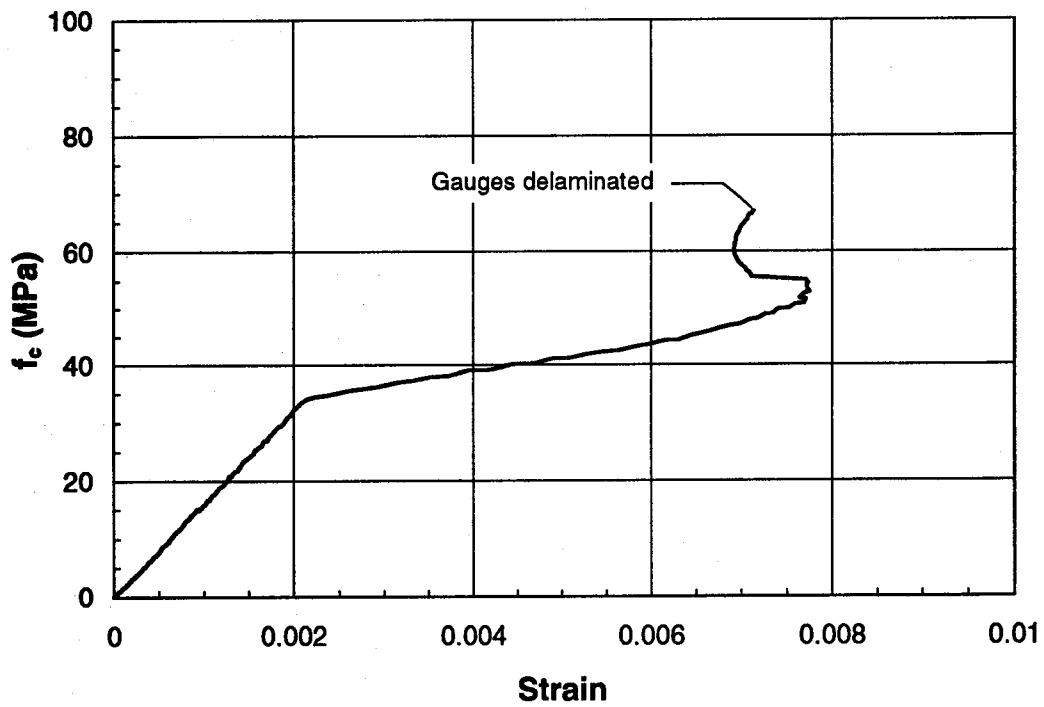
Figure B.40 Column Strain through Slab (Specimen B-4)

151
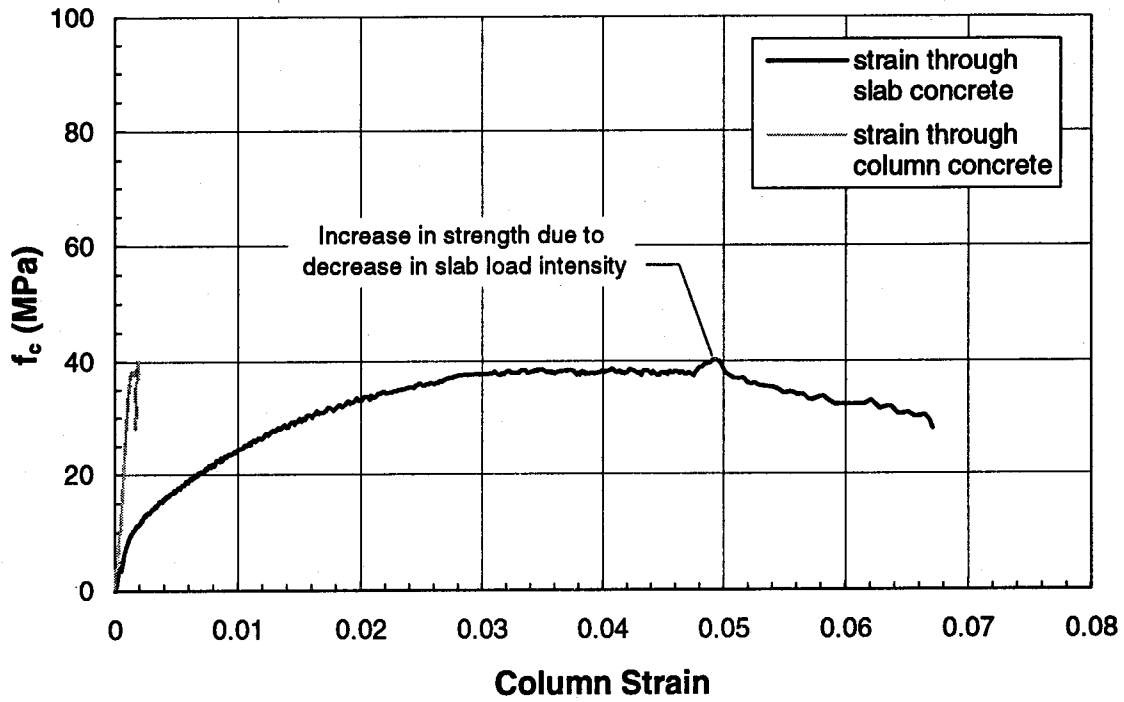
Figure B.41 Stress-Strain Behaviour (Specimen B-5)
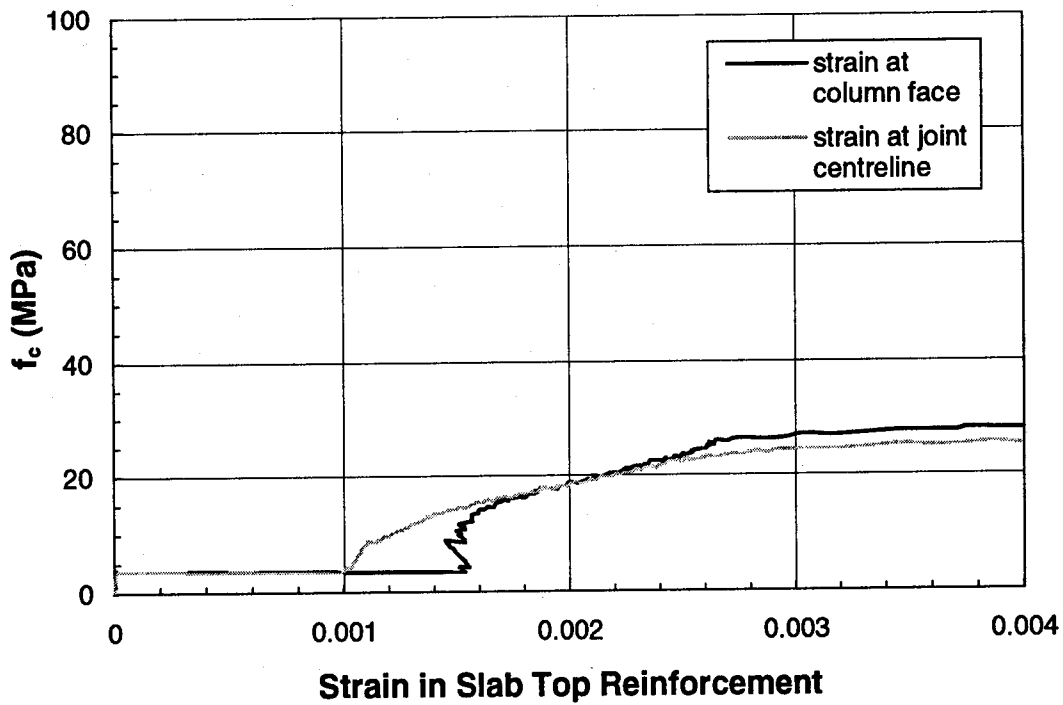
Figure B.42 Slab Transverse Strain (Specimen B-5)
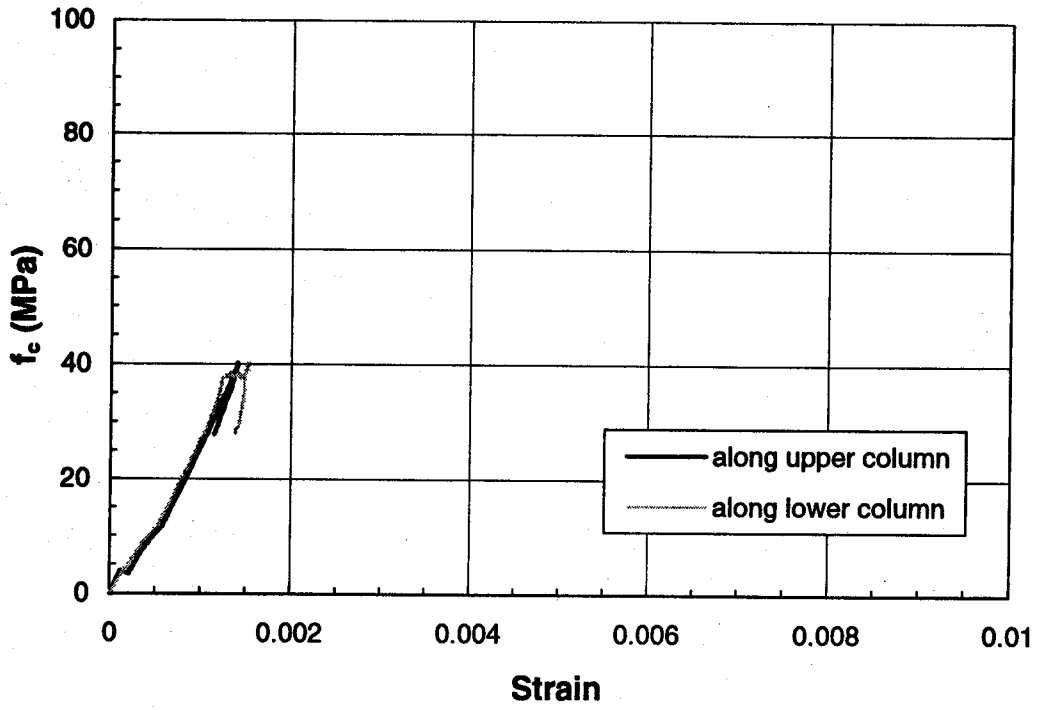
Figure B.43   Column Longitudinal Strain (Specimen B-5)
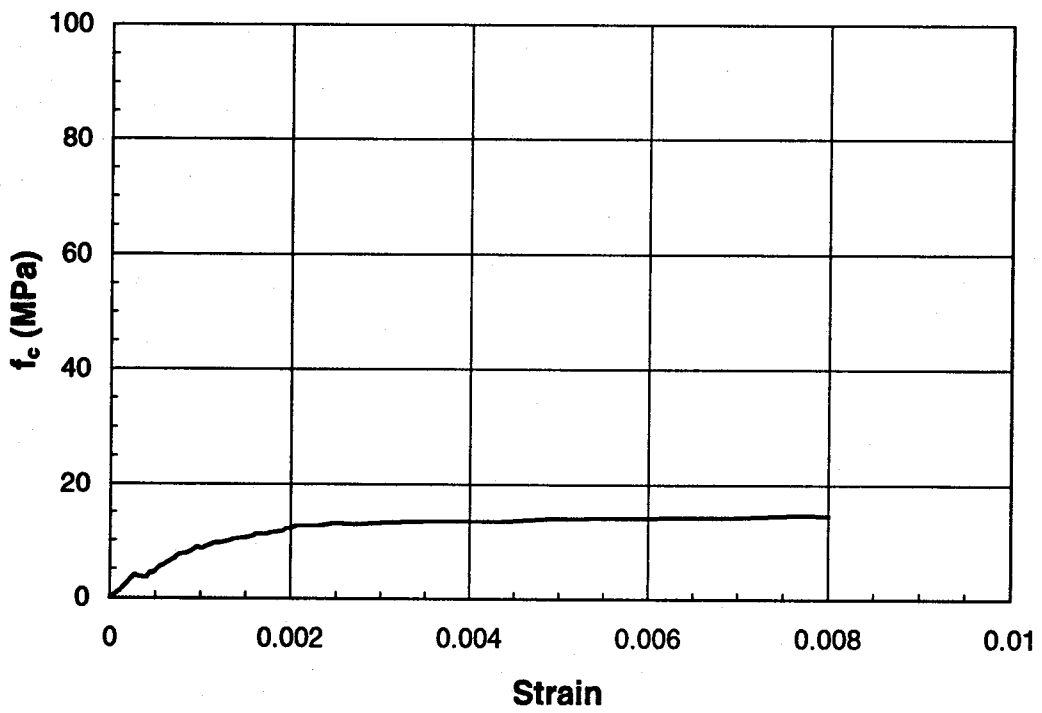
Figure B.44 Column Strain through Slab (Specimen B-5)

153
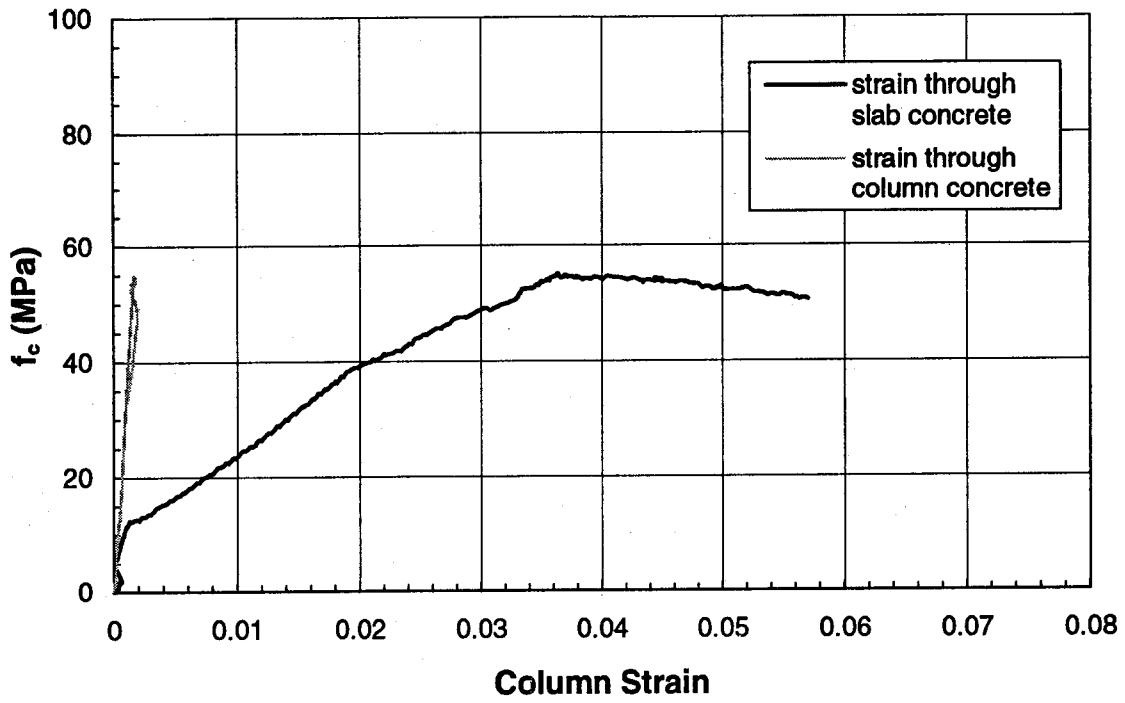
Figure B.45 Stress-Strain Behaviour (Specimen B-6)
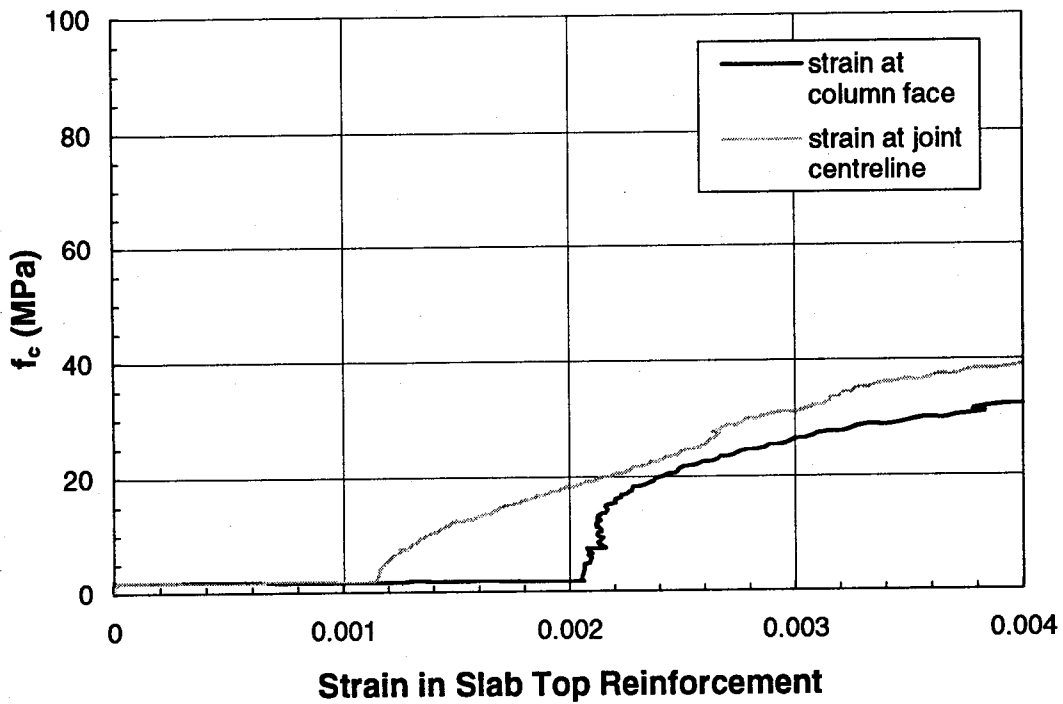
Figure B.46 Slab Transverse Strain (Specimen B-6)

154
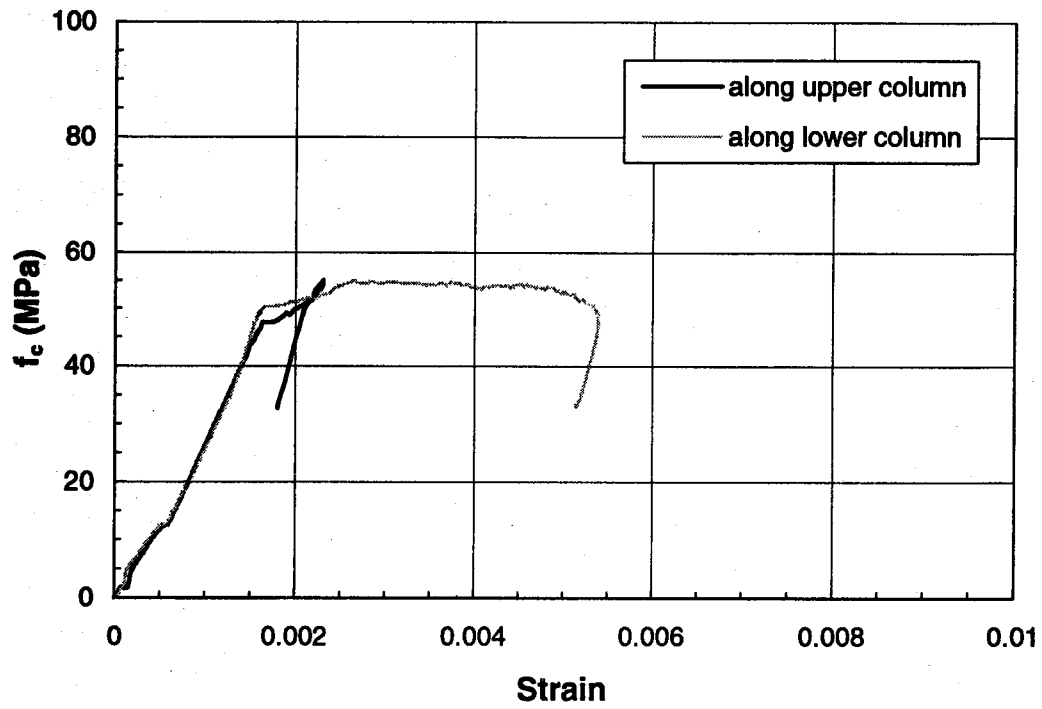
Figure B.47   Column Longitudinal Strain (Specimen B-6)
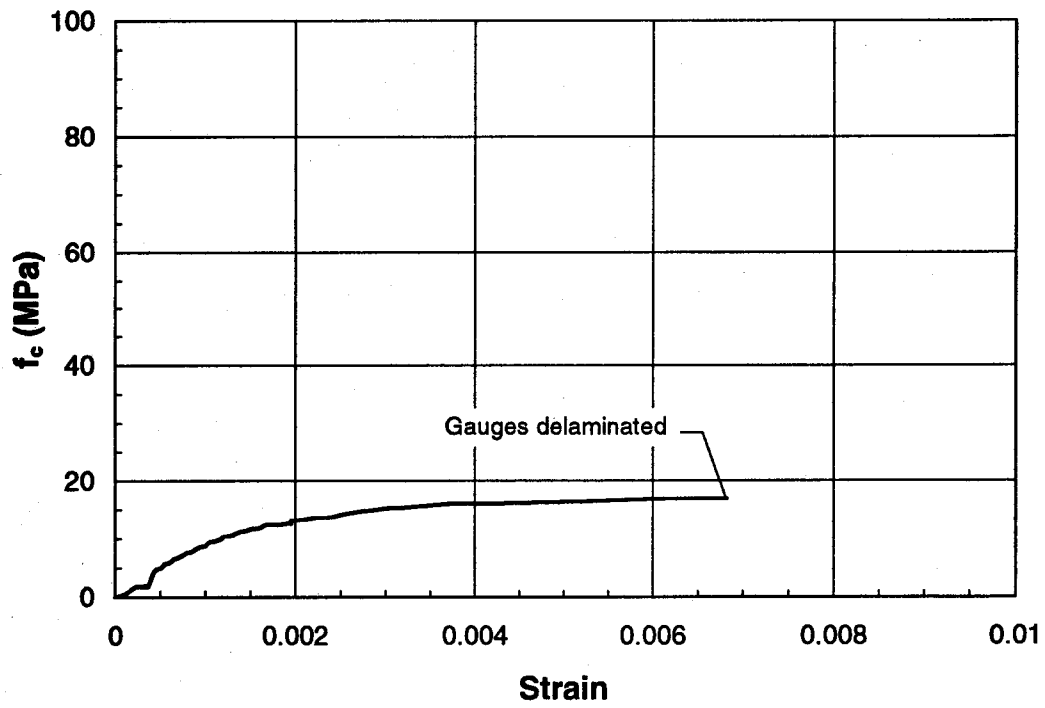
Figure B.48 Column Strain through Slab (Specimen B-6)

155
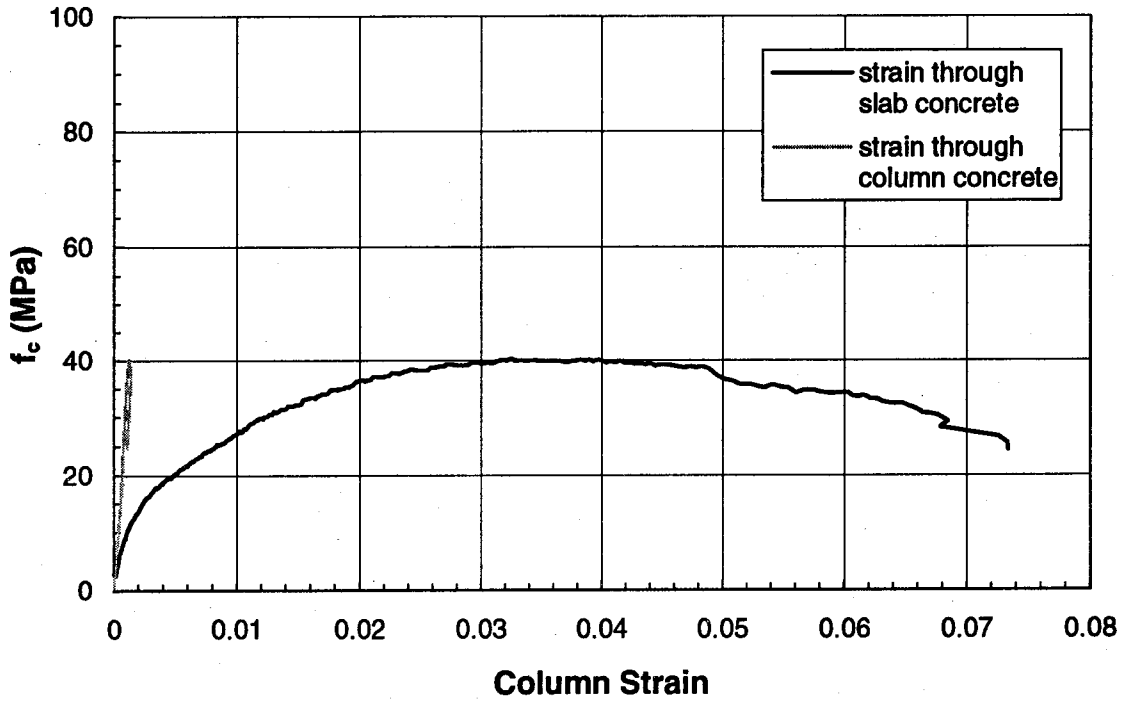
Figure B.49   Stress-Strain Behaviour (Specimen B-7)
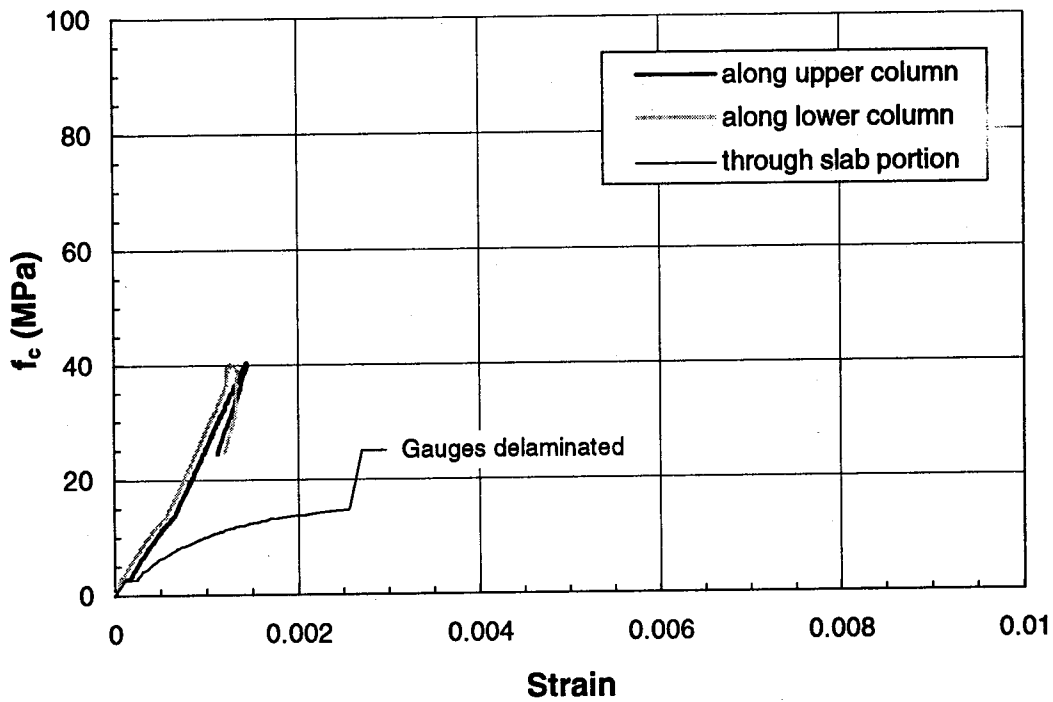
Figure B.50   Column Longitudinal Strain (Specimen B-7)

156
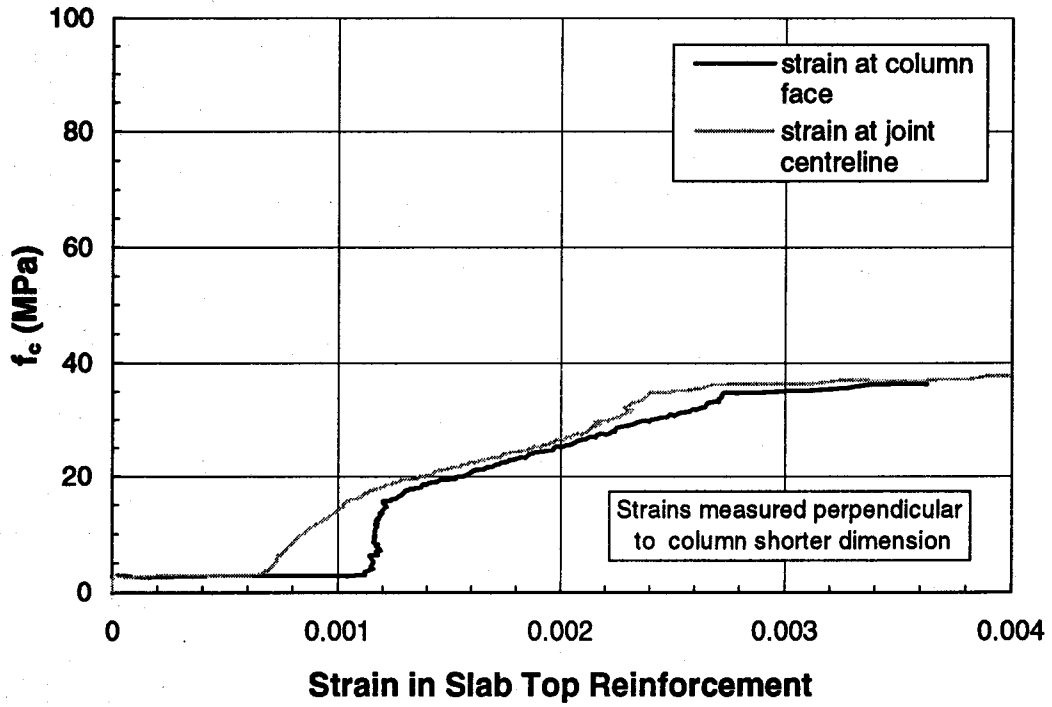
Figure B.51   Slab Transverse Strain (Specimen B-7)
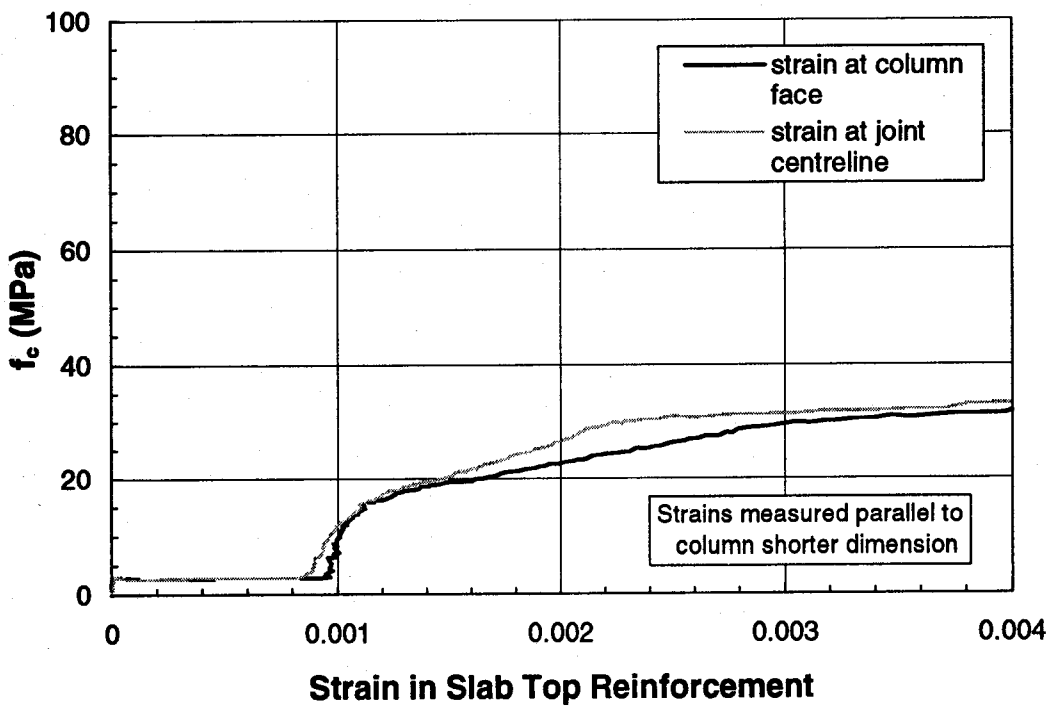
Figure B.52   Slab Transverse Strain (Specimen B-7)
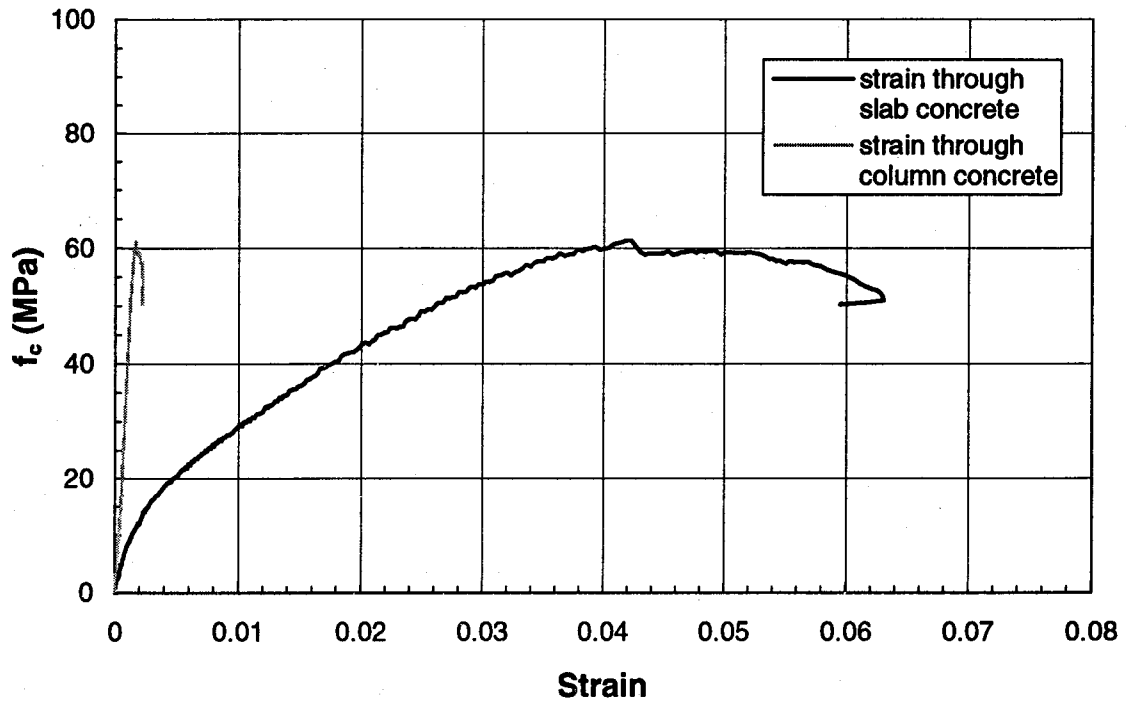
Figure B.53   Stress-Strain Behaviour (Specimen B-8)
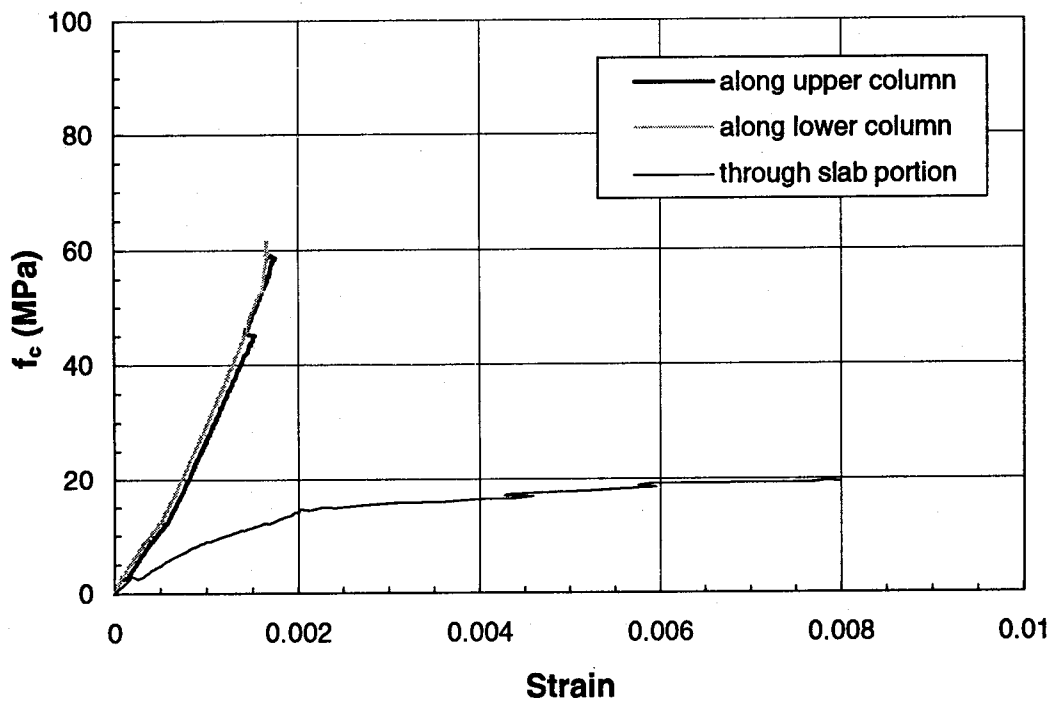
Figure B.54   Column Longitudinal Strain (Specimen B-8)

158
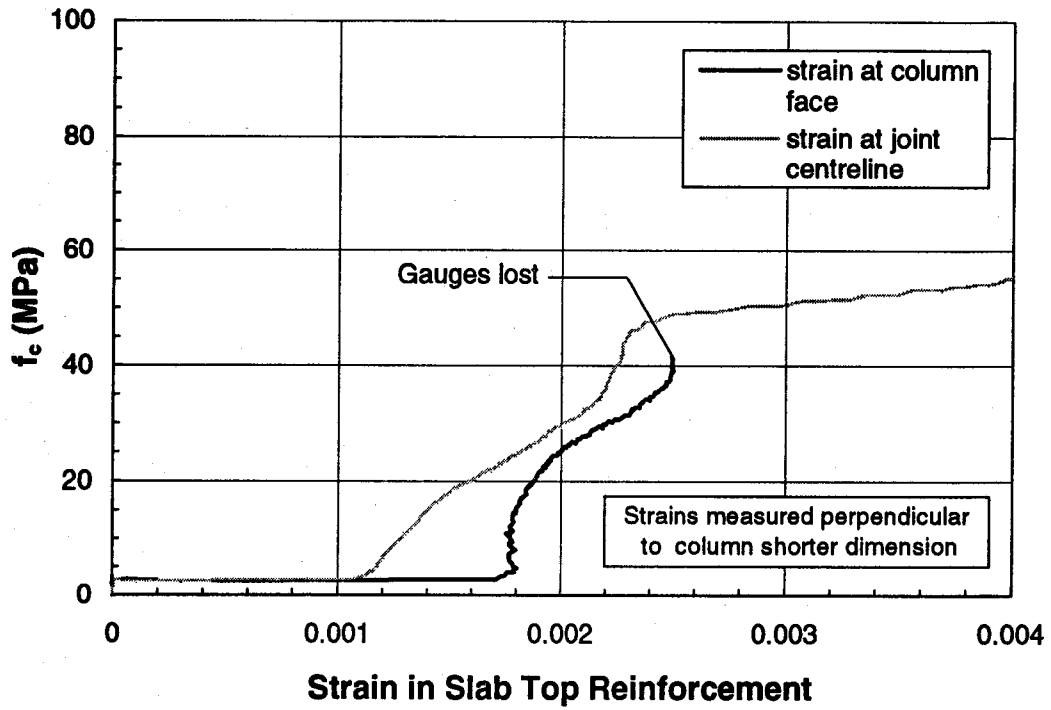
Figure B.55 Slab Transverse Strain (Specimen B-8)
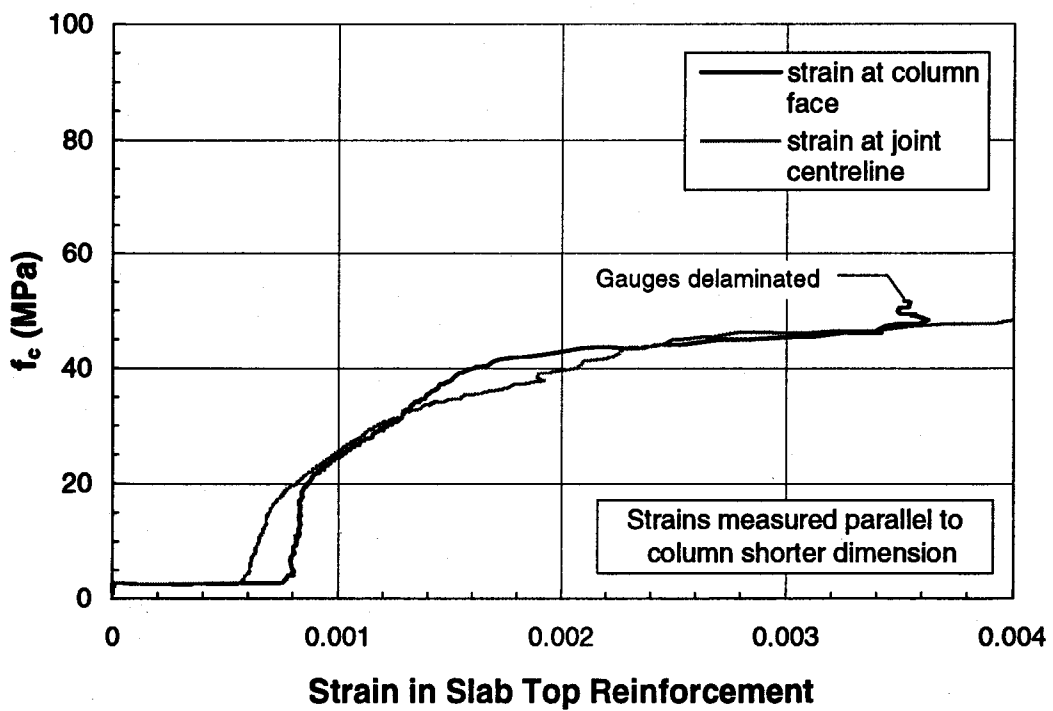
Figure B.56 Slab Transverse Strain (Specimen B-8)

Series C Specimens

- Edge Sandwich Plates -
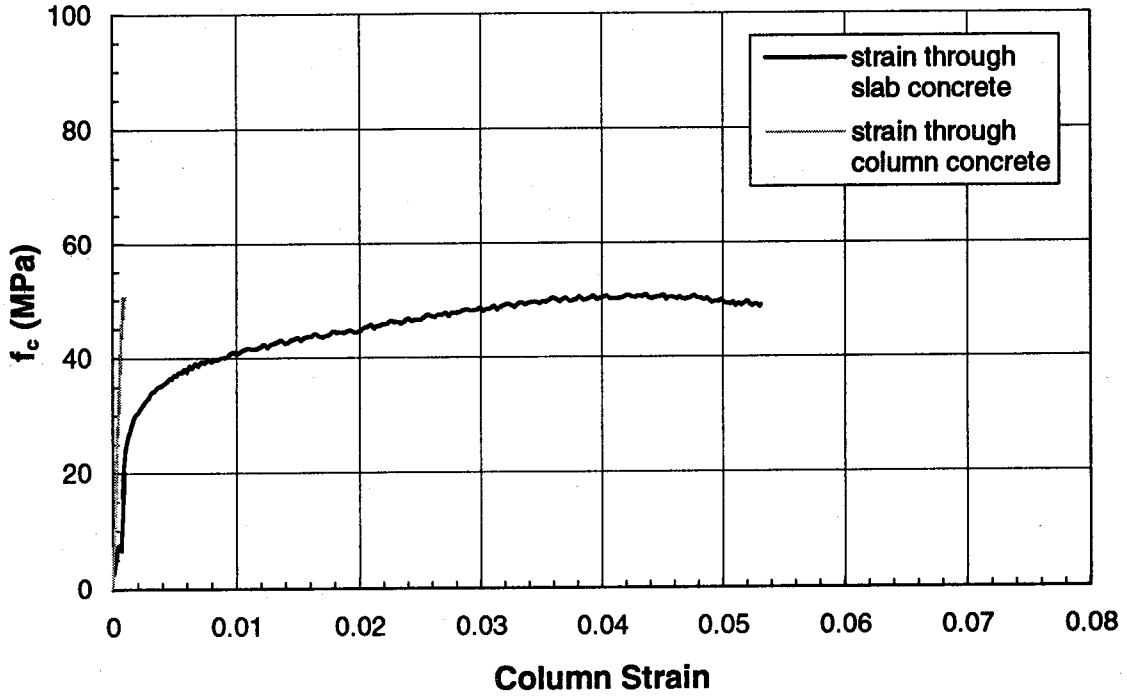
Figure B.57   Stress-Strain Behaviour (Specimen C1-A)
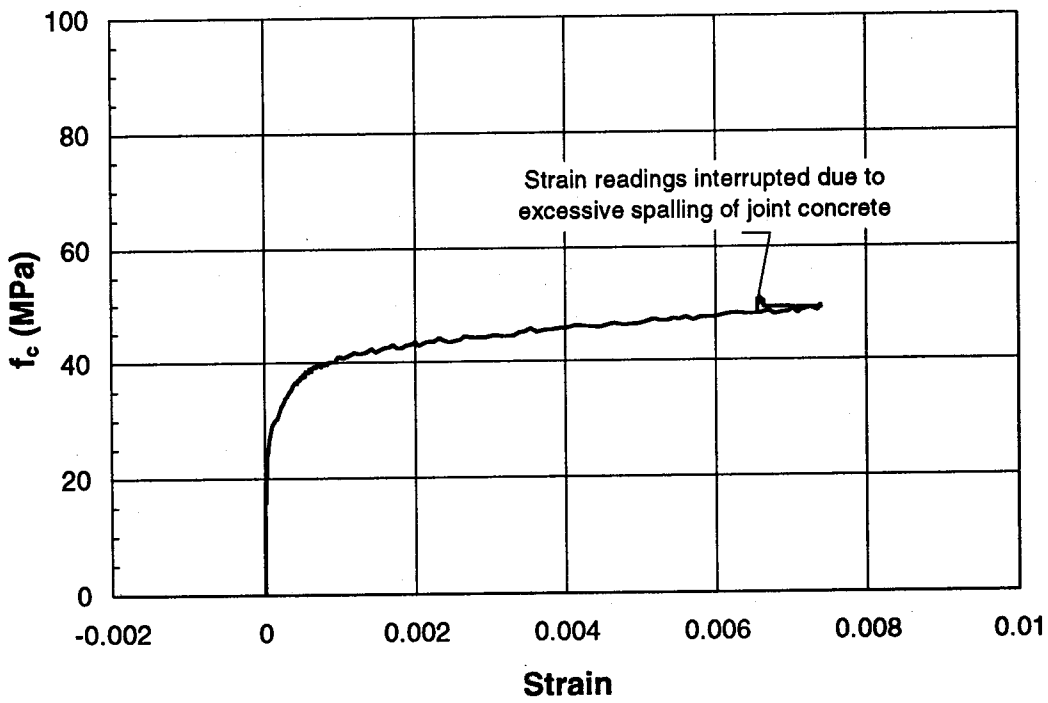
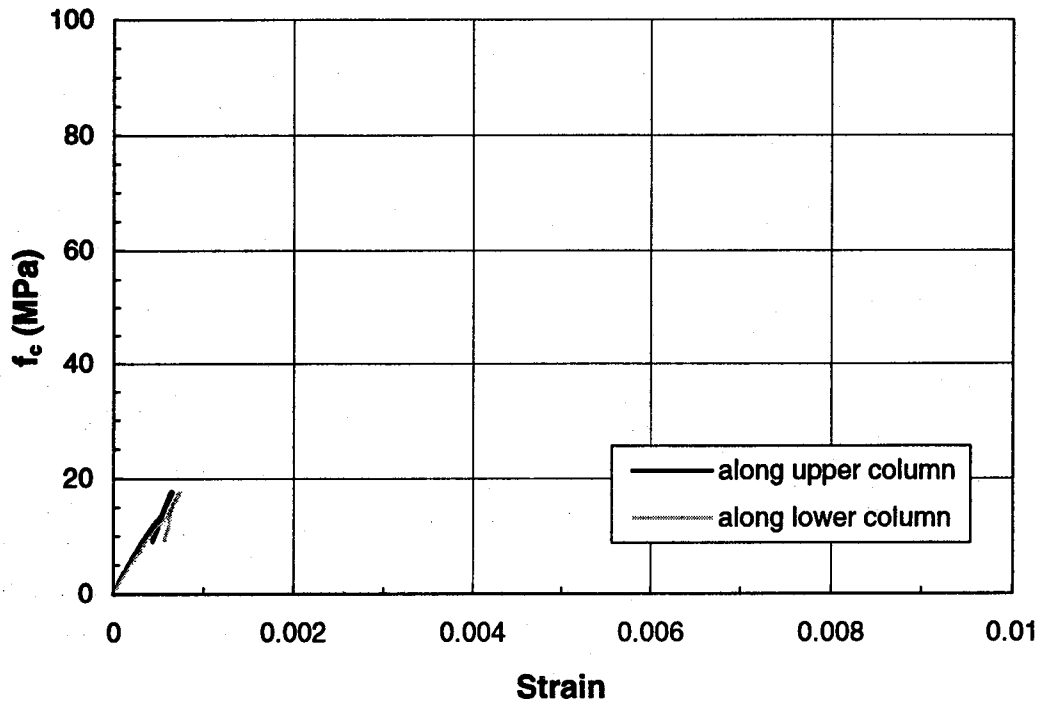

Figure B.58   Joint Lateral Deformation (Specimen C1-A)

162
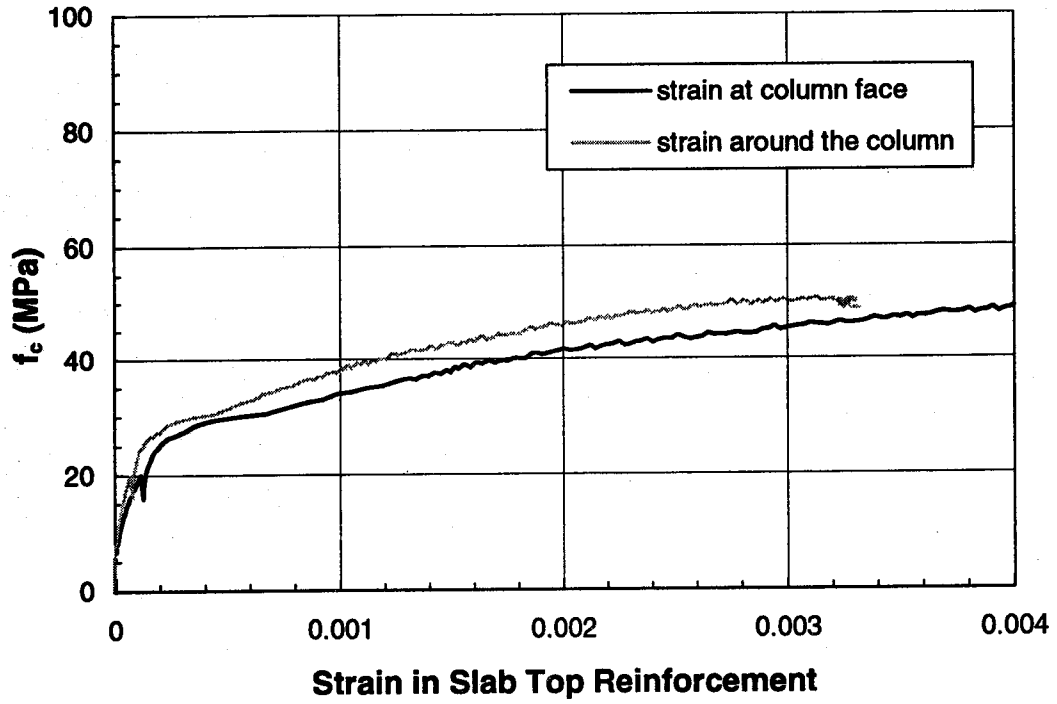
Figure B.59 Slab Top Transverse Strain (C1-A)
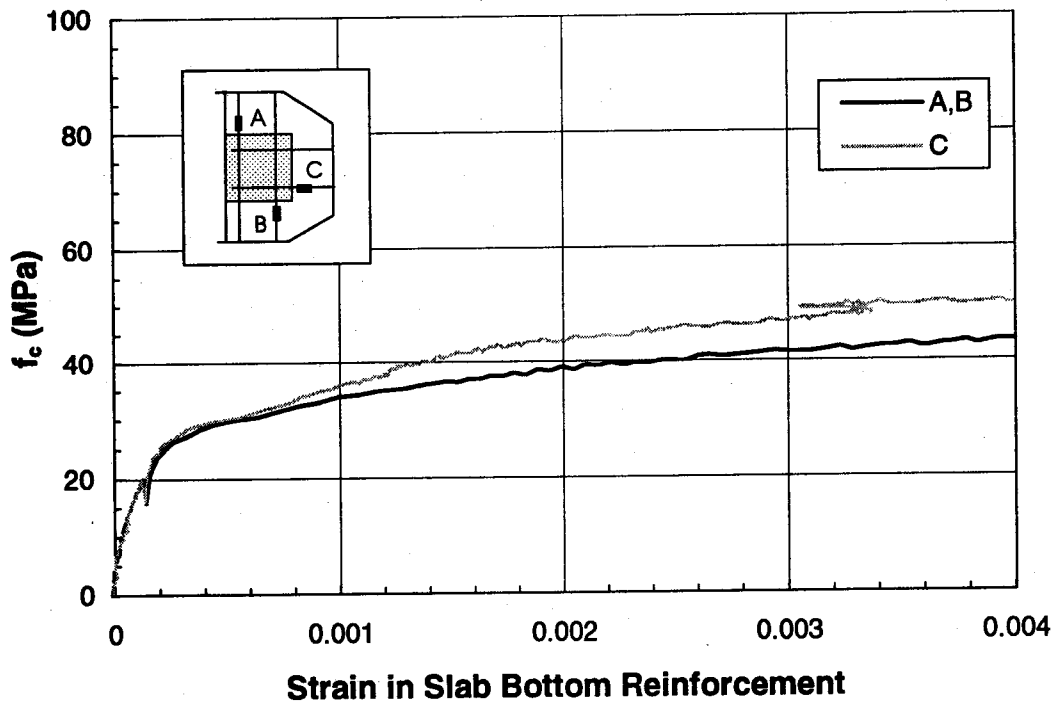
Figure B.60 Slab Bottom Transverse Strain (C1-A)

163
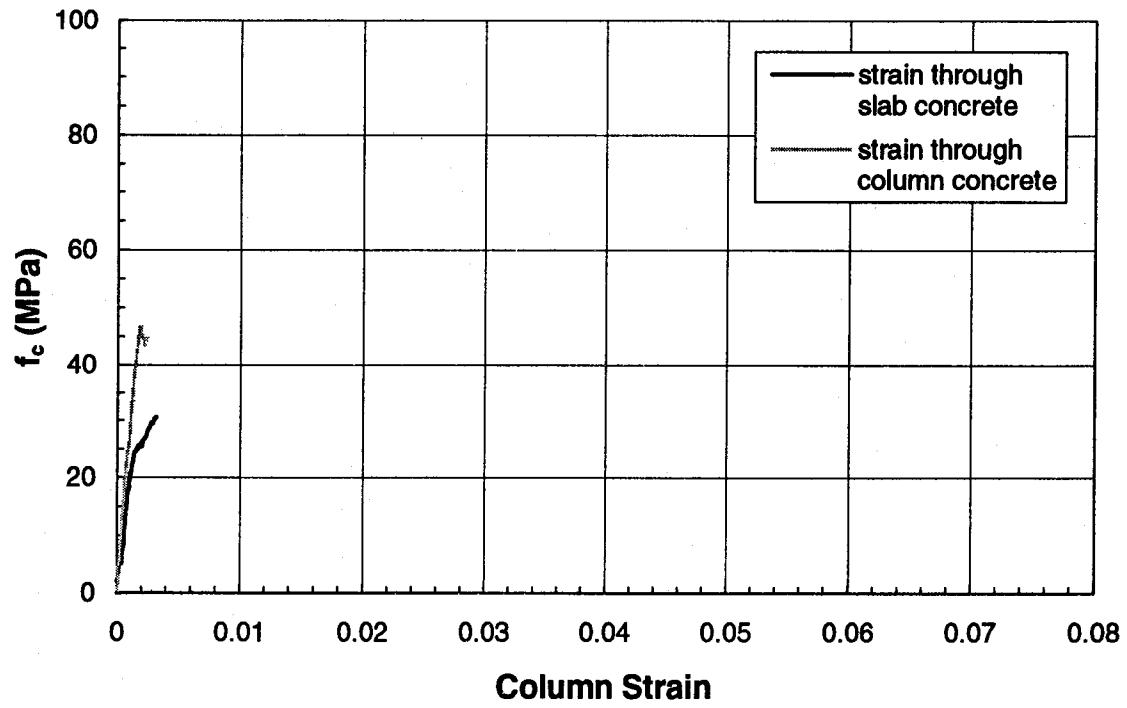
Figure B.61   Stress-Strain Behaviour (Specimen C1-B)
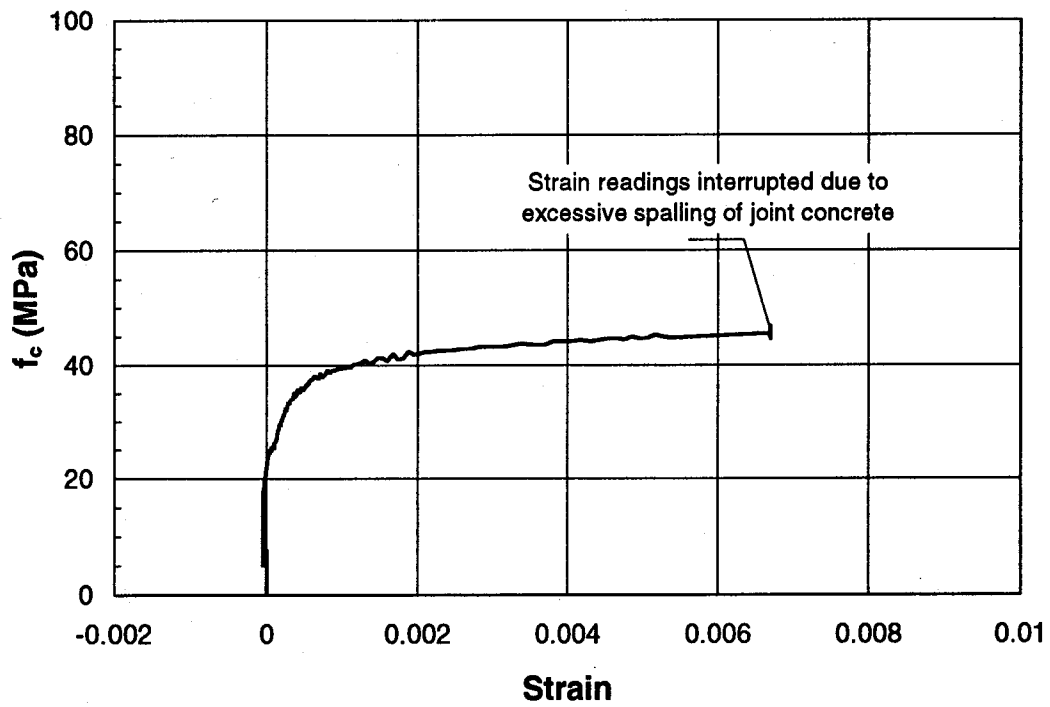
Figure B.62   Joint Lateral Deformation (Specimen C1-B)

164
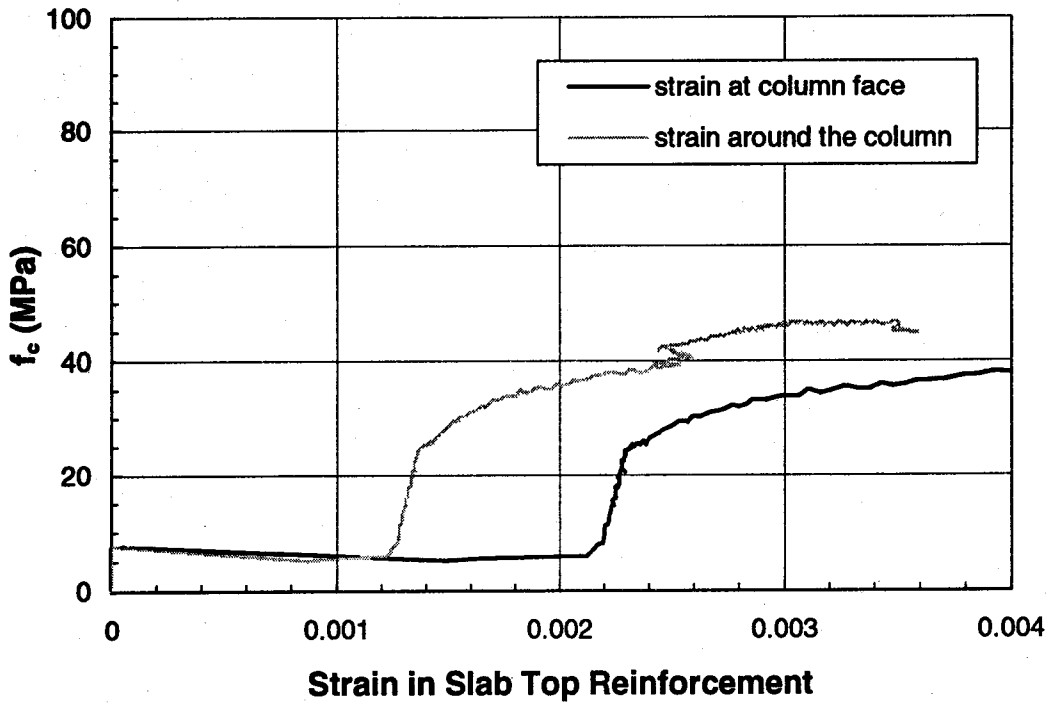
Figure B.63 Slab Top Transverse Strain (C1-B)
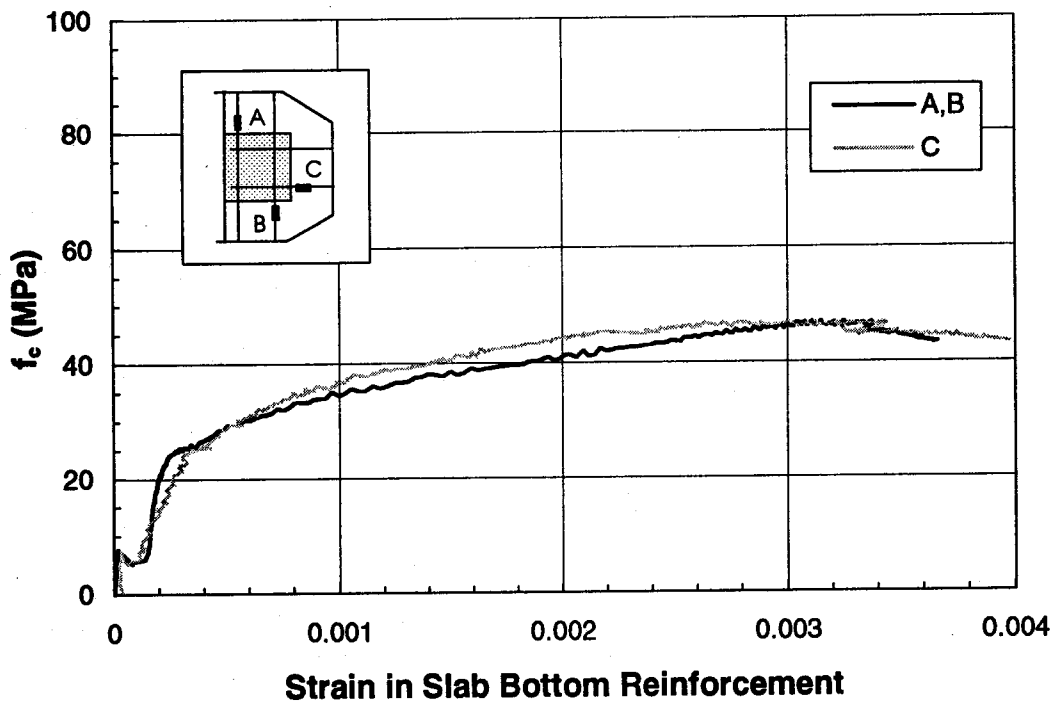
Figure B.64 Slab Bottom Transverse Strain (C1-B)

165
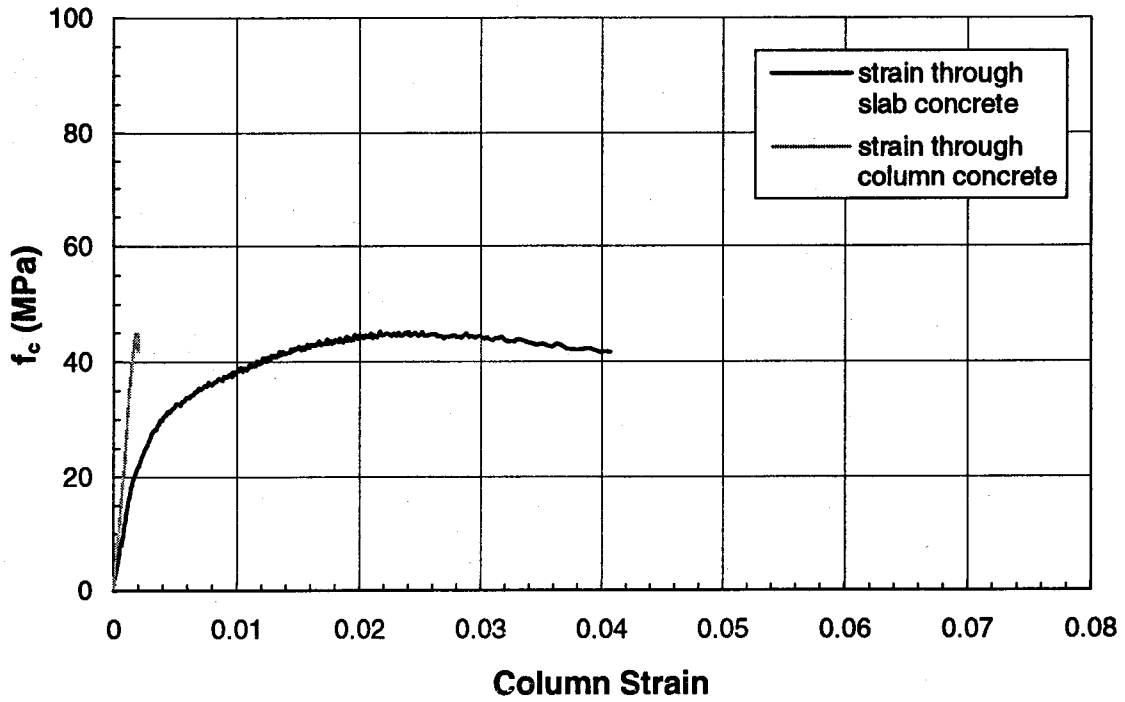
Figure B.65   Stress-Strain Behaviour (Specimen C1-C)
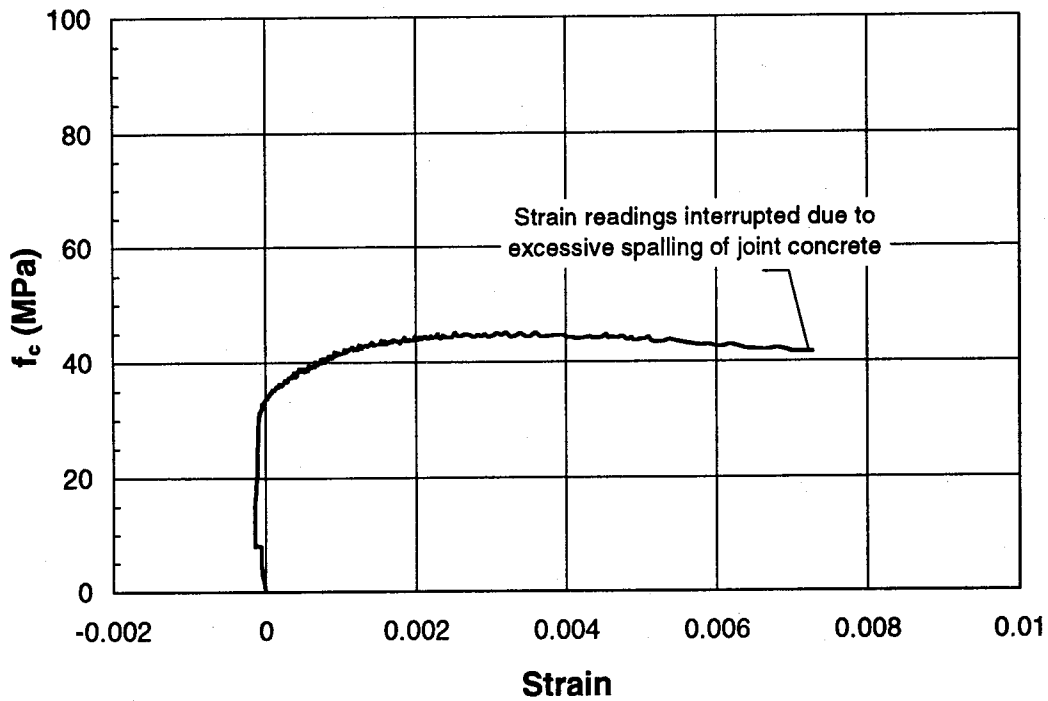
Figure B.66   Joint Lateral Deformation (Specimen C1-C)

166
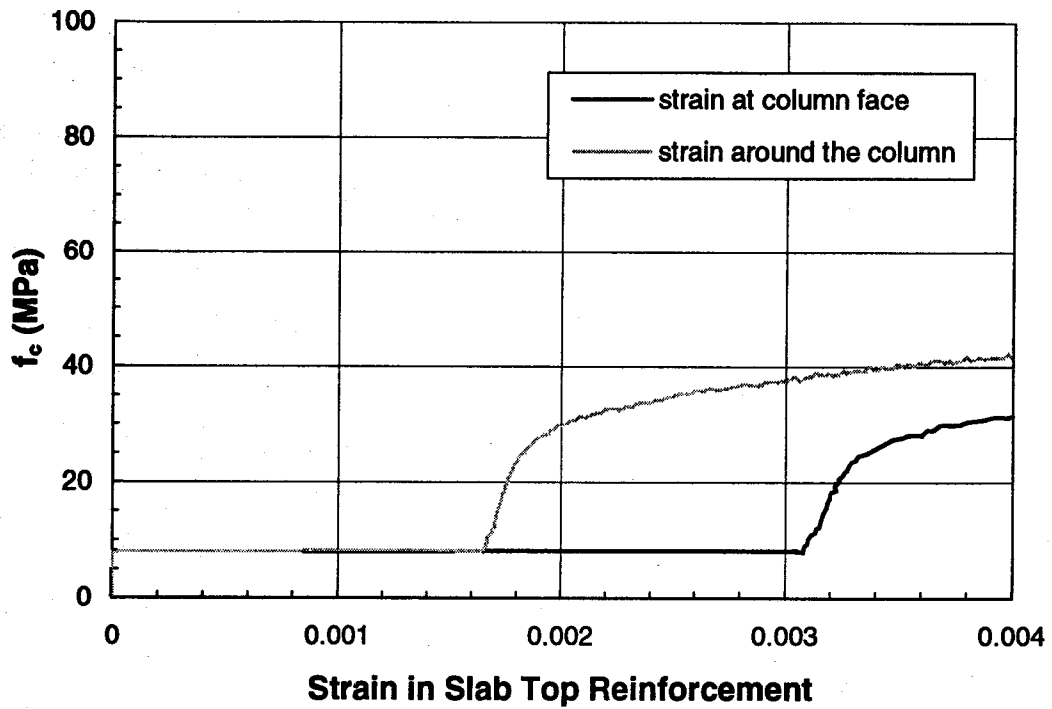
Figure B.67   Slab Top Transverse Strain (C1-C)
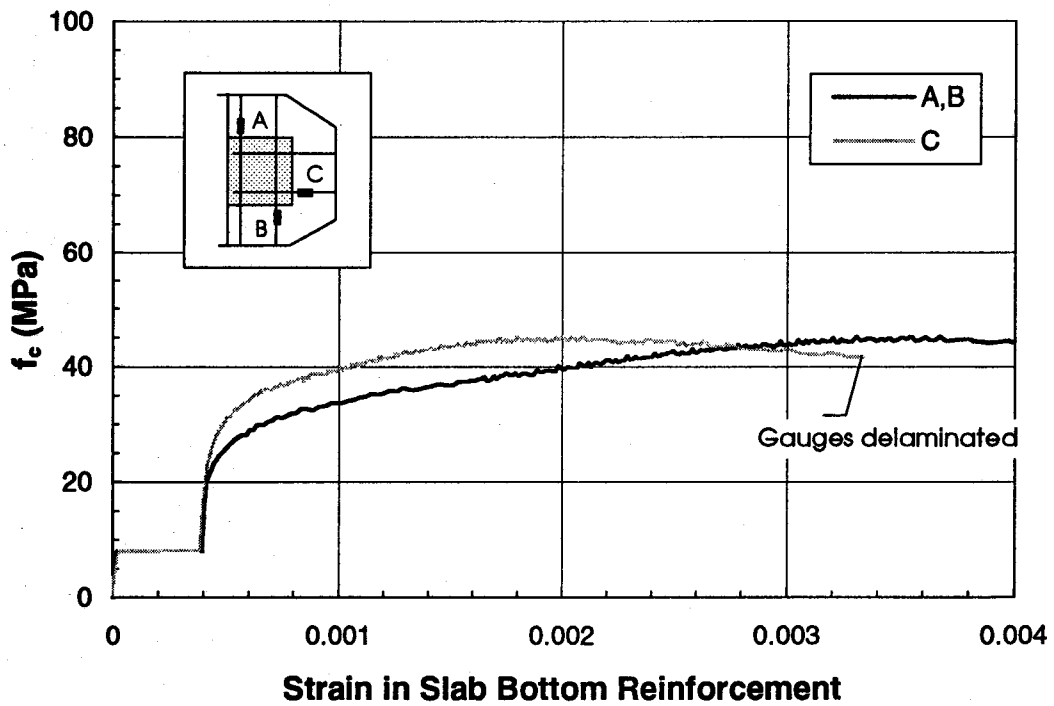
Figure B.68   Slab Bottom Transverse Strain (C1-C)
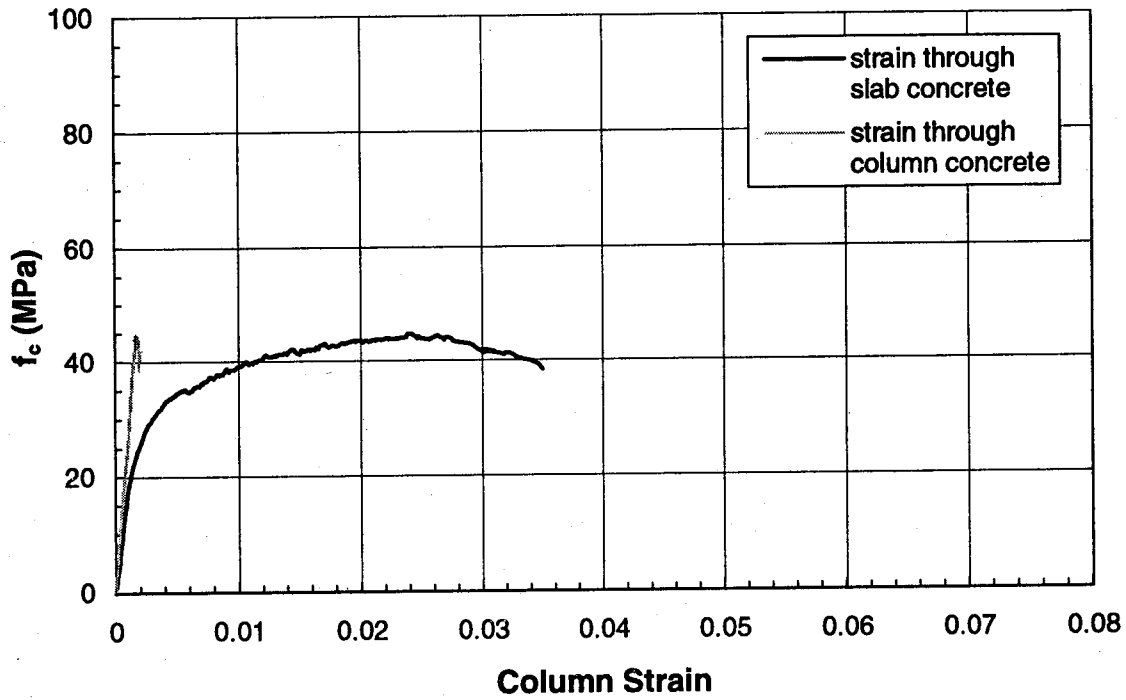
Figure B.69   Stress-Strain Behaviour (Specimen C2-A)

Strain readings interrupted due to
excessive spalling of joint concrete
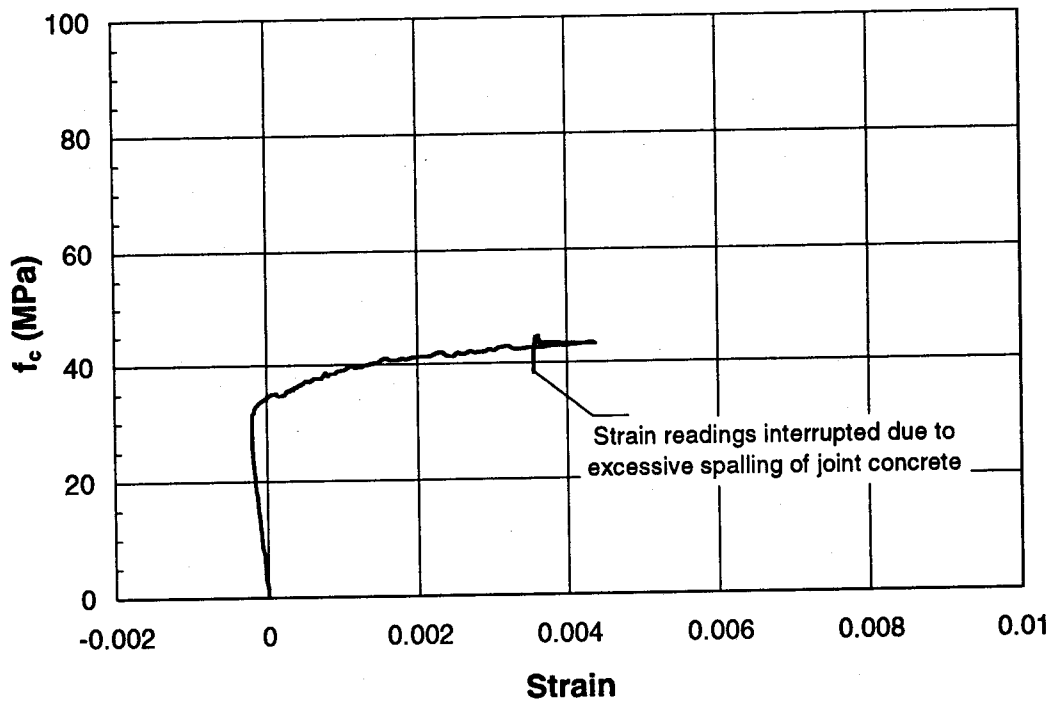
Figure B.70   Joint Lateral Deformation (Specimen C2-A)

168
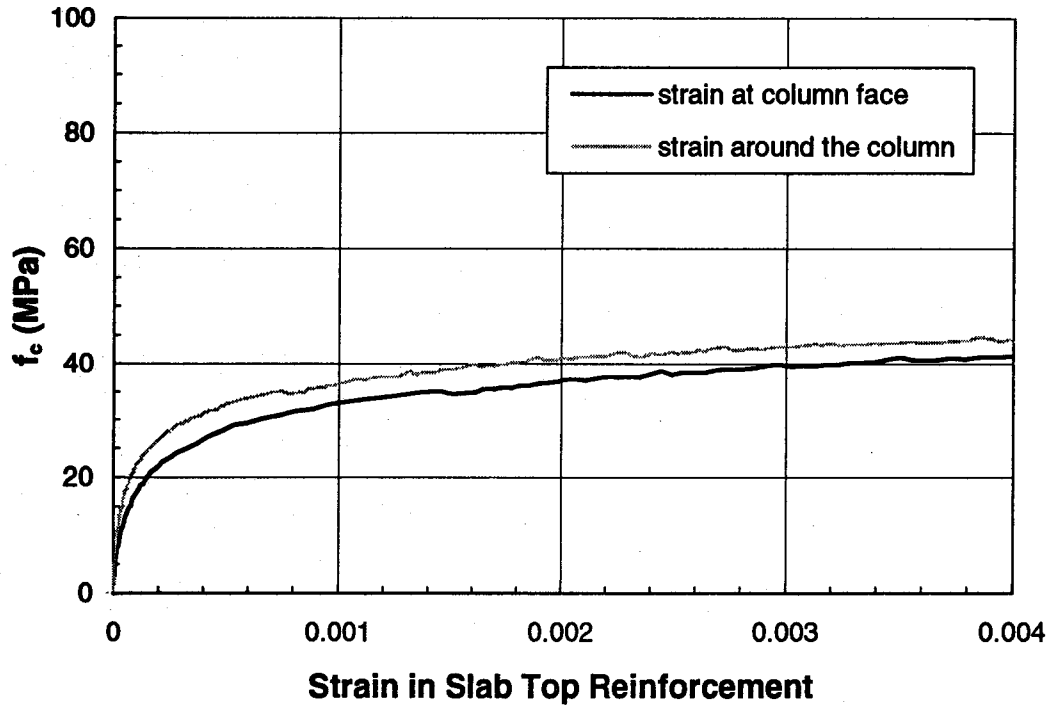
Figure B.71   Slab Top Transverse Strain   (C2-A)
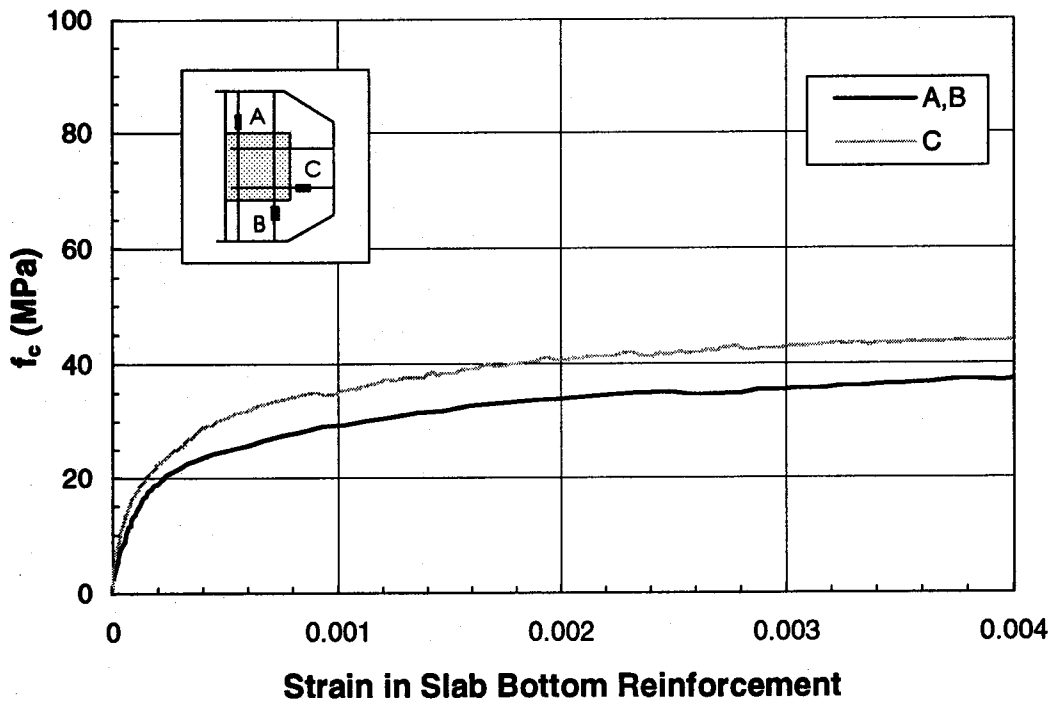
Figure B.72   Slab Bottom Transverse Strain   (C2-A)
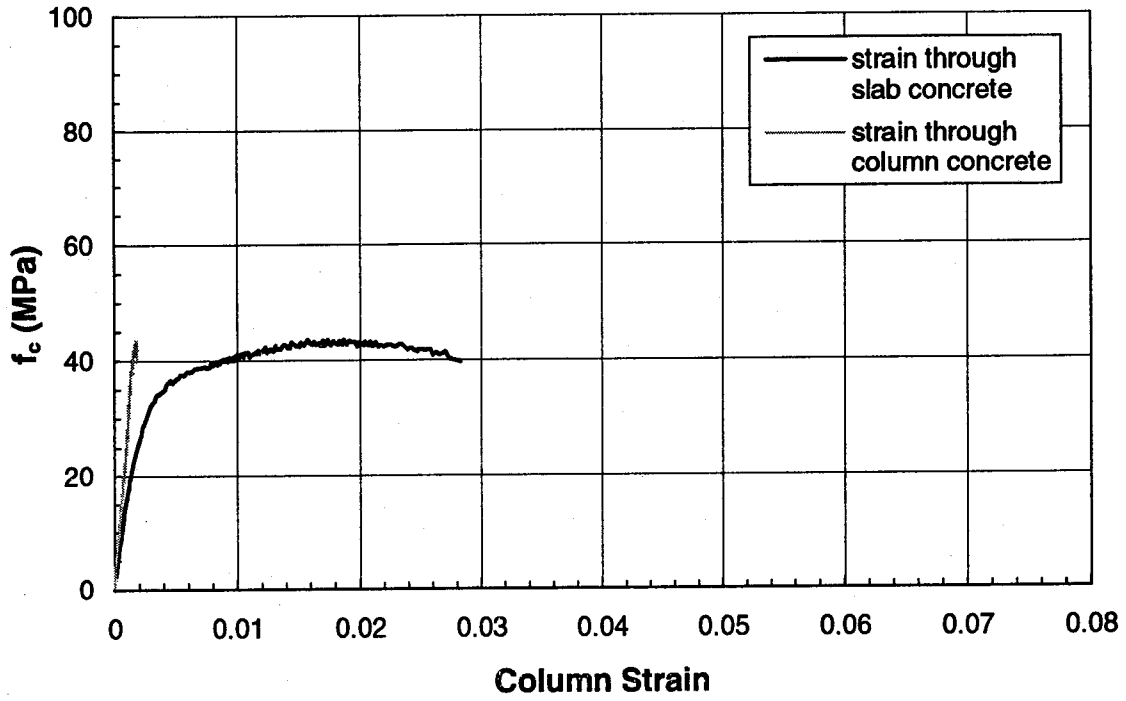
Figure B.73   Stress-Strain Behaviour (Specimen C2-B)
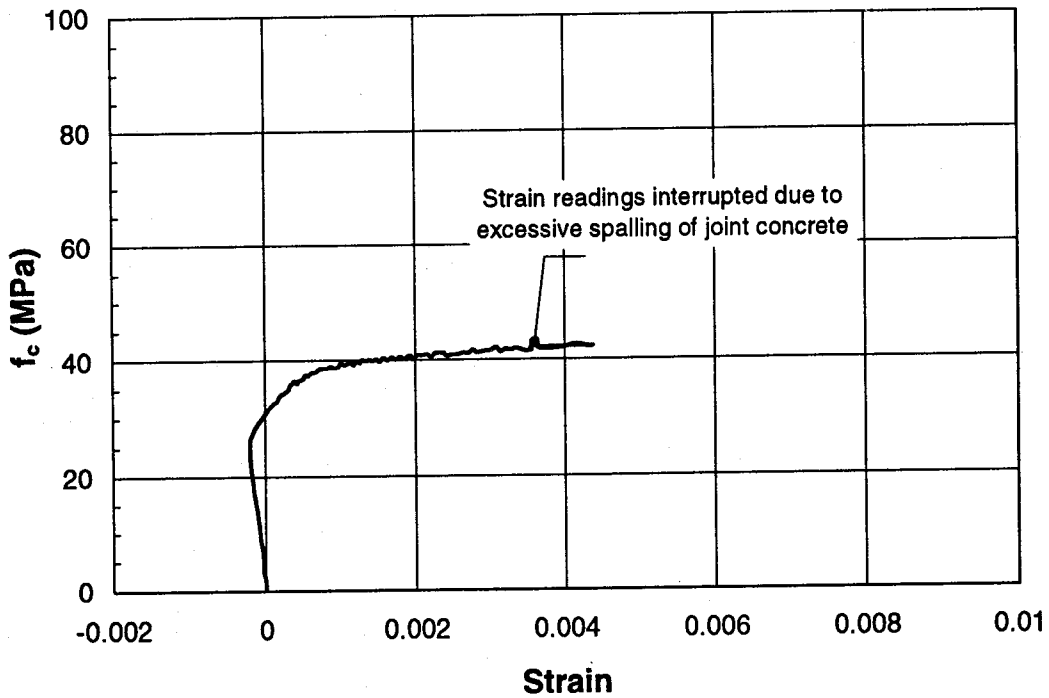
Figure B.74   Joint Lateral Deformation (Specimen C2-B)

170
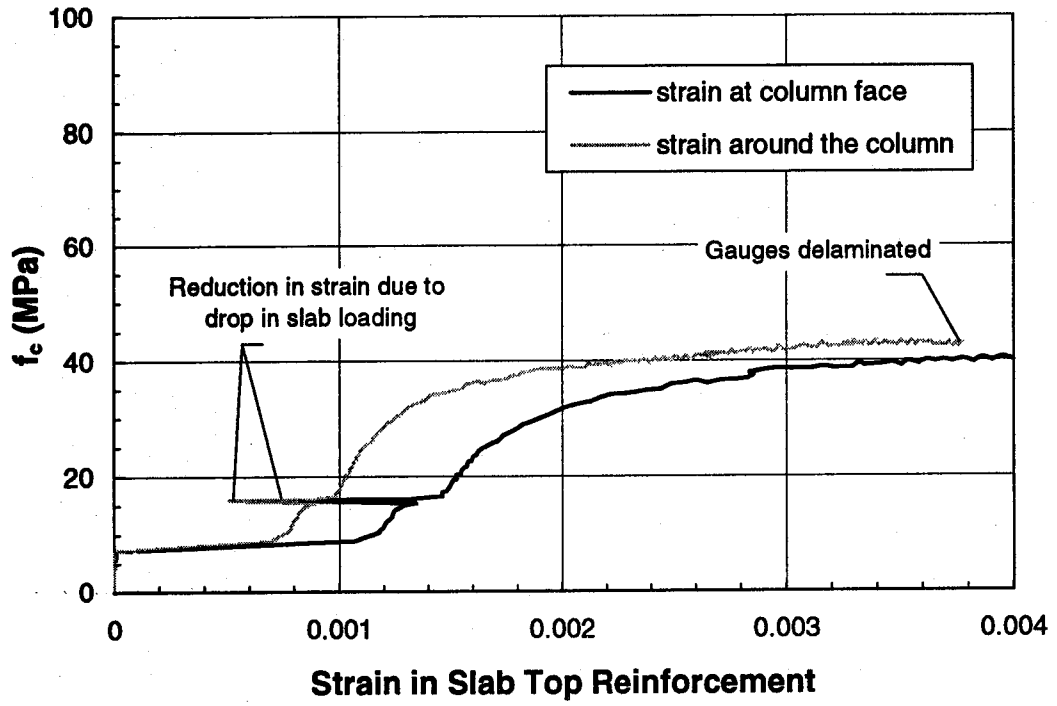
Figure B.75   Slab Top Transverse Strain (C2-B)

Strain in Slab Bottom Reinforcement
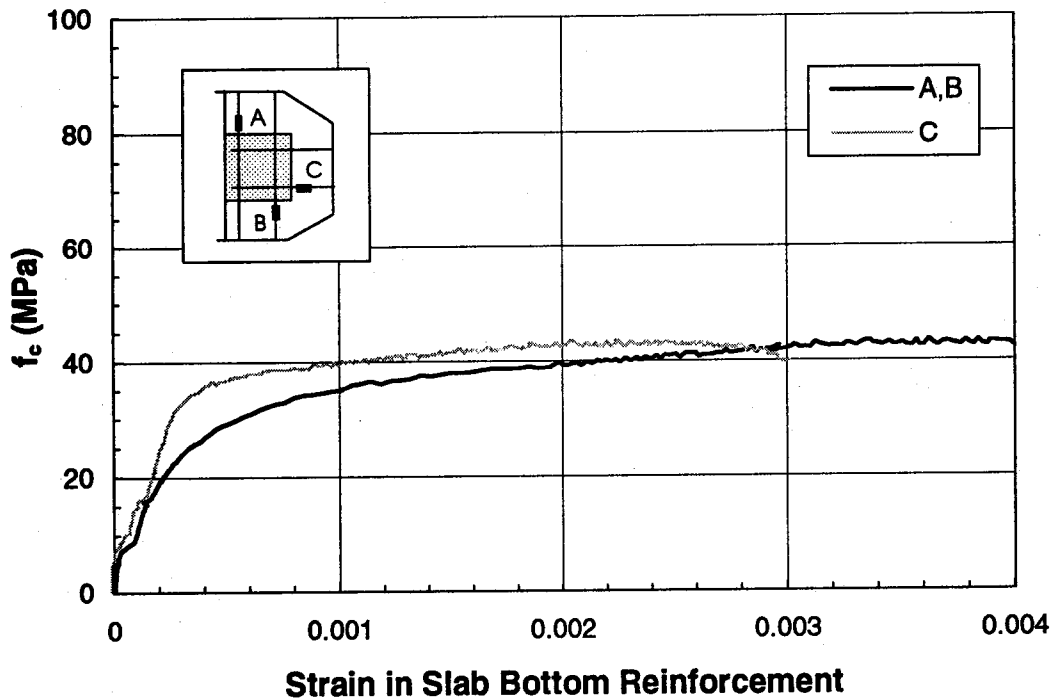
Figure B.76   Slab Bottom Transverse Strain (C2-B)

171
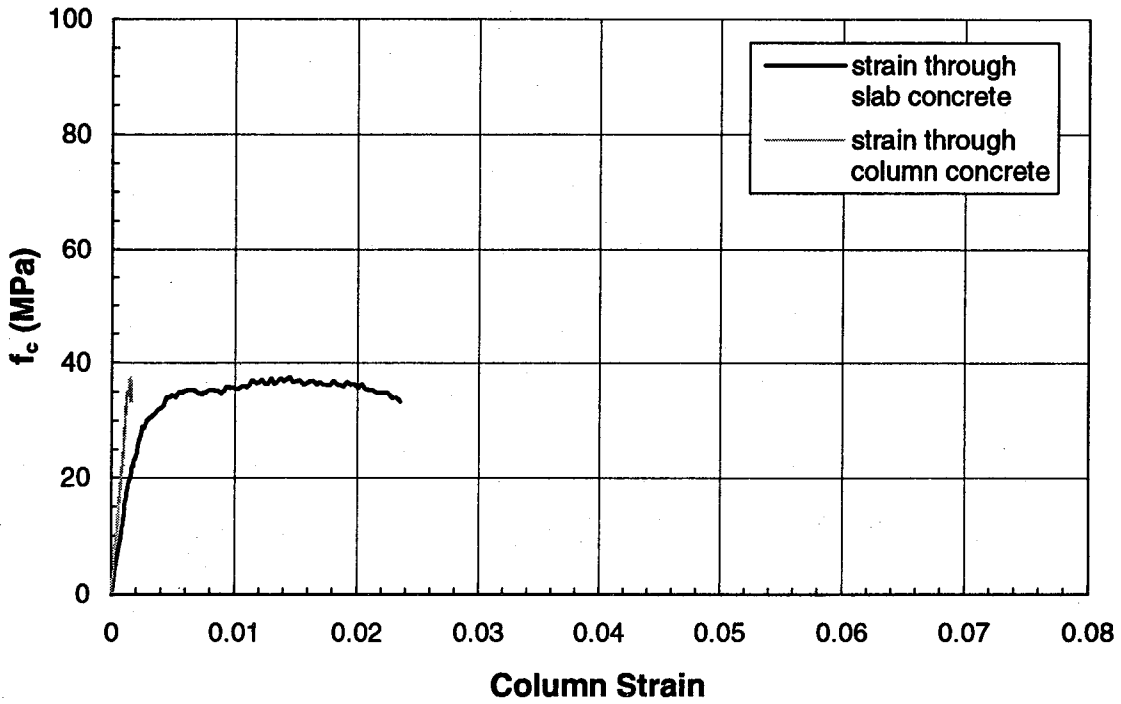
Figure B.77   Stress-Strain Behaviour (Specimen C2-C)
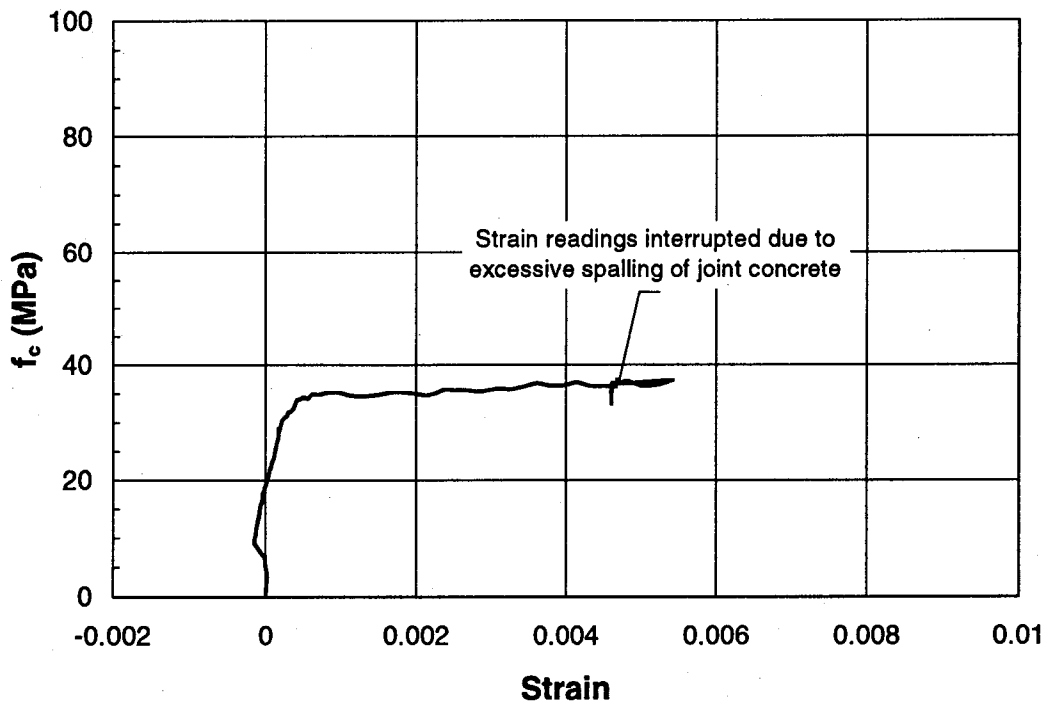
Figure B.78   Joint Lateral Deformation (Specimen C2-C)

172
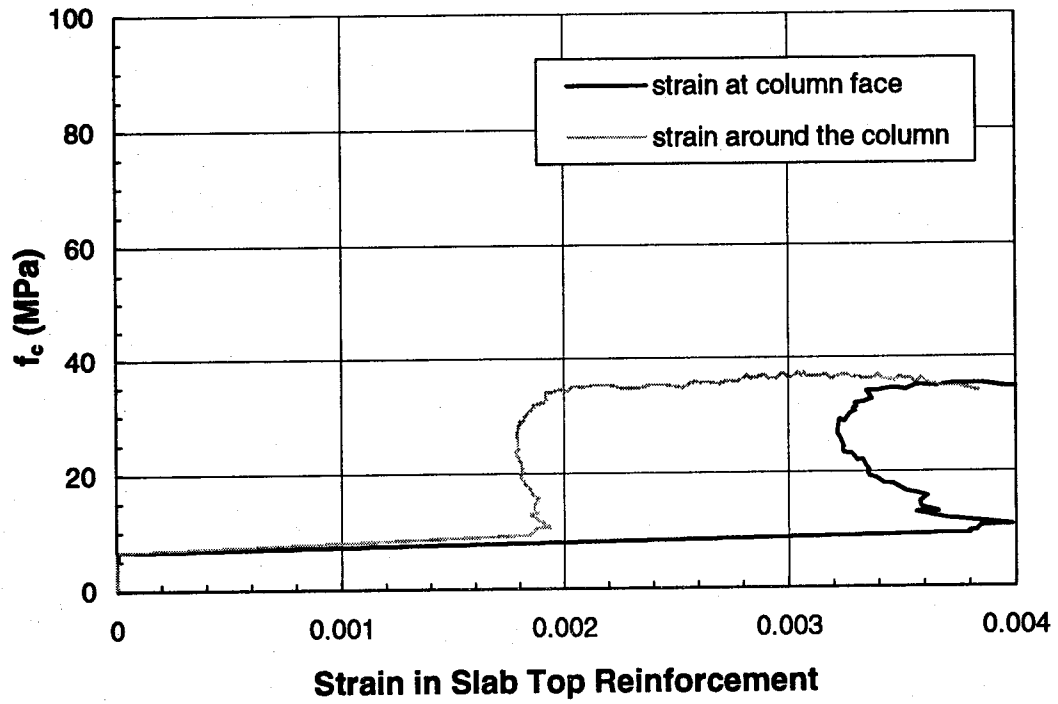
Figure B.79   Slab Top Transverse Strain (C2-C)
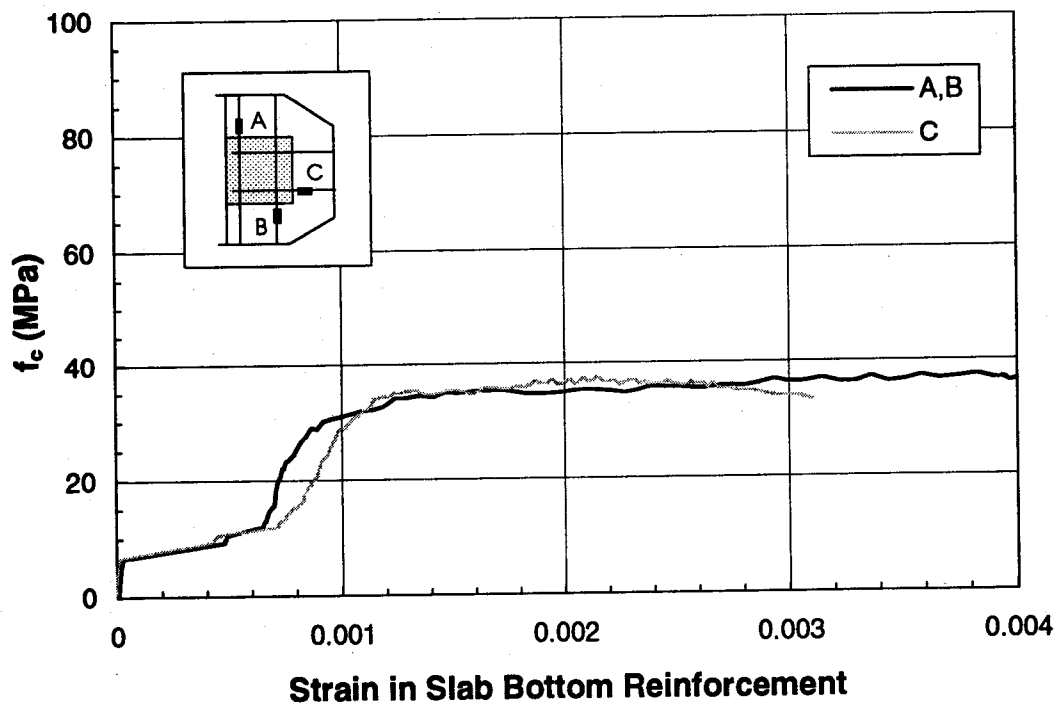
Figure B.80   Slab Bottom Transverse Strain (C2-C)

173

Series D Specimens

- Sandwich Columns -
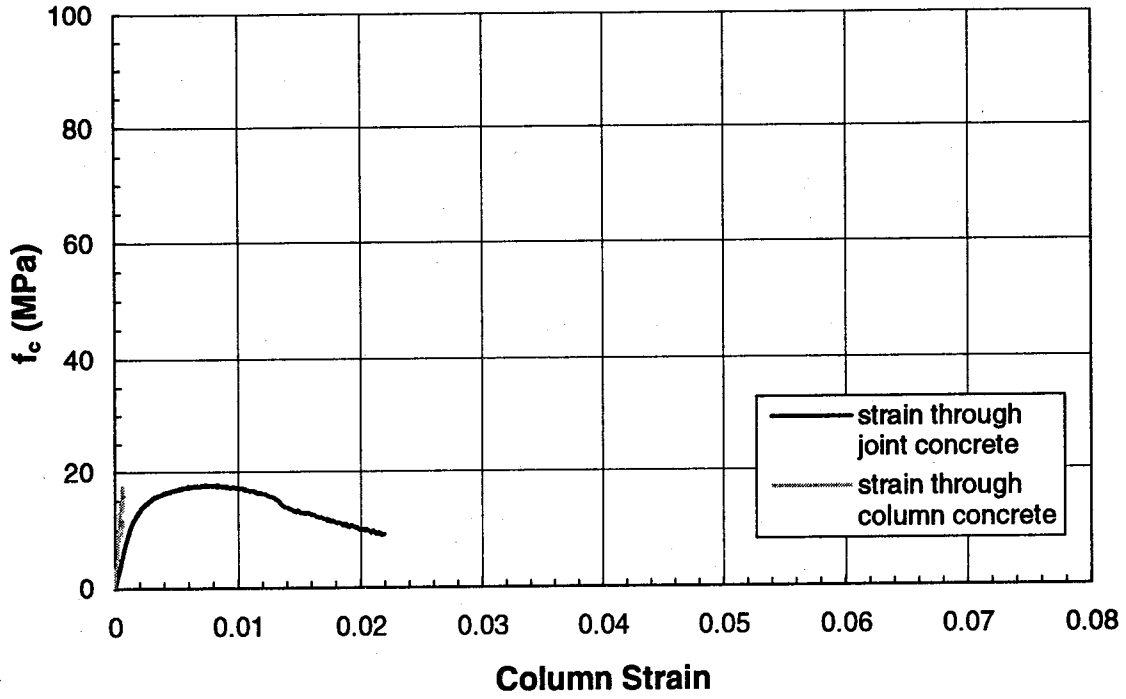
Figure B.81 Stress-Strain Behaviour (Specimen D-SC1)
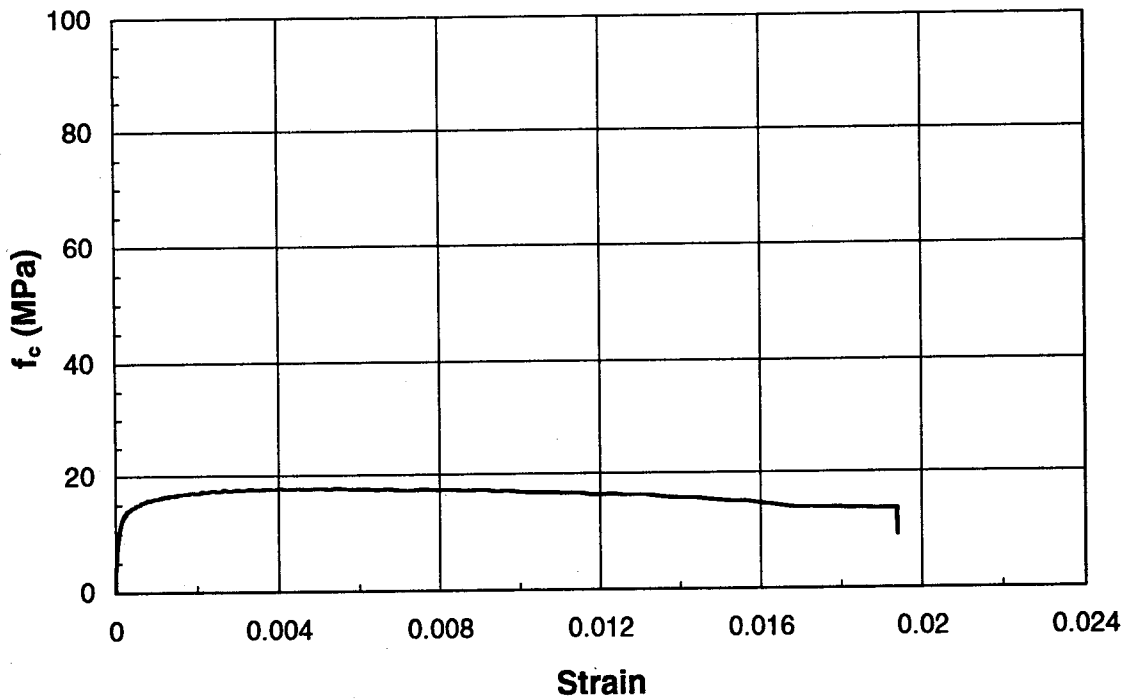
Figure B.82 Joint Lateral Deformation (Specimen D-SC1)

176

Figure B.83   Column Longitudinal Strain (D-SC1)
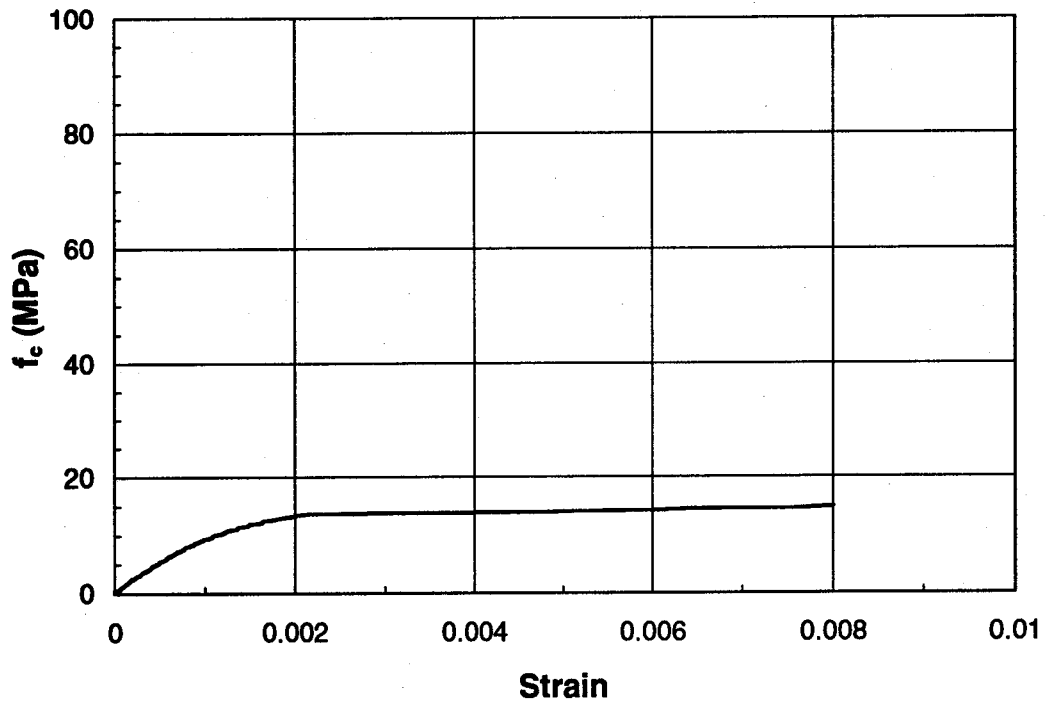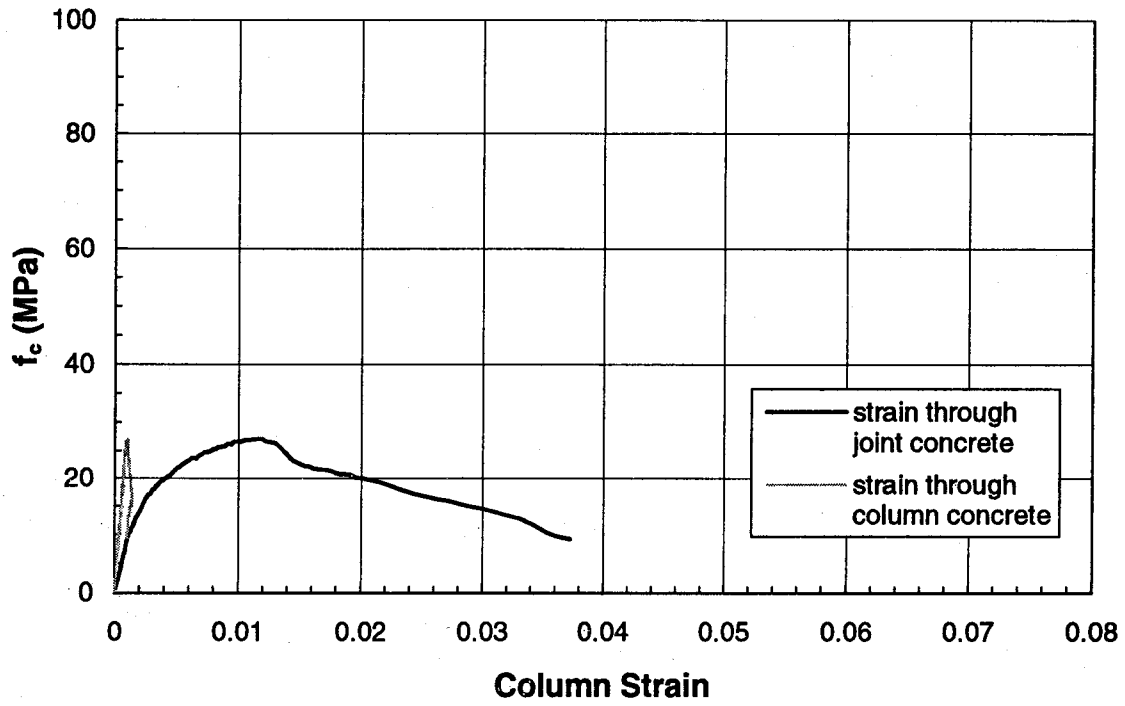

Figure B.84   Column Strain through Joint (D-SC1)

177
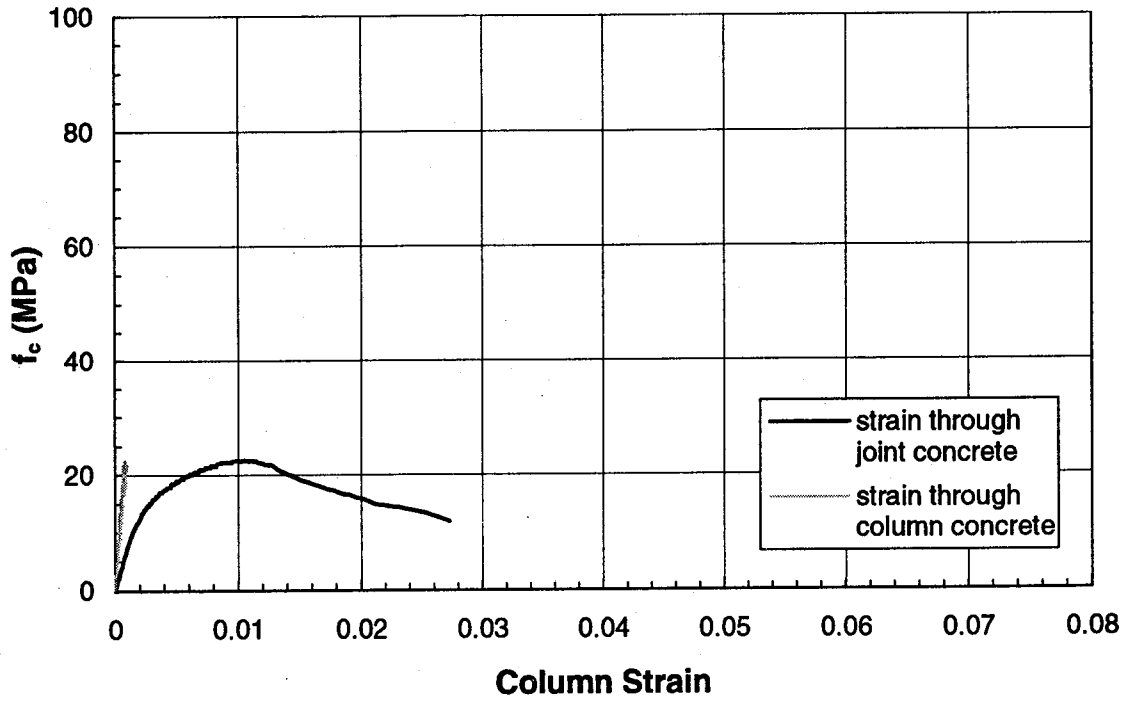
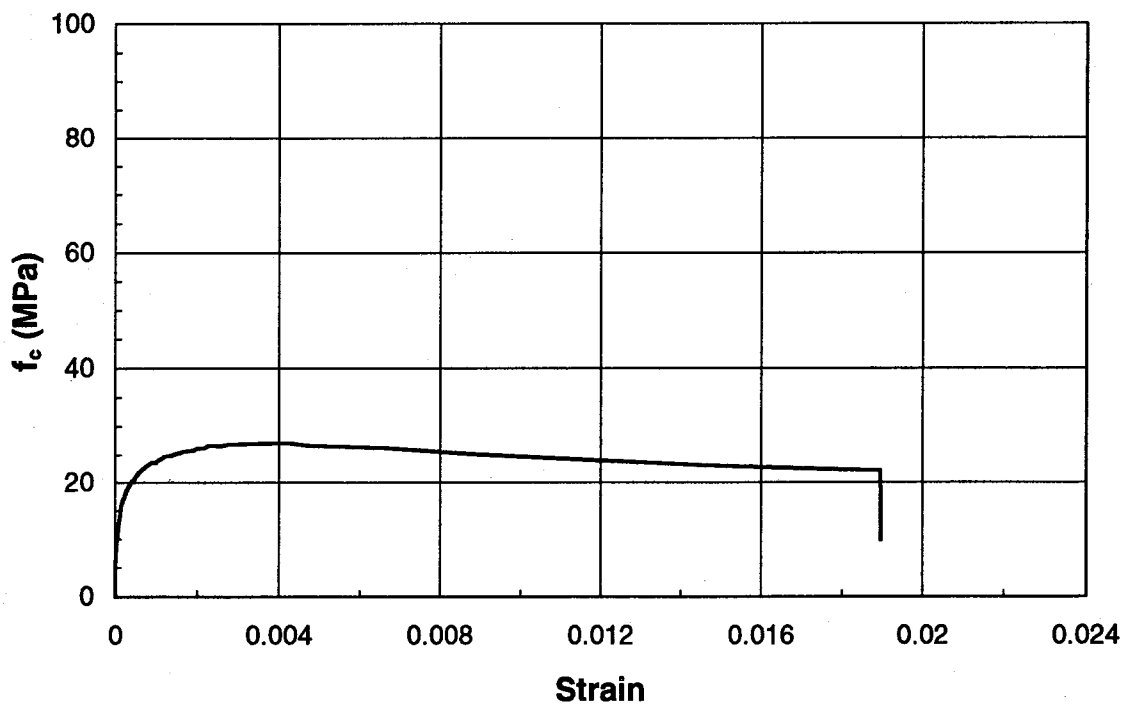**Figure B.85   Stress-Strain Behaviour (Specimen D-SC2)**
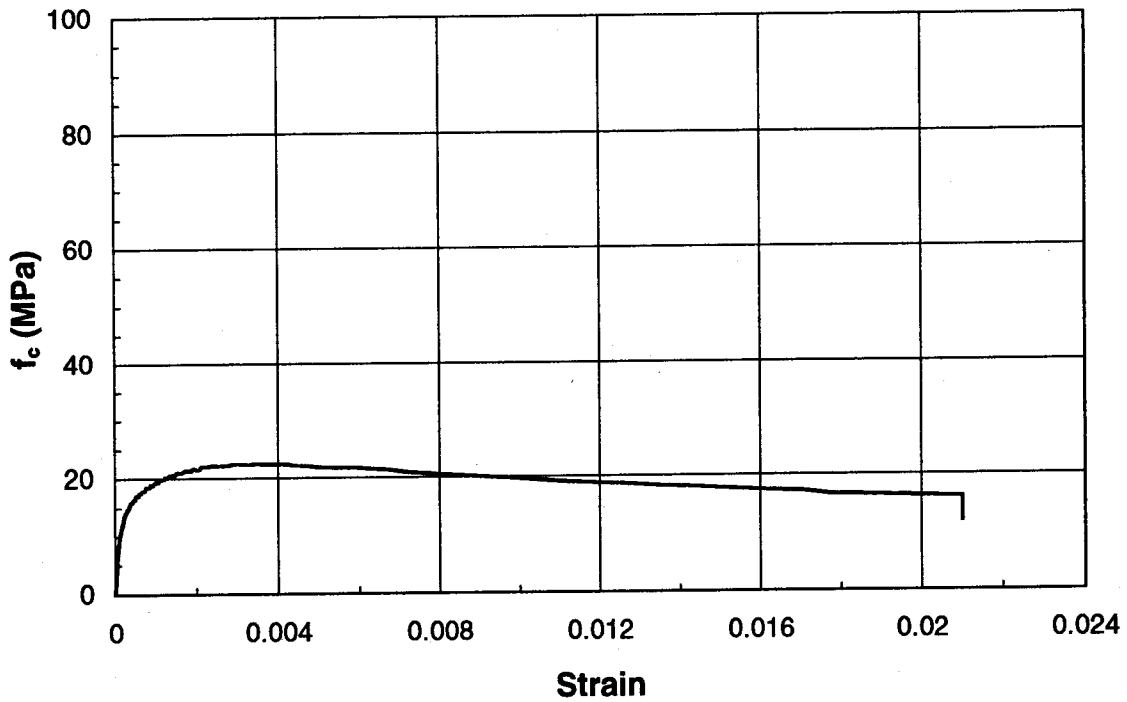
Figure B.86   Joint Lateral Deformation (Specimen D-SC2)

178
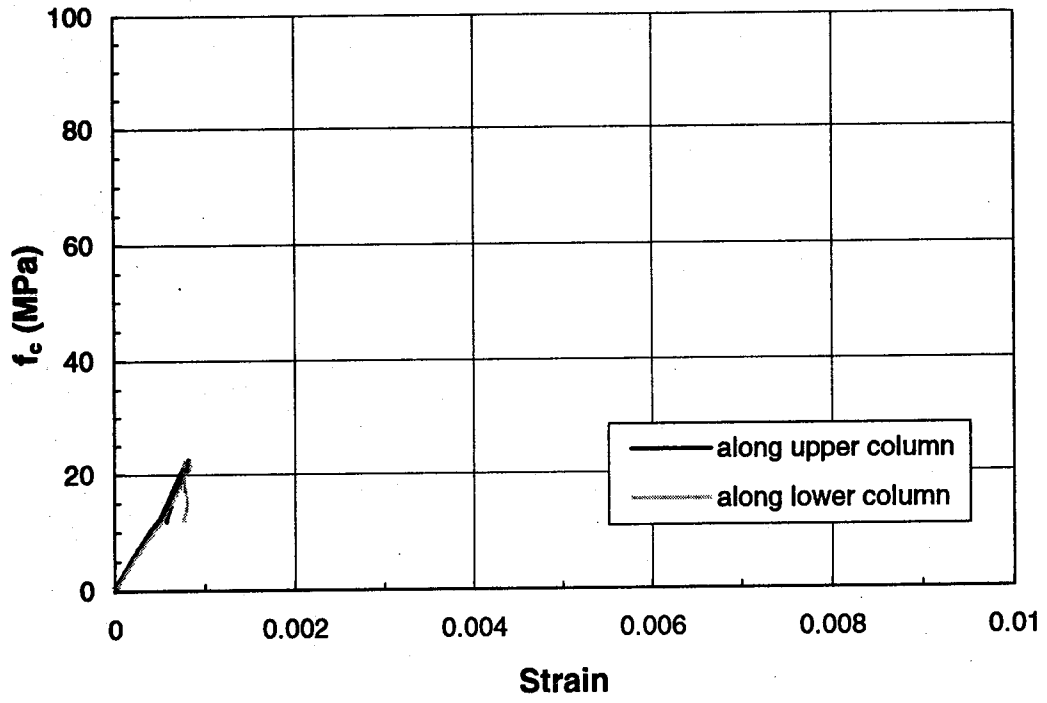
Figure B.87   Column Longitudinal Strain (D-SC2)
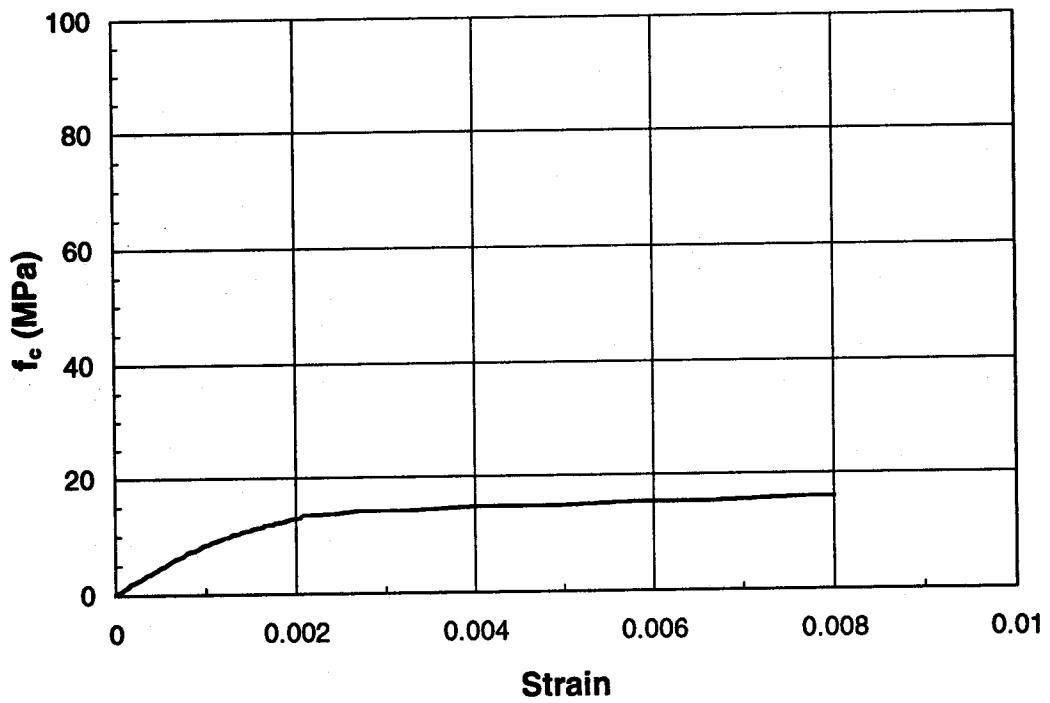
Figure B.88   Column Strain through Joint (D-SC2)

Figure B.89   Stress-Strain Behaviour (Specimen D-SC3)

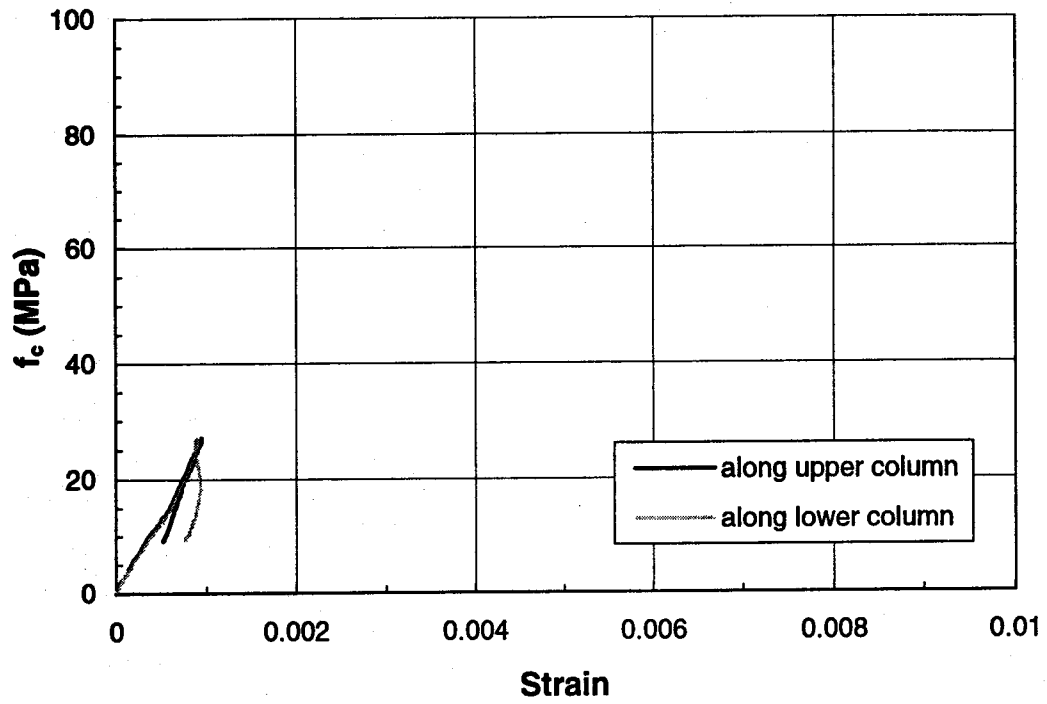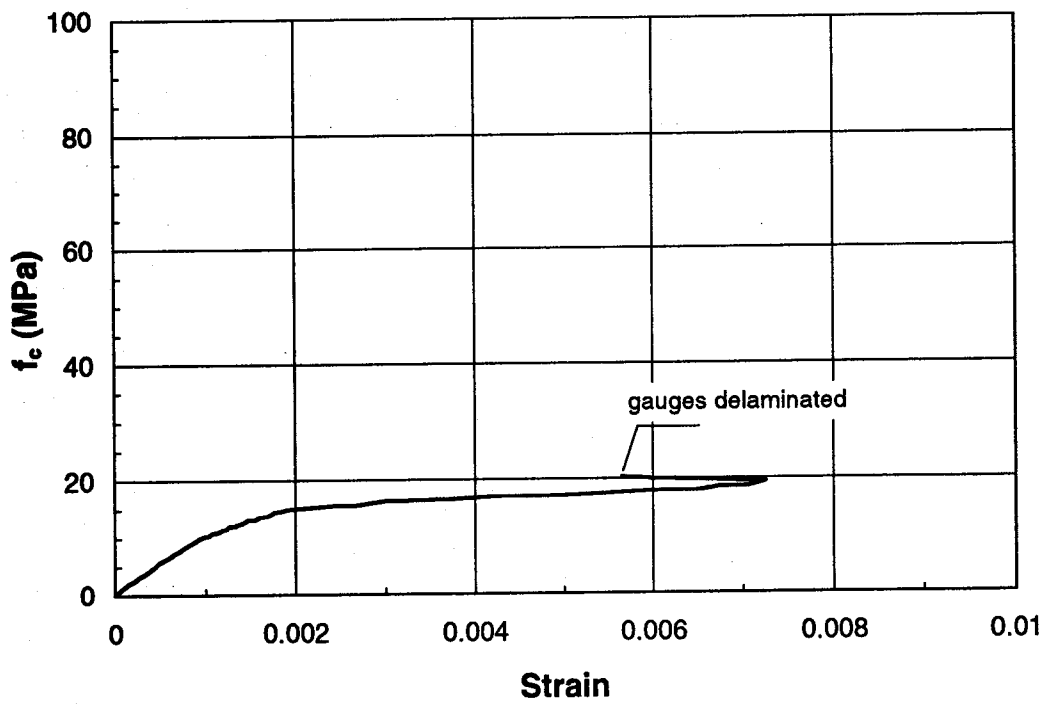**Figure B.90   Joint Lateral Deformation (Specimen D-SC3)**

180

Figure B.91   Column Longitudinal Strain (D-SC3)
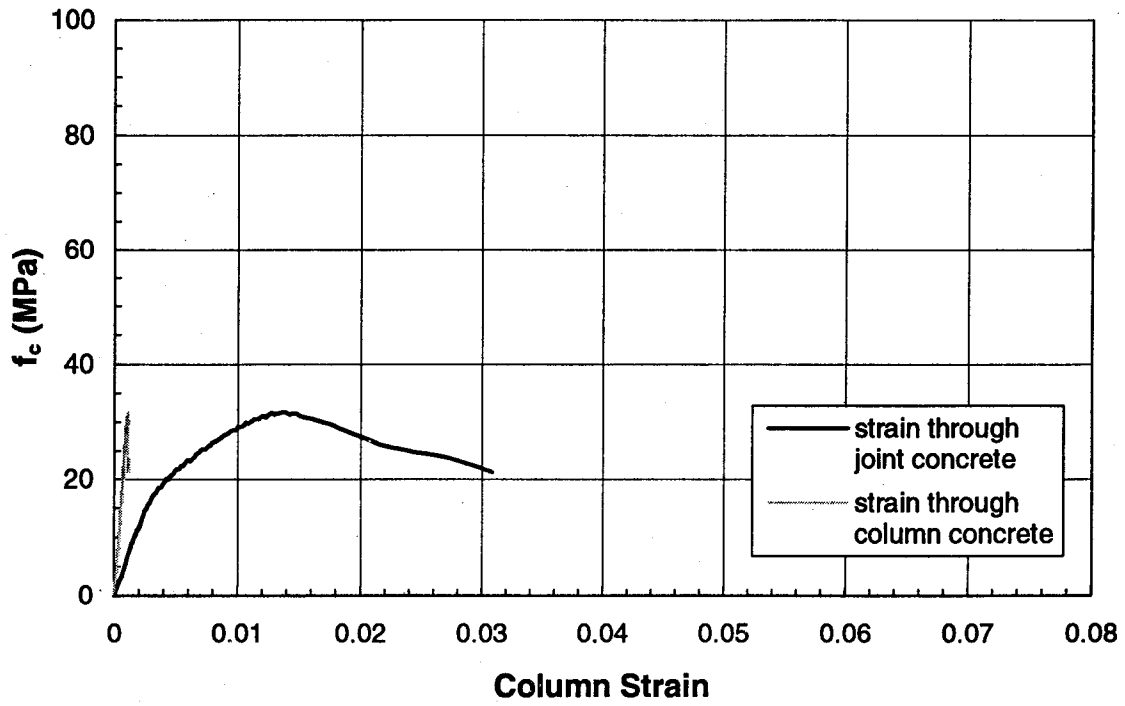

Figure B.92   Column Strain through Joint (D-SC3)
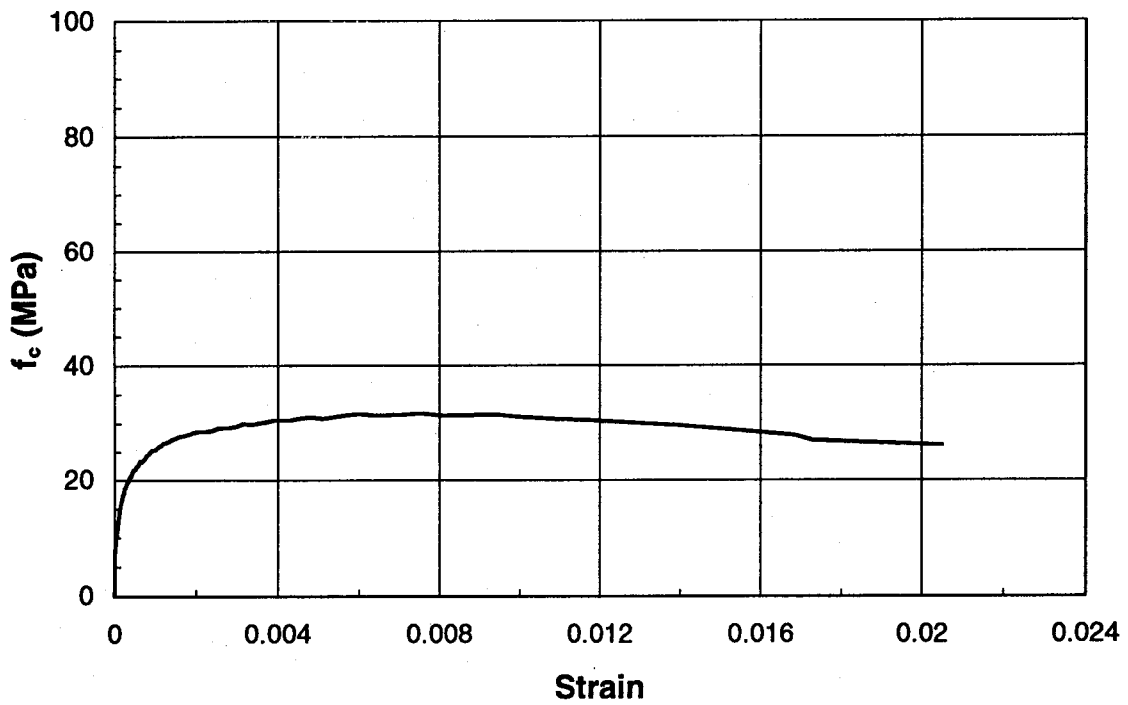
181

Figure B.93   Stress-Strain Behaviour (Specimen D-SC4)

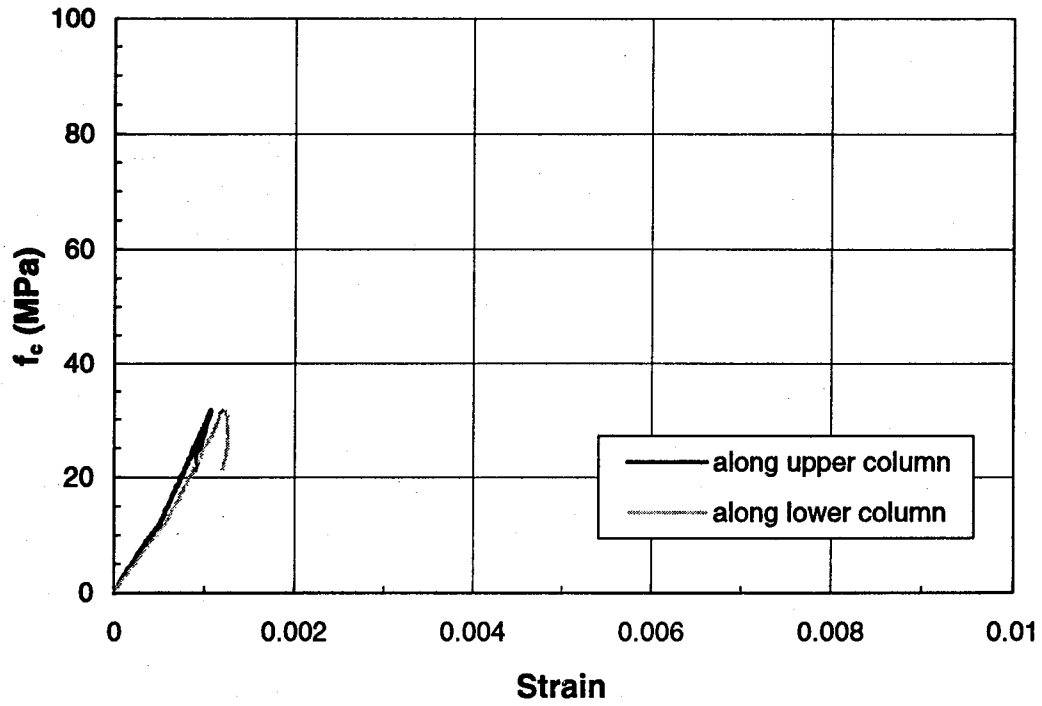**Figure B.94   Joint Lateral Deformation (Specimen D-SC4)**

182

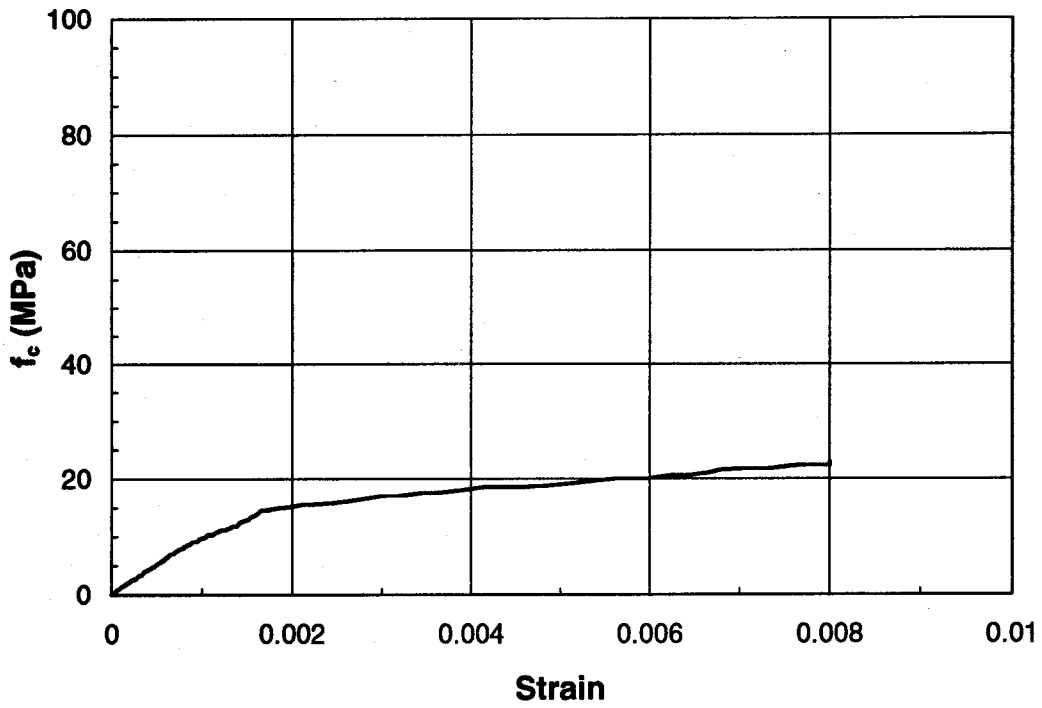**Figure B.95   Column Longitudinal Strain (D-SC4)**

Figure B.96   Column Strain through Joint (D-SC4)

199. *The Flexural Creep Behavior of OSB Panels Under Various Climatic Conditions* by N. Zhao, J.J.R. Cheng and L. Bach, June 1994.

200. *High Performance Concrete Under High Sustained Compressive Stresses* by S. Iravani and J.G. MacGregor, June 1994.

201. *Strength and Installation Characteristics of Tension - Control Bolts* by S.T. Undershute and G.L. Kulak, August 1994.

202. *Deformational Behavior of Line Pipe* by M. Mohareb, A.E. Elwi, G.L. Kulak and D.W. Murray, September 1994.

203. *Behavior of Girth-Welded Line Pipe,* by N. Yoosef-Ghodsi, G.L. Kulak and D.W. Murray, September 1994.

204. *Numerical Investigation of Eccentrically Loaded Tied High Strength Concrete Columns* by J. Xie, A.E. Elwi and J.G. MacGregor, October 1994.

205. *Shear Strengthening of Concrete Girders Using Carbon Fibre Reinforced Plastic Sheets* by E.H. Drimoussis and J.J.R. Cheng, October 1994.

206. *Shrinkage and Flexural Tests of a Full-Scale Composite Truss* by M.B. Maurer and D.J.L. Kennedy, December 1994.

207. *Analytical Investigation of the Compressive Behavior and Strength of Steel Gusset Plate Connections* by M.C.H. Yam and J.J.R. Cheng, December 1994.

208. *The Effect of Tension Flange Movement of the Strength of Point Loaded I-Beams* by D. Mullin and J.J.R. Cheng, January 1995.

209. *Experimental Study of Transversely Loaded Continuous Steel Plates* by K.P. Ratzlaff and D.J.L. Kennedy, May 1995.

210. *Fatigue Tests of Riveted Bridge Girders* by D. Adamson and G.L. Kulak, July 1995.

211. *Fatigue of Riveted Tension Members* by J. DiBattista and G.L. Kulak, November 1995.

212. *Behaviour of Masonry Cavity Walls Subjected to Vertical Eccentric Loads* by R. Wang, A.E. Elwi, M.A. Hatzinikolas and J. Warwaruk, Feburary 1996.

213. *Thermal Ice Loads on Structures* by Azarnejad, A. and Hrudey, T.M., November 1996.

214. *Transmission of High Strength Concrete Column Loads Through Concrete Slabs* by C.E. Ospina and S.D.B. Alexander, January 1997.